

2011

# Natural oil-based composites reinforced with natural fillers, and conjugation/isomerization of carbon-carbon double bonds

Rafael Lopes Quirino  
*Iowa State University*

Follow this and additional works at: <https://lib.dr.iastate.edu/etd>

 Part of the [Chemistry Commons](#)

## Recommended Citation

Quirino, Rafael Lopes, "Natural oil-based composites reinforced with natural fillers, and conjugation/isomerization of carbon-carbon double bonds" (2011). *Graduate Theses and Dissertations*. 10316.  
<https://lib.dr.iastate.edu/etd/10316>

This Dissertation is brought to you for free and open access by the Iowa State University Capstones, Theses and Dissertations at Iowa State University Digital Repository. It has been accepted for inclusion in Graduate Theses and Dissertations by an authorized administrator of Iowa State University Digital Repository. For more information, please contact [digirep@iastate.edu](mailto:digirep@iastate.edu).

**Natural oil-based composites reinforced with natural fillers, and  
conjugation/isomerization of carbon-carbon double bonds**

by

**Rafael Lopes Quirino**

A dissertation submitted to the graduate faculty  
In partial fulfillment of the requirements for the degree of  
DOCTOR OF PHILOSOPHY

Major: Chemistry

Program of Study Committee:  
Richard C. Larock, Co-major Professor  
Michael Kessler, Co-major Professor  
Malika El-Jeffries  
John Verkade  
Yan Zhao

Iowa State University

Ames, Iowa

2011

Copyright © Rafael Lopes Quirino 2011. All rights reserved.

To Larissa, Gabriela, Nathan, Alba, Hécio, Vera, Waldir, Leticia and Igor  
for their unconditional love and support

## TABLE OF CONTENTS

|  |     |
|--|-----|
| LIST OF ABBREVIATIONS  | v   |
| ABSTRACT   | vii |
| CHAPTER 1. GENERAL INTRODUCTION  | 1   |
| Preface  | 1   |
| Dissertation Organization  | 7   |
| References   | 8   |
| CHAPTER 2. SYNTHESIS AND PROPERTIES OF SOY HULL-REINFORCED<br>BIOCOMPOSITES FROM CONJUGATED SOYBEAN OIL            | 10  |
| Abstract   | 10  |
| Introduction   | 11  |
| Experimental   | 13  |
| Results and Discussion   | 15  |
| Conclusions  | 34  |
| Acknowledgements   | 35  |
| References   | 35  |
| CHAPTER 3. RICE HULL BIOCOMPOSITES. PART 1: PREPARATION OF A<br>LINSEED OIL-BASED RESIN REINFORCED WITH RICE HULLS | 37  |
| Abstract   | 37  |
| Introduction   | 37  |
| Experimental   | 39  |
| Results and Discussion   | 42  |
| Conclusions  | 62  |
| Acknowledgements   | 62  |
| References   | 63  |
| CHAPTER 4. RICE HULL BIOCOMPOSITES. PART 2: EFFECT OF THE<br>RESIN COMPOSITION ON THE PROPERTIES OF THE COMPOSITE  | 65  |
| Abstract   | 65  |
| Introduction   | 66  |
| Experimental   | 68  |
| Results and Discussion   | 71  |
| Conclusions  | 87  |
| Acknowledgements   | 88  |
| References   | 88  |

|   |     |
|---|-----|
| CHAPTER 5. SOYBEAN AND LINSEED OIL-BASED COMPOSITES<br>REINFORCED WITH WOOD FLOUR AND WOOD FIBERS | 90  |
| Abstract  | 90  |
| Introduction  | 91  |
| Experimental  | 93  |
| Results and Discussion  | 96  |
| Conclusions   | 112 |
| Acknowledgements  | 113 |
| References  | 114 |
| CHAPTER 6. SUGAR-CANE BAGASSE COMPOSITES FROM VEGETABLE<br>OILS                                   | 116 |
| Abstract  | 116 |
| Introduction  | 116 |
| Experimental  | 119 |
| Results and Discussion  | 122 |
| Conclusion  | 137 |
| Acknowledgements  | 138 |
| References  | 138 |
| CHAPTER 7. OAT HULL COMPOSITES FROM CONJUGATED NATURAL<br>OILS                                    | 141 |
| Abstract  | 141 |
| Introduction  | 141 |
| Experimental  | 145 |
| Results and Discussion  | 147 |
| Conclusion  | 162 |
| Acknowledgements  | 164 |
| References  | 164 |
| CHAPTER 8. Rh-BASED BIPHASIC ISOMERIZATION OF CARBON-<br>CARBON DOUBLE BONDS                      | 166 |
| Abstract  | 166 |
| Introduction  | 166 |
| Experimental  | 170 |
| Results and Discussion  | 175 |
| Conclusion  | 192 |
| Acknowledgements  | 193 |
| References  | 193 |
| CHAPTER 9. GENERAL CONCLUSIONS  | 196 |
| ACKNOWLEDGEMENTS  | 202 |
| CURRICULUM VITAE  | 203 |

## LIST OF ABBREVIATIONS

|                  |  |
|------------------|--|
| $^1\text{H}$ NMR | proton nuclear magnetic resonance          |
| AA               | acrylic acid                               |
| ADMET            | acyclic diene metathesis                   |
| AIBN             | azobisisobutyronitrile                     |
| ASTM             | American Society for Testing and Materials |
| BMA              | <i>n</i> -butyl methacrylate               |
| CCO              | conjugated corn oil                        |
| CFO              | conjugated fish oil                        |
| CLA              | conjugated linoleic acid                   |
| CLO              | conjugated linseed oil                     |
| CSO              | conjugated soybean oil                     |
| CTAB             | cetyltrimethylammonium bromide             |
| DCPD             | dicyclopentadiene                          |
| DHA              | docosa-4,7,10,13,16,19-hexaenoic acid      |
| DMA              | dynamic mechanical analysis                |
| dppba            | 4-(diphenylphosphino)benzoic acid          |
| DSC              | differential scanning calorimetry          |
| DTA              | derivative of thermogravimetric analysis   |
| DVB              | divinylbenzene                             |
| <i>E</i>         | Young's modulus                            |
| <i>E'</i>        | storage modulus                            |
| <i>E''</i>       | loss modulus                               |
| EPA              | eicosa-5,8,11,14,17-pentaenoic acid        |
| EtOH             | ethanol                                    |
| GC/MS            | gas chromatography/mass spectrometry       |
| HDPE             | high density polyethylene                  |
| <i>i</i> -PrOH   | 2-propanol                                 |
| ICP-MS           | induced coupled plasma-mass spectrometry   |
| MA               | maleic anhydride                           |
| MeOH             | methanol                                   |

|                |   |
|----------------|---|
| PP             | polypropylene   |
| PrOH           | propanol  |
| PTS            | polyoxyethanyl- $\alpha$ -tocopheryl sebacate               |
| ROMP           | ring opening metathesis polymerization                      |
| SDS            | sodium dodecyl sulfate                                      |
| SEM            | scanning electron microscopy                                |
| SH             | soybean hulls   |
| SOY            | soybean oil   |
| ST             | styrene   |
| <i>t</i> -BuOH | <i>tert</i> -butanol  |
| $T_{10}$       | temperature at 10% weight loss                              |
| $T_{50}$       | temperature at 50% weight loss                              |
| $T_7$          | temperature at 7% weight degradation                        |
| $T_{95}$       | temperature at 95% weight loss                              |
| TBPO           | di- <i>t</i> -butyl peroxide                                |
| $T_f$          | temperature after which no weight loss is detected          |
| $T_g$          | glass transition temperature                                |
| TGA            | thermogravimetric   |
| $T_{max}$      | temperature at maximum degradation rate                     |
| tppms          | triphenylphosphine monosulfonate sodium salt                |
| tppts          | triphenylphosphine-3,3',3''-trisulfonic acid trisodium salt |
| ttp            | tris- <i>p</i> -tolylphosphine                              |
| TUN            | tung oil  |

**ABSTRACT**

The tensile and flexural properties of new thermosetting composites made by the free radical polymerization of natural oil-based resins reinforced with natural fillers have been determined for various oils, fillers, and resin compositions. Tung, and conjugated corn, soybean, linseed, and fish oils have been co-polymerized with varying amounts of divinylbenzene (0-15 wt %), dicyclopentadiene (0-10 wt %), *n*-butyl methacrylate (20-35 wt %), and maleic anhydride (0-15 wt %). The natural fillers used include widely produced and underused agricultural residues, such as sugar-cane bagasse, soybean, rice, and oat hulls, as well as residues from the wood industry, such as wood flours and wood fibers. The thermal stability of the new materials has been determined by TGA and the wt % of monomer incorporation has been calculated after Soxhlet extraction and analysis of the extracts by <sup>1</sup>H NMR. Scanning electron microscopy of selected samples revealed improvement on the filler-resin interaction for samples containing maleic anhydride. Composites with Young's modulus and tensile strength as high as 4.3 GPa and 17.6 MPa, respectively, have been prepared. The materials obtained show promising application in the automotive, aerospace and housing industries as decorative, light-weight panels. The conjugation of the oils used in this study involves the use of an efficient homogeneous Rh catalyst that is completely discarded after the reaction. The conversion of that catalyst into a biphasic system can turn this reaction into an economically viable, and greener process. In the present work, we have optimized the conversion of the homogeneous catalyst  $[\text{RhCl}_2(\text{C}_8\text{H}_{14})_2]_2$  into a complex that works under biphasic conditions for the conjugation/positional isomerization of carbon-carbon double bonds. A maximum yield of 96% has been obtained at optimal conditions using soybean oil as the substrate.



## CHAPTER 1. GENERAL INTRODUCTION

Portions of the General Introduction have been adapted from a book chapter published in the ACS Symposium series book *Renewable and Sustainable Polymers*, as well as from a chapter submitted for inclusion in the book *Sustainable Composites and Advanced Materials* by Destech Publications.

### Preface

With the tremendous commercial importance of the plastics and coatings industries, it is obvious that the replacement of petroleum-based materials by useful novel bioplastics from inexpensive, renewable, natural resources, like natural oils and agricultural residues, has an enormous impact economically, environmentally, and energy-wise. The advantages of bio-based materials are their ready availability in large quantities, their usually competitive price in comparison to currently used petroleum-based monomers, the potential of producing more bio-degradable materials than virtually indestructible petroleum-based polymers, the possibility of producing new materials with properties not currently available in commercial petroleum-based products, and the overall intrinsic low toxicity of such bio-based products.

The use of renewable resources in energy and material-related applications is receiving increasing attention in both industry and academia. Several factors contribute to frequent dramatic fluctuations in the price of oil, which is reflected in the production cost of all petroleum-based goods. This situation creates an urgent need, from an industrial point of view, for starting materials from an alternative source. For the reasons mentioned earlier, bio-based products have the potential to partially replace petroleum-based materials. Thus,

research and development of new biopolymers is extremely important in attaining oil independence and sustainable industrial development.

Currently, the polymer industry is responsible for approximately 7 % of all oil and gas used worldwide.<sup>1</sup> As a matter of fact, 15 % of all soybean oil produced from 2001 to 2005 was employed for industrial uses.<sup>2</sup> Besides vegetable oils, other widely used renewable raw materials are polysaccharides (cellulose and starch), wood, and proteins.<sup>3</sup> A variety of chemicals have been prepared from these starting materials. Bio-oil and syngas are obtained by the pyrolysis of wood and agricultural wastes.<sup>4</sup> Proteins are denatured and aligned during processing to make protein-based biopolymers,<sup>5</sup> and vegetable oils find uses in paints,<sup>6</sup> bio-coatings,<sup>7</sup> biofuels,<sup>8</sup> and as building blocks for bio-based polymers.<sup>9</sup>

Recently, a variety of vegetable oil-based polymers with good thermal and mechanical properties have been developed through the cationic, free radical, or thermal copolymerization of regular and conjugated natural oils with several petroleum-based comonomers.<sup>9,10</sup> Other polymerization methods, such as ring-opening metathesis polymerization (ROMP) and acyclic diene metathesis (ADMET),<sup>9,11</sup> have also been recently employed to synthesize vegetable oil-based polymers. Bio-based materials with improved thermophysical and mechanical properties can be obtained by simply reinforcing the aforementioned polymeric matrices with inorganic fillers and natural fibers.<sup>12-17</sup> Various agricultural residues and natural fibers, such as spent germ,<sup>14</sup> corn stover,<sup>15</sup> wheat straw,<sup>16</sup> and switch grass<sup>17</sup> have been added to the aforementioned vegetable oil-based resins to prepare biocomposites with up to 85 wt % of bio-based content.

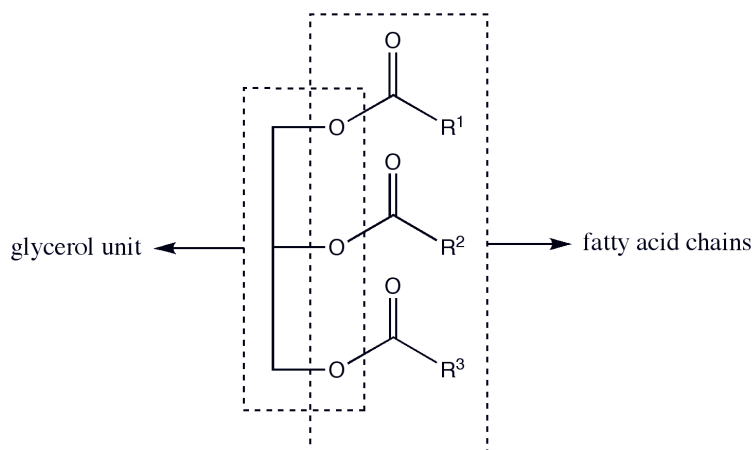
The general chemical structure of natural oils consists of triglycerides of various fatty acid compositions. The main difference between different natural oils is the length of the fatty acid chains, the number and the position of the carbon-carbon double bonds along those fatty acid chains, and the presence of specific functional groups. These characteristics of the oils vary according to the plants from which the oils are extracted and their corresponding growing conditions.<sup>18</sup> A common representation of a triglyceride is given in Figure 1, along with the chemical structure of the most abundant fatty acids found in natural oils. Table I summarizes the fatty acid composition of the most commonly used oils.

As can be seen from Figure 1 and Table I, naturally-occurring fatty acids contain an even number of carbons, and most of the carbon-carbon double bonds present in the unsaturated fatty acids have a *cis* configuration. Furthermore, some fatty acids, such as ricinoleic acid, bear functional groups on specific positions along the fatty acid chain.

In natural oil-based systems, one of the important reactive sites in the triglyceride is the carbon-carbon double bonds. Overall, the reactivity of vegetable oils towards cationic and free radical polymerization processes is significantly higher if the carbon-carbon double bonds in the fatty acid chains are conjugated.<sup>19</sup> For the remainder of this dissertation, the term “conjugated” refers to carbon-carbon double bonds that are conjugated (as in a 1,3-diene).

Conjugated vegetable oils from the isomerization of carbon-carbon double bonds have been initially reported as by-products of reactions involving vegetable oils.<sup>20</sup> Since then, the production of conjugated fatty acids and triglycerides using heterogeneous catalysts has been studied and optimized.<sup>21</sup>

A



R<sup>1</sup>, R<sup>2</sup>, R<sup>3</sup> = distinct aliphatic hydrocarbon chains with varying length, number and position of carbon-carbon double bonds, and functional groups

B

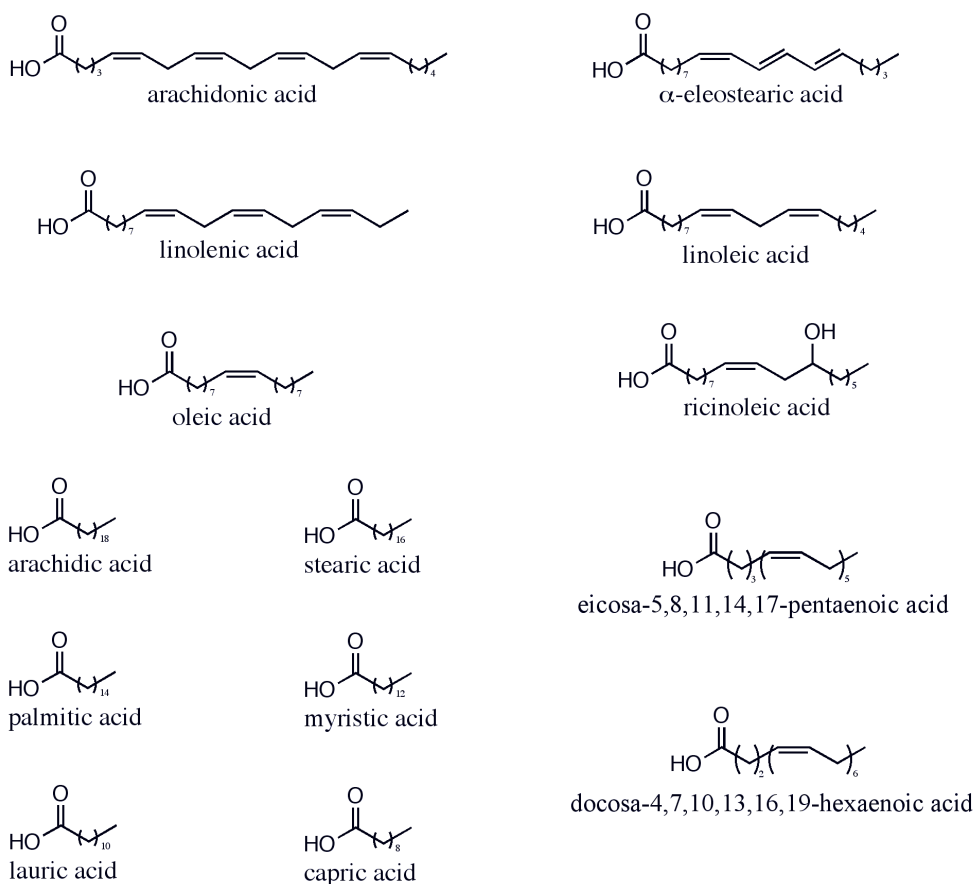


**Figure 1.** (A) General chemical structure of a vegetable oil. (B) Most common fatty acids present in vegetable oils and their chemical structures.

**Table I.** Fatty acid composition of vegetable oils commonly used in the preparation of new bio-based materials.

| Oil                    | Linolenic acid content (%) | Linoleic acid content (%) | Oleic acid content (%) | Stearic acid content (%) | Palmitic acid content (%) |
|------------------------|----------------------------|---------------------------|------------------------|--------------------------|---------------------------|
| Tung <sup>a</sup>      | -                          | 9                         | 4                      | -                        | 6                         |
| Linseed                | 57                         | 15                        | 19                     | 4                        | 6                         |
| Walnut                 | 3                          | 73                        | 18                     | 1                        | 5                         |
| Low saturation soybean | 9                          | 57                        | 31                     | 1                        | 3                         |
| Safflower              | -                          | 78                        | 12                     | 2                        | 7                         |
| Sunflower              | 1                          | 54                        | 37                     | 3                        | 5                         |
| Soybean                | 8                          | 53                        | 23                     | 4                        | 11                        |
| Corn                   | 1                          | 60                        | 25                     | 2                        | 11                        |
| Grapeseed              | -                          | 63                        | 27                     | 3                        | 7                         |
| Canola                 | 9                          | 21                        | 61                     | 2                        | 4                         |
| Sesame                 | 1                          | 43                        | 41                     | 6                        | 9                         |
| Peanut                 | -                          | 32                        | 47                     | 2                        | 11                        |
| Olive                  | 1                          | 6                         | 80                     | 3                        | 9                         |
| Castor <sup>b</sup>    | 1                          | 4                         | 5                      | 1                        | 2                         |
| Fish <sup>c</sup>      | -                          | -                         | 11-25                  | -                        | 10-22                     |

<sup>a</sup> Approximately 84 % of the fatty acid chains in tung oil are alpha-eleostearic acid, a naturally conjugated triene (12).

<sup>b</sup> Approximately 85 % of the fatty acid chains in castor oil are ricinoleic acid.

<sup>c</sup> Approximately 32% of the fatty acid chains in fish oil are eicosa-5,8,11,14,17-pentaenoic acid (EPA) and approximately 25% of the fatty acid chains are docosa-4,7,10,13,16,19-hexaenoic acid (DHA)

Conjugated vegetable oils are also useful as drying oils for paints and coatings.<sup>19</sup> While some natural oils can be used without further structural modification to produce coatings,<sup>22</sup> cheaper and more readily available vegetable oils can be conjugated in order to increase their drying properties and reduce production costs.<sup>19</sup> Conjugated vegetable oils can

also be used as a source of conjugated linoleic acid (CLA).<sup>19</sup> CLA has been shown to possess anti-cancer and anti-atherosclerosis activity, and serves as a fat reducing agent.<sup>19</sup> Vegetable oils with a high content of linoleic acid have great potential for the production of CLA upon conjugation.

Several conjugation processes for vegetable oils have been developed to date.<sup>19-21</sup> In most of these processes, transition metal hydrides interact with the unsaturation in the triglyceride through an addition-elimination mechanism and the carbon-carbon double bonds “move” along the fatty acid chain to yield conjugated species. A very efficient homogeneous conjugation system that uses a Rh-based pre-catalyst ( $[\text{RhCl}(\text{C}_8\text{H}_{14})_2]_2$ ) has given more than 95% conversion for several natural oils.<sup>19</sup> The conjugation of vegetable oils in the presence of this catalyst system has been carried out under mild reaction conditions and affords very little in the way of hydrogenated species, a typical side product in such processes.<sup>19</sup> Although very efficient, this catalyst is usually completely discarded after conjugation. Being a homogeneous catalyst, filtration of the products to recover the metal complex is very difficult and time consuming. Therefore, the catalyst's reuse is currently not an attractive process, despite its high price.

Finding a recyclable and reusable catalyst for the conjugation of triglycerides represents a key step towards the development of greener technologies for preparing conjugated natural oils. Many alternatives to homogeneous catalysts have been proposed, including solid catalysts.<sup>21</sup> More recently, polymer-bound complexes, and active species tethered to inorganic supports have shown reactivities similar to their homogeneous counterparts, with the advantage of being more easily recoverable.<sup>23</sup>

Along those lines, an interesting alternative is an ethanol-soluble complex that works under biphasic conditions. This catalyst has the potential advantage of using an environmentally-friendly solvent and being easily recovered using simple liquid/liquid separation techniques for subsequent use, without the need for further purification of the active species or the products.

The technology involved in the new natural oil-based materials and products investigated here is remarkably simple and should be readily adapted to existing industry. The transition from petroleum to bio-based products provides major economical advantages, and even more importantly, generates more environmentally-friendly processes and products.

### **Dissertation Organization**

This dissertation is divided into seven chapters. The tensile and flexural properties of new thermosetting composites made by the free radical polymerization of a conjugated soybean oil-based resin reinforced with soybean hulls are discussed in the first chapter. The effects of reinforcement particle size and filler/resin ratio have been assessed, as well as the thermal stability and the wt % of oil incorporation into the new materials. In this study, the resin is initially composed of conjugated soybean oil (CSO), divinylbenzene (DVB), and *n*-butyl methacrylate (BMA). Dicyclopentadiene (DCPD) has been tested as a potential cheaper crosslinker substitute for DVB.

The second and third chapters deal with conjugated linseed oil (CLO)-based free radical thermosets reinforced with rice hulls. The second chapter focuses on a cure sequence study and on the effect of different parameters, such as pressure, filler load, drying and grinding of the filler on the final properties of the composites, while the third chapter focuses

on a study of the effects of the resin composition on composite properties. A comparison between CLO and CSO as the major resin component has been carried out, and maleic anhydride (MA) has been added to the formulation as a filler-resin compatibilizer.

In the fourth chapter, a detailed analysis of the influence of the cure time on the properties of composites consisting of a CLO- or CSO-based thermoset reinforced with wood flour and wood fibers is presented, and in the fifth chapter, the post-cure process of vegetable oil-based thermosets reinforced with washed sugar-cane bagasse is studied in detail. Important observations about the initial washing and drying of the filler indicate that these processes have an impact on the final properties of the composites. The sixth chapter is concerned with structure-property relationships of oat hull composites prepared from various regular and conjugated natural oils as the major resin components.

The biphasic conjugation of soybean and other natural oils, as well as the positional isomerization of various alkenes, has been examined using a biphasic rhodium catalyst. This study and the corresponding results are described and discussed in detail in the seventh chapter.

### References

1. C. K. Williams, M. A. Hillmyer, *Polym. Rev.* **2008**, *48*, 1.
2. M. N. Belgacem, A. Gandini, *Monomers, Polymers and Composites from Renewable Resources*, Elsevier, Oxford, **2008**.
3. G. W. Huber, S. Iborra, A. Corma, *Chem. Rev.* **2006**, *106*, 4044.
4. A. Demirbas, *Energy Convers. Manage.* **2009**, *50*, 2782.
5. G. Srinivasan, D. Grewell, *67<sup>th</sup> ANTEC*, **2009**, 2610.
6. M. R. Van De Mark, K. Sandefur, *Industrial Uses of Vegetable Oil*, Editor, S. Z. Erhan, AOCS Press, Peoria, IL, **2005**, 143-162.
7. Y. Lu, R. C. Larock, *ChemSusChem* **2010**, *3*, 329.



8. D. G. Lima, V. C. D. Soares, E. B. Ribeiro, D. A. Carvalho, E. C. V. Cardoso, F. C. Rassi, K. C. Mundim, J. C. Rubim, P. A. Z. Suarez, *J. Anal. Appl. Pyrolysis* **2004**, *71*, 987.
9. Y. Lu, R. C. Larock, *ChemSusChem* **2009**, *2*, 136.
10. P. P. Kundu, R. C. Larock, *Biomacromolecules* **2005**, *6*, 797.
11. A. Rybak, P. A. Fokou, M. A. R. Meier, *Eur. J. Lipid Sci. Technol.* **2008**, *110*, 797.
12. Y. Lu, R. C. Larock, *J. Appl. Polym. Sci.* **2006**, *102*, 3345.
13. Y. Lu, R. C. Larock, *Biomacromolecules* **2006**, *7*, 2692.
14. D. P. Pfister, J. R. Baker, P. H. Henna, Y. Lu, R. C. Larock, *J. Appl. Polym. Sci.* **2008**, *108*, 3618.
15. D. P. Pfister, R. C. Larock, *Bioresour. Technol.* **2010**, *101*, 6200.
16. D. P. Pfister, R. C. Larock, *Composites: Part A* **2010**, *41*, 1279.
17. D. P. Pfister, *Green Composites and Coatings from Agricultural Feedstocks*, Ph.D. dissertation, Iowa State University, Ames, Iowa, **2010**.
18. M. A. R. Meier, J. O. Metzger, U. S. Schubert, *Chem. Soc. Rev.* **2007**, *36*, 1788.
19. D. D. Andjelkovic, B. Min, D. Ahn, R. C. Larock, *J. Agric. Food Chem.* **2006**, *54*, 9535.
20. M. O. Jung, S. H. Yoon, M. Y. Jung, *J. Agric. Food Chem.* **2001**, *49*, 3010.
21. O. A. Simakova, A. Leino, B. Campo, P. Maki-Arvela, K. Kordas, J. Mikkola, D. Y. Murzin, *Catalysis Today* **2010**, *150*, 32.
22. H. Wexler, *Chem. Rev.* **1964**, *64*, 591.
23. D. E. Bergbreiter, *Chem. Rev.* **2002**, *102*, 3345.

## CHAPTER 2. SYNTHESIS AND PROPERTIES OF SOY HULL-REINFORCED BIOCOMPOSITES FROM CONJUGATED SOYBEAN OIL

A Paper Published in Journal of Applied Polymer Science, 112, 2033-2043.  
Copyright © 2009, Wiley-Blackwell

Rafael L. Quirino, Richard C. Larock\*

*Department of Chemistry, Iowa State University, Ames, Iowa 50011*

### Abstract

The tensile and flexural properties of new thermosetting composites made by the free radical polymerization of a conjugated soybean oil-based resin reinforced with soy hulls have been determined for various resin compositions. The effects of reinforcement particle size and filler/resin ratio have been assessed. The thermal stability of the new materials has been determined by TGA and the wt % of oil incorporation has been calculated after Soxhlet extraction (the extracts have been identified by  $^1\text{H}$  NMR spectroscopy). The resin consists initially of 50 wt % conjugated soybean oil and varying amounts of divinylbenzene (5-15 wt %), dicyclopentadiene (0-10 wt%) and *n*-butyl methacrylate (25-35 wt %). Two soy hull particle sizes have been tested ( $<177\ \mu\text{m}$  and  $<425\ \mu\text{m}$ ) and two different filler/resin ratios have been compared (50:50 and 60:40). An appropriate cure sequence has been established by DSC analysis. The results show a decrease in the properties whenever divinylbenzene or *n*-butyl methacrylate is substituted by dicyclopentadiene. Also, larger particle sizes and higher filler/resin ratios are found to have a negative effect on the tensile properties of the new materials.

## Introduction

The replacement of petroleum-based products by materials prepared from natural biorenewable resources has been intensively investigated in recent years in an attempt to reduce man's dependence on crude oil. One promising approach involves the use of vegetable oils in substitution or in addition to petroleum derivatives. Interesting applications as biofuels,<sup>1</sup> coatings<sup>2</sup> and biomaterials<sup>3</sup> (biopolymers and biocomposites) have been reported.

The use of vegetable oils as comonomers in the synthesis of new biopolymers is known and a variety of processes and materials have already been reported in the literature using different vegetable oils.<sup>4-6</sup> A simple and promising procedure that yields thermosets with unique mechanical properties involves the reaction of the carbon-carbon double bonds in the fatty acid chains of triglycerides with other reactive monomers (divinylbenzene, styrene, acrylonitrile, dienes, acrylates, etc.) to form a network of crosslinked polymer chains. These materials can be obtained through cationic,<sup>7-10</sup> thermal<sup>11,12</sup> or free radical polymerization.<sup>13,14</sup> Initially, our group focused on the development of new resins using a range of vegetable oils, including soybean,<sup>7,10,14</sup> corn,<sup>8</sup> tung<sup>11</sup> and linseed<sup>12,13</sup> oils.

Soybeans are among America's largest crops, being mainly used in the food industry. Soybean oil represents a readily available and low cost starting material that can be used for the purposes indicated earlier.<sup>1-3</sup> The fatty acid composition of soybean oil is as follows: 51% linoleic acid (C18:2), 23% oleic acid (C18:1), 10% palmitic acid (C16:0), 7% linolenic acid (C18:3), 4% stearic acid (C18:0) and 5% of other fatty acids in negligible amounts.<sup>15</sup>

With an average of 4.5 double bonds per triglyceride,<sup>10</sup> soybean oil is only moderately active towards free radical species, but the reactivity can be considerably

increased by conjugation of the carbon-carbon double bonds of the fatty acid chains. Several studies regarding the double bond isomerization of vegetable oils have been reported in the literature.<sup>16-19</sup> Our group has developed a homogeneous isomerization procedure employing  $[\text{RhCl}(\text{C}_8\text{H}_{14})_2]_2$  as a pre-catalyst.<sup>20</sup> The reaction yields >95% conjugation for several vegetable oils tested and has been used frequently in our work on bioplastics.<sup>7,13,21-24</sup>

Free radical resins developed in our group so far include conjugated linseed oil-<sup>13</sup> and conjugated soybean oil-<sup>14</sup> containing biopolymers. The results obtained in these studies revealed that a vegetable oil content ranging from 40 wt % to 65 wt % maximizes the oil incorporation in the final matrix.<sup>14</sup> More recently, in an attempt to obtain stronger materials, we have reported the preparation and properties of composites containing a tung oil-based resin (cured by free radical polymerization) reinforced with spent germ, an underused agricultural by-product from wet mill ethanol production.<sup>25</sup>

Soy hulls, another example of an abundant underused agricultural by-product, are essentially the outer skin of the soybean.<sup>26</sup> They are normally used as a low cost feedstock or discarded during processing of the soybeans. The large quantity of soy hulls produced and their lack of industrial application account for their low price.<sup>27</sup> The chemical composition of soy hulls is approximately 11% protein, 11% galactomannans, 12% acidic polysaccharides, 10% xylan hemicellulose, 40% cellulose and 16% lignin.<sup>27</sup> Due to their relatively high fiber content (lignin, cellulose and hemicellulose), low cost and ready availability, soy hulls are particularly attractive as an economical and environmentally-friendly reinforcement for biocomposites.

In this work, we've studied the mechanical and flexural properties of composites

prepared from conjugated soybean oil (CSO) reinforced with soy hulls. An appropriate cure sequence has been established by means of differential scanning calorimetry (DSC). Young's ( $E$ ) and storage ( $E'$ ) moduli, as well as tensile strengths and glass transition temperatures ( $T_g$ 's) have been determined as the resin composition is varied. We have also looked into the effect of the particle size and the filler/resin ratio on the properties of the final materials. Their thermal stability has been assessed by thermogravimetric analysis (TGA), the wt % incorporation of CSO in the resin has been determined by Soxhlet extraction with  $\text{CH}_2\text{Cl}_2$ , and the extracts have been identified by  $^1\text{H}$  NMR spectroscopy. A scanning electron microscopy (SEM) study has shown visual proof of the filler-resin arrangements in the final composites.

### Experimental

**Materials.** *n*-Butyl methacrylate (BMA) and dicyclopentadiene (DCPD) were purchased from Alfa Aesar (Ward Hill, MA). Divinylbenzene (DVB) and *t*-butyl peroxide (TBPO) were purchased from Aldrich Chemical Co. (Milwaukee, WI). All chemicals were used as received. The soybean oil (*Carlini* brand – Aldi Inc., Batavia, IL) was purchased in a local grocery store and conjugation was carried out using a homogeneous Rh catalyst, as described in the literature,<sup>20</sup> to produce CSO. The soy hulls were provided by West Central Co-op (Ralston, IA). They were ground and sieved into two different particle sizes, <425  $\mu\text{m}$  diameter (>40 mesh) and <177  $\mu\text{m}$  diameter (>80 mesh). The sieved soy hulls were then dried overnight at 70 °C in a vacuum oven prior to their use.

**Preparation of the Composites.** The crude resin was obtained by mixing the designated amounts of each component (CSO, DVB, DCPD and BMA) in a beaker. All resins have been

prepared using 50 wt % CSO. For the radical initiator TBPO, five wt % of the total resin was added. As an example of the nomenclature adopted in this work, the sample DVB10-DCPD5-BMA35 represents a resin containing 10 wt % of DVB, 5 wt % of DCPD and 35 wt % of BMA (the other 50 wt % of the resin being CSO). The dried soy hulls were impregnated with the resin (in the ratios designated in the text) and compression molded at 276 psi (unless otherwise specified). The filler content could not be reduced below 50 wt %, because, during compression molding, the excess of resin leaks when pressure is applied. If cure occurs at atmospheric pressure, then the fillers accumulate on the bottom of the mold and a non-uniform composite is obtained. For filler compositions above 60 wt % the opposite effect is observed. The amount of resin was insufficient to completely wet the soy hulls yielding materials that tended to crumble when handled. All composites were cured for 5 hours at 130 °C and then post-cured at 150 °C for another 2 hours.

**Characterization.** The optimal cure sequence was determined by DSC using a Q20 DSC (TA Instruments, New Castle, DE) under a N<sub>2</sub> atmosphere over a temperature range of -20 °C to 400 °C at a rate of 20 °C/min. The samples weighed approximately 11 mg.

The tensile test experiments were conducted at 25 °C according to ASTM D638 using an Instron universal testing machine (model 5569) equipped with a video extensometer and operating at a crosshead speed of 2.0 mm/min. The dogbone-shaped test specimens had the following gauge dimensions: 57 mm x 12.7 mm x 4.5 mm (length, width and thickness, respectively).

The dynamic mechanical analysis (DMA) was conducted on a TA Instruments Q800 DMA using a three-point bending mode. A rectangular specimen of about 22 mm × 8.5 mm ×

1.5 mm (length × width × thickness) was cut from the samples. Each specimen was cooled to -60 °C and then heated at 3 °C/min to 250 °C at a frequency of 1 Hz under air.

A Q50 TGA instrument (TA Instruments, New Castle, DE) was used to measure the weight loss of the samples under an air atmosphere. The samples were heated from room temperature to 650 °C at a heating rate of 20 °C/min. The samples weighed approximately 10 mg.

Soxhlet extraction was conducted to determine the amount of soluble materials in the composites. A 2 g sample was extracted for 24 hours with 110 mL of dichloromethane (CH<sub>2</sub>Cl<sub>2</sub>). After extraction, the resulting solution was concentrated on a rotary evaporator and both the soluble and insoluble materials were dried in a vacuum oven at 70 °C overnight before weighing. The soluble fraction of each extracted sample was dissolved in CDCl<sub>3</sub> and proton nuclear magnetic resonance (<sup>1</sup>H NMR) spectroscopic analysis was carried out in order to determine its composition. The <sup>1</sup>H NMR spectra were obtained with a Varian Unity spectrometer (Varian Associates, Palo Alto, CA) operating at 300 MHz.

Scanning Electron Microscopy (SEM) analysis was conducted using a Hitachi S-2460N variable pressure scanning electron microscope. The parameters used were: 20 kVolts accelerating voltage, 60 Pa Helium atmosphere and 15 mm working distance. The equipment was set with a tetra backscattered electron detector. Each sample analyzed was frozen with liquid N<sub>2</sub> prior to fracture for the cryo-fractured analysis. For comparative reasons, the samples were also cut using a razor blade and analyzed by SEM.

## Results and Discussion

**Cure Sequence Determination.** A preliminary determination of the best cure sequence was

conducted by means of DSC experiments with a partially cured composite sample (Figure 1A) and with soy hulls alone (Figure 1B). In Figure 1A, the DSC curve of the sample DVB15-BMA35 with 50 wt % soy hulls and a particle size  $<425 \mu\text{m}$  diameter heated at  $130^\circ\text{C}$  for 4 hours shows two exothermic peaks at approximately  $135^\circ\text{C}$  and  $170^\circ\text{C}$ , as well as a pronounced absorption of heat at  $220^\circ\text{C}$  and two exothermic peaks at  $260^\circ\text{C}$  and  $350^\circ\text{C}$ . Any transitions occurring after  $400^\circ\text{C}$  are related to decomposition of the resin as explained in our previous work.<sup>25</sup> The heat flow observed between  $200^\circ\text{C}$  and  $400^\circ\text{C}$  corresponds to decomposition of the hemicellulose and cellulose present in significant amounts in the soy hulls.<sup>28</sup> This same feature can be seen in Figure 1B. The exothermic peaks at  $135^\circ\text{C}$  and  $170^\circ\text{C}$  in Figure 1A are probably related to further cure of the resin.

A comparison of Figures 1A and 1B confirms that the heat flow observed in the range  $200\text{-}400^\circ\text{C}$  in Figure 1A is related to changes in the soy hulls. The lower degradation temperature for the soy hulls alone (the heat absorption starts at  $160^\circ\text{C}$ ) when compared to the composite analysis (Figure 1A, the heat absorption starts at  $198^\circ\text{C}$ ) suggests that the resin helps thermally stabilize the filler, increasing considerably the degradation temperatures.

To fully cure the soybean oil-based resin during the composite processing, a longer cure sequence at higher temperatures was clearly required (see Figure 1A). For that reason, the cure time was increased to 5 hours at  $130^\circ\text{C}$  and 276 psi. To ensure complete cure of the resin, a post cure of 2 hours at  $150^\circ\text{C}$  and atmospheric pressure was tried. Figure 1C shows the DSC of a sample subjected to that cure sequence. In Figure 1C, the peaks at  $135^\circ\text{C}$  and  $170^\circ\text{C}$  have completely disappeared, indicating that the resin was completely cured after the



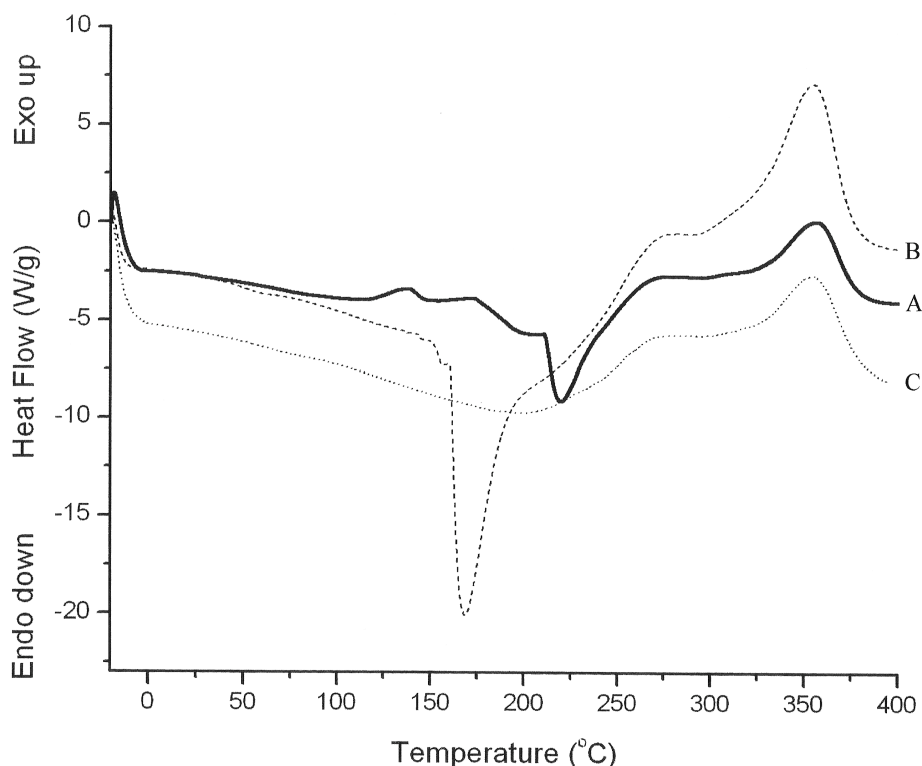


**Figure 1.** DSC curves of (A) DVB15-BMA35 composite heated at 130 °C for 4 hours, (B) soy hulls, and (C) DVB15-BMA35 composite heated at 130 °C for 5 hours at 276 psi and postcured at 150 °C for 2 hours.

longer heating sequence. Also, it is noticeable that the endothermic peak in Figure 1C is much less pronounced than in Figures 1A and 1B. This peak is attributed to volatilization of compounds during thermal degradation of the hemicellulose.<sup>28</sup> This volatilization process occurs more easily in the absence of resin or in the presence of partially cured resin. The completely cured polymer network entraps soy hull particles, inhibiting volatilization. This particle entrapment is not as effective in the presence of the partially cured resin as the network isn't fully formed and contains regions of lower molecular weight chains and lower crosslink density in the composite. Another reason for the lower endothermic peak in Figure

1C may be partial degradation of the hemicellulose during the longer cure process. A comparison of the DTA curves for the soy hulls (Figure 2) and the DVB15-BMA35 composite (Figure 3) also shows that degradation of hemicellulose starts at lower temperatures in the absence of the resin. As a fully cured resin was desired for the preparation of composites in this work, all the samples prepared here were subjected to the same heat treatment: 5 hours at 130 °C and 276 psi, followed by a post cure of 2 hours at 150 °C and atmospheric pressure (the pressure was different than 276 psi where indicated).

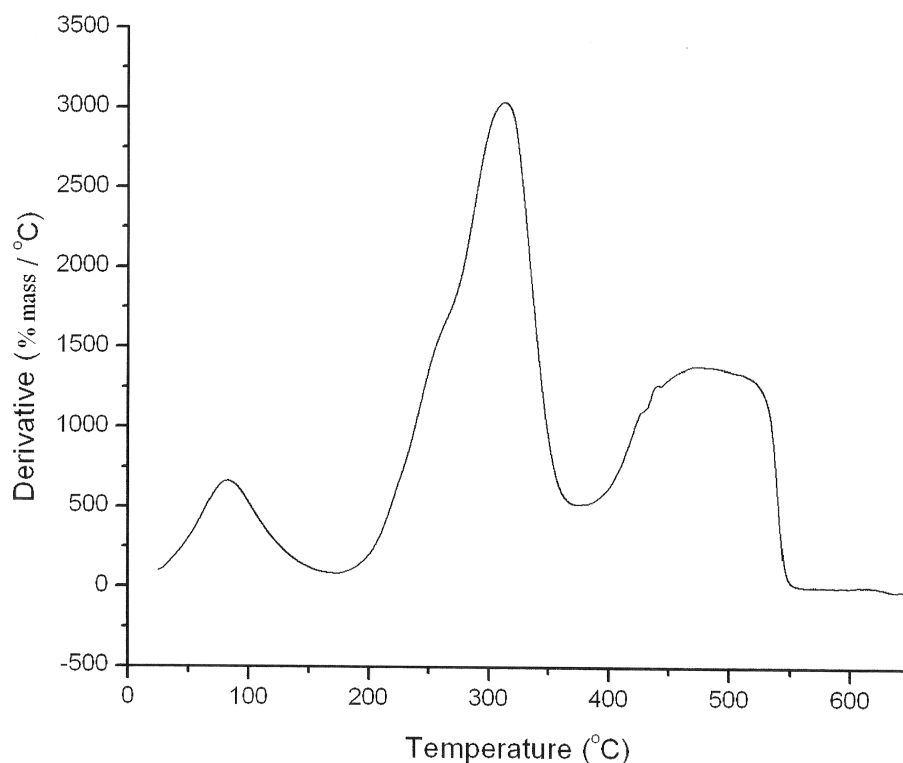


**Figure 2.** DTA curve of soy hulls.

**Dynamic Mechanical Analysis (DMA).** From Table I, the effects of filler/resin ratio, particle size and resin composition on the flexural properties of the composites can be

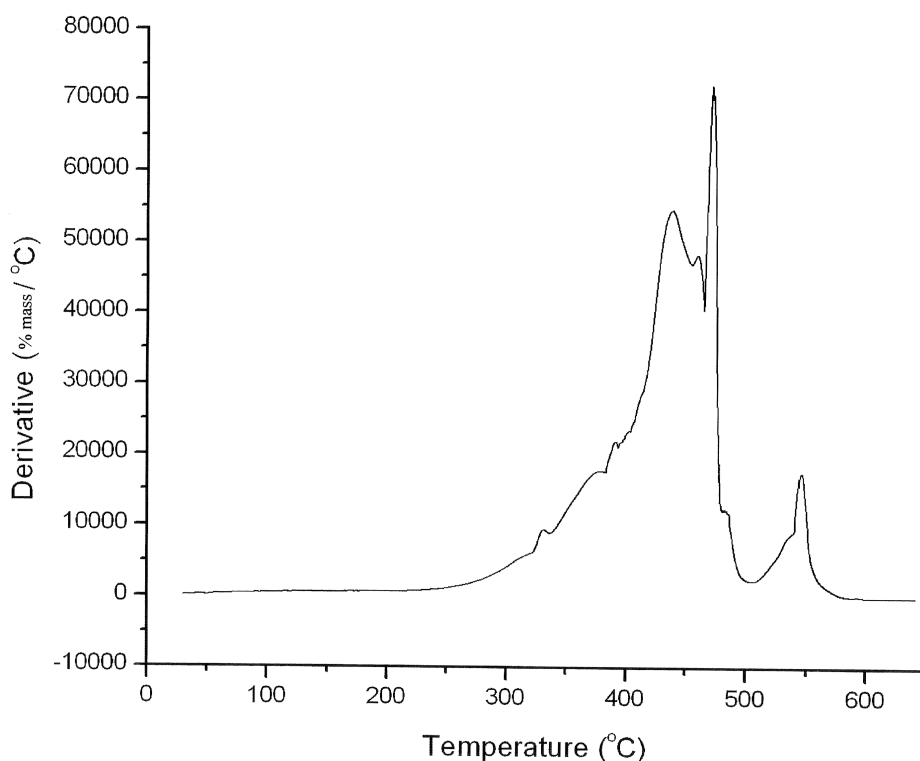


**Figure 3.** DTA curve of DVB15-BMA35 (filler/resin ratio = 50:50 and particle size <math><425\ \mu\text{m}</math>).

obtained through analysis of the storage modulus ( $E'$ ) at 25 °C. Table I also shows the glass transition temperatures ( $T_g$ 's) of each sample as obtained from the tan delta curve by DMA.

The most distinctive characteristic of the composites prepared is the formation of a phase separated matrix upon cure of the resin. The presence of two distinct  $T_g$ 's in all samples is evidence that compounds with different reactivity (such as CSO and DVB, for example) have polymerized at different rates, producing a phase separation. For all samples, the first  $T_g$  ( $T_{g1}$ ) occurred below -6 °C, while the second  $T_g$  ( $T_{g2}$ ) occurred above 57 °C. The large difference between  $T_{g1}$  and  $T_{g2}$  indicates formation of two phases with very different properties and compositions. The phase associated with  $T_{g1}$  is believed to be a CSO-rich phase, composed mainly of less reactive species derived from CSO and DCPD. The phase

**Table I.** Glass transition temperatures ( $T_g$ 's) and storage modulus ( $E'$ ) at 25 °C of the composites prepared.

| Entry | Sample <sup>a</sup> | Filler/Resin Ratio (wt %) | Particle Size ( $\mu\text{m}$ ) | $T_{g1}$ (°C) | $T_{g2}$ (°C) | $T_{g2} - T_{g1}$ (°C) | $E'$ at 25 °C (MPa) |
|-------|---------------------|---------------------------|---------------------------------|---------------|---------------|------------------------|---------------------|
| 1     | Resin <sup>b</sup>  | -                         | -                               | -31           | 57            | 88                     | 152                 |
| 2     | 92 psi              | 50/50                     | <425                            | -24           | 60            | 84                     | 298                 |
| 3     | 184 psi             | 50/50                     | <425                            | -26           | 74            | 100                    | 315                 |
| 4     | DVB15-BMA35         | 50/50                     | <425                            | -32           | 75            | 107                    | 536                 |
| 5     | 368 psi             | 50/50                     | <425                            | -31           | 76            | 107                    | 356                 |
| 6     | DVB10-DCPD5-BMA35   | 50/50                     | <425                            | -12           | 68            | 80                     | 492                 |
| 7     | DVB5-DCPD10-BMA35   | 50/50                     | <425                            | -8            | 73            | 81                     | 340                 |
| 8     | DVB15-DCPD10-BMA25  | 50/50                     | <425                            | -14           | 74            | 88                     | 686                 |
| 9     | DVB10-DCPD10-BMA30  | 50/50                     | <425                            | -18           | 69            | 87                     | 291                 |
| 10    | DVB15-BMA35         | 60/40                     | <425                            | -32           | 76            | 108                    | 416                 |
| 11    | DVB10-DCPD5-BMA35   | 60/40                     | <425                            | -17           | 75            | 92                     | 318                 |
| 12    | DVB5-DCPD10-BMA35   | 60/40                     | <425                            | -7            | 65            | 72                     | 234                 |
| 13    | DVB15-DCPD10-BMA25  | 60/40                     | <425                            | -13           | 84            | 97                     | 384                 |
| 14    | DVB15-BMA35         | 60/40                     | <177                            | -36           | 74            | 110                    | 456                 |
| 15    | DVB10-DCPD5-BMA35   | 60/40                     | <177                            | -12           | 72            | 84                     | 326                 |
| 16    | DVB5-DCPD10-BMA35   | 60/40                     | <177                            | -13           | 73            | 86                     | 262                 |
| 17    | DVB15-DCPD10-BMA25  | 60/40                     | <177                            | -29           | 79            | 108                    | 411                 |
| 18    | DVB10-DCPD10-BMA30  | 60/40                     | <177                            | -32           | 65            | 97                     | 333                 |

<sup>a</sup>The cure was conducted at 276 psi unless otherwise noted.

<sup>b</sup>DVB15-BMA35 without filler.

associated with  $T_{g2}$  is probably a DVB-rich phase.

The reinforcing effect obtained when soy hulls are added to the resin can be clearly

seen by comparing the values of  $T_g2$  for entry 1 and any other entry in Table I. For all reinforced samples (entries 2-18),  $T_g2$  occurs at a higher temperature than that of the unreinforced resin (entry 1, 57.3 °C). The increase in  $T_g2$  ranges from 5% for entry 2 (60.2 °C) to 46% for entry 13 (83.5 °C). The effect is even more significant for the storage modulus, showing a minimum increase of 1.5 times in  $E'$  for entry 12 (234 MPa compared with 152 MPa for entry 1). The only property that doesn't seem to be significantly affected by the presence of reinforcement is  $T_g1$ . Indeed,  $T_g1$  is more sensitive to variations in the resin composition as will be explained later.

By increasing the pressure applied during cure from 92 psi to 368 psi (Table I, entries 2-5), a trend can be observed for  $E'$ . The storage modulus increases significantly from 298 MPa (entry 2) to 536 MPa (entry 4). When the applied pressure was 368 psi (entry 5), the storage modulus decreased to 356 MPa. The pressure during cure had a definite effect on the observed phase separation of the matrix as evidenced by the values of  $T_g2 - T_g1$  (Table I). As the pressure was increased from 92 psi to 276 psi, the difference in  $T_g$ 's went from 84 °C to 107 °C (entries 2-4, Table I), indicating an increase in the incompatibility of the two phases. Increasing the pressure to 368 psi showed no further effect on phase separation (entries 4 and 5, Table I). The relationship between cure pressure and phase separation is not fully understood at the present time and further tests are necessary to better explain these observations. One could argue that higher pressures force the resin to physically interact with the filler structure during cure (hence the increase in both  $T_g$ 's, entries 2-4, Table I) and that this might favor stabilization of the CSO-rich phase through mixing with residual soybean oil from the soy hulls (see Table IV, entry 1), yielding an even lower polymerization rate for CSO and a greater phase separation. The influence of the residual oil from the filler on the  $T_g$

of the resin has been noted previously, where samples prepared with extracted filler showed higher  $T_g$ 's than samples prepared with fillers containing residual oil.<sup>25</sup> In the current work, the presence of fillers clearly contributes to phase separation of the resin, as noticed from the  $T_{g2} - T_{g1}$  values for entries 1, 4, 10, and 14 in Table I (88 °C, 107 °C, 108 °C, and 110 °C, respectively).

As seen from a comparison of entries 4, 6-8 and 10-13 in Table I,  $E'$  decreases considerably (at least 31% from entry 7 to entry 12) when a higher load of filler is used. Indeed, the higher filler content affects the dispersion and polymerization of the resin, yielding materials with increased flaws and/or weak points. The effect of filler/resin ratio on the  $T_g$ 's isn't clear, as most of the variations are negligible, except for the  $T_{g2}$  of entries 8 and 13 where there is a variation of 10 °C.

The particle size of soy hulls has less of an effect in  $E'$  than the filler/resin ratio, with a maximum improvement of approximately 10% when smaller particles are used (compare entries 10 and 14 in Table I). Comparison of entries 10-13 and 14-17 in Table I reveals an overall improvement in storage modulus whenever smaller particles are used as the filler. At the same wt %, soy hulls having a smaller particle size present a higher density, accounting for a lower volume of material and a higher surface area when compared to larger particle sizes. The smaller particles allow better dispersion of the filler in the resin, enhancing the filler-resin interaction and consequently improving the composites' mechanical properties. Although some variations in  $T_g$ 's can be observed when comparing entries 10-13 and 14-17 in Table I, they don't follow any particular trend that can be related to the properties of the final composites.

As expected from its structure and reactivity, DVB is the major structural comonomer in the resin; so  $E'$  is expected to drop whenever DVB is substituted by DCPD. As a matter of fact, this can be observed throughout Table I, and the most evident change is seen when comparing entries 14 and 16, where substitution of 10 wt % DVB by 10 wt % DCPD represents a loss of nearly 43% in  $E'$ . As far as the  $T_g$ 's are concerned, a net increase in  $T_{g1}$  is observed when larger amounts of DCPD are present in the resin, whereas  $T_{g2}$  isn't affected by the resin composition to the same extent (entries 10-12, for example). This suggests that DCPD is incorporated preferentially into the CSO-rich phase, increasing its crosslink density and augmenting  $T_{g1}$ . Another overall trend can be observed when comparing the values of  $T_{g2} - T_{g1}$  for various resin compositions. As DVB is replaced by DCPD, a significantly lower difference in the two  $T_g$ 's is obtained.

**Tensile Tests.** The tensile test results for all composites prepared in this work are shown in Table II. From the results obtained, it can be seen that the tensile strength of the composites is lower for higher filler/resin ratios (Table II; entries 3, 5-7 and 9-12). A similar trend is observed for the Young's modulus, when these first two sets of results are compared, with the exception of entry 5. Although the variations in Young's modulus are proportionally less significant than those for the tensile strength, it's expected that high loads of filler affect the dispersion and polymerization of the resin, as mentioned earlier during the discussion of the DMA results. These observations are in agreement with previously published data.<sup>25</sup>

The effect of particle size was assessed by comparing the results summarized in entries 9-12 and 13-16 in Table II (samples having soy hull diameters  $<425 \mu\text{m}$  and  $<177 \mu\text{m}$ , respectively). The results show an improvement in tensile strength whenever smaller particles are used as the filler, except for the results reported in entry 16 of Table II. The

**Table II.** Young's modulus and tensile strength of the composites prepared.

| Entry | Sample <sup>a</sup> | Filler/Resin Ratio (wt %) | Particle Size ( $\mu\text{m}$ ) | Young's Modulus (MPa) | Tensile Strength (MPa) |
|-------|---------------------|---------------------------|---------------------------------|-----------------------|------------------------|
| 1     | 92 psi              | 50/50                     | <425                            | 542 $\pm$ 27          | 2.4 $\pm$ 0.1          |
| 2     | 184 psi             | 50/50                     | <425                            | 414 $\pm$ 18          | 1.4 $\pm$ 0.3          |
| 3     | DVB15-BMA35         | 50/50                     | <425                            | 672 $\pm$ 31          | 2.6 $\pm$ 0.2          |
| 4     | 368 psi             | 50/50                     | <425                            | 551 $\pm$ 60          | 2.4 $\pm$ 0.1          |
| 5     | DVB10-DCPD5-BMA35   | 50/50                     | <425                            | 480 $\pm$ 58          | 1.8 $\pm$ 0.1          |
| 6     | DVB5-DCPD10-BMA35   | 50/50                     | <425                            | 473 $\pm$ 62          | 1.5 $\pm$ 0.2          |
| 7     | DVB15-DCPD10-BMA25  | 50/50                     | <425                            | 645 $\pm$ 74          | 2.3 $\pm$ 0.2          |
| 8     | DVB10-DCPD10-BMA30  | 50/50                     | <425                            | 441 $\pm$ 51          | 1.4 $\pm$ 0.2          |
| 9     | DVB15-BMA35         | 60/40                     | <425                            | 663 $\pm$ 59          | 2.0 $\pm$ 0.3          |
| 10    | DVB10-DCPD5-BMA35   | 60/40                     | <425                            | 636 $\pm$ 73          | 1.5 $\pm$ 0.2          |
| 11    | DVB5-DCPD10-BMA35   | 60/40                     | <425                            | 406 $\pm$ 46          | 0.7 $\pm$ 0.1          |
| 12    | DVB15-DCPD10-BMA25  | 60/40                     | <425                            | 569 $\pm$ 81          | 2.2 $\pm$ 0.1          |
| 13    | DVB15-BMA35         | 60/40                     | <177                            | 804 $\pm$ 63          | 2.5 $\pm$ 0.2          |
| 14    | DVB10-DCPD5-BMA35   | 60/40                     | <177                            | 468 $\pm$ 47          | 1.7 $\pm$ 0.3          |
| 15    | DVB5-DCPD10-BMA35   | 60/40                     | <177                            | 351 $\pm$ 50          | 0.9 $\pm$ 0.2          |
| 16    | DVB15-DCPD10-BMA25  | 60/40                     | <177                            | 641 $\pm$ 18          | 1.8 $\pm$ 0.3          |
| 17    | DVB10-DCPD10-BMA30  | 60/40                     | <177                            | 490 $\pm$ 79          | 1.3 $\pm$ 0.3          |

<sup>a</sup>The cure was conducted at 276 psi unless otherwise noted.

overall trend observed here is in agreement with the observations made when discussing the DMA results. Similar effects were observed with spent germ biocomposites prepared from a tung oil resin.<sup>25</sup> For the Young's modulus, no regular trend was observed when comparing



samples with different filler particle sizes.

Variations in the resin composition can affect significantly both the Young's modulus and the tensile strength of the composites, as can be seen when comparing entries 13 and 15 in Table II. For example, a difference of more than 50% in both properties is observed when 10 wt % DVB in the resin is substituted by 10 wt % DCPD. Indeed, due to differences in reactivity and stability of the monomers, gradual substitution of 5 wt % of DVB by 5 wt % DCPD yields materials with lower tensile strength and Young's modulus (compare entries 3, 5, 6, 9-11 and 13-15 in Table II).

Substitution of BMA by DCPD has a lesser effect on the composites' properties than replacement of DVB by DCPD, as shown above. When 10 wt % of the comonomer BMA was replaced by 10 wt % DCPD (Table II, entries 7, 12, and 16 compared to entries 3, 9 and 13), a drop in both the Young's modulus and the tensile strength was observed. The change is within the experimental error for the tensile strengths observed in entries 9 and 12 (2.0 MPa and 2.2 MPa, respectively), but represents a decrease of up to 28% between entries 13 and 16 (2.5 MPa and 1.8 MPa, respectively). The decrease in Young's modulus follows the same trend with up to a 20% decrease seen when comparing entries 13 and 16 (804 MPa and 642 MPa, respectively). Those results are closely related to the structure and reactivity of DCPD. The presence of two double bonds in this latter compound accounts for its role as a crosslinker in the same manner as DVB. For that reason, samples containing 25 wt % of DVB + DCPD show a high crosslink density that compensates for the low reactivity of DCPD towards free radical processes. When the amount of crosslinkers drops to 20 wt % by substituting 5 wt % of DVB by 5 wt % of BMA (entries 8 and 17 in Table II), a significant

loss in tensile properties is observed. The Young's modulus decreases to 441 MPa (entry 8) and 490 MPa (entry 17) while the tensile strength drops to 1.4 and 1.3 respectively (entries 8 and 17) because of a lower crosslink density. Therefore, it can be concluded that DVB is the component that is primarily responsible for the tensile properties in the composites we have prepared.

Further investigation of the influence of the processing pressure on the final composites' properties is needed in order to explain the results observed. So far, no regular trend is evident for either the Young's modulus or the tensile strength when the pressure is increased from 92 psi to 368 psi (entries 1-4, Table II). The best results were obtained for the sample cured at 276 psi. The Young's modulus for that sample is 672 MPa and the tensile strength is 2.6 MPa (Table II, entry 3).

**Thermogravimetric Analysis (TGA).** The thermal stability of the composites has been studied by TGA and the results obtained are presented in Table III. From the thermal degradation pattern of the composites, 3 temperatures are of particular interest: (1) the temperature at which 10 wt % of the sample has degraded ( $T_{10}$ ), (2) the temperature at which 50 wt % of the sample has degraded ( $T_{50}$ ), and (3) the temperature at which 95 wt % of the sample has degraded ( $T_{95}$ ).

From entry 1 of Table III, it can be seen that initial degradation of the soy hulls starts near 200 °C ( $T_{10} = 204$  °C) and the fibers are 95% degraded at 545 °C ( $T_{95} = 545$  °C). For the unreinforced resin (Table III, entry 2), degradation starts near 344 °C ( $T_{10} = 344$  °C) and is mostly finished at 586 °C ( $T_{95} = 586$  °C). By reinforcing the resin with soy hulls, the thermal stability of the filler is significantly increased as the  $T_{10}$  values for all samples (entries 2-19)

**Table III.** Degradation temperatures for the composites.

| Entry | Sample <sup>a</sup> | Filler/Resin Ratio (wt %) | Particle Size (μm) | T <sub>10</sub> (°C) | T <sub>50</sub> (°C) | T <sub>95</sub> (°C) |
|-------|---------------------|---------------------------|--------------------|----------------------|----------------------|----------------------|
| 1     | Soy Hulls           | -                         | <425               | 204                  | 325                  | 545                  |
| 2     | Resin <sup>b</sup>  | -                         | -                  | 344                  | 436                  | 585                  |
| 3     | 92 psi              | 50/50                     | <425               | 278                  | 384                  | 624                  |
| 4     | 184 psi             | 50/50                     | <425               | 274                  | 375                  | 594                  |
| 5     | DVB15-BMA35         | 50/50                     | <425               | 275                  | 383                  | 610                  |
| 6     | 368 psi             | 50/50                     | <425               | 279                  | 384                  | 572                  |
| 7     | DVB10-DCPD5-BMA35   | 50/50                     | <425               | 265                  | 357                  | 624                  |
| 8     | DVB5-DCPD10-BMA35   | 50/50                     | <425               | 264                  | 352                  | 535                  |
| 9     | DVB15-DCPD10-BMA25  | 50/50                     | <425               | 271                  | 383                  | 642                  |
| 10    | DVB10-DCPD10-BMA30  | 50/50                     | <425               | 266                  | 367                  | 578                  |
| 11    | DVB15-BMA35         | 60/40                     | <425               | 276                  | 381                  | 567                  |
| 12    | DVB10-DCPD5-BMA35   | 60/40                     | <425               | 267                  | 360                  | 609                  |
| 13    | DVB5-DCPD10-BMA35   | 60/40                     | <425               | 269                  | 365                  | 623                  |
| 14    | DVB15-DCPD10-BMA25  | 60/40                     | <425               | 268                  | 364                  | 609                  |
| 15    | DVB15-BMA35         | 60/40                     | <177               | 266                  | 378                  | 551                  |
| 16    | DVB10-DCPD5-BMA35   | 60/40                     | <177               | 267                  | 373                  | 540                  |
| 17    | DVB5-DCPD10-BMA35   | 60/40                     | <177               | 255                  | 355                  | 588                  |
| 18    | DVB15-DCPD10-BMA25  | 60/40                     | <177               | 261                  | 366                  | 601                  |
| 19    | DVB10-DCPD10-BMA30  | 60/40                     | <177               | 266                  | 379                  | 590                  |

<sup>a</sup>The cure was conducted at 276 psi unless otherwise noted.

<sup>b</sup>DVB15-BMA35 without filler.

are higher than 255 °C, representing an increase of at least 25%. This can be confirmed by analysis of the DTA curves of the soy hulls (Figure 2) and the DVB15-BMA35 composite

(Figure 3). As seen in Figure 2, after the initial loss of water, the soy hulls start to degrade above 190 °C, whereas the composite degradation only starts above 260 °C.  $T_{50}$  is also improved in the presence of the resin, although a maximum increase of only 18% is seen (entries 5, 6 and 9).  $T_{95}$  seems to be affected in an irregular manner by the resin, so no conclusions can be drawn here.

Other parameters, such as pressure during cure, filler/resin ratio, particle size and resin composition, seem to have no clear cut effect on the  $T_{10}$ ,  $T_{50}$  and  $T_{95}$  values. Indeed,  $T_{10}$  varies from 256 °C (entry 17) to 279 °C (entry 6), while  $T_{50}$  ranges from 352 °C (entry 8) to 384 °C (entry 3), and  $T_{95}$  goes from 535 °C (entry 8) to 642 °C (entry 9) without any regular pattern being evident.

**Soxhlet Extraction.** The Soxhlet extraction results are presented in Table IV. Figure 4 shows the  $^1\text{H}$  NMR spectra of soybean oil (SOY), conjugated soybean oil (CSO) and the extracts of soy hulls (SH), the pure resin and one of the composites prepared (DVB15-BMA35).

From the results in Table IV, it can be observed that the majority of the starting materials (82-92 wt %) get incorporated into the final composites, forming a material that is relatively insoluble in  $\text{CH}_2\text{Cl}_2$ . Soy hulls alone (Table IV, entry 1) yield 10 wt % of soluble materials, identified as being mainly soybean oil by  $^1\text{H}$  NMR spectroscopic analysis (Figure 4C). The unreinforced resin (entry 2) shows a total of 13 wt % of soluble materials after Soxhlet extraction. Characterization of the extract by  $^1\text{H}$  NMR spectroscopic analysis indicates CSO to be the major component and traces of BMA can be detected (peak at 4.05 ppm) (Figure 4D).

The difference in pressure during the cure seems to have no effect on the % soluble

**Table IV.** Extraction results.

| Entry | Sample <sup>a</sup>    | Filler/Resin<br>Ratio (wt<br>%) | Particle Size<br>( $\mu\text{m}$ ) | % Soluble | %<br>Insoluble |
|-------|------------------------|---------------------------------|------------------------------------|-----------|----------------|
| 1     | Soy Hulls              | -                               | <425                               | 10        | 90             |
| 2     | Resin <sup>b</sup>     | -                               | -                                  | 13        | 87             |
| 3     | 92 psi                 | 50/50                           | <425                               | 14        | 86             |
| 4     | 184 psi                | 50/50                           | <425                               | 14        | 86             |
| 5     | DVB15-BMA35            | 50/50                           | <425                               | 14        | 86             |
| 6     | 368 psi                | 50/50                           | <425                               | 12        | 88             |
| 7     | DVB10-DCPD5-<br>BMA35  | 50/50                           | <425                               | 8         | 92             |
| 8     | DVB5-DCPD10-<br>BMA35  | 50/50                           | <425                               | 10        | 90             |
| 9     | DVB15-DCPD10-<br>BMA25 | 50/50                           | <425                               | 9         | 91             |
| 10    | DVB10-DCPD10-<br>BMA30 | 50/50                           | <425                               | 11        | 89             |
| 11    | DVB15-BMA35            | 60/40                           | <425                               | 12        | 88             |
| 12    | DVB10-DCPD5-<br>BMA35  | 60/40                           | <425                               | 9         | 91             |
| 13    | DVB5-DCPD10-<br>BMA35  | 60/40                           | <425                               | 14        | 86             |
| 14    | DVB15-DCPD10-<br>BMA25 | 60/40                           | <425                               | 9         | 91             |
| 15    | DVB15-BMA35            | 60/40                           | <177                               | 14        | 86             |
| 16    | DVB10-DCPD5-<br>BMA35  | 60/40                           | <177                               | 15        | 85             |
| 17    | DVB5-DCPD10-<br>BMA35  | 60/40                           | <177                               | 18        | 82             |
| 18    | DVB15-DCPD10-<br>BMA25 | 60/40                           | <177                               | 15        | 85             |
| 19    | DVB10-DCPD10-<br>BMA30 | 60/40                           | <177                               | 16        | 84             |

<sup>a</sup>The cure was conducted at 276 psi unless otherwise noted.

<sup>b</sup>DVB15-BMA35 without filler.

materials obtained from the composites (Table IV, entries 3-6). In fact, the 2 wt % difference observed between entries 6 and 3-5 is negligible. Also, the filler/resin ratio shows no

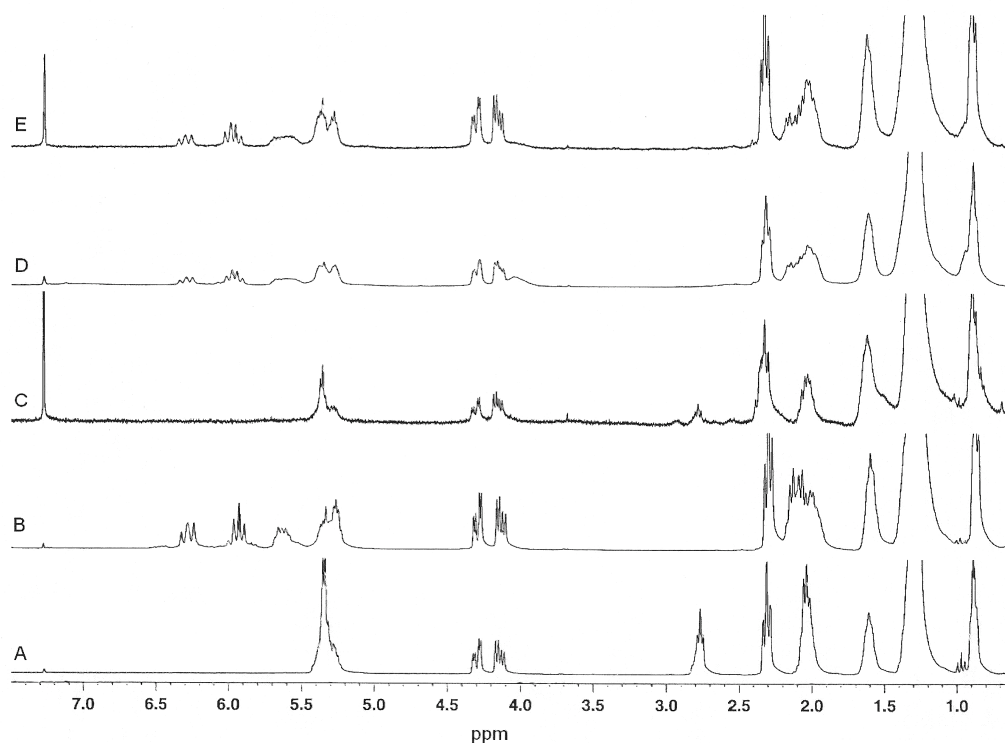


**Figure 4.**  $^1\text{H}$  NMR spectra of (A) soybean oil, (B) CSO, (C) soy hulls' extract, (D) unreinforced resin extract (composition: 50 wt % CSO, 35 wt % BMA and 15 wt % DVB), and (E) composite extract (composition: resin = DVB15-BMA35, filler/resin ratio = 50/50 and particle size  $<425\ \mu\text{m}$ ). Spectrum E is representative of extracts from all composites.

significant effect on the % soluble materials from the composites. Considering that the resin and the soy hulls are each responsible for 10-13 wt % of soluble materials, a higher filler/resin ratio wasn't expected to change the final amount of soluble materials in the composites. Indeed, a comparison of the % soluble materials for similar resins with different filler/resin ratios (Table IV; entries 5, 7-9 and 11-14) shows a maximum difference of 4 wt % between entries 8 and 13 in Table IV.

Unlike the filler/resin ratio, the particle size does seem to affect the % of soluble

materials in the final composites. A comparison of entries 11-14 and 15-18 in Table IV shows an average increase of 5 wt % in the amount of soluble materials when particles smaller than 177  $\mu\text{m}$  diameter are used, instead of particles smaller than 425  $\mu\text{m}$  diameter. With a higher surface area, smaller particles are expected to have a greater interaction with the resin. As proposed earlier when discussing the DMA results, the greater interaction between filler and resin may lead to mixture of the unreactive residual oil from the soy hulls with the CSO-based resin, which would decrease the overall reactivity of the matrix, yielding more soluble content. The reasons behind this observations aren't fully clear at this time and further studies are necessary in order to determine the origin of the observed behavior.

Finally, no particular pattern has been observed for the effect of resin composition on the amount of soluble material in the composites. It is assumed that all components are similarly incorporated into the matrix, with the exception of CSO. From a comparison of the  $^1\text{H}$  NMR spectra (Figures 4B and 4E), the extract of the composites is believed to be primarily conjugated soybean oil (CSO), confirming our prediction that CSO is not likely to be fully incorporated due to its lower reactivity.

**Scanning Electron Microscopy (SEM).** Figure 5 shows the SEM images of cryo-fractured (A-D) and cut (E-H) surfaces of composite samples. Taking as the reference the sample shown in Figures 5A and 5E, the images illustrate the effect of having the same resin composition and different cure pressures (Figures 5B and 5F), filler/resin ratios (Figures 5C and 5G), and filler particle sizes (Figures 5D and 5H). By analyzing the images, it is possible to better understand how some parameters change the filler-resin interaction and to correlate these effects with some of the properties obtained for the composites.

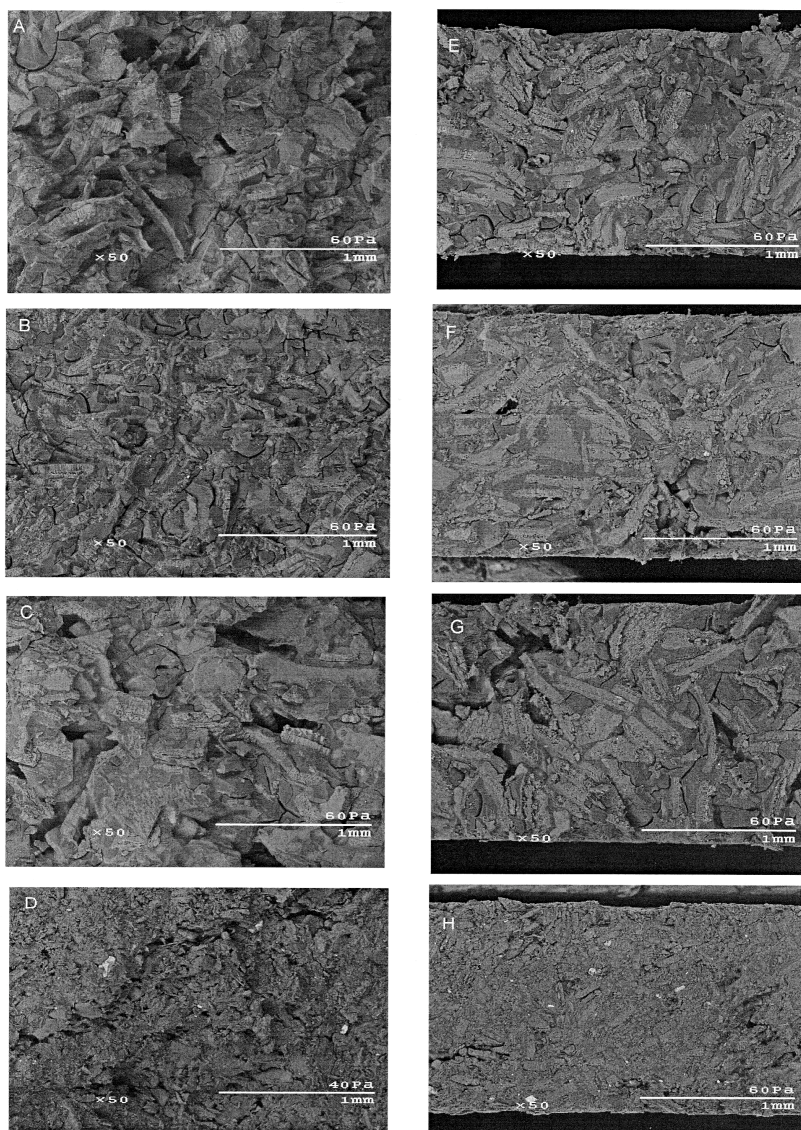


**Figure 5.** SEM images of (A) cryo-fractured DVB15-BMA35, 50:50 filler/resin ratio, particle size  $<425\ \mu\text{m}$ , cured under 92 psi; (B) cryo-fractured DVB15-BMA35, 50:50 filler/resin ratio, particle size  $<425\ \mu\text{m}$ , cured under 276 psi; (C) cryo-fractured DVB15-BMA35, 60:40 filler/resin ratio, particle size  $<425\ \mu\text{m}$ , cured under 276 psi; (D) cryo-fractured DVB15-BMA35, 60:40 filler/resin ratio, particle size  $<177\ \mu\text{m}$ , cured under 276 psi; (E) cut DVB15-BMA35, 50:50 filler/resin ratio, particle size  $<425\ \mu\text{m}$ , cured under 92 psi; (F) cut DVB15-BMA35, 50:50 filler/resin ratio, particle size  $<425\ \mu\text{m}$ , cured under 276 psi; (G) cut DVB15-BMA35, 60:40 filler/resin ratio, particle size  $<425\ \mu\text{m}$ , cured under 276 psi; and (H) cut DVB15-BMA35, 60:40 filler/resin ratio, particle size  $<177\ \mu\text{m}$ , cured under 276 psi.

The cryo-fractured images (Figures 5A-D) provide important information about the filler-resin interaction. From the absence of holes caused by fiber pull-out or other similar



events during fracture, it appears that there is a good interaction between the soy hulls and the matrix. The voids observed in the images are mainly the result of shrinkage during cure (Figure 5A-C). In Figure 5D, the smaller soy hulls and their relatively good dispersion throughout the matrix make it difficult to distinguish between shrinkage cracks and structural voids in the sample.

In an attempt to evaluate the filler dispersion in the matrix, the composites were cut and the cross sections observed by SEM (Figures 5E-H). The effect of pressure during cure can be assessed by the comparison of Figures 5E and 5F. It can be seen that considerably fewer shrinkage cracks appear in the sample cured at 276 psi (Figure 5F) than in the sample cured at 92 psi (Figure 5E), yielding a more compact structure with less voids and more particles completely surrounded by the polymer matrix. This could explain the improvement in dynamic flexural properties for the sample cured at a higher pressure (Table I, entries 2 and 4). Improvements in tensile properties were also observed for these samples (Table II, entries 1 and 3), although a consistent explanation fails for the samples cured at 184 psi and 368 psi (Table I, entry 5, and Table II, entries 2 and 4).

A comparison of Figures 5F and 5G gives information about filler/resin ratio effects on the structure of the composites. The sample having a higher filler/resin ratio (Figure 5G) exhibits considerably bigger flaws and voids than the sample with a 50:50 filler/resin ratio (Figure 5F). This is presumably caused by an absence of resin between the filler particles in some regions of the composite. This can explain the drop in storage modulus observed in Table I, entries 4, 6-8, and 10-13. For the tensile test, an overall decrease in  $E$  and in the tensile strength was observed (Table II, entries 3, 5-7, and 9-12), but again a consistent

explanation fails when comparing the Young's modulus of entries 5 and 10 in Table II.

The most significant differences are observed when comparing particle size effects in the structure of the composites (Figures 5G and 5H). From the SEM images, it is clear that composites prepared with smaller particle sizes exhibit better dispersion of the soy hulls in the matrix. It is easily seen that the voids present in Figure 5H are much smaller than those in Figure 5G, which may explain the better properties obtained for the former composite (Table I, entries 10 and 14, and Table II, entries 9 and 13). The higher contact surface between the soy hulls and the resin may account for the earlier mentioned effect on the percent soluble materials (Table IV, entries 11 and 15).

### Conclusions

In this work, biocomposites have been prepared by the free radical polymerization of a conjugated soybean oil-based resin reinforced with soy hulls. An ideal cure sequence of 5 hours at 130 °C, followed by a postcure at 150 °C for 2 hours, has been established by a DSC study of the cure process. The effects of filler/resin ratio, particle size and pressure during cure have been evaluated. It has been observed that the properties of the composites tend to decrease when higher filler/resin ratios or larger particle sizes are used. This behavior is closely related to impregnation of the filler by the resin; whenever good dispersion of the filler in the matrix is compromised, the mechanical properties of the composites are negatively affected. As the pressure applied during cure is increased up to 276 psi, an overall increase in the mechanical properties is detected by tensile test and DMA. The properties decrease when a higher pressure (368 psi) is applied.

The matrix is identified as being phase separated, which is probably related to the

difference in reactivity of CSO and the other monomers employed in the resin. Although good thermal stabilities and promising properties are obtained for the composites presented here, better results might be achieved by using more reactive oils, such as conjugated linseed oil.

In terms of resin composition, a significant dependence of the properties on the DVB content is observed. Replacement of DVB by DCPD affects considerably the properties due to differences in the reactivity of these two compounds. A loss in reactivity of the resin upon substitution of BMA by DCPD is compensated for by a higher crosslink density, but the final properties of the composites are still lower than those of the reference resin (DVB15-BMA35).

### **Acknowledgements**

We gratefully acknowledge the financial support of the Iowa Biotechnology Consortium through the USDA and the Recycling and Reuse Technology Transfer Center of the University of Northern Iowa. We would like to thank West Central Co-op for the soy hulls, and Professor Michael Kessler from the Department of Material Sciences and Engineering and Dr. Richard Hall from the Department of Natural Resource Ecology and Management at Iowa State University for the use of their facilities.

### **References**

1. Ma, F.; Hanna, M.A. *Bioresource Technol* 1999, 70, 1.
2. Wexler, H. *Chem Rev* 1964, 64, 591.
3. Sharma, V.; Kundu, P. P. *Prog Polym Sci* 2006, 31, 983.
4. Jin, F.; Park, S. *Polym Int* 2008, 57, 577.
5. Mosiewicki, M.; Aranguren, M. I.; Borrajo, J. *J Appl Polym Sci* 2005, 97, 825.

6. Miyagawa, H.; Mohanty, A. K.; Burgueno, R.; Drzal, L. T.; Misra, M. *J Polym Sci Part B: Polym Phys* 2007, 45, 698.
7. Li, F.; Larock, R. C. *J Appl Polym Sci* 2001, 80, 658.
8. Li, F.; Hasjim, J.; Larock, R. C. *J Appl Polym Sci* 2003, 90, 1830.
9. Andjelkovic, D. D.; Valverde, S. M.; Henna, P. H.; Li, F.; Larock, R. C. *Polymer* 2005, 46, 9674.
10. Andjelkovic, D. D.; Larock, R. C. *Biomacromolecules* 2006, 7, 927.
11. Li, F.; Larock, R. C. *Biomacromolecules* 2003, 4, 1018.
12. Kundu, P. P.; Larock, R. C. *Biomacromolecules* 2005, 6, 797.
13. Henna, P. H.; Andjelkovic, D. D.; Kundu, P. P.; Larock, R. C. *J Appl Polym Sci* 2007, 104, 979.
14. Valverde, M. S.; Andjelkovic, D. D.; Kundu, P. P.; Larock, R. C. *J Appl Polym Sci* 2008, 107, 423.
15. Lima, D. G.; Soares, V. C. D.; Ribeiro, E. B.; Carvalho, D. A.; Cardoso, E. C. V.; Rassi, F. C.; Mundim, K. C.; Rubim, J. C.; Suarez, P. A. Z. *J Anal Appl Pyrolysis* 2004, 71, 987.
16. Pakdeechanuan, P.; Intarapichet, K.; Fernando, L. N.; Grun, I. U. *J Agric Food Chem* 2005, 53, 923.
17. Mitchell, J. H.; Kraybill, H. R. *J Am Chem Soc* 1942, 64, 988.
18. Jung, M. O.; Yoon, S. H.; Jung, M. Y. *J Agric Food Chem* 2001, 49, 3010.
19. Jung, M. Y.; Ha, Y. L. *J Agric Food Chem* 1999, 47, 704.
20. Larock, R. C.; Dong, X.; Chung, S.; Reddy, C. K.; Ehlers, L. E. *J Am Oil Chem Soc* 2001, 78, 447.
21. Li, F.; Larock, R. C. *J Appl Polym Sci* 2000, 78, 1044.
22. Li, F.; Hanson, M. V.; Larock, R. C. *Polymer* 2001, 42, 1567.
23. Li, F.; Larock, R. C. *J Polym Environ* 2002, 10, 59.
24. Lu, Y.; Larock, R. C. *Biomacromolecules* 2006, 7, 2692.
25. Pfister, D. P.; Baker, J. R.; Henna, P. H.; Lu, Y.; Larock, R. C. *J Appl Polym Sci* 2008, 108, 3618.
26. Laszlo, J. A. *J Agric Food Chem* 1987, 35, 593.
27. Sessa, D. J. *J Sci Food Agric* 2004, 84, 75.
28. Yang, H.; Yan, R.; Chen, H.; Lee, D. H.; Zheng, C. *Fuel* 2007, 86, 1781.

### **CHAPTER 3. RICE HULL BIOCOMPOSITES. PART 1: PREPARATION OF A LINSEED OIL-BASED RESIN REINFORCED WITH RICE HULLS**

A Paper Published in Journal of Applied Polymer Science, 121, 2039-2049.

Copyright © 2011, Wiley-Blackwell

Rafael L. Quirino, Richard C. Larock\*

*Department of Chemistry, Iowa State University, Ames, Iowa 50011*

#### **Abstract**

Biocomposites consisting of a conjugated linseed oil-based thermoset reinforced with rice hulls have been prepared by free radical polymerization initiated by *t*-butyl peroxide. The resin composition was kept constant at 50 wt % conjugated linseed oil, 35 wt % *n*-butyl methacrylate, and 15 wt % divinylbenzene. Tensile tests, DMA, TGA, Soxhlet extraction, and DSC have been employed to establish the ideal cure sequence. The pressure during cure, filler load, and drying and grinding of the filler have been varied and their effect on the final properties of the composites have been assessed. Optimal conditions have been established for the preparation of rice hull biocomposites. SEM showed a weak filler-resin interaction and X-ray mapping suggested the presence of silica in the rice hulls, which may account for the high thermal and mechanical properties obtained for these composites.

#### **Introduction**

The rapid increase in petroleum prices over recent years has encouraged the development of alternative sources of energy and materials. In that context, biorenewable-based products, such as biofuels, bioplastics, and biocoatings are especially appealing, since

they are readily prepared from naturally occurring starting materials that are constantly being generated by nature. Although the complete substitution of petroleum-derived products in our current society is highly unlikely, great progress has been made recently towards the development of products with the potential to compete with petroleum goods in times of high oil prices.

With that in mind, our group has been investigating the synthesis and properties of new biomaterials derived mainly from agricultural oils. Materials, such as soybean oil-based polyurethane coatings,<sup>1, 2</sup> soybean,<sup>3, 4</sup> and linseed oil-based bio-rubbers,<sup>5</sup> and various bioplastics containing at least 40 wt % of vegetable or modified vegetable oils, such as soybean,<sup>6</sup> corn,<sup>7</sup> tung,<sup>8</sup> and linseed oils,<sup>9</sup> have been prepared and analyzed. These latter materials range from soft rubbers to hard plastics, depending on the resin composition and the co-monomers added to the matrix.<sup>10</sup>

The use of natural fibers to reinforce polymeric materials has been explored by several groups in the last decade. There are reports of the reinforcement of polypropylene (PP) with sisal fiber,<sup>11</sup> rice hulls and kenaf fiber,<sup>12</sup> palm and coir fibers,<sup>13</sup> wheat straw,<sup>14</sup> sunflower hulls,<sup>15</sup> and abaca strands.<sup>16</sup> High density polyethylene (HDPE) has also been reinforced with banana fiber,<sup>17</sup> sugar cane bagasse and wood flour.<sup>18</sup> Polyester and epoxy resins have been reinforced with jute fiber,<sup>19</sup> and there are reports of the use of hemp fiber,<sup>20</sup> and poultry feathers as reinforcements for composites,<sup>21</sup> among several other combinations of resins and natural fibers that are not cited here.

Recently, our group reported the preparation and analysis of a soybean oil-based thermoset resin reinforced with corn stover.<sup>22</sup> The same resin has been previously reinforced

by us with soybean hulls,<sup>23</sup> and a tung oil variation of the resin was reinforced with spent germ.<sup>24, 25</sup> Unlike previous work, where rice hulls were used to reinforce thermoplastics,<sup>12</sup> we report herein the preparation of a linseed oil-based free-radical thermoset resin reinforced with rice hulls. The resin is a copolymer of conjugated linseed oil (CLO), divinylbenzene (DVB) and *n*-butyl methacrylate (BMA). The composites were compression molded and the influence of pressure during cure, cure temperatures, cure time, filler load, filler particle size, and drying of the filler on the final properties of the composites has been assessed and optimum preparation conditions are proposed. The techniques used for the analysis of the biocomposites are tensile tests, dynamic mechanical analysis (DMA), differential scanning calorimetry (DSC), thermogravimetric analysis (TGA), Soxhlet extraction, proton nuclear magnetic resonance spectroscopy (<sup>1</sup>H NMR), scanning electron microscopy (SEM), and X-ray mapping.

## Experimental

**Materials.** BMA was purchased from Alfa Aesar (Ward Hill, MA). DVB and *t*-butyl peroxide (TBPO) were purchased from Sigma-Aldrich (Milwaukee, WI). All were used as received. Superb linseed oil was provided by ADM (Red Wing, MN) and conjugated using a rhodium catalyst, following a method developed and frequently used by our group.<sup>26</sup> The rice hulls were provided by the Missouri Crop Improvement Association (Columbia, MO). They were ground to <1 mm diameter particle size and dried overnight at 70 °C in a vacuum oven before use. Three samples have been made using as-received (non-ground and/or non-dried) rice hulls for comparison of the properties with the composites reinforced with the ground and dried rice hulls.

**General procedure for preparation of the biocomposites.** The crude resin was obtained by mixing 15.0 g (50 wt %) of the conjugated linseed oil (CLO), 10.5 g (35 wt %) of BMA, and 4.5 g (15 wt %) of DVB in a beaker. Then 1.5 g of the free-radical initiator TBPO, corresponding to an extra 5 wt % with respect to the total resin weight, was added to the monomer mixture and stirred. The rice hulls were impregnated with the crude resin and compression molded for 5 hours (unless otherwise specified) at different temperatures (cure sequences I-VII, Table I). The composites were then removed from the mold and post-cured in a convection oven for 2 hours at different temperatures (cure sequences I-V, Table I). As observed with soybean hull biocomposites,<sup>23</sup> the filler content could not be reduced below 50 wt % because, during compression molding, the excess of resin leaks out from the mold when pressure is applied. If the cure is carried out at atmospheric pressure, the filler accumulates in the bottom of the mold and a non-uniform composite is obtained. The cure temperatures, the pressure during the cure, and the filler load have been varied as indicated in the text. Finally, four composites were prepared with fillers under different conditions to evaluate the effect of drying and grinding the rice hulls.

**Characterization of the composites.** Tensile tests were conducted at room temperature according to ASTM D-638 using an Instron universal testing machine (model 5569) equipped with a video extensometer and operating at a crosshead speed of 2.0 mm/min. Dogbone-shaped test specimens were machined from the original samples to give the following gauge dimensions: 57.0 mm x 12.7 mm x 4.5 mm (length x width x thickness, respectively). For each composite, seven dog-bones were cut and tested. The results presented in the text are the average of these measurements along with the calculated



standard deviation. A Student's t-test was used to confirm that each pair of results is statistically different.

DMA experiments were conducted on a Q800 DMA (TA Instruments, New Castle, DE) using a three point bending mode with a 15.0 mm clamp. Rectangular specimens of 22.0 mm x 8.5 mm x 1.5 mm (length x width x thickness, respectively) were cut from the original samples. Each specimen was cooled to -60 °C and then heated at 3 °C/min to 250 °C at a frequency of 1 Hz and an amplitude of 14 μm under air. Two runs for each sample were carried out and the results presented in the text reflect the average of the two measurements.

A Q50 TGA instrument (TA Instruments, New Castle, DE) was used to measure the weight loss of the samples under an air atmosphere. The samples (~10 mg) were heated from room temperature to 650 °C at a rate of 20 °C/min.

Soxhlet extraction was conducted to determine the amount of soluble materials in the composites. A 2.0 g sample of each composite was extracted for 24 h using refluxing dichloromethane (CH<sub>2</sub>Cl<sub>2</sub>). After extraction, the solubles were recovered by evaporating the CH<sub>2</sub>Cl<sub>2</sub> under vacuum. Both soluble and insoluble materials were dried overnight at 70 °C. The dried soluble fraction was then dissolved in deuterated chloroform (CDCl<sub>3</sub>) and the <sup>1</sup>H NMR spectrum was obtained using a Varian Unity spectrometer (Varian Associates, Palo Alto, CA) operating at 300 MHz. The <sup>1</sup>H NMR spectra helped determine the identity of the solubles in each sample.

DSC experiments were performed on a Q20 DSC (TA Instruments, New Castle, DE) under a N<sub>2</sub> atmosphere over a temperature range of -20 °C to 400 °C, while heating at a rate of 20 °C/min. The samples weighed ~10 mg.

For the SEM analysis, each sample was frozen with liquid nitrogen prior to fracture (cryofracture). A second section of the sample was mechanically cut and shaved with a razor blade to provide a smooth cross section. Both cryofractured and cut samples were examined using an Hitachi S-2460N variable-pressure SEM. The microscope was operated at 20 kV accelerating voltage, with 60 Pa of helium atmosphere, and a 25 mm working distance. Backscattered electron images were collected using a Tetra BSE detector (Oxford Instruments) at 35x and 100x magnifications. An Oxford ISIS X-ray analyzer with a light-element detector was used to collect an X-ray map of a section of the cut surface at 200x magnification.

## Results and Discussion

**Cure sequence study.** In order to determine the optimum cure sequence, seven samples bearing the same resin composition and filler load (70 wt %) were exposed to different temperatures, as shown in Table I. The cured composites were then analyzed by a tensile test, DMA, TGA, and Soxhlet extraction. The results are presented in Table II.

For an assessment of the reproducibility of the composites' properties, cure sequence I was applied to composites from different batches, under otherwise identical conditions (cure sequence I<sup>a</sup>, Table II). The results show an overall agreement between the properties measured for the two samples, especially when the differences between the properties obtained for cure sequences I and I<sup>a</sup> are compared to the variations observed for the other cure sequences employed (cure sequences II-VII, Table I).

**Table I.** Cure temperatures used in preparation of the biocomposites.

| Cure Sequence <sup>a</sup> | Cure Temperature (°C) | Post-cure Temperature (°C) |
|----------------------------|-----------------------|----------------------------|
| I                          | 130                   | 150                        |
| II                         | 140                   | 160                        |
| III                        | 155                   | 175                        |
| IV                         | 180                   | 200                        |
| V                          | 230                   | 250                        |
| VI                         | 180                   | -                          |
| VII                        | 180 <sup>b</sup>      | -                          |

<sup>a</sup> The composites were cured under 400 psi.

<sup>b</sup> The sample was cured for 7 hours.

**Table II.** Tensile test, DMA, TGA and Soxhlet extraction results for composites cured under 400 psi, and different temperatures and times.

| Cure sequence  | $E$ (GPa) | Tensile strength (MPa) | $T_g$ (°C)          | $E'$ at 130°C (MPa) | $T_{10}$ (°C) | Residue (wt %) | Soluble fraction (wt %) <sup>d</sup> |
|----------------|-----------|------------------------|---------------------|---------------------|---------------|----------------|--------------------------------------|
| I              | 0.8 ± 0.1 | 2.4 ± 0.4              | 26                  | 102                 | 289           | 15             | 6                                    |
| I <sup>a</sup> | 0.7 ± 0.1 | 3.2 ± 0.3              | 25                  | 98                  | 290           | 15             | 6                                    |
| II             | 1.2 ± 0.1 | 3.7 ± 0.3              | 30, 73 <sup>b</sup> | 137                 | 294           | 14             | 6                                    |
| III            | 1.4 ± 0.4 | 5.4 ± 0.8              | 43                  | 209                 | 291           | 14             | 6                                    |
| IV             | 1.8 ± 0.1 | 6.7 ± 0.7              | 68                  | 336                 | 304           | 14             | 5                                    |
| V              | 1.7 ± 0.1 | 5.8 ± 2.7              | 66                  | 149                 | 352           | 21             | 4                                    |
| VI             | 1.0 ± 0.5 | 0.7 ± 0.5              | 59                  | 45                  | 297           | 14             | 14                                   |
| VII            | 1.1 ± 0.4 | 0.8 ± 0.3              | - <sup>c</sup>      | - <sup>c</sup>      | 298           | 14             | 13                                   |

<sup>a</sup> Composite made under the same conditions, but from a different batch.

<sup>b</sup> Two distinct  $T_g$ 's were observed (30 °C and 73 °C).

<sup>c</sup> The sample submitted to cure sequence VII tended to crumble very easily when handled; therefore, DMA specimens could not be machined for determination of the  $T_g$  and storage modulus at 130 °C.

<sup>d</sup> Determined by Soxhlet extraction.

From the tensile test results, there is an overall increase in both the Young's modulus and the tensile strength when the cure temperature increases from 130 °C to 180 °C (cure sequences I-IV, Table II). A significant drop in the tensile strength is observed when the composite is cured at 230 °C (cure sequence V, Table II). In that case, the exceedingly high cure temperature employed in cure sequence V initiates thermal degradation of the rice hulls, affecting the tensile properties of the final composite. The absence of a post-cure step during cure sequences VI and VII has a dramatic effect on the tensile properties of the composites, independent of the duration of the cure. The Young's modulus decreases to around 1.0 GPa for composites cured at 180 °C for 5 and 7 hours (cure sequences VI and VII, Table II). A more pronounced decrease is observed in the tensile strength of these composites (compare cure sequences VI and VII with cure sequence IV, Table II). This indicates that the post-cure is a key step during the preparation of the biocomposites. It helps to maximize the mechanical properties through an increase in the crosslink density and full incorporation of all of the co-monomers used in the synthesis.

The glass transition temperatures ( $T_g$ ) were determined from the tan delta curves obtained by DMA. Similar to the Young's modulus and the tensile strength, an increase in the  $T_g$  for the composites is seen with increasing cure temperatures. The  $T_g$  increases from 26 °C to 68 °C when the cure temperature is increased from 130 °C to 180 °C (cure sequences I-IV, Table II). This increase in  $T_g$  may indicate a higher degree of cure obtained when higher temperatures are used during processing. At lower temperatures, the polymerization rate is low and the product obtained after the process isn't fully cured. As the cure temperature increases, a higher polymerization rate yields a higher degree of cure, increasing the final  $T_g$  as a consequence. The occurrence of a second  $T_g$  for cure sequence II is not completely

understood. In some of our previous work,<sup>23</sup> the appearance of two  $T_g$ 's was observed when a resin containing co-monomers with distinctly different reactivities (for example, conjugated soybean oil, BMA and DVB) was cured under high pressures and high filler loads, but here these parameters are kept constant. By increasing the cure temperature to 230 °C (cure sequence V, Table II), a slight decrease in the  $T_g$  is observed. The absence of a post-cure step (cure sequence VI, Table II) results in a composite that is only partially cured. The composite cured under cure sequence VII crumbled too easily when handled to be analyzed by DMA.

The storage modulus of the biocomposites was determined at 130 °C, significantly above the  $T_g$ , where a better relationship could be established between the parameters changed and the storage modulus of the composites analyzed. Overall, the results follow the same trend observed for the tensile properties. An increase in storage modulus ( $E'$ ) is seen with an increase in the cure temperature. A significant drop in the storage modulus is observed when comparing cure sequences IV and V in Table II, and a dramatic decrease in  $E'$  is detected when no post-cure is applied (cure sequence VI, Table II). These results suggest that the post-cure is essential to get a fully cured composite and cure sequence IV seems to be optimal for this system.

$T_{10}$  represents the temperature at 10 wt % degradation of the composites, as determined by TGA. This temperature occurs between 289 °C and 352 °C for all composites included in Table II. There is an overall increase in this value with an increase in the cure temperature (cure sequences I-V, Table II). However, the small differences observed between cure sequences I, II, and III are insignificant considering the overall trend and may be attributed to experimental variation. As mentioned before, with higher cure temperatures,

partial degradation of the less stable filler components (such as hemicellulose) increases during the cure. Indeed, reports indicate that hemicellulose starts to degrade at temperatures as low as 175 °C.<sup>27</sup> When performing the TGA of those partially degraded materials (cure sequences IV-VII), a higher temperature is required to attain  $T_{10}$ , since the composite has a higher content of more stable components. The  $T_{10}$  values of samples that were not post-cured (cure sequences VI and VII, Table II) are slightly lower than the  $T_{10}$  of the composite cured under cure sequence IV (Table II). This indicates that the two hour post-cure at 200 °C (cure sequence IV, Table I) is probably responsible for partial degradation of the filler. Furthermore, the rice hulls alone exhibit a  $T_{10}$  of 286 °C (result not shown in Table II), which implies that temperatures lower than  $T_{10}$  for the composites may already start degrading the filler.

With the exception of three entries in Table II, the residue left after 650 °C during the TGA corresponds to 14 wt %. For the reasons expressed earlier, the composite cured under cure sequence V had a higher residue content. Presumably, the higher temperature employed during the cure degraded the less stable filler components to a greater extent, leaving a higher concentration of minerals and more stable structures in the composite. The slightly higher residue content found for the sample cured using cure sequence I may be attributed to experimental variables when weighing the filler and resin for preparation of the composite. The residue is rich in silica, as confirmed later during X-ray map analysis and as reported in the literature for rice straw.<sup>28</sup>

Finally, most of the composites afforded 4-6 wt % of soluble materials after cure (cure sequences I-V, Table II). This indicates that the majority of the resin components were

incorporated into the resin during the cure and that a high crosslink density has been attained. In the two cure sequences where a post-cure step has not been employed (cure sequences VI and VII, Table II), a much larger soluble content has been found. From the  $^1\text{H}$  NMR spectra of the extracts, it can be clearly seen that the soluble content recovered from the composites (Figures 1A and 1B) resembles the unreacted CLO (Figure 1D). The intensity of the peaks in Figure 1A is much lower than that of Figures 1B and 1D due to the low amount of soluble materials recovered, but the presence of the methylene hydrogen peaks between 4.0 ppm and 4.5 ppm confirms the presence of a triglyceride unit in the extract. Also worth mentioning is the fact that the rice hulls alone exhibited a soluble content of 10 wt % (result not shown in Table II), consisting of an oily material rich in hydrocarbon residues as can be seen from the peaks between 0.5 ppm and 2.5 ppm in the  $^1\text{H}$  NMR spectrum (Figure 1C), which correspond to hydrogens attached to  $\text{sp}^3$  hybridized carbons.

A comparison of the DSC curves of rice hulls and composites cured under different cure sequences is provided in Figure 2. The most distinctive feature of these curves is the endothermic peak that occurs at 194 °C for the rice hulls (Figure 2C). This peak is attributed to volatilization of compounds formed during degradation of the hemicellulose,<sup>29</sup> and matches the beginning of the second weight loss step observed in the TGA curve (figure not shown). The rice hulls also exhibit a change in the baseline at 152 °C that is not presently understood. In the composite undergoing cure sequence VII (Figure 2A), the endothermic peak is less intense and shifts to a lower temperature (190 °C). This phenomenon can be related to partial degradation of the hemicellulose during the cure process. Indeed, during thermal degradation, the hemicellulose chain is broken down to smaller structures that

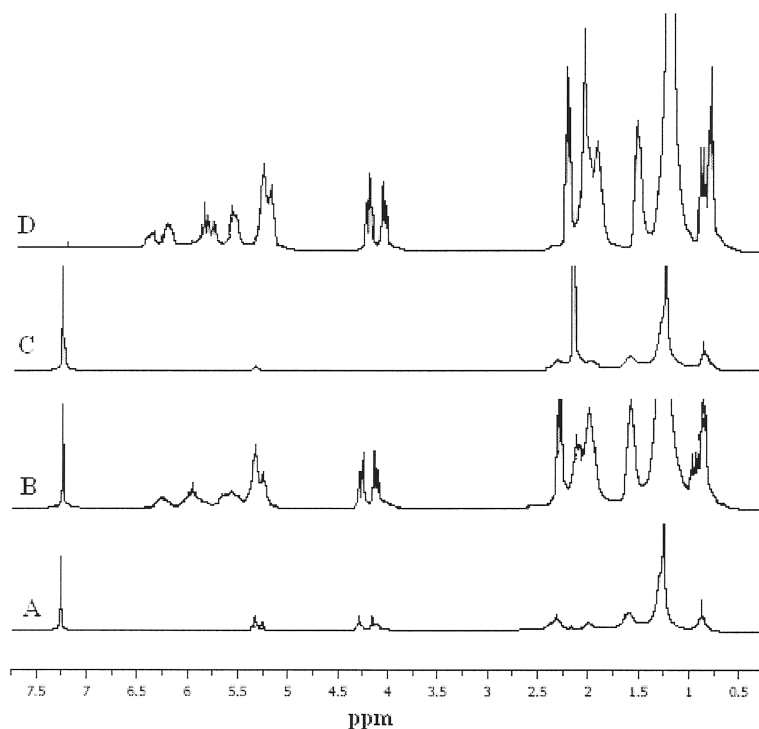


**Figure 1.**  $^1\text{H}$  NMR spectra of: (A) extract of a composite cured under cure sequence IV, (B) extract of a composite cured under cure sequence VII, (C) extract of rice hulls, (D) conjugated linseed oil.

require lower temperatures to volatilize. Also, since some components had already volatilized during cure, the intensity of the peak is noticeably lower. For the composite cured under cure sequence IV (Figure 2B), the endothermic peak has completely disappeared and no transitions are observed between 0 °C and 250 °C, indicating that the resin is fully cured and the composite is completely stable in that temperature range. The transitions occurring after 250 °C can be attributed to thermal degradation of the samples and won't be individually analyzed here.



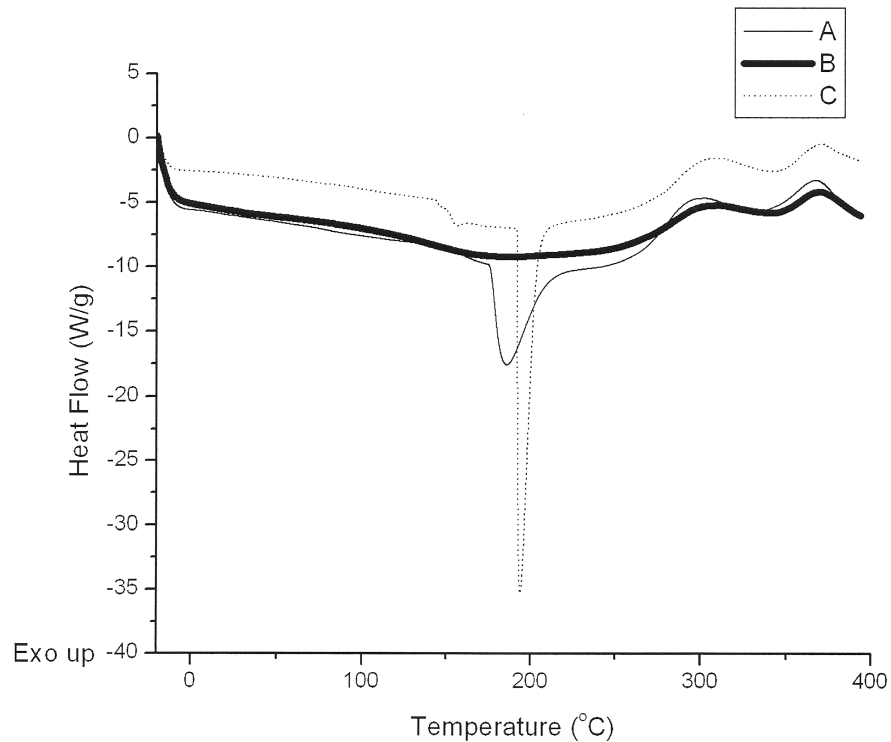


**Figure 2.** DSC curves of: (A) a composite cured under cure sequence VII, (B) a composite cured under cure sequence IV, (C) rice hulls.

Given the results presented so far, cure sequence IV yields a fully cured resin and a composite with the best mechanical properties among those prepared in this section. Therefore, cure sequence IV has been used in the preparation of all composites in the remainder of this work.

### **Influence of pressure during cure on the properties of the rice hull biocomposites.**

Variation of the cure pressure during preparation of the composites has an impact on the final properties obtained, as can be seen in Table III. Young's modulus increases when the pressure increases from 276 psi to 600 psi. In this case, an increase in the pressure forces, by a purely mechanical action, unfavorable interactions between the hydrophobic resin and the hydrophilic filler. The increase in pressure minimizes the presence of micro-voids in the final

composites, and therefore improves the modulus. For the tensile strength, there is a decrease when the pressure is increased from 400 psi to 600 psi (Table III). Lower tensile strengths indicate that the composites are less tolerant to deformations and they become more brittle when higher pressures are used during the cure. When a very low pressure (276 psi) is used in the preparation of the composite, the presence of micro-voids is so significant that even the tensile strength of the material is compromised.

**Table III.** Tensile test, DMA, TGA and Soxhlet extraction results for rice hull composites containing 70 wt % rice hulls, cured under various pressures using cure sequence IV.

| Pressure (psi) | E (GPa)   | Tensile strength (MPa) | $T_g$ (°C) | E' at 130°C (MPa) | $T_{10}$ (°C) | Residue (wt %) | Soluble fraction (wt %) <sup>a</sup> |
|----------------|-----------|------------------------|------------|-------------------|---------------|----------------|--------------------------------------|
| 276            | 1.6 ± 0.3 | 5.5 ± 1.2              | 66         | 37                | 309           | 15             | 6                                    |
| 400            | 1.8 ± 0.1 | 6.7 ± 0.7              | 68         | 336               | 304           | 14             | 5                                    |
| 500            | 2.0 ± 0.3 | 6.2 ± 0.8              | 69         | 417               | 306           | 15             | 6                                    |
| 600            | 2.3 ± 0.5 | 5.9 ± 0.6              | 52         | 220               | 304           | 15             | 5                                    |

<sup>a</sup> Determined by Soxhlet extraction.

A slight increase in the  $T_g$  is observed by increasing the pressure from 276 psi to 500 psi (Table III), but due to the very low variability of  $T_g$  in that pressure range, it is difficult to establish a relationship between cure pressure and the glass transition temperature of the composites, as can be observed in Figure 3. Nevertheless, the composite cured under 600 psi exhibited a  $T_g$  of 52 °C. This constitutes a significant decrease from the  $T_g$  of the composite cured at 500 psi. In one of our previous studies,<sup>23</sup> it was demonstrated that the cure pressure can affect the polymerization of the resin. Here, it can be assumed that the high pressure affected the mobility and dispersion of the resin co-monomers through the filler particles during polymerization, and as a consequence, a matrix with a lower  $T_g$  was obtained. The

storage moduli follow the same trends observed for the  $T_g$ 's, with an increase when the cure pressure increases from 276 psi to 500 psi (Table III, Figure 3), and a significant decrease in modulus when the pressure increases from 500 psi to 600 psi. The remarkably low modulus obtained using a 276 psi cure pressure (Figure 3) can be attributed to poor filler-resin interaction, which compromises the stress transfer from the matrix to the filler.

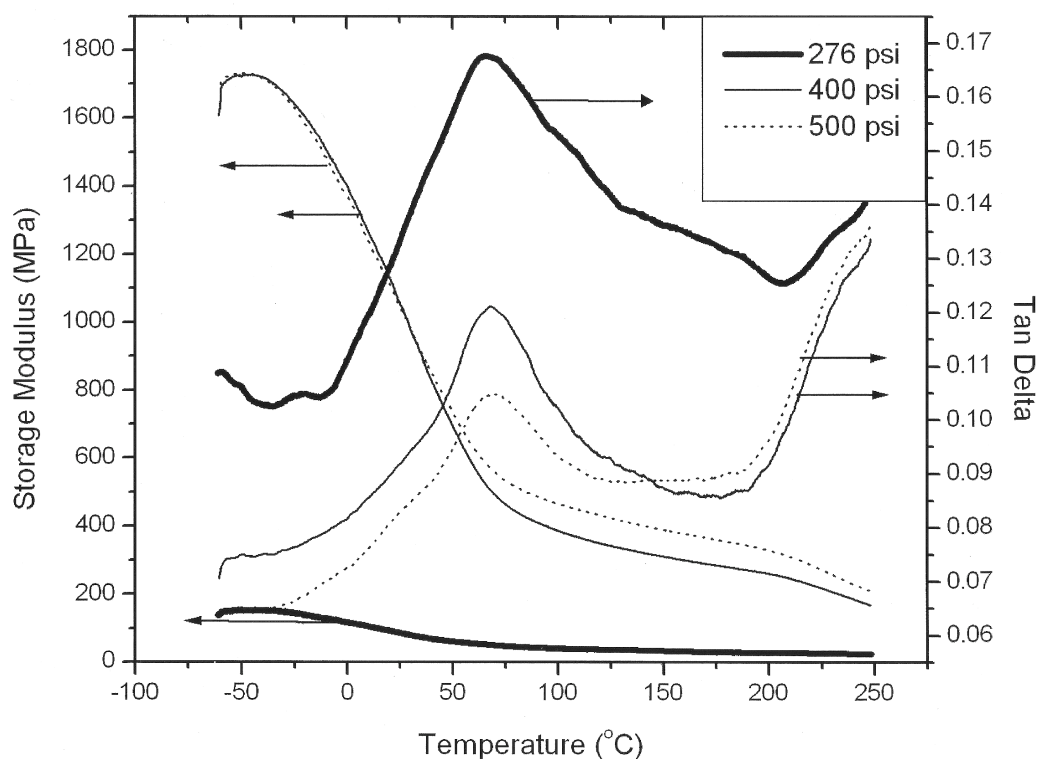


**Figure 3.** Storage modulus and tan delta curves for samples cured under 276 psi, 400 psi, and 500 psi. The composites have 70 wt % of ground filler and were cured under the specified pressure using cure sequence IV.

The  $T_{10}$  values, residue and soluble fraction change very little when different cure pressures are used during preparation of the composites. The  $T_{10}$  value and the residue are closely related to the resin and material composition, whereas the soluble fraction is an indirect measurement of the crosslink density of the matrix. Since the filler material and resin

composition have been kept constant throughout this study, no significant changes were expected for the thermal degradation profile of the composites, and a soluble content of approximately 5 wt % is expected for any composite cured under cure sequence IV (Table II).

Since the aim of this work is to produce a rigid composite with good mechanical properties for possible replacement of petroleum-derived polymers, the cure pressure that gives the stiffest material (600 psi) has been chosen for use in the remainder of this work.

**Influence of filler load on the properties of the rice hull biocomposites.** Table IV shows the effect of the filler load on the composite properties. There is an increase in Young's modulus, tensile strength, and storage modulus when the filler load is increased from 50 wt % to 70 wt %. The increase in the mechanical properties reveals the reinforcement behavior of the rice hulls in the composite, in a filler load range where there is enough resin to wet all of the filler particles. This reinforcing behavior of the rice hulls can also be observed when comparing the storage modulus of an unreinforced conjugated soybean oil-based resin and any of the composites shown in Table IV. Indeed, a significant increase is observed whenever rice hulls are present. Beyond 70 wt % filler load, a decrease in the tensile properties is seen. This drop in the tensile properties is attributed to a lack of resin to bind all the filler particles efficiently, resulting in agglomeration of the filler and weak points in the composite structure that are responsible for the lower performance of the material. The same phenomenon was observed previously with soybean hull composites.<sup>23</sup> As for the storage modulus, there is a significant decrease above 70 wt % filler load (Table IV) for reasons

mentioned above. The variation in storage modulus for samples containing 80 wt % and 90 wt % filler is negligible when compared to the drop observed between 70 wt % and 80 wt %.

**Table IV.** Tensile test, DMA, TGA and Soxhlet extraction results for rice hull biocomposites prepared under cure sequence IV and 600 psi with varying filler loads.

| Filler load (wt %) | $E$ (GPa) | Tensile strength (MPa) | $T_g$ (°C)           | $E'$ at 130°C (MPa) | $T_{10}$ (°C) | Residue (wt %) | Soluble fraction (wt %) <sup>c</sup> |
|--------------------|-----------|------------------------|----------------------|---------------------|---------------|----------------|--------------------------------------|
| - <sup>a</sup>     | -         | -                      | -51, 37 <sup>b</sup> | 44                  | 344           | 0              | 13                                   |
| 50                 | 0.6 ± 0.2 | 1.1 ± 0.8              | 32                   | 82                  | 308           | 9              | 7                                    |
| 60                 | 1.4 ± 0.4 | 4.7 ± 1.6              | 63                   | 172                 | 302           | 10             | 5                                    |
| 70                 | 2.3 ± 0.5 | 5.9 ± 0.6              | 52                   | 220                 | 304           | 15             | 5                                    |
| 80                 | 1.7 ± 0.8 | 2.6 ± 1.6              | -18, 93 <sup>b</sup> | 83                  | 294           | 12             | 5                                    |
| 90                 | 0.9 ± 0.5 | 0.6 ± 0.5              | -29, 66 <sup>b</sup> | 87                  | 292           | 13             | 4                                    |

<sup>a</sup> Unreinforced resin containing 50 wt % of conjugated soybean oil, 35 wt % of *n*-butyl methacrylate, and 15 wt % of divinylbenzene.<sup>23</sup>

<sup>b</sup> Two distinct  $T_g$ 's were observed.

<sup>c</sup> Determined by Soxhlet extraction.

Between 50 wt % and 70 wt % filler load, no regular pattern in the  $T_g$  values could be distinguished (Table IV). However, two  $T_g$ 's were observed when the filler load was 80 wt % and 90 wt % (Table IV). In these instances, the high filler load may have compromised the dispersion of the different co-monomers throughout the system, affecting the chain growth during polymerization. For the unreinforced conjugated soybean oil-based resin, a difference in the reactivity of the co-monomers promoted a phase separation of the resin. Indeed, a phase separation of vegetable oil-based resins has been previously observed,<sup>10, 22, 23</sup> and it is believed that the two phases formed consist of a vegetable oil-rich phase and a DVB-rich phase.

The  $T_{10}$  values do not vary much for filler contents varying between 50 wt % and 70 wt %, and no specific trend is observed (Table IV). There is a 10 °C drop in  $T_{10}$  for 80 wt % and 90 wt % filler loads with respect to the 70 wt % and 60 wt % composites, respectively. As mentioned before, the  $T_{10}$  value of the rice hulls alone (286 °C) is lower than that of the resin (344 °C). So in systems where the rice hulls are in a large excess (80 wt % and beyond), it is normal to observe a decrease in  $T_{10}$ . The percent residue increases when the filler load increases from 50 wt % to 70 wt % (Table IV). The rice hulls alone exhibited a residue content of 18 wt % (result not shown in Table IV), while the unreinforced resin had left no residue. This indicates that the majority of the residue left after thermal degradation comes from the reinforcement. Therefore, it is expected that an increase in the filler content will produce an increase in the residue left after degradation. This trend was not observed for the samples containing 80 wt % and 90 wt % of the filler, which exhibit essentially the same residue, with a negligible difference.

Figure 4 provides a comparison of the thermal degradation patterns of the unreinforced resin and samples containing 50 wt % and 70 wt % rice hulls. From this comparison, a few key features from degradation of the filler stand out, like the loss of water between 100 °C and 150 °C, and the two distinct degradation steps before and after 450 °C, which are related to the cellulose/lignin composition of the filler. There is also a noticeable increase in residue percentage with filler content.

There was not a significant variation in the soluble fraction recovered from the composites with different filler loads. The values ranged from 4 wt % to 7 wt % solubles (Table IV). With such a small variation, it is impossible to establish a reliable relationship

between the filler content and the amount of solubles recovered after Soxhlet extraction. The unreinforced resin, on the other hand, exhibited 13 wt % of soluble materials, consisting mainly of unreacted oil. These results suggest that the resin is the main source of soluble content in the composites, corroborating the results shown in Figure 1.

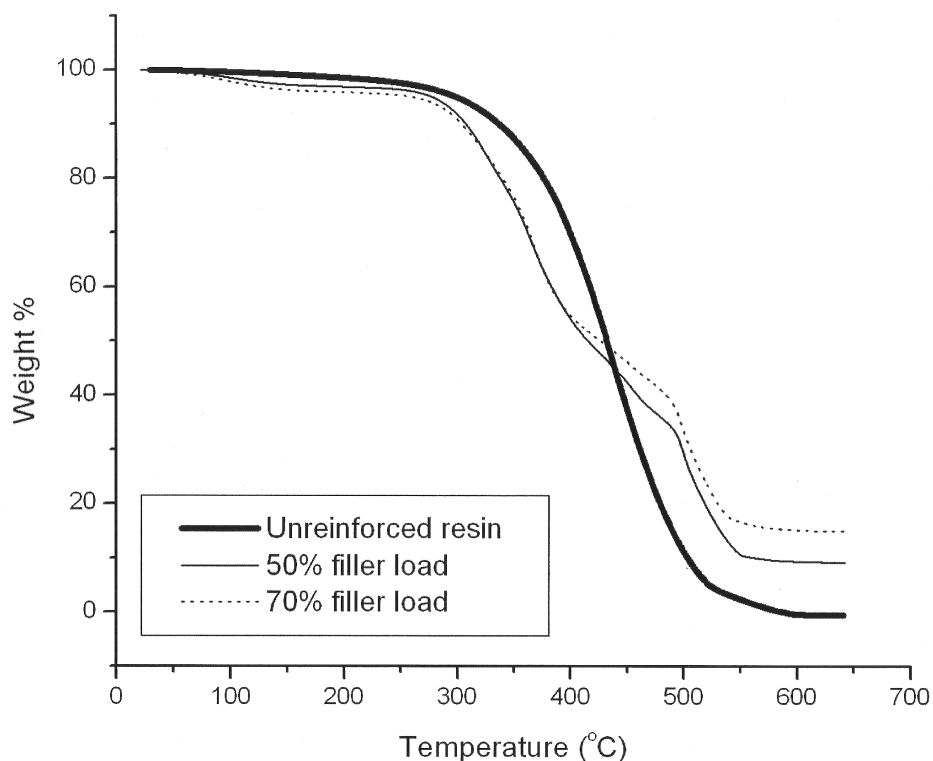


**Figure 4.** TGA curves for a soybean oil-based unreinforced resin, and composites containing 50 wt % and 70 wt % rice hulls. The resin composition was 50 wt % of conjugated vegetable oil, 35 wt % of *n*-butyl methacrylate, and 15 wt % of divinylbenzene.

As stated before, the goal of this work is to find a rice hull biocomposite with the best mechanical properties possible. Considering the results presented in Table IV, a filler load of 70 wt % gave the best overall properties and has, therefore, been used to study the influence of drying and grinding the filler on the final properties of the composite.

**Influence of drying and grinding the filler on the properties of the rice hull biocomposites.** Table V summarizes the properties obtained for four composites prepared under the same conditions, differing only with respect to the condition of the rice hulls used as the filler. The rice hulls used were (a) as received; (b) dried, but not ground; (c) non-dried, but ground; (d) dried and ground.

**Table V.** Tensile test, DMA, TGA and Soxhlet extraction results for rice hull biocomposites prepared under cure sequence IV and 600 psi containing 70 wt % of various rice hull fillers.

| Rice hulls        | $E$ (GPa)     | Tensile strength (MPa) | $T_g$ (°C) | $E'$ at 130°C (MPa) | $T_{10}$ (°C) | Residue (wt %) | Soluble fraction (wt %) <sup>a</sup> |
|-------------------|---------------|------------------------|------------|---------------------|---------------|----------------|--------------------------------------|
| as received       | $0.7 \pm 0.4$ | $1.4 \pm 0.8$          | 40         | 21                  | 297           | 16             | 6                                    |
| dried, non-ground | $2.3 \pm 0.4$ | $5.7 \pm 0.6$          | 41         | 280                 | 303           | 16             | 5                                    |
| non-dried, ground | $1.0 \pm 0.3$ | $1.7 \pm 1.0$          | 58         | 199                 | 298           | 17             | 5                                    |
| dried, ground     | $2.3 \pm 0.5$ | $5.9 \pm 0.6$          | 52         | 220                 | 304           | 15             | 5                                    |

<sup>a</sup> Determined by Soxhlet extraction.

The mechanical properties of these biocomposites reveal a great improvement in the composite's performance whenever the rice hulls are dried before use. Indeed, the Young's modulus increases when the whole rice hulls are dried before being impregnated with the resin (Table V). Similarly, there's an increase in the Young's modulus when the ground rice hulls are dried (Table V). The tensile strength of the composites show the same trend, with increases when drying the whole and the ground rice hulls (Table V). Along the same lines, the storage modulus at 130 °C increases when using dried versus non-dried whole rice hulls, and also increases when drying the ground rice hulls before use. This increase in the



mechanical properties is probably related to the fact that the lower moisture content in the dried rice hulls may lead to a better filler-resin interaction, which gives better stress transfer from the matrix to the reinforcement, and consequently better tensile properties.

Grinding the rice hulls had little effect on the tensile properties of the composites, in comparison to the variations observed between dried and non-dried fillers. The slight increase in the Young's modulus observed when comparing non-dried, whole rice hulls and ground rice hulls can be neglected, since it falls within the standard deviations of the corresponding samples (Table V). Also, virtually no change was observed when comparing dried rice hulls (Table V). The same happens with the tensile strength; increases within the standard deviation of the samples are observed for non-dried, whole and ground rice hulls, and for dried, whole and ground rice hulls (Table V). The better tensile properties normally obtained for composites with smaller particle sizes are compensated for here by a loss in the aspect ratio of the non-ground rice hulls. Therefore, grinding the rice hulls means going from an elongated structure with better tensile properties, but lower dispersion in the matrix, to more spherical particles, which disperse better in the matrix, but show lower tensile properties.

For the storage modulus at 130 °C, drying the rice hulls has an effect similar to that observed on the tensile properties. A significant increase occurs when drying the whole rice hulls (Table V). A more subtle increase is observed between non-dried and dried, ground rice hulls (Table V). The effect on the storage modulus at 130 °C of grinding the rice hulls is unclear as opposite trends were observed for dried and non-dried fillers. An increase was observed when comparing whole and ground, non-dried rice hulls, whereas a decrease was

observed when comparing whole and ground, dried rice hulls (Table V). The  $T_g$ , on the other hand, appears to be more sensitive to variations in the filler particle size. Indeed, grinding the rice hulls increases the  $T_g$  of the composite by at least 11 °C (Table V). This effect has been observed previously with soybean hull composites,<sup>23</sup> and is attributed to a better mix of resin and filler when smaller particle sizes are used. Very little effect was observed when comparing the  $T_g$ 's of non-dried and dried, whole rice hulls or when comparing non-dried and dried, ground rice hulls (Table V).

The  $T_{10}$  values were only slightly changed when comparing dried and non-dried rice hulls. The slight differences observed between the  $T_{10}$  values of non-dried and dried, whole rice hulls, and of non-dried and dried, ground rice hulls are due to the moisture content of the filler. When the filler is dried before use, it loses approximately 7 wt % due to moisture (result not shown in Table V). For the composites reinforced with non-dried rice hulls,  $T_{10}$  reflects the loss of that moisture content from the filler, along with partial volatilization of some resin components, and, as the moisture should be completely lost at around 100 °C, the  $T_{10}$  value of those materials is slightly shifted to lower temperatures. From the negligible difference observed between the  $T_{10}$  values of non-ground and ground, dried hulls, and non-ground and ground, non-dried hulls (Table V), it can be concluded that grinding the rice hulls has no effect on the  $T_{10}$  values of the composites.

Finally, there's virtually no variation in residue content and soluble content extracted upon drying and/or grinding the rice hulls (Table V). As mentioned before, those properties are related to the amount of filler and the composition of the resin used in the preparation of

the composites, and, since those parameters are kept constant for all of the samples shown in Table V, no variation was expected here.

**SEM analysis of the rice hull biocomposites.** Figure 5 depicts the SEM image of cryofractured and cut biocomposite samples. Samples made with dried and non-dried rice hulls were analyzed and compared. Both composites had a filler load of 70 wt % and were cured under 600 psi at 180 °C for 5 hours and then post-cured at ambient pressure for 2 hours at 200 °C.

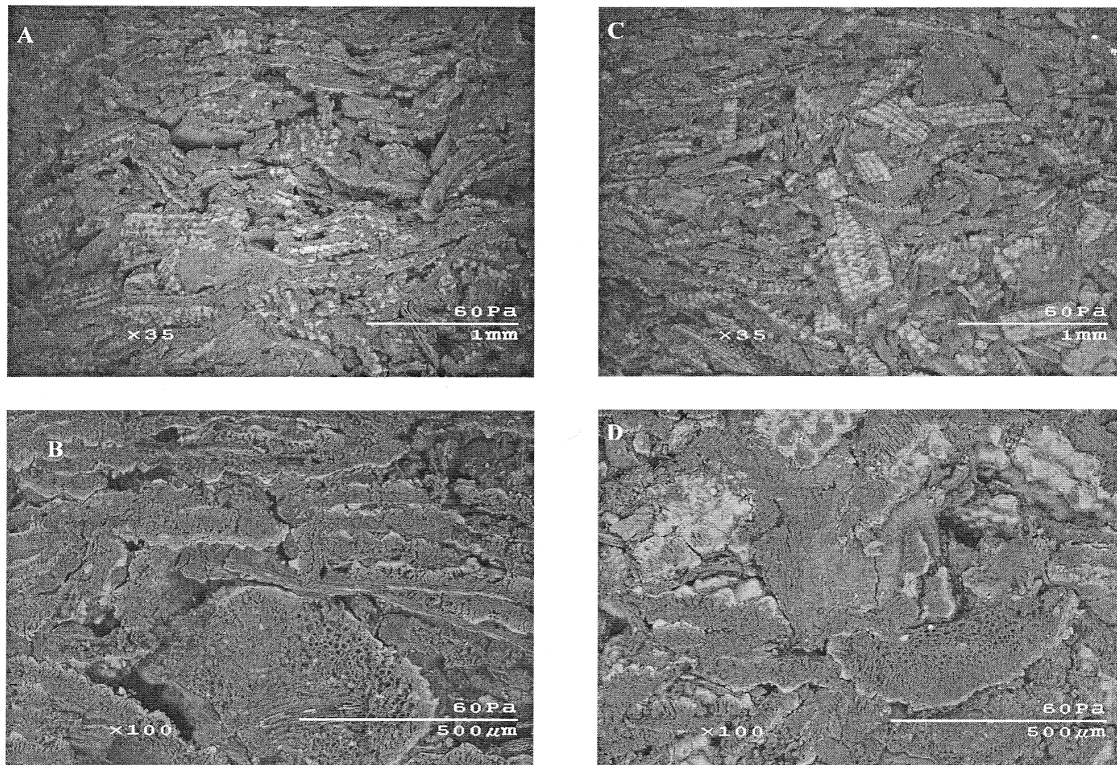


**Figure 5.** SEM images of: (A) a cryofractured biocomposite reinforced with dried rice hulls (35x magnification), (B) a cut biocomposite reinforced with dried rice hulls (100x magnification), (C) a cryofractured biocomposite reinforced with non-dried rice hulls (35x magnification), (D) a cut biocomposite reinforced with non-dried rice hulls (100x magnification). Both composites had 70 wt % of ground filler and were cured under 600 psi at 180 °C for 5 hours and then post-cured at ambient pressure for 2 hours at 200 °C.

The brighter regions on the images represent structures of higher density, located mostly on the surface of the rice hulls. Those structures will be further discussed later in the text. The porous structures observed, for example, in Figure 5B, correspond to rice hull particles. As expected, the large amount of rice hulls employed (70 wt %), resulted in composites where the resin is present in minimal amounts, and functions mainly as a binder between the rice hull particles. Significant voids are observed in all four images, which indicate the overall bad interaction between filler and resin. The presence of voids also indicates weak regions in the composites where cracks can be easily generated and/or propagated.

The images of cryofractured composites (Figures 5A and 5C) show a more significant exposition of the silica structures, again indicating poor resin-filler adhesion. When the samples were fractured, the crack propagated along the resin-filler interface, leaving the rice hull particle surfaces exposed. Comparatively more of the silica structures can be seen in Figure 5C, where non-dried rice hulls were used. This is an indication that worse resin-filler interactions are obtained when non-dried filler particles are used, due to the incompatibility of the hydrophobic resin and the hydrophilic filler. Furthermore, Figure 5A shows more resin artifacts covering the rice hull particles.

Figures 5B and 5D show, in more detail, the filler-resin interface. The central area in Figure 5B shows a region where resin and filler interact well (there is no discontinuity between matrix and reinforcement). Nothing similar is observed in the entirety of Figure 5D, supporting the idea that worse filler-resin interactions are present when the fillers are not dried before their use as a reinforcement in manufacture of the biocomposites.

**X-ray map of a rice hull biocomposite sample.** An X-ray map of a rice hull biocomposite sample cured at 600 psi, under cure sequence IV, is shown in Figure 6. Figure 6A shows the SEM image of the cut biocomposite at 200x magnification. From that image, it is clear that the denser region (brighter areas) is more abundant on the surface of the rice hull particles. The presence of significant amounts of silica in rice straw ash suggests that these high-density structures are most likely  $\text{SiO}_2$ .<sup>28</sup>

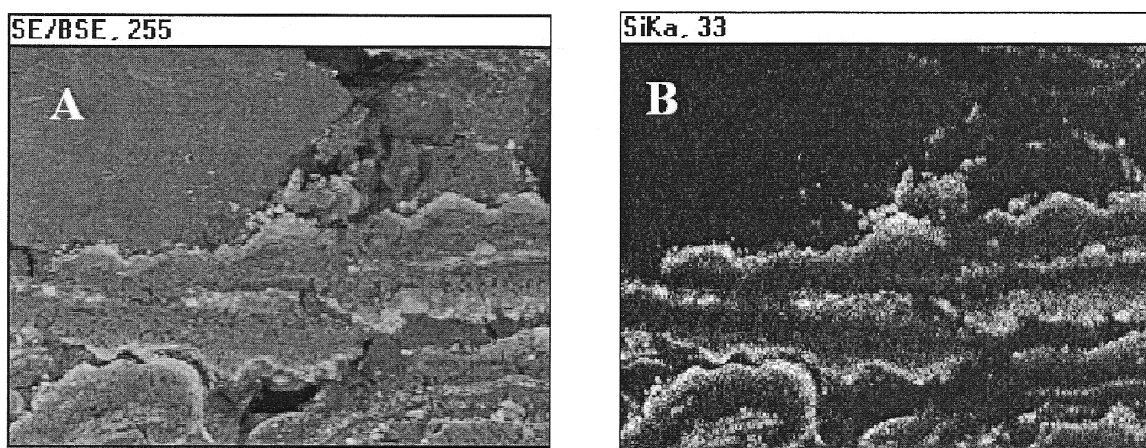


**Figure 6.** Si X-ray map. (A) 200x magnification SEM image of a biocomposite with 70 wt % of ground filler, cured under 600 psi at 180 °C for 5 hours and then post-cured at ambient pressure for 2 hours at 200 °C. (B) X-ray map of line Si Ka on the same section shown in (A).

Figure 6B shows the Si X-ray map. By comparing Figures 6A and 6B, it becomes clear that rice hulls are rich in Si and that the Si-containing structures are more abundant on the surface of the rice hulls. The presence of silica in the rice hulls explains the high mechanical properties obtained for the biocomposites prepared in this work.

## Conclusions

Rice hull biocomposites have been prepared by the free radical polymerization of a CLO-based resin. After a cure study, an optimal cure sequence of 5 hours at 180 °C under pressure, followed by a 2 hour post-cure under ambient pressure, has been established. Mechanical data, along with TGA, Soxhlet extraction and DSC results show that the post-cure step is crucial in order to get a fully cured resin, and the best CLO incorporation in the matrix. The effects of pressure during cure, filler load, and drying and grinding the filler on the final properties of the biocomposites have been assessed and optimal conditions have been established for preparation of the rice hull-reinforced composites. A pressure of 600 psi during the cure has resulted in the stiffest material. The use of 70 wt % of dried and ground (<1 mm diameter particle size) filler affords the best overall properties. SEM shows evidence of weak filler-resin interaction due to differences in the hydrophilicity of the matrix and the reinforcement. The SEM analysis also provides an indication of a denser material present on the surface of the rice hulls. The Si X-ray map indicated a high Si content in that material, which consists, most likely, of silica. The presence of significant amounts of silica in the rice hulls may account for the high thermal stability and the high mechanical properties obtained for the rice hull biocomposites. A thorough resin composition study is currently being carried out and will soon be reported.

## Acknowledgments

The authors thank the Recycling and Reuse Technology Transfer Center of the University of Northern Iowa for financial support, the Missouri Crop Improvement Association for the rice hulls, Professor Michael Kessler from the Department of Material

Sciences and Engineering and Dr. Richard Hall from the Department of Natural Resource Ecology and Management at Iowa State University for the use of their facilities, Warren Straszheim from the Department of Material Sciences and Engineering for help with the SEM and X-ray mapping experiments, and Dr. Douglas Stokke from the Department of Natural Resource Ecology and Management for important information concerning the rice hulls.

### References

1. Lu, Y.; Larock, R. C. *Biomacromolecules* 2007, 8, 3108.
2. Lu, Y.; Larock, R. C. *Biomacromolecules* 2008, 9, 3332.
3. Andjelkovic, D. D.; Larock, R. C. *Biomacromolecules* 2006, 7, 927.
4. Andjelkovic, D. D.; Lu, Y.; Kessler, M. R.; Larock, R. C. *Macromol. Mater. Eng.* 2009, 294, 472.
5. Jeong, W.; Mauldin, T. C.; Larock, R. C.; Kessler, M. R. *Macromol. Mater. Eng.* 2009, 294, 756.
6. Valverde, M.; Andjelkovic, D.; Kundu, P. P.; Larock, R. C. *J. Appl. Polym. Sci.* 2008, 107, 423.
7. Li, F.; Hasjim, J.; Larock, R. C. *J. Appl. Polym. Sci.* 2003, 90, 1830.
8. Li, F.; Larock, R. C. *Biomacromolecules* 2003, 4, 1018.
9. Henna, P. H.; Andjelkovic, D. D.; Kundu, P. P.; Larock, R. C. *J. Appl. Polym. Sci.* 2007, 104, 979.
10. Andjelkovic, D. D.; Valverde, M.; Henna, P.; Li, F.; Larock, R. C. *Polymer* 2005, 46, 9674.
11. Jarukumjorn, K.; Suppakarn, N. *Composites: Part B* 2009, 40, 623.
12. Srebrenkoska, V.; Gaceva, G. B.; Dimeski, D. *Maced. J. Chem. Chem. Eng.* 2009, 28, 99.
13. Haque, M. M.; Hasan, M.; Islam, M. S.; Ali, M. E. *Bioresour. Technol.* 2009, 100, 4903.
14. Panthapulakkal, S.; Zereshkian, A.; Sain, M. *Bioresour. Technol.* 2006, 97, 265.
15. Sui, G.; Fuqua, M. A.; Ulven, A. A.; Zhong, W. H. *Bioresour. Technol.* 2009, 100, 1246.
16. Vilaseca, F.; Valady-Gonzalez, A.; Herrera-Franco, P. J.; Pelach, M. A.; Lopez, J. P.; Mutje, P. *Bioresour. Technol.* 2010, 101, 387.
17. Liu, H.; Wu, Q.; Zhang, Q. *Bioresour. Technol.* 2009, 100, 6088.

18. Xu, Y.; Wu, Q.; Lei, Y.; Yao, F. *Bioresour. Technol.* 2010, 101, 3280.
19. Onal, L.; Karaduman, Y. *J. Comp. Mat.* 2009, 43, 1751.
20. Hapuarachchi, T. D.; Ren, G.; Fan, M.; Hogg, P. J.; Peijs, T. *Appl. Compos. Mater.* 2007, 14, 251.
21. Reddy, N.; Yang, Y. *J. Appl. Polym. Sci.* 2010, 116, 3668.
22. Pfister, D. P.; Larock, R. C. *Bioresour. Technol.* 2010, 101, 6200.
23. Quirino, R. L.; Larock, R. C. *J. Appl. Polym. Sci.* 2009, 112, 2033.
24. Bhuyan, S.; Sundararajan, S.; Pfister, D.; Larock, R. C. *Tribol. Int.* 2010, 43, 171.
25. Pfister, D. P.; Baker, J. R.; Henna, P. H.; Lu, Y.; Larock, R. C. *J. Appl. Polym. Sci.* 2008, 108, 3618.
26. Larock, R. C.; Dong, X.; Chung, S.; Reddy, C. K.; Ehlers, L. E. *J. Am. Oil Chem. Soc.* 2001, 78, 447.
27. Barneto, A. G.; Carmona, J. A.; Alfonso, J. E. M.; Alcaide, L. J. *Bioresour. Technol.* 2009, 100, 3963.
28. Abdel-Mohdy, F. A.; Abdel-Halim, E. S.; Abu-Ayana, Y. M.; El-Sawy, S. M. *Carbohydr. Polym.* 2009, 75, 44.
29. Yang, H.; Yan, R.; Chen, H.; Lee, D. H.; Zheng, C. *Fuel* 2007, 86, 1781.



**CHAPTER 4. RICE HULL BIOCOMPOSITES. PART 2: EFFECT OF THE RESIN  
COMPOSITION ON THE PROPERTIES OF THE COMPOSITE**

A Paper Published in Journal of Applied Polymer Science, 121, 2050-2059.

Copyright © 2011, Wiley-Blackwell

Rafael L. Quirino, Richard C. Larock\*

*Department of Chemistry, Iowa State University, Ames, Iowa 50011*

**Abstract**

A free radical thermoset resin consisting of a copolymer of conjugated linseed oil (CLO) or conjugated soybean oil (CSO), *n*-butyl methacrylate (BMA), divinylbenzene (DVB), and maleic anhydride (MA) has been reinforced with rice hulls. Composites containing 70 wt % of the filler were compression molded, the conjugated oil content in the resin was kept constant at 50 wt %, and the relative amounts of BMA, DVB, and MA were varied to afford composites with different resin compositions. Tensile tests, DMA, TGA, and Soxhlet extraction of the different composites prepared have been employed to establish the relationship between resin composition and the properties of the composites. Overall, the mechanical properties tend to improve when MA is introduced into the resin. SEM of selected samples showed a better filler-resin interaction for MA-containing composites and samples prepared from CLO exhibit better properties than those prepared from CSO.

## Introduction

With the shortage in petroleum and growing concerns about the environment, the use of biorenewable materials for the production of bioplastics and biocomposites has recently gained increasing attention. Natural oils, which consist of triglycerides often containing polyunsaturated carbon chains, represent a promising component in the preparation of biobased materials due to their ready availability and low cost.

In particular, linseed and soybean oils have been used as major components in various resin formulations. Semi-conducting materials have been prepared from a poly(urethane amide) of linseed oil blended with poly(1-naphthylamine).<sup>1</sup> Linseed oil monoglyceride maleates have been co-polymerized with styrene to form a matrix for wood flour composites.<sup>2</sup> Clay composites have also been prepared using a matrix where conjugated linseed oil was co-polymerized with divinylbenzene (DVB) and acrylic acid (AA),<sup>3</sup> and a similar resin, containing linseed oil, DVB, styrene (ST) and AA, has also been studied.<sup>4</sup> Linseed oil has also been used as the starting material in the preparation of an AA-esterified monomer for later co-polymerization with ST.<sup>5</sup> Also, polyester amides have been made from linseed oil.<sup>6</sup> Along the same lines, polyurethanes,<sup>7</sup> an epoxy resin for glass fiber composites,<sup>8</sup> and multicomponent thermoset resins from soybean oil have been reported among several other reports not cited here.<sup>9</sup>

The high degree of unsaturation in these oils (approximately 6 C=C per triglyceride for linseed oil and 4.5 for soybean oil) makes them very attractive as comonomers in free radical resins. The fatty acid composition of linseed oil follows: 4% stearic acid, 19% oleic acid, 15% linoleic acid, 57% linolenic acid, and 5% of other fatty acids,<sup>10</sup> while soybean oil

consists of 14% palmitic acid, 4% stearic acid, 24% oleic acid, 52% linoleic acid, and 6% linolenic acid.<sup>11</sup> Despite the high number of carbon-carbon double bonds in these oils, it is known that a significantly higher reactivity towards free radical polymerization processes is attained upon conjugation of the carbon-carbon double bonds.<sup>12</sup> Our group has investigated resins formed by the free radical copolymerization of conjugated linseed oil with acrylonitrile and DVB,<sup>10</sup> and the thermal polymerization of conjugated linseed oil in the presence of ST and DVB.<sup>13</sup> The cationic polymerization of a modified linseed oil and dicyclopentadiene (DCPD) has also been studied by the Larock group,<sup>14</sup> as well as various resins containing conjugated soybean oil.<sup>15-17</sup>

More recently, we have studied the reinforcement of a conjugated soybean oil-based thermoset matrix containing DVB and *n*-butyl methacrylate (BMA) with corn stover,<sup>18</sup> and soybean hulls.<sup>19</sup> In the latter system, DCPD was employed in the resin to partially substitute either DVB or BMA in an attempt to improve the mechanical properties and lower the cost of the resulting composite. A similar resin, containing unmodified tung oil, has been reinforced with spent germ by us.<sup>20, 21</sup>

Rice hulls are a major agricultural by-product from the rice industry and very few uses have been proposed for it. It normally ends up being disposed of in landfills or just burned to produce an ash rich in silica.<sup>22</sup> The use of rice hulls as a reinforcement for polypropylene composites has been reported recently, and the promising results suggest that it may work as a good filler in the preparation of bio-based composites.<sup>23</sup> The preparation of rice hull composites from conjugated linseed oil has been optimized in Part 1 of this project.<sup>24</sup> The effect of cure sequence, pressure, filler load, particle size, and drying of the

filler on the composite properties has been studied and the best conditions for preparation of these rice hull-reinforced materials have been established.<sup>24</sup>

In Part 2 of this project, we report the preparation of rice hull composites with resins of various compositions. All of the resins studied here contain 50 wt % of the conjugated vegetable oil and different concentrations of maleic anhydride (MA), BMA, and DVB. MA, in this system, acts as a compatibilizer between the hydrophobic matrix and the hydrophilic filler. The effect of the concentration of the different comonomers used on the final composite properties has been assessed by means of tensile tests, dynamic mechanical analysis (DMA), thermogravimetric analysis (TGA), Soxhlet extraction, scanning electron microscopy (SEM), and proton nuclear magnetic resonance spectroscopy (<sup>1</sup>H NMR).

### Experimental

**Materials.** BMA was purchased from Alfa Aesar (Ward Hill, MA). DVB, MA and di-*t*-butyl peroxide (TBPO) were purchased from Sigma-Aldrich (St. Louis, MO). All were used as received. Superb linseed oil was provided by ADM (Red Wing, MN) and soybean oil (*Great Value* brand – Bentonville, AR) was purchased in a local grocery store. Both oils have been conjugated using a rhodium catalyst, following a method developed and frequently used by our group.<sup>12</sup> The rice hulls were provided by the Missouri Crop Improvement Association (Columbia, MO). They were ground to <1 mm diameter particle size and dried overnight at 70 °C in a vacuum oven before use.

**General procedure for preparation of the composites.** The crude resin was obtained by mixing the conjugated vegetable oil, BMA and DVB in a beaker. MA was melted in a hot water bath and quickly added to the crude resin mixture under agitation, along with the free

radical initiator TBPO. The rice hulls were impregnated with the crude resin and compression molded for 5 hours at 180 °C and 600 psi. The composites were then removed from the mold and post-cured in a convection oven for 2 hours at 200 °C at ambient pressure. An optimal filler load of 70 wt % had been pre-established in Part 1 of this project and has been kept constant throughout Part 2.<sup>24</sup> In all composites produced, the resin has a conjugated vegetable oil content of 50 wt % and the optimal amount of TBPO has been determined to be, in preliminary tests, an extra 5 wt % of the total resin weight. The amounts of DVB, BMA and MA have been varied, as indicated in the text, to produce composites of various compositions.

**Characterization of the composites.** Tensile tests were conducted at room temperature according to ASTM D-638 using an Instron universal testing machine (model 5569) equipped with a video extensometer and operating at a crosshead speed of 2.0 mm/min. Dogbone-shaped test specimens were machined from the original samples to give the following gauge dimensions: 57.0 mm x 12.7 mm x 4.5 mm (length x width x thickness, respectively). For each composite, seven dog-bones were cut and tested. The results presented in the text are the average of these measurements along with the calculated standard deviation.

DMA experiments were conducted on a Q800 DMA (TA Instruments, New Castle, DE) using a three point bending mode with a 15.0 mm clamp. Rectangular specimens of 22.0 mm x 8.5 mm x 1.5 mm (length x width x thickness, respectively) were cut from the original samples. Each specimen was cooled to -60 °C and then heated at 3 °C/min to 250 °C. The experiment was conducted using a frequency of 1 Hz and an amplitude of 14 µm

under air. Two runs for each sample were carried out and the results presented in the text reflect the average of the two measurements.

A Q50 TGA instrument (TA Instruments, New Castle, DE) was used to measure the weight loss of the samples under an air atmosphere. The samples (~10 mg) were heated from room temperature to 650 °C at a rate of 20 °C/min.

Soxhlet extraction was conducted to determine the amount of soluble materials in the composites. A 2.0 g sample of each composite was extracted for 24 h with dichloromethane ( $\text{CH}_2\text{Cl}_2$ ). After extraction, the solubles were recovered by evaporating the  $\text{CH}_2\text{Cl}_2$  under vacuum. Both soluble and insoluble materials were dried overnight at 70 °C. The dried soluble fraction was then dissolved in deuterated chloroform ( $\text{CDCl}_3$ ) and the  $^1\text{H}$  NMR spectrum was obtained using a Varian Unity spectrometer (Varian Associates, Palo Alto, CA) operating at 300 MHz. The  $^1\text{H}$  NMR spectra helped to determine the identity of the solubles in each sample.

For the SEM analysis, each sample was frozen with liquid nitrogen prior to fracture (cryofracture). A second section of the sample was mechanically cut and shaved with a razor blade to provide a smooth cross section. Both cryofractured and cut samples were examined using an Hitachi S-2460N variable-pressure SEM. The microscope was operated at 20 kV accelerating voltage, with 60 Pa of helium atmosphere, and a 25 mm working distance. Backscattered electron images were collected using a Tetra BSE detector (Oxford Instruments) at 35x and 100x magnifications.

## Results and Discussion

**Mechanical properties of conjugated linseed oil (CLO)-containing composites.** The tensile test and DMA results of all samples made with CLO are summarized in Table I. Young's moduli, tensile strengths, storage moduli at 130 °C, and  $T_g$ 's are reported for the CLO-containing composites with different resin compositions.

**Table I.** Tensile tests and DMA results for biocomposites made from conjugated linseed oil (CLO).

| Entry | BMA (wt %) | DVB (wt %) | MA (wt %) | Young's Modulus (GPa) | Tensile Strength (MPa) | Storage Modulus at 130 °C (MPa) | $T_g$ (°C)         |
|-------|------------|------------|-----------|-----------------------|------------------------|---------------------------------|--------------------|
| 1     | 35         | 15         | -         | 2.3 ± 0.5             | 5.9 ± 0.6              | 220                             | 52                 |
| 2     | 35         | 10         | 5         | 1.9 ± 0.4             | 7.9 ± 1.6              | 609                             | 64                 |
| 3     | 35         | 5          | 10        | 1.9 ± 0.3             | 7.1 ± 1.0              | 391                             | 45                 |
| 4     | 35         | -          | 15        | 1.7 ± 0.4             | 5.8 ± 0.9              | 345                             | 33                 |
| 5     | 30         | 15         | 5         | 2.1 ± 0.7             | 7.0 ± 1.3              | 141                             | 0, 69 <sup>a</sup> |
| 6     | 25         | 15         | 10        | 2.1 ± 0.3             | 8.4 ± 1.2              | 350                             | 63                 |
| 7     | 20         | 15         | 15        | 2.3 ± 0.4             | 9.1 ± 1.7              | 255                             | 75                 |
| 8     | 30         | 10         | 10        | 1.7 ± 0.5             | 7.8 ± 1.3              | 332                             | 71                 |
| 9     | 30         | 5          | 15        | 2.1 ± 0.6             | 8.0 ± 1.3              | 258                             | 68                 |
| 10    | 25         | 10         | 15        | 1.8 ± 0.3             | 7.7 ± 1.0              | 476                             | 78                 |

<sup>a</sup> Two  $T_g$ 's were observed.

Comparing entries 1-4 in Table I, the effect of gradual substitution of DVB by MA on the mechanical properties can be assessed. There is an overall decrease in Young's modulus ( $E$ ) from 2.3 GPa to 1.7 GPa when 15 wt % DVB is replaced by MA (entries 1 and 4, respectively, Table I). Although the loss in  $E$  isn't dramatic, it reveals that DVB is

probably the component mainly responsible for the stiffness of the resin. A similar trend was observed when DVB was replaced by DCPD in soybean hull composites.<sup>19</sup>

The tensile strength of the composites exhibits a different trend upon gradual substitution of DVB by MA (entries 1-4, Table I). There is an increase in the tensile strength for the samples containing 5 wt % and 10 wt % MA (7.9 MPa and 7.1 MPa, respectively, entries 2 and 3, Table I) in comparison with the sample where MA is completely absent (5.9 MPa, entry 1, Table I). This reveals that MA behaves as a compatibilizer between the resin and the filler in this system. Indeed, the C-C double bond in MA can be co-polymerized with the resin, while the anhydride group can be opened by the hydroxyl groups present in the cellulose and hemicellulose in the rice hulls at the high temperatures employed during the cure. With a better filler-resin interaction whenever MA is present, there is better stress transfer from the matrix to the filler, resulting in a higher tensile strength for the composite. For entry 4 (Table I), the decrease in tensile strength (5.8 MPa) is related to the absence of DVB in the resin. In this case, the loss in mechanical properties due to the absence of DVB is not compensated for by the better filler-resin interaction imparted by the presence of MA.

A similar trend is observed for the storage modulus at 130 °C ( $E'$ ) and the  $T_g$  of the samples when substituting DVB by MA (entries 1-4, Table I). In both cases, there is an increase in the value when 5 wt % MA is introduced into the resin (entry 2, Table I).  $E'$  increases from 220 MPa to 609 MPa while  $T_g$  increases from 52 °C to 64 °C (entries 1 and 2, Table I). As mentioned earlier, this increase is related to a better filler-resin interaction imparted by the presence of the MA. When the amount of DVB in the resin is below 10 wt % (entries 3 and 4, Table I), a decrease in  $E'$  from 609 MPa (entry 2) to 345 MPa (entry 4)



and  $T_g$  from 64 °C (entry 2) to 33 °C (entry 4) is observed, due to the loss in rigidity of the system.

When BMA is gradually substituted by MA, (entries 1 and 5-7, Table I) the Young's modulus isn't significantly affected, which reveals that, structurally, both molecules have similar characteristics. On the other hand, the tensile strength increases remarkably from 5.9 MPa (entry 1, Table I) to 9.1 MPa (entry 7, Table I) when BMA is substituted by MA, showing, once again, the better filler-resin effect imparted by MA. No specific trend could be distinguished for the storage modulus at 130 °C when BMA was substituted by MA. There is an overall increase in  $T_g$  from 52 °C (entry 1, Table I) to 75 °C (entry 7, Table I) by substituting BMA with MA. The appearance of two  $T_g$ 's (entry 5, Table I) isn't completely understood. In our previous work with soybean hulls,<sup>19</sup> the appearance of two  $T_g$ 's was related to the presence of comonomers with distinctly different reactivities (for example, conjugated soybean oil, BMA and DVB).

When 5 wt % of DVB and 5 wt % of BMA are replaced with 10 wt % of MA, there is a decrease in Young's modulus from 2.3 GPa (entry 1, Table I) to 1.7 GPa (entry 8, Table I) due to the decrease in DVB content, as explained earlier. The tensile strength, storage modulus at 130 °C and  $T_g$  increase from 5.9 MPa, 220 MPa, and 52 °C to 7.8 MPa, 332 MPa, and 71 °C, respectively. These variations show, once again, the gain in mechanical properties due to the addition of MA to the resin and the better filler-resin interaction. When an additional 5 wt % of DVB is replaced by MA (entry 9, Table I), the tensile properties are not significantly affected, since the difference in the Young's modulus and the tensile strength between entries 8 and 9 (Table I) falls within the standard deviation of the

measurements. On the other hand, the storage modulus at 130 °C and the  $T_g$  decrease from 332 MPa and 71 °C (entry 8, Table I) to 258 MPa and 68 °C (entry 9, Table I), respectively.

Finally, the tensile properties of the sample with 25 wt % of BMA, 10 wt % of DVB, and 15 wt % of MA (entry 10, Table I) are comparable to those of the sample in entry 8, Table I. The difference in  $E$  and tensile strength fall within the standard deviation of the experiment and can be neglected. The only significant differences occur in the storage modulus at 130 °C, with an increase from 332 MPa (entry 8, Table I) to 476 MPa and in  $T_g$ , with an increase from 71 °C (entry 8, Table I) to 78 °C.

The curves showing loss modulus ( $E''$ ) versus temperature for selected formulations are given in Figure 1. For all of the curves shown, there is an overall decrease in loss modulus with an increase in temperature. This behavior is most likely the result of further reaction of the remaining carbon-carbon double bonds in the resin, which increases the crosslink density and gradually inhibits the dissipation of the energy through movement of the polymer chains. It is interesting to observe that the loss modulus plateaus at approximately 120 °C, when all carbon-carbon double bonds in the resin have, most likely, reacted. In the case of the sample containing 10 wt % DVB (Figure 1B), the lower amount of the crosslink agent results in a higher loss modulus, when compared to the other curves in Figure 1, for the entire temperature range studied. Indeed, if a lower crosslink density is attained, the polymer chains in the matrix are more free to dissipate the stress energy into movement, resulting in a higher loss modulus. For samples with the same DVB content (Figures 1A, 1C, and 1D), one can correlate the loss modulus behavior with the presence of MA in the resin. When MA is present (Figures 1C and 1D), the resulting better filler-resin

interaction provides more efficient stress transfer from the matrix to the reinforcement, preventing significant dissipation of energy into polymer chain motion, and as a consequence, a decrease in the loss modulus is observed (compare to Figure 1A). When comparing Figures 1C and 1D, a logical relationship between the amount of MA in the resin and the loss modulus can be established for temperatures lower than 25 °C. With a higher MA content, Figure 1D exhibits a lower loss modulus for the reasons already discussed. However, an interesting inversion of the loss modulus behavior is observed after 25 °C. This phenomenon may be related to the overall reactivity of the resin components. Indeed, the loss modulus decreases from 43 MPa to 18 MPa over the temperature range studied and shown in Figure 1D, whereas, for Figure 1C, the decrease observed is from 49 MPa to 9 MPa, suggesting that more carbon-carbon double bonds remain unreacted for resins containing less MA.

**Thermal properties and Soxhlet extraction results of CLO-containing composites.** The TGA and Soxhlet extraction results are summarized in Table II.  $T_{10}$  corresponds to the temperature required to attain loss of 10 wt % of the initial sample;  $T_{50}$  corresponds to the temperature required to attain loss of 50 wt % of the initial sample; and  $T_f$  corresponds to the temperature after which no further weight loss was detected.

From the results in Table II, it can be seen that the changes in  $T_{10}$  are very subtle, when comparing composites with different resin compositions. Indeed, the  $T_{10}$  values vary only from 299 °C (entry 4, Table II) to 306 °C (entry 6, Table II) with no obvious trend, leading to the conclusion that this initial 10 % wt loss is not related to any component of the resin. It could be related, in fact, to initial degradation of the hemicellulose from the rice hulls.<sup>25</sup>

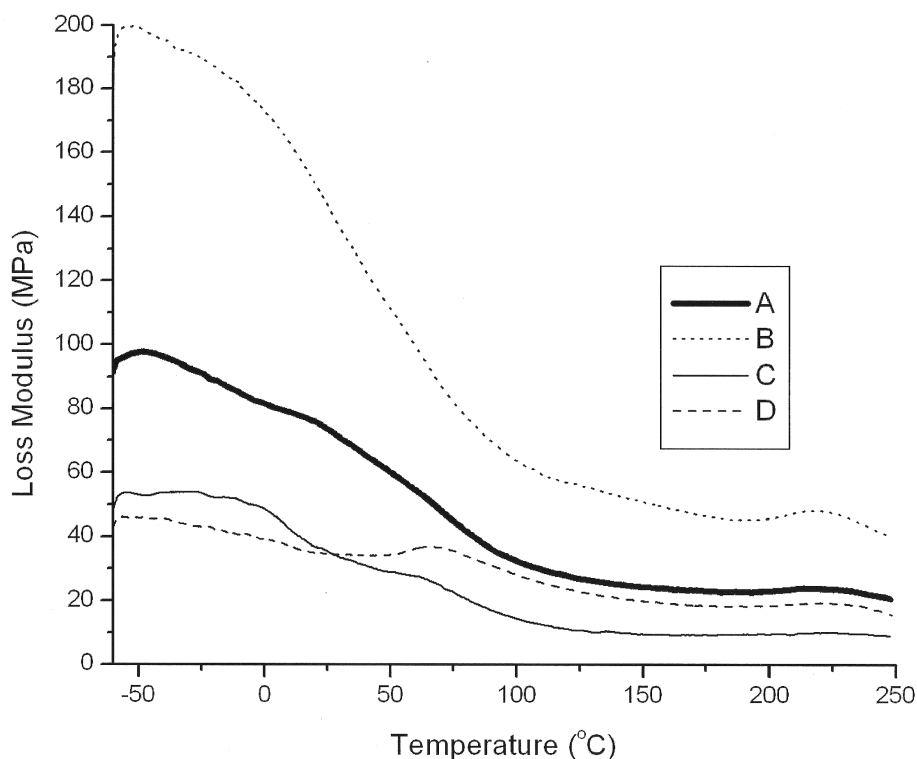


**Figure 1.** Loss modulus versus temperature for rice hull-reinforced composites with selected formulations: (A) 50 wt % CLO, 35 wt % BMA, and 15 wt % DVB; (B) 50 wt % CLO, 35 wt % BMA, 10 wt % DVB, and 5 wt % MA; (C) 50 wt % CLO, 30 wt % BMA, 15 wt % DVB, and 5 wt % MA; (D) 50 wt % CLO, 20 wt % BMA, 15 wt % DVB, and 15 wt % MA.

For the  $T_{50}$  values, however, some general trends can be identified. For example, samples with 15 wt % of DVB exhibit a  $T_{50}$  value that varies from 425 °C (entry 5, Table II) to 433 °C (entries 6 and 7, Table II). When the DVB content is below 15 wt %, the  $T_{50}$  value ranges from 413 °C (entry 9, Table II) to 420 °C (entry 4, Table II), the exception being entry 2 in Table II (408 °C). This suggests that DVB, with its higher reactivity in free radical polymerization processes, is readily polymerized. Therefore, samples with a higher DVB content possess a network with a higher crosslink density and, as a consequence, higher temperatures are required to attain a loss of 50 wt %.

**Table II.** TGA and Soxhlet extraction results for biocomposites made from conjugated linseed oil (CLO).

| Entry | BMA (wt %) | DVB (wt %) | MA (wt %) | $T_{10}$ (°C) | $T_{50}$ (°C) | $T_f$ (°C) | Residue (wt %) | Solubles (wt %) <sup>a</sup> | Insolubles (wt %) <sup>a</sup> |
|-------|------------|------------|-----------|---------------|---------------|------------|----------------|------------------------------|--------------------------------|
| 1     | 35         | 15         | -         | 304           | 426           | 606        | 15             | 5                            | 95                             |
| 2     | 35         | 10         | 5         | 300           | 408           | 635        | 11             | 4                            | 96                             |
| 3     | 35         | 5          | 10        | 304           | 419           | 611        | 11             | 5                            | 95                             |
| 4     | 35         | -          | 15        | 299           | 420           | 595        | 12             | 6                            | 94                             |
| 5     | 30         | 15         | 5         | 304           | 425           | 614        | 11             | 4                            | 96                             |
| 6     | 25         | 15         | 10        | 306           | 433           | 599        | 11             | 5                            | 95                             |
| 7     | 20         | 15         | 15        | 305           | 433           | 638        | 11             | 4                            | 96                             |
| 8     | 30         | 10         | 10        | 302           | 418           | 601        | 11             | 5                            | 95                             |
| 9     | 30         | 5          | 15        | 304           | 413           | 622        | 11             | 5                            | 95                             |
| 10    | 25         | 10         | 15        | 301           | 416           | 607        | 10             | 5                            | 95                             |

<sup>a</sup> Determined by Soxhlet extraction using CH<sub>2</sub>Cl<sub>2</sub> for 24 hours.

Only a few trends could be distinguished when analyzing the  $T_f$  values obtained for the composites prepared in this work. By comparison of entries 1 and 2 in Table II, it can be seen that substitution of 5 wt % of DVB by MA imparts an increase in  $T_f$  from 606 °C to 635 °C. This increase is probably related to the better interaction between filler and matrix after addition of MA, which gives the material a lower rate of weight loss in the later stages of thermal degradation. The same analysis can be made when comparing entries 1 and 5 in Table II. In this case, substitution of 5 wt % of BMA by MA also imparts an increase in the  $T_f$  value, from 606 °C to 614 °C. These observations correlate well with the results for the tensile strength (entries 1, 2 and 5, Table I). Comparing entries 2-4 in Table II, the  $T_f$  value decreases with the percentage of DVB in the resin, from 635 °C (entry 2, Table II) to 595 °C (entry 4, Table II). The results summarized in entries 1 and 8 (Table II) show a very similar thermal degradation profile for the corresponding samples. As mentioned earlier, the loss in

thermal stability by the lower amount of DVB in entry 8 is compensated for by the addition of MA, which gives a better matrix-filler interaction. For entries 6, 7, 9 and 10 (Table II), no specific trend is observed with a variation in the resin composition.

The TGA and DTA curves of some selected formulations, along with the data for pure rice hulls, are given in Figure 2. The TGA curves shown in Figures 2B and 2C are representative of all MA-containing composites. For those samples, little variation in the residue left after thermal degradation is observed independent of the changes in resin composition. As discussed earlier, the rice hulls are the main source of residue in these composites. Figure 2D shows that approximately 18 wt % of the residue is left after thermal degradation of the rice hulls alone. This relatively high residue content has been associated with the presence of significant amounts of silica on the surface of the rice hulls.<sup>24</sup> When comparing all of the resin formulations studied here, it can be observed that when no MA is present in the resin (entry 1, Figure 2A and Table II), a higher percentage of residue is left after thermal degradation. The close interaction of the anhydride groups in MA with the hydroxyl groups from cellulose and hemicellulose on the surface of the rice hulls may facilitate the degradation of the filler particles during the TGA experiment. For all of the other formulations, the variation in residue left after TGA is insignificant (Table II).

The DTA curves in Figure 2 show that the thermal degradation of the materials occurs in five distinct steps. The first step, around 100 °C, consists of loss of water from the rice hulls. The second step, occurring at 330 °C has two components, one associated with degradation of the hemicellulose from the rice hulls<sup>25</sup> (clearly observed in Figures 2A and

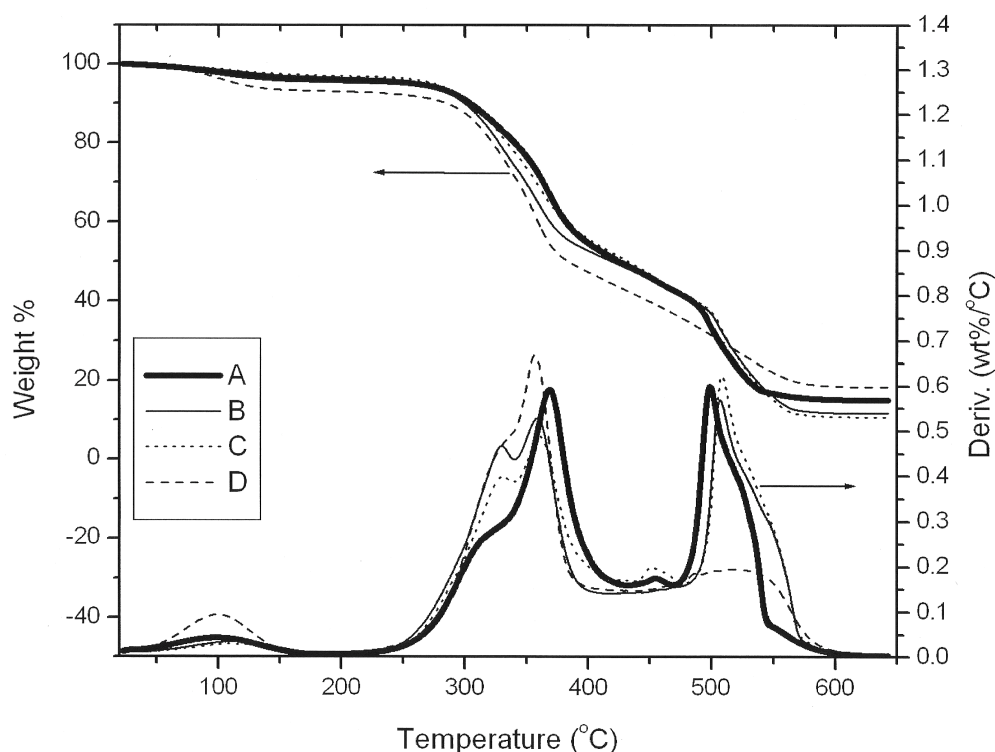


**Figure 2.** TGA and DTA curves for rice hull-reinforced composites with selected formulations: (A) 50 wt % CLO, 35 wt % BMA, and 15 wt % DVB; (B) 50 wt % CLO, 35 wt % BMA, and 15 wt % MA; (C) 50 wt % CLO, 20 wt % BMA, 15 wt % DVB, and 15 wt % MA; and pure rice hulls (D).

2D) and another associated with the degradation of MA. This latter component can be easily identified in Figures 2B and 2C. The third step occurs between 360 °C and 370 °C, and is associated with degradation of the cellulose from the rice hulls.<sup>25</sup> It is therefore present in all curves shown in Figure 2. The fourth step, at 455 °C, is only seen in Figures 2A and 2C, and can be associated with degradation of the DVB component of the resin. The last step occurs between 490 °C and 550 °C, and can be associated with the dissociation of carbon-carbon bonds from the lignin in the rice hulls<sup>25</sup> and the vegetable oil in the resin.

Finally, all of the composites presented in Table II afforded 4-6 wt % of soluble materials after Soxhlet extraction with CH<sub>2</sub>Cl<sub>2</sub> for 24 hours. Considering that the rice hulls

alone afford 10 wt % of soluble material (data not shown in Table II)<sup>24</sup>, this indicates that the majority of the resin components were incorporated into the resin during the cure and that a high crosslink density has been attained with essentially no differences between the various composite samples.

**SEM study of rice hull-reinforced composites.** The SEM images of cut and cryofractured composites with different resin compositions is shown in Figure 3. Figures 3A and 3B show the cut cross section of composites where the resin composition is 50 wt % CLO, 35 wt % BMA, and 15 wt % DVB; and 50 wt % CLO, 20 wt % BMA, 15 wt % DVB, and 15 wt % MA; respectively. A comparison of Figures 3A and 3B reveals visual evidence of the better resin-filler interaction obtained when MA is added to the resin. Indeed, a greater number of voids can easily be seen in Figure 3A. Furthermore, Figure 3B indicates an overall better dispersion of the rice hull particles in the matrix. These observations are in agreement with the results in Tables I and II.

Figures 3C and 3D show the cryofractured cross section of the same composites shown in Figures 3A and 3B at a higher magnification (100x). Here, again, it is possible to confirm the better filler-resin interaction obtained when MA is used as a comonomer in the resin. In Figure 3C, a gap can be seen between the resin and the filler particles, whereas in Figure 3D, it is almost impossible to discern any discontinuity in the interface between the resin and the filler.

**Comparison of the properties of conjugated soybean oil (CSO)- and CLO-containing composites.** Table III summarizes the tensile test and DMA results for composites made



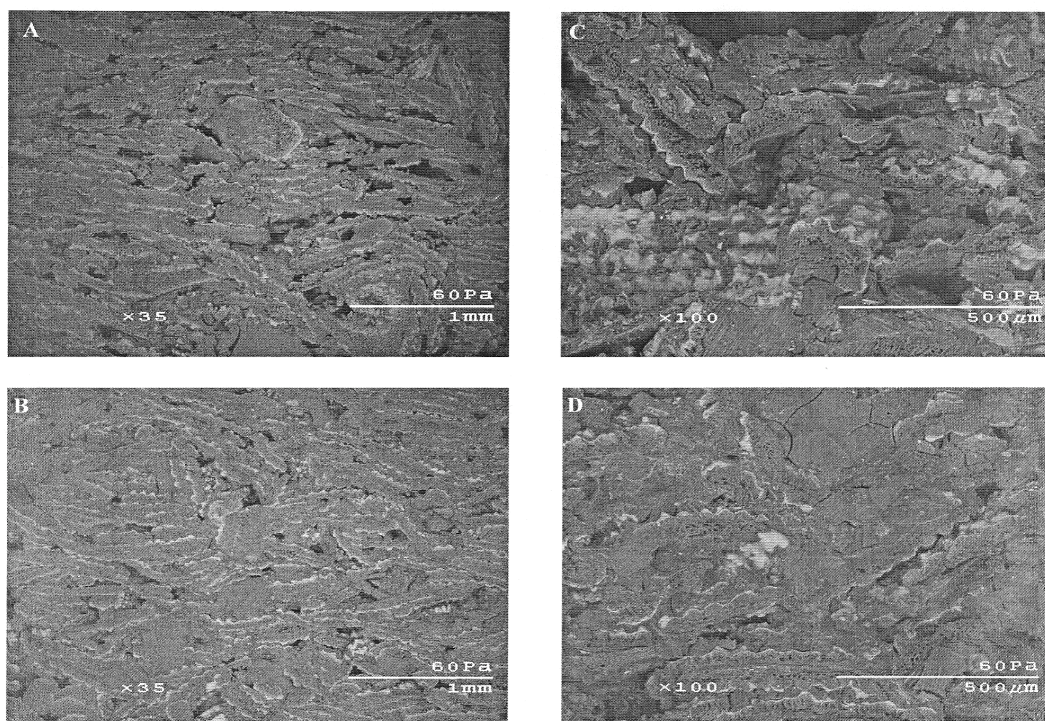


**Figure 3.** SEM images of: (A) cross section of a cut rice hull-reinforced composite (35x magnification) with resin composition 50 wt % CLO, 35 wt % BMA, and 15 wt % DVB; (B) cross section of a cut rice hull-reinforced composite (35x magnification) with resin composition 50 wt % CLO, 20 wt % BMA, 15 wt % DVB, and 15 wt % MA; (C) cross section of a cryofractured rice hull-reinforced composite (100x magnification) with resin composition 50 wt % CLO, 35 wt % BMA, and 15 wt % DVB; (D) cross section of a cryofractured rice hull-reinforced composite (100x magnification) with resin composition 50 wt % CLO, 20 wt % BMA, 15 wt % DVB, and 15 wt % MA.

from CSO and CLO. There is an increase in the tensile strength whenever 15 wt % of BMA is substituted by MA, independent of the oil used. For the CSO-containing samples, the tensile strength increases from 4.2 MPa to 7.0 MPa when MA is added to the resin (entries 1 and 2, Table III). For the CLO-containing samples, the tensile strength increases from 5.9 MPa to 9.1 MPa (entries 3 and 4, Table III). As mentioned earlier, MA acts as a compatibilizer between the matrix and the filler, helping in stress transfer and therefore improving the tensile strength. An increase in Young's modulus from 1.2 GPa to 2.2 GPa

(entries 1 and 2, Table III) is also observed when BMA is partially replaced by MA in the CSO-containing composites. For CLO-containing composites, there is no change in  $E$  upon substitution of BMA by MA (2.3 GPa, entries 3 and 4 in Table III). As expected, the use of CLO gives composites with better tensile properties than those made from CSO. In the absence of MA, the Young's modulus and the tensile strength increase, respectively, from 1.2 GPa and 4.2 MPa to 2.3 GPa and 5.9 MPa (entries 1 and 3 in Table III) by changing the oil in the resin composition from CSO to CLO. The same is observed for the composites containing MA.  $E$  and the tensile strength increase, respectively, from 2.2 GPa and 7.0 MPa to 2.3 GPa and 9.1 MPa (entries 2 and 4 in Table III). This effect is related to the higher number of carbon-carbon double bonds present in the linseed oil compared to soybean oil. The higher degree of unsaturation of linseed oil results in a resin with a higher crosslink density.

**Table III.** Tensile tests and DMA results for biocomposites made from conjugated linseed oil (CLO) and conjugated soybean oil (CSO).

| Entry | Oil<br>(50 wt %) | BMA<br>(wt %) | DVB<br>(wt %) | MA<br>(wt %) | Young's<br>Modulus<br>(GPa) | Tensile<br>Strength<br>(MPa) | Storage<br>Modulus<br>at 130 °C<br>(MPa) | $T_g$ (°C)          |
|-------|------------------|---------------|---------------|--------------|-----------------------------|------------------------------|--|---------------------|
| 1     | CSO              | 35            | 15            | -            | 1.2 ± 0.3                   | 4.2 ± 0.7                    | 215                                      | 24, 78 <sup>a</sup> |
| 2     | CSO              | 20            | 15            | 15           | 2.2 ± 0.9                   | 7.0 ± 1.2                    | 613                                      | 0, 92 <sup>a</sup>  |
| 3     | CLO              | 35            | 15            | -            | 2.3 ± 0.5                   | 5.9 ± 0.6                    | 220                                      | 52                  |
| 4     | CLO              | 20            | 15            | 15           | 2.3 ± 0.4                   | 9.1 ± 1.7                    | 255                                      | 75                  |

<sup>a</sup> Two  $T_g$ 's were observed.

An increase in storage modulus is also observed when 15 wt % of BMA is replaced by MA. In composites containing CSO, the increase is more substantial (from 215 MPa to

613 MPa, entries 1 and 2 in Table III) than in those containing CLO (from 220 MPa to 255 MPa, entries 3 and 4 in Table III). The effect of the oil on the storage modulus isn't clear as an increase from 215 MPa to 220 MPa is observed when CSO is replaced by CLO in MA-free composites (entries 1 and 3 in Table III), whereas a substantial decrease from 613 MPa to 255 MPa is observed for the MA-containing composites (entries 2 and 4 in Table III).

The glass transition temperatures measured by DMA and reported in Table III reveal an interesting phenomenon observed in previous studies.<sup>19</sup> The presence of two very distinct  $T_g$ 's for CSO-containing samples indicates that there is, most likely, a phase separation of the resin during polymerization of the different co-monomers. Due to its lower reactivity in comparison to CLO, CSO polymerizes at a slower rate during the cure of the resin. This slower polymerization rate results in an initially formed phase which is richer in the more reactive co-monomers, such as DVB. When most of the DVB is polymerized, a CSO-rich phase starts to form, thereby explaining the two  $T_g$ 's observed.

The tan delta curves of samples containing CSO and CLO are shown in Figure 4. Figure 4A is representative of all resin compositions containing CLO and MA (Table I). The CSO-containing composites (Figures 4B and 4C) exhibit two tan delta peaks, which is indicative of a possible phase separation that results in two distinct  $T_g$  values, as discussed earlier. The first peak is very obvious and occurs at temperatures lower than 50 °C, whereas the second transition is less obvious and occurs at higher temperatures. When comparing composites made with the same vegetable oil (Figures 4A and 4C, for example), sharper tan delta peaks are obtained when MA is not a part of the formulation. This result implies that although a better filler-resin interaction is obtained when MA is added to the resin, a more

heterogeneous matrix is formed. The difference in reactivity between the vegetable oil and the other co-monomers may result in an initially formed oil-poor phase containing anhydride units that can strongly interact with the filler particles. The interaction between MA and the rice hulls compromises the overall dispersion of growing polymer chains among the filler particles, resulting in a more heterogeneous polymer phase.

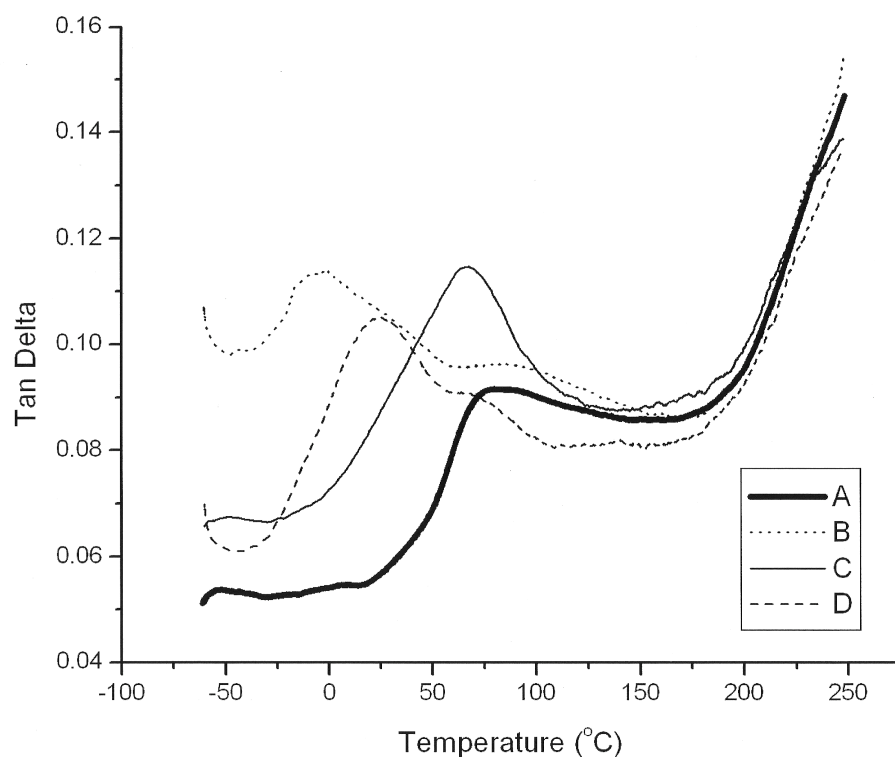


**Figure 4.** Tan Delta curves of: (A) rice hull-reinforced composite with resin composition 50 wt % CLO, 20 wt % BMA, 15 wt % DVB, and 15 wt % MA; (B) rice hull-reinforced composite with resin composition 50 wt % CSO, 20 wt % BMA, 15 wt % DVB, and 15 wt % MA; (C) rice hull-reinforced composite with resin composition 50 wt % CLO, 35 wt % BMA, and 15 wt % DVB; (D) rice hull-reinforced composite with resin composition 50 wt % CSO, 35 wt % BMA, and 15 wt % DVB.

Table IV presents the TGA and extraction data for composites containing CSO and CLO. Little variation was found for the  $T_{10}$  values of the composites listed in Table IV, with

a maximum  $T_{10}$  value of 306 °C for the CSO-containing composite without MA and a minimum of 301 °C for the CSO-containing composite with MA (entries 1 and 2 in Table IV). As discussed previously, this initial 10 wt % loss is related to initial degradation of the filler, and therefore, switching from CLO to CSO should have no effect on the  $T_{10}$  value.

**Table IV.** TGA and Soxhlet extraction results for biocomposites made from conjugated linseed oil (CLO) and conjugated soybean oil (CSO).

| Entry | Oil<br>(50 wt %) | BMA<br>(wt %) | DVB<br>(wt %) | MA<br>(wt %) | $T_{10}$ (°C) | $T_{50}$ (°C) | $T_f$ (°C) | Solubles<br>(wt %) <sup>a</sup> | Insolubles<br>(wt %) <sup>a</sup> |
|-------|------------------|---------------|---------------|--------------|---------------|---------------|------------|---------------------------------|-----------------------------------|
| 1     | CSO              | 35            | 15            | -            | 306           | 405           | 592        | 4                               | 96                                |
| 2     | CSO              | 20            | 15            | 15           | 301           | 419           | 600        | 4                               | 96                                |
| 3     | CLO              | 35            | 15            | -            | 304           | 426           | 606        | 5                               | 95                                |
| 4     | CLO              | 20            | 15            | 15           | 305           | 433           | 638        | 4                               | 96                                |

<sup>a</sup>Determined by Soxhlet extraction using CH<sub>2</sub>Cl<sub>2</sub> for 24 hours.

The  $T_{50}$  values, on the other hand, show a close relationship to the resin composition. There is an increase in the  $T_{50}$  value whenever MA is added to the resin. For CSO-containing composites, the  $T_{50}$  value increases from 405 °C to 419 °C (entries 1 and 2 in Table IV), while the increase in CLO-containing composites occurs from 426 °C to 433 °C (entries 3 and 4 in Table IV). This behavior was previously attributed to the better filler-resin interaction imparted by the presence of MA. When the  $T_{50}$  values of CSO- and CLO-containing composites are compared, it becomes evident that CLO gives higher numbers. Indeed, there is an increase in the  $T_{50}$  value from 405 °C to 426 °C when CSO is substituted by CLO in MA-free composites (entries 1 and 3 in Table IV). Also, an increase from 419 °C to 433 °C in the  $T_{50}$  value is seen when CLO substitutes CSO in MA-containing composites (entries 2 and 4 in Table IV). As mentioned earlier, CLO is expected to give a resin with a

higher crosslink density than CSO, which would account for the higher temperatures required to attain 50 wt % degradation.

The  $T_f$  values for the samples listed in Table IV exhibit a very similar trend to the  $T_{50}$  values. An increase in the  $T_f$  value was detected whenever MA is added to the resin (from 592 °C to 600 °C for the CSO-containing composites and from 606 °C to 638 °C for the CLO-containing composites, entries 1 and 2, and 3 and 4 in Table IV). Also, an increase in  $T_f$  is observed when CSO is replaced by CLO (from 592 °C to 606 °C for the MA-free composites and from 600 °C to 638 °C for the MA-containing samples; entries 1 and 3, and 2 and 4 in Table IV).

The percentage of solubles determined by Soxhlet extraction of the composites doesn't reveal much, since only a minimal variation was detected. All samples analyzed afforded 4-5 wt % of soluble material (Table IV), thus showing that the amount of material retained in the composite after extraction is not strongly dependent on the resin composition variations introduced here. The Soxhlet extraction results reflect how much of the monomers have been incorporated into the matrix. In fact, both CSO and CLO can crosslink, to different degrees, through their multiple carbon-carbon double bonds. So no significant variations in the extraction results were expected among the samples shown in Table IV. From the  $^1\text{H}$  NMR spectra of the extracts of selected samples, it can be clearly seen that the soluble content recovered from the composites (Figures 5A and 5C) resembles the unreacted CLO and CSO (Figures 5B and 5D, respectively). The methylene hydrogen peaks between 4.0 ppm and 4.5 ppm in Figures 5A and 5B confirm the presence of a triglyceride unit in the extract. The absence of other distinctive peaks in the spectra indicates that, with the

exception of the conjugated oil, all the other co-monomers are fully incorporated into the cured resin.

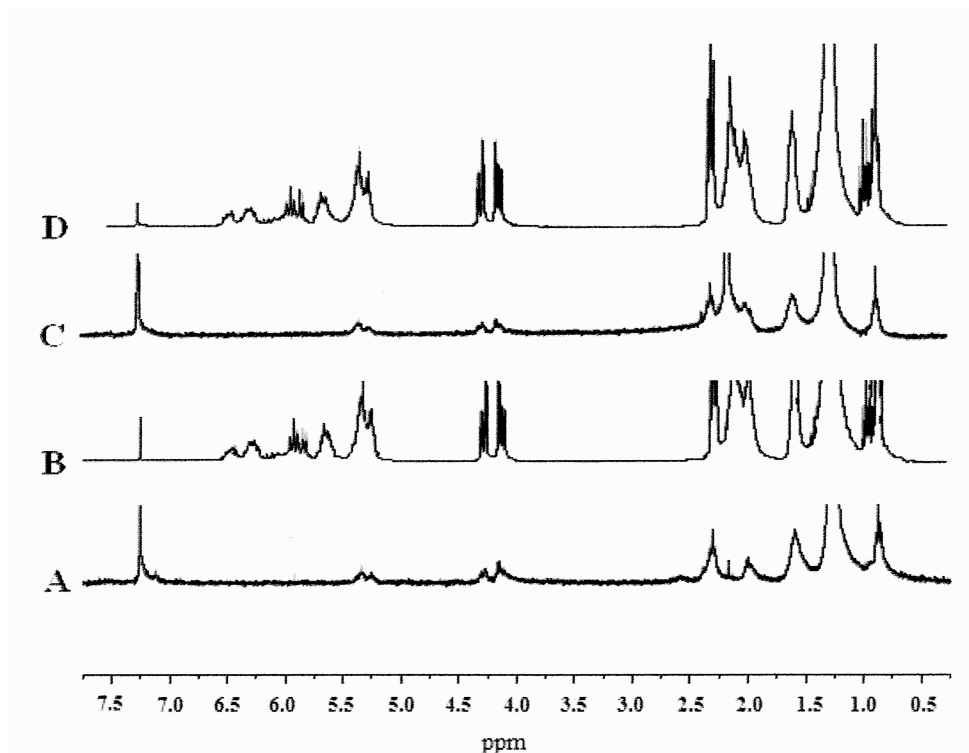


**Figure 5.**  $^1\text{H}$  NMR spectra of: (A) extract of a rice hull biocomposite with resin composition 50 wt % CLO, 35 wt % BMA, and 15 wt % DVB; (B) conjugated linseed oil; (C) extract of a rice hull biocomposite with resin composition 50 wt % CSO, 20 wt % BMA, 15 wt % DVB, and 15 wt % MA; (D) conjugated soybean oil.

### Conclusions

Rice hull-reinforced composites have been prepared by the free radical polymerization of resins with different compositions. The resins used had a constant conjugated vegetable oil (CLO or CSO) content of 50 wt % and a variable amount of BMA, DVB, and MA. The pressure, cure sequence, filler load and particle size were kept constant. Tensile tests, DMA, and TGA experiments showed an overall improvement in the

composites' properties whenever MA was added as a co-monomer in the resin. MA acts as a compatibilizer between the filler particles and the matrix. These results have been corroborated by SEM images showing a better filler-resin interaction in composites where the matrix contains MA. A comparison between CSO and CLO as the major resin component showed that composites made from CLO exhibited better overall properties than those made with CSO. The Soxhlet extraction experiments, along with the  $^1\text{H}$  NMR spectra of the extracts, demonstrate that most of the monomers used were fully incorporated into the cured resin, with the exception of the conjugated oils.

### **Acknowledgments**

The authors thank the Recycling and Reuse Technology Transfer Center of the University of Northern Iowa for financial support, the Missouri Crop Improvement Association for the rice hulls, Professor Michael Kessler from the Department of Material Sciences and Engineering and Dr. Richard Hall from the Department of Natural Resource Ecology and Management at Iowa State University for the use of their facilities, Warren Straszheim from the Department of Material Sciences and Engineering for help with the SEM and X-ray mapping experiments, and Dr. Douglas Stokke from the Department of Natural Resource Ecology and Management for important information concerning the rice hulls.

### **References**

1. Ashraf, S. M.; Ahmad, S.; Riaz, U. *Polym Int* 2007, 56, 1173.
2. Mosiewicki, M.; Borrajo, J.; Aranguren, M. I. *Polym Int* 2007, 56, 779.
3. Sharma, V.; Banait, J. S.; Kundu, P. P. *J Appl Polym Sci* 2009, 114, 446.
4. Sharma, V.; Banait, J. S.; Kundu, P. P. *J Appl Polym Sci* 2009, 111, 1816.



5. Gultekin, M.; Beker, U.; Guner, F. S.; Erciyes, A. T.; Yagci, Y. *Macromol Mater Eng* 2000, 283, 15.
6. Sharma, H. O.; Alam, M.; Riaz, U.; Ahmad, S.; Ashraf, S. M. *Int J Polymer Mater* 2007, 56, 437.
7. Wang, C.; Yang, L.; Ni, B.; Shi, G. *J Appl Polym Sci* 2009, 114, 125.
8. Thulasiraman, V.; Rakesh, S.; Sarojadevi, M. *Polymer Composites* 2009, 30, 49.
9. Bhuyan, S.; Holden, L. S.; Sundararajan, S.; Andjelkovic, D.; Larock, R. C. *Wear* 2007, 263, 965.
10. Henna, P. H.; Andjelkovic, D. D.; Kundu, P. P.; Larock, R. C. *J Appl Polym Sci* 2007, 104, 979.
11. Lima, D. G.; Soares, V. C. D.; Ribeiro, E. B.; Carvalho, D. A.; Cardoso, E. C. V.; Rassi, F. C.; Mundim, K. C.; Rubim, J. C.; Suarez, P. A. Z. *J Anal Appl Pyrolysis* 2004, 71, 987.
12. Larock, R. C.; Dong, X.; Chung, S.; Reddy, C. K.; Ehlers, L. E. *J Am Oil Chem Soc* 2001, 78, 447.
13. Kundu, P. P.; Larock, R. C. *Biomacromolecules* 2005, 6, 797.
14. Xia, Y.; Henna, P. H.; Larock, R. C. *Macromol Mater Eng* 2009, 294, 590.
15. Andjelkovic, D. D.; Larock, R. C. *Biomacromolecules* 2006, 7, 927.
16. Andjelkovic, D. D.; Lu, Y.; Kessler, M. R.; Larock, R. C. *Macromol Mater Eng* 2009, 294, 472.
17. Valverde, M.; Andjelkovic, D.; Kundu, P. P.; Larock, R. C. *J Appl Polym Sci* 2008, 107, 423.
18. Pfister, D. P.; Larock, R. C. *Bioresour Technol* 2010, 101, 6200.
19. Quirino, R. L.; Larock, R. C. *J Appl Polym Sci* 2009, 112, 2033.
20. Bhuyan, S.; Sundararajan, S.; Pfister, D.; Larock, R. C. *Tribol Int* 2010, 43, 171.
21. Pfister, D. P.; Baker, J. R.; Henna, P. H.; Lu, Y.; Larock, R. C. *J Appl Polym Sci* 2008, 108, 3618.
22. Teng, H.; Wei, Y. *Ind Eng Chem Res* 1998, 37, 3806.
23. Srebrenkoska, V.; Gaceva, G. B.; Dimeski, D. Maced. *J. Chem. Chem. Eng.* 2009, 28, 99.
24. Quirino, R. L.; Larock, R. C. *J Appl Polym Sci*, accepted.
25. Barneto, A. G.; Carmona, J. A.; Alfonso, J. E. M.; Alcaide, L. J. *Bioresour Technol* 2009, 100, 3963.

**CHAPTER 5. SOYBEAN AND LINSEED OIL-BASED COMPOSITES  
REINFORCED WITH WOOD FLOUR AND WOOD FIBERS**

A Paper Accepted for Publication in Journal of Applied Polymer Science.

Copyright © 2011, Wiley-Blackwell

Rafael L. Quirino, John Woodford, Richard C. Larock\*

*Department of Chemistry, Iowa State University, Ames, Iowa 50011*

**Abstract**

Composites consisting of a conjugated linseed or soybean oil-based thermoset reinforced with wood flour and wood fibers have been prepared by free radical polymerization. The thermoset resin consists of a copolymer of conjugated linseed oil (CLO) or conjugated soybean oil (CSO), *n*-butyl methacrylate (BMA), divinylbenzene (DVB), and maleic anhydride (MA). The composites were cured at 180 °C and 600 psi and post-cured for two hours at 200 °C under atmospheric pressure. The effect of varying filler load, time of cure, filler particle size, origin of the fillers, and resin composition has been assessed by means of tensile tests, DMA, TGA, Soxhlet extraction followed by <sup>1</sup>H NMR spectroscopic analysis of the extracts, and DSC. The best processing conditions have been established for the pine wood flour composites. It has been observed that the addition of MA to the resin composition improves the filler-resin interaction.

## Introduction

With the current desire to find replacements for petroleum-derived chemicals and materials, several bio-based resin systems have been developed in the past few years.<sup>1-15</sup> These biopolymers consist of linseed and soybean oil-based resins,<sup>1-8</sup> polyurethanes,<sup>1,2</sup> polyester amides,<sup>3</sup> multicomponent thermosets,<sup>4-7</sup> and cyanate esters.<sup>8</sup> Some of these systems have been reinforced with inorganic fillers, such as nanoclays,<sup>9,10</sup> and glass fibers.<sup>11,12</sup> Another approach, adopted by several authors, for the preparation of “green” composites, is the reinforcement of standard petroleum-derived thermoplastics with a variety of natural fillers.<sup>13-19</sup> Only recently, some progress on the reinforcement of blends of petroleum-derived unsaturated epoxy resins and 10 wt % of epoxidized soybean oil with natural fillers has been reported.<sup>20</sup>

The Larock group at Iowa State University has focused its initial efforts in the study of bio-based thermosets on high natural oil content (~40-60 wt %) materials.<sup>21-24</sup> The cationic co-polymerization of modified vegetable oils and other vinylic comonomers results in homogeneous bio-based materials with a smooth surface.<sup>25</sup> Due to the problems associated with the cure of vegetable oil-based systems in the presence of free radical initiators, such as the entrapment of bubbles in the resin and crack formation, free radical resins received little attention in the early stages of our research.<sup>26</sup> The thermal copolymerization of such systems has also been investigated, but the process is not considered to be practical due to the high temperatures and long times required in order to obtain viable materials.<sup>27</sup>

More recently, in an attempt to improve the mechanical properties of the aforementioned bio-based polymers, the Larock group has used inorganic<sup>28,29</sup> and natural

fillers as reinforcements for the preparation of “green” composites.<sup>30-34</sup> The natural filler-reinforced composites contain up to 85 wt % of bio-based materials, including the resin and the filler.<sup>30-34</sup> In the preparation of such materials, it has been demonstrated that free radical initiators are quite effective in crosslinking the carbon-carbon double bonds in the oils and the other monomers used. The presence of ligno-cellulosic filler particles minimizes shrinkage of the resin and only minimal micro-cracks have been detected by scanning electron microscopy (SEM) of soybean hull composites.<sup>31</sup> Recent results from the study of natural filler-reinforced composites in the Larock group suggested that maleic anhydride (MA) can serve as a good filler-resin compatibilizer and help improve the stress transfer from the matrix to the reinforcement, resulting in an overall increase of the mechanical properties.<sup>33,34</sup>

With an estimated annual production of 21.2 billion pounds in 2007,<sup>35</sup> soybean oil is one of the most prevalent vegetable oils in the United States. Soybean oil consists of a triglyceride with a fatty acid composition of 11% palmitic acid, 3% stearic acid, 22% oleic acid, 55% linoleic acid, and 9% linolenic acid.<sup>36</sup> The total average number of carbon-carbon double bonds per triglyceride in soybean oil is 4.5.<sup>37</sup> When these carbon-carbon double bonds are isomerized and brought into conjugation using methodology developed by the Larock group and widely used by us,<sup>38</sup> soybean oil can readily polymerize and crosslink in a free radical process to form a rigid thermoset. With a similar fatty acid composition (4% stearic acid, 19% oleic acid, 15% linoleic acid, 57% linolenic acid, and 5% of other fatty acids), but a higher degree of unsaturation (6.0 carbon-carbon double bonds per triglyceride), linseed oil is also a potential bio-based monomer for the preparation of “green” composites.<sup>23</sup>

The use of wood flour and wood fibers as reinforcements in the preparation of “green” composites is known.<sup>13,15</sup> However, in most cases, petroleum-derived thermoplastics have been used as the matrix.<sup>13,15</sup> Here, we report the preparation of soybean and linseed oil-based thermosets reinforced with pine, oak, and maple wood flours and a mixture of hardwood fibers. Parameters, such as cure time, filler load, filler particle size, origin of the filler, and resin composition, have been varied and the resulting properties of the “green” composites have been assessed by differential scanning calorimetry (DSC), thermogravimetric analysis (TGA), tensile tests, dynamic mechanical analysis (DMA), and Soxhlet extraction followed by proton nuclear magnetic resonance (<sup>1</sup>H NMR) spectroscopic analysis of the extracts. After analysis of the results, optimal conditions have been suggested for the preparation of such composites, and the effect of MA as a filler-resin compatibilizer has been verified.

## Experimental

**Materials.** *n*-Butyl methacrylate (BMA) was purchased from Alfa Aesar (Ward Hill, MA). DVB, MA and *t*-butyl peroxide (TBPO) were purchased from Sigma-Aldrich (St. Louis, MO). All were used as received. Soybean oil (Great Value brand – Bentonville, AR) was purchased in a local grocery store, and Superb linseed oil was provided by ADM (Red Wing, MN). The carbon-carbon double bonds in both oils have been isomerized and brought into conjugation using a rhodium catalyst, following a method developed and frequently used by our group.<sup>38</sup> The products contain conjugated carbon-carbon double bonds, like in a 1,3-diene, and will be referred to in the text as conjugated oils. The wood flours of different particle sizes and wood fibers were provided by American Wood Fibers (Schofield, WI). The

fillers were dried overnight at 70 °C in a vacuum oven right before impregnation with the resin to improve filler-resin compatibility.

**General procedure for preparation of the composites.** *Wood flour composites.* The crude resin was obtained by mixing the conjugated vegetable oil, BMA and DVB in a beaker. MA was melted in a hot water bath and quickly added to the crude resin mixture under agitation, along with the free radical initiator TBPO. The natural fillers were manually mixed with the crude resin in a large beaker using a spatula, resulting in thorough impregnation of the fillers. The impregnated fillers were then transferred to a 6" x 6" mold, and compression molded at 180 °C and 600 psi. The composites were removed from the mold and post-cured in a convection oven for 2 hours at 200 °C at ambient pressure. In all composites produced, the resin has a conjugated vegetable oil content of 50 wt % and the optimum amount of TBPO has been determined to be, in preliminary tests, an extra 5 wt % of the total resin weight. The amounts of DVB, BMA and MA have been varied, as indicated in the text, to produce composites of various compositions.

*Wood fiber composites.* Due to the very low density of the wood fibers, and the difficulties associated with handling that material, only one composite has been prepared using mixed hardwood fibers, which exhibit a wide variation in the aspect ratio, as reinforcement. The aspect ratio of the mixed wood fibers has not been determined by us, and the fibers have been used as received. Following the same procedure described for the preparation of the wood flour composites, the wood fibers were impregnated with a resin containing 50 wt % of conjugated linseed oil (CLO), 35 wt % of BMA, 15 wt % of DVB, and an extra 5 wt % of the total resin weight of TBPO. The final filler to resin ratio obtained was 50/50. The mixture

was compression molded at 130 °C and 400 psi for 5 hours, and post-cured in a convection oven at 150 °C for 2 hours at ambient pressure. For comparison purposes, a pine wood flour (particle size diameter <310 μm) composite was prepared using the same parameters.

**Characterization of the composites.** Tensile tests were conducted at room temperature according to ASTM D-638 using an Instron universal testing machine (model 5569) equipped with a video extensometer and operating at a crosshead speed of 2.0 mm/min. Dog bone-shaped test specimens were machined from the original samples to give the following gauge dimensions: 57.0 mm x 12.7 mm x 4.5 mm (length x width x thickness, respectively). For each composite, seven dog bones were cut and tested. The results presented in the text are the average of these measurements along with the calculated standard deviation.

DMA experiments were conducted on a Q800 DMA (TA Instruments, New Castle, DE) using a three point bending mode with a 10.0 mm clamp. Rectangular specimens of 22.0 mm x 8.5 mm x 1.5 mm (length x width x thickness, respectively) were cut from the original samples. Each specimen was cooled to -60 °C and then heated at 3 °C/min to 250 °C. The experiment was conducted using a frequency of 1 Hz and an amplitude of 14 μm under air. Two runs for each sample were carried out and the results presented in the text reflect the average of the two measurements.

Soxhlet extraction was conducted to determine the amount of soluble materials in the composites. A 2.0 g sample of each composite was extracted for 24 h with dichloromethane (CH<sub>2</sub>Cl<sub>2</sub>). After extraction, the solubles were recovered by evaporating the CH<sub>2</sub>Cl<sub>2</sub> under vacuum. Both soluble and insoluble materials were dried overnight at 70 °C. The dried soluble fraction was then dissolved in deuterated chloroform (CDCl<sub>3</sub>) and the <sup>1</sup>H NMR

spectrum was obtained using a Varian Unity spectrometer (Varian Associates, Palo Alto, CA) operating at 300 MHz. The  $^1\text{H}$  NMR spectra helped to identify the solubles in each sample.

A Q50 TGA instrument (TA Instruments, New Castle, DE) was used to measure the weight loss of the samples under an air atmosphere. The samples (~10 mg) were heated from room temperature to 650 °C at a rate of 20 °C/min.

DSC experiments were performed on a Q20 DSC instrument (TA Instruments, New Castle, DE) under a  $\text{N}_2$  atmosphere over a temperature range of -20 °C to 400 °C, while heating at a rate of 20 °C/min. The samples weighed ~10 mg.

## Results and Discussion

**Filler load evaluation.** In order to determine the optimal filler to resin ratio for the preparation of wood flour composites, samples containing 60-85 wt % of pine wood flour have been prepared and their mechanical properties have been measured by tensile tests and DMA. Table I summarizes the results obtained for composites with a constant resin composition equal to 50 wt % of conjugated soybean oil (CSO), 35 wt % of BMA, and 15 wt % of DVB. The pine flour particle size diameter was also held constant at <310  $\mu\text{m}$ . The composites have been cured at 180 °C and 600 psi for 5 hours, followed by a post-cure step at 200 °C and ambient pressure for 2 hours.

From the tensile test results presented in Table I, one can see an overall increase in both the Young's modulus and the tensile strength of the composites with increasing filler loads. The increase in the tensile properties is clearer for filler loads comprised between 60



**Table I.** Tensile tests, DMA, and extraction results for pine wood flour composites with varying filler loads

| Filler Load (wt %) <sup>a</sup> | <i>E</i> (GPa) | Tensile Strength (MPa) | <i>E'</i> at 130 °C (MPa) | <i>T<sub>g1</sub></i> (°C) | <i>T<sub>g2</sub></i> (°C) | Soluble Fraction (%) <sup>b</sup> |
|---------------------------------|----------------|------------------------|---------------------------|----------------------------|----------------------------|-----------------------------------|
| - <sup>c</sup>                  | -              | -                      | 44                        | -51                        | 37                         | 13                                |
| 60                              | 1.5 ± 0.1      | 9.1 ± 1.0              | 739                       | 1                          | 75                         | 8                                 |
| 70                              | 1.8 ± 0.1      | 9.5 ± 2.0              | 946                       | -4                         | 78                         | 8                                 |
| 75                              | 2.8 ± 0.9      | 9.5 ± 1.6              | 1033                      | -3                         | 85                         | 9                                 |
| 80                              | 2.8 ± 0.9      | 11.7 ± 2.4             | 1072                      | 4                          | 79                         | 5                                 |
| 85                              | 3.3 ± 0.4      | 10.5 ± 0.7             | 1026                      | 7                          | 61                         | 4                                 |

<sup>a</sup> Filler particle size diameter <310 μm. Cure conditions: 180 °C and 600 psi for 5 hours, followed by a post-cure step at 200 °C and ambient pressure for 2 hours.

<sup>b</sup> Determined by Soxhlet extraction.

<sup>c</sup> Unreinforced resin containing 50 wt % of CSO, 35 wt % of BMA, and 15 wt % of DVB

wt % and 75 wt %. Beyond that point, the differences in Young's modulus fall within the standard deviation associated with the measurements. Although a high value of 3.3 GPa is observed for the sample containing 85 wt % of pine wood flour, there is no statistical difference between the samples. The same situation is observed for the tensile strength of samples containing 80 wt % and 85 wt % of filler. In this case, the strength peaks at 11.7 MPa, for the sample prepared with 80 wt % of pine flour, but the difference with respect to the sample containing 85 wt % of pine flour falls within the standard deviation of the two measurements.

When the flexural properties of samples prepared with varying amounts of pine flour are compared, a clear increase in the storage modulus at 130 °C (well above the detected *T<sub>g</sub>*'s) is observed when the filler load is increased from 60 wt % to 80 wt %. This increase reflects the reinforcement imparted by the filler, which is a consequence of the stress transfer from

the matrix to the filler particles, avoiding dissipation of the energy in polymer chain motions and therefore yielding a higher storage modulus. An even higher effect is obtained when comparing the unreinforced resin and the sample containing 60 wt % of the filler. In that case, there is approximately a 17 fold improvement in the storage modulus! Nevertheless, as noted in our previous work with soybean and rice hulls,<sup>31,33</sup> when the filler load is exceedingly high (85 wt %, Table I), the amount of resin in the system isn't enough to bind all of the filler particles, leading to filler agglomeration and formation of weak points in the composite morphology that negatively impact the storage modulus.

Another interesting observation from the flexural tests is the presence of two distinct  $T_g$ 's for the systems presented in Table I. This phenomenon has been observed and analyzed previously by us and is attributed to a phase separation of the resin due to the very distinct reactivity of the co-monomers towards free radicals, most noticeably CSO and DVB.<sup>31,33</sup>

The soluble content recovered after Soxhlet extraction of the composites bearing different filler loads is also presented in Table I. The soluble content of the pure resin corresponds to 13 wt %, and it has been identified as being mainly unreacted CSO.<sup>31</sup> Indeed, the  $^1\text{H}$  NMR spectrum of the resin extract (Figure 1B) matches very closely that of pure CSO (Figure 1A), except for small peaks at 4.0 ppm and 7.0 ppm in the spectrum of the resin extract. Those peaks are most likely related to either residual unreacted BMA and DVB respectively or to non-crosslinked oligomers containing those units. Some differences in the pattern of the 1.9-2.2 ppm signal are also observed when comparing Figures 1A and 1B. Those differences are possibly related to the presence of BMA, DVB, and/or non-crosslinked oligomers in the extract of the resin. It is, however, extremely hard to attribute the observed

differences in that range to specific components of the system due to the extensive overlap of signals related to aliphatic protons of the various resin components.

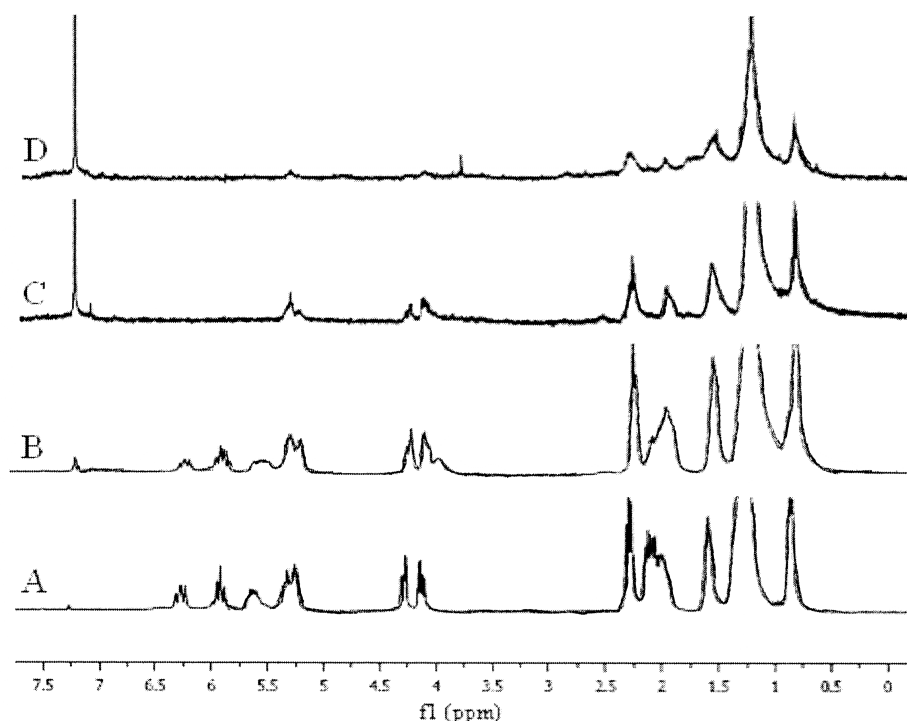


**Figure 1.**  $^1\text{H}$  NMR spectra of (A) conjugated soybean oil (CSO), (B) extract of a resin containing 50 wt % of CSO, 35 wt % of BMA, and 15 wt % of DVB, (C) extract of a pine wood flour composite containing an 80/20 filler to resin ratio and cured for 4 hours, (D) extract of pine wood flour.

Pine wood flour only yields 9 wt % of an unidentified soluble material (result not shown in Table I). Thus, it is expected that an increase in the filler content will result in a decrease of the recovered solubles after Soxhlet extraction as is observed in Table I. The material extracted from the wood flour is rich in carbon-hydrogen bonds as evidenced by the peaks in the 0.8-2.5 ppm range (Figure 1D) with the possibility of the presence of carbon-carbon double bonds and/or oxygenated functional groups evident from the small peaks

located at 3.7 ppm and 5.3 ppm. Since this material has not been identified yet, it is impossible to predict what role it plays in the system studied. When analyzing the spectrum of a composite extract (Figure 1C), it is possible to identify most of the features found in the spectrum of the resin extract, confirming that the majority of what is extracted comes from the matrix and is most likely unreacted CSO and trace amounts of the other comonomers. The intensity of the solvent peak (7.26 ppm) indicates how concentrated the solutions used to obtain the corresponding spectra were. It is noteworthy that only a very small amount of extract has been recovered from samples C and D, resulting in more dilute samples and more intense solvent peaks.

The thermal stability of the wood flour composites can be assessed by a comparison of the TGA curves of some selected samples shown in Figure 2. Due to the high filler load present in the composites (70 wt % and 80 wt %, Figures 2C and 2D, respectively), their thermal degradation profile more closely resembles that of the pure pine wood flour (Figure 2B) rather than the resin (Figure 2A). After the initial loss of water by the filler particles (around 100 °C, Figure 2), the composites and the pure filler start to degrade at approximately 225 °C, whereas the pure resin only starts degrading at approximately 275 °C. Thus, the fillers are less thermally stable than the resin.

It is interesting to note that despite the higher thermal stability of the resin system, the composites degrade slightly faster than the pure filler. This is confirmed by the first peak of the DTA curves ( $T_{max1}$ ). While the pure filler exhibits a  $T_{max1}$  of 348 °C, samples C and D exhibit a  $T_{max1}$  of 334 °C and 329 °C, respectively. This first degradation peak can be

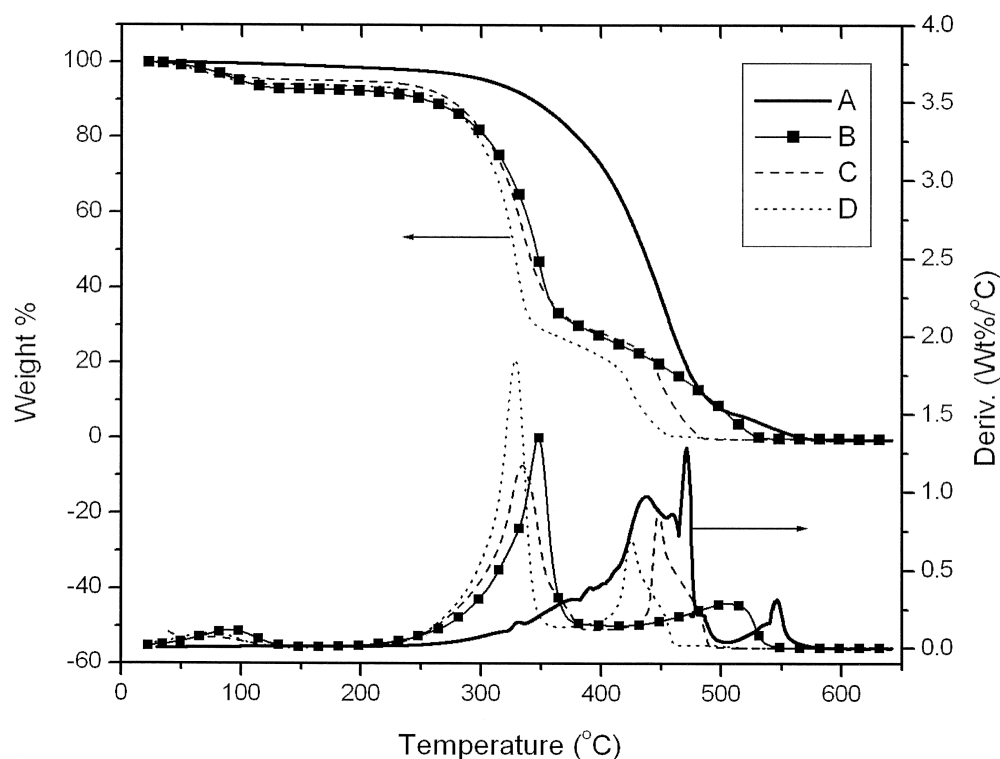


**Figure 2.** TGA and DTA curves of (A) an unreinforced resin with the following composition: 50 wt % of CSO, 35 wt % of BMA, and 15 wt % of DVB; (B) pine wood flour; (C) a composite containing 70 wt % of pine wood flour (particle size diameter  $<310 \mu\text{m}$ ) and 30 wt % of resin A; and (D) a composite containing 80 wt % of pine wood flour (particle size diameter  $<310 \mu\text{m}$ ) and 20 wt % of resin A.

attributed to the hemicellulose component of the ligno-cellulosic materials.<sup>31,33</sup> The negative effect that the resin has on the thermal stability of the wood flour differs from our earlier data using soybean and rice hulls as reinforcements,<sup>31,33</sup> and is not yet fully understood. The other DTA peaks observed for samples B, C, and D are, most likely, a combination of the degradation of cellulose, lignin, and some of the resin components. The degradation pattern of the resin is more complex and it is hard to attribute the DTA peaks for sample A (Figure 2) to specific components of the system. Nevertheless, it is noteworthy that  $T_{max1}$  occurs at

approximately 445 °C for the pure resin, a much higher temperature than that observed for the composites or the pure filler.

Given the results presented so far for composites made with different amounts of filler, an 80/20 filler to resin ratio yields a composite with the overall best mechanical properties. Furthermore, despite the statistical equivalence of the tensile properties of samples containing 80 wt % and 85 wt % of wood flour, and taking into account the processability of the crude resin and wood flour mixture, the 80/20 filler to resin ratio proved to be the most practical one to handle prior to curing. Therefore, this filler load has been used in the preparation of all composites in the remainder of this work.

**Cure time analysis.** To determine the best cure time for the system, pine wood flour composites with a constant filler to resin ratio of 80/20, and a constant resin composition (50 wt % of CSO, 35 wt % of BMA, and 15 wt % of DVB) have been prepared and cured at 600 psi and 180 °C for different times. The results from the tensile tests, DMA, and Soxhlet extraction are presented in Table II.

When the cure time is varied from 30 minutes to 3 hours, there is no significant variation in the Young's modulus of the pine wood flour composites as the differences between the values fall within the standard deviations of the measurements. The Young's modulus reaches its maximum at 4.3 GPa when the composite is cured for 4 hours, but once again, no statistical differences have been found between the samples cured for 4 and 5 hours. For the tensile strength, with the exception of the sample cured for 30 minutes, all of the other composites exhibit values that range within the standard deviations of the

**Table II.** Tensile tests, DMA, and extraction results for pine wood flour composites cured at 180 °C and 600 psi for different times, and post-cured at 200 °C for 2 hours at ambient pressure

| Cure Time (h) <sup>a</sup> | <i>E</i> (GPa) | Tensile Strength (MPa) | <i>E'</i> at 130 °C (MPa) | <i>T<sub>g1</sub></i> (°C) | <i>T<sub>g2</sub></i> (°C) | Soluble Fraction (%) <sup>b</sup> |
|----------------------------|----------------|------------------------|---------------------------|----------------------------|----------------------------|-----------------------------------|
| 5                          | 2.8 ± 0.9      | 11.7 ± 2.4             | 1072                      | 4                          | 79                         | 5                                 |
| 4                          | 4.3 ± 1.1      | 12.4 ± 1.1             | 742                       | 3                          | 93                         | 4                                 |
| 3                          | 3.1 ± 0.6      | 12.3 ± 1.9             | 704                       | -2                         | 77                         | 6                                 |
| 2                          | 3.3 ± 0.7      | 13.9 ± 1.6             | 831                       | 2                          | 90                         | 5                                 |
| 1                          | 3.5 ± 0.9      | 13.0 ± 0.9             | 1292                      | -1                         | 71                         | 5                                 |
| 0.5                        | 3.1 ± 0.6      | 11.4 ± 1.2             | 864                       | -7                         | 97                         | 5                                 |

<sup>a</sup> Filler particle size diameter <310 μm. Filler/resin ratio = 80/20.

<sup>b</sup> Determined by Soxhlet extraction.

measurements. These results indicate that although very little variation is obtained in the tensile properties by varying the cure time, a 30 minute cure is inappropriate due to the very low tensile strength obtained. This is probably because the resin is not completely cured after such a short time. On the other hand, a 4 hour cure sequence results in the stiffest material and is therefore considered the optimum cure time for the preparation of wood flour composites.

With respect to the storage modulus at 130 °C, there is no obvious trend between the values observed and the cure time. A maximum storage modulus is observed when the composite is cured for one hour. However, the results suggest a tendency for *E'* to increase with cure time for cure sequences lasting between three and five hours.

During curing, two competing phenomena are responsible for the minor variation in the mechanical properties measured as a function of the cure time. Indeed, one would expect the tensile and flexural properties to improve significantly with cure time as the crosslink

density of the resin increases and further reactions of the comonomers are expected to yield stiffer and stronger materials. Furthermore, it has been shown that the post-cure step is essential for achieving a fully crosslinked resin.<sup>33</sup> This finding supports the claim that samples submitted to the same post-cure conditions exhibit a similar crosslink density, and similar properties as a consequence. However, degradation of the filler components starts at fairly low temperatures (see Figure 3), and the loss of properties due to partial filler degradation under the cure conditions is a possibility. With both phenomena occurring simultaneously, one effect compensates for the other and this is reflected in the overall measurements, as can be seen in Table II.

It has been previously shown, with rice hull composites cured at different temperatures, that a cure temperature of 180 °C maximizes the crosslinking of the resin, resulting in materials with better properties.<sup>33</sup> A cure temperature of 130 °C has been employed in the preparation of a wood flour composite, resulting in a sample with significantly lower properties than the one cured at 180 °C (compare the results presented in Tables I and IV).

Once again, two distinct  $T_g$ 's have been observed for the wood flour composites prepared with CSO (Table II). As discussed earlier, this is a result of a phase separation due to the difference in reactivity of the comonomers that form the matrix of the composites. The lower  $T_g$ , most likely associated with a CSO-rich phase, varied from -7 °C to 4 °C in a non-regular pattern, as the cure time increased from 30 minutes to 5 hours. The higher  $T_g$ , most likely related to a DVB-rich phase, shows a broader variation from 71 °C to 97 °C within the same cure time range. These results show that the phase separation doesn't depend on the



cure time and that the DVB-rich phase is readily formed at the cure temperature (180 °C), even when the cure only lasts for 30 minutes. Once the DVB-rich phase is formed and the concentration of free DVB monomer has dropped, the CSO-rich phase starts to form. Surprisingly, the change in soluble material with cure time is minimal, which suggests that both phases are mostly formed within the first 30 minutes of the cure, and that only a small amount of the monomers are left unreacted. For the remainder of the time, during longer cure sequences, processes such as crosslinking, polymer chain growth, and oligomer incorporation into the matrix occur, resulting in materials with slightly better mechanical properties.

Another evidence of the effect of the cure time on the composites is shown in Figure 3, where the DSC plots of composites cured for different times are pictured. Composites cured for 3 and 4 hours have been omitted due to their similarity to the composite cured at 2 hours and to achieve better quality plots.

As discussed in our previous publication on soybean hull composites,<sup>31</sup> the exothermic peaks occurring after 250 °C in the DSC of ligno-cellulosic composites correspond to the decomposition of hemicellulose and cellulose from the filler. Since the composition of the materials is the same for all four samples shown in Figure 3, no significant variation is detected between 250 °C and 400 °C. The sharp heat absorption observed between 150 °C and 200 °C for samples cured between 30 minutes and 2 hours is attributed to volatilization of compounds during hemicellulose thermal degradation, as previously demonstrated with soybean hull composites.<sup>31</sup> This peak occurs at 190 °C for samples cured for 30 minutes and 2 hours. It is unclear to us why a lower temperature was obtained for the composite cured for 1 hour. However, the main focus of the present

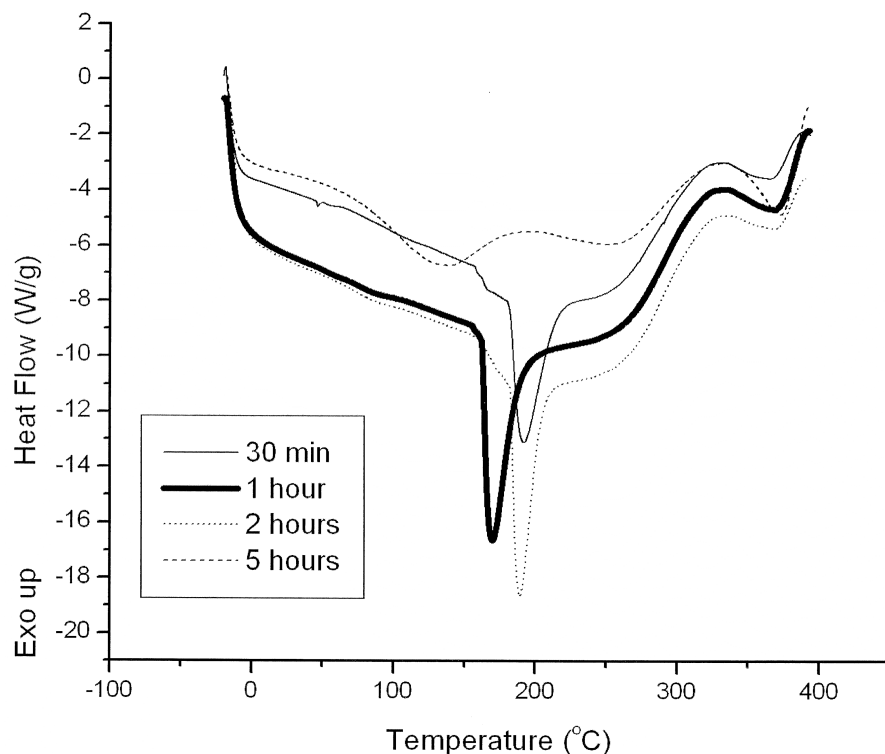


**Figure 3.** DSC of composites cured at 180 °C and 600 psi for different times, and post-cured at 200 °C and ambient pressure for 2 hours. The composites have a filler/resin ratio of 80/20, and a resin composition of 50 wt % of CSO, 35 wt % of BMA, and 15 wt % of DVB.

discussion is the change in the resin using different cure sequences. Regarding the DSC of the composite cured for 5 hours, the endothermic peak is much less intense, and appeared at a considerably lower temperature (135 °C). This is an indication that the exceedingly long cure time initiated the thermal degradation of the filler, and, therefore, less energy was required during volatilization of the compounds in the DSC experiment.

The most important feature of the DSC curves shown in Figure 3 is a change in the baseline occurring right before the heat absorption. This feature is clearly seen at 160 °C for the composite cured for 30 minutes, and is most likely related to further cure of the resin, as discussed for soybean hull composites.<sup>31</sup> The same feature, although much less intense is

observed, at the same temperature, for the composite cured for 1 hour, indicating that a longer cure time indeed results in a more complete cure of the resin. For the composite cured for 2 hours, the change in the baseline is much smoother and actually hard to detect, corroborating the idea that a longer heating time results in further cure of the resin. The aforementioned feature is completely nonexistent in the DSC of the composite cured for 5 hours. In fact, in this instance, the resin is completely cured, but the filler is significantly degraded, and a burnt smell has been noticed when removing the composite from the mold after preparation.

**Filler particle size, filler origin, and resin composition effects.** Table III shows the properties of composites made with different wood flours containing varying particle sizes and resin compositions. Comparing the properties of composites made with pine wood flour of different particle sizes (entries 1-3, Table III), it is evident that the overall best values have been obtained from the composite prepared with particles  $<310 \mu\text{m}$  (entry 2, Table III). The only exception being the storage modulus at  $130^\circ\text{C}$ , for which the composite prepared with filler particles  $<470 \mu\text{m}$  (entry 1, Table III) exhibited the highest value. We have observed previously with soybean hulls that the use of fillers of smaller particle sizes tends to result in a better dispersion of the resin and higher mechanical properties.<sup>31</sup> Larger particles, on the contrary, agglomerate more easily, forming weak points in the composite.<sup>31</sup> Here, probably due to a difference in the filler structure and composition (grain shell *versus* ground wood), a different trend is observed. The optimum intermediate particle size ( $<310 \mu\text{m}$ ) most likely prevents agglomeration of the filler. This trend changed when maple/oak composites were prepared with a resin that contains the compatibilizer MA (entries 7-9, Table III). In that case, the expected trend of smaller particle sizes ( $<224 \mu\text{m}$ ) yielding composites with better

properties is verified. Once again the exception being the storage modulus at 130 °C, for which the highest value is observed for the composite prepared with particles <310 μm (entry 8, Table III).

**Table III.** Filler particle size, filler origin, and resin composition effects on the properties of wood flour reinforced composites.

| Entry | Filler           | Resin Composition <sup>a</sup> | Particle size (μm) | <i>E</i> (GPa) | Tensile Strength (MPa) | <i>T<sub>g1</sub></i> (°C) | <i>T<sub>g2</sub></i> (°C) | <i>E'</i> at 130 °C (MPa) |
|-------|------------------|--------------------------------|--------------------|----------------|------------------------|----------------------------|----------------------------|---------------------------|
| 1     | pine flour       | CSO-DVB-BMA35                  | <470               | 3.2 ± 0.6      | 8.3 ± 0.8              | 2                          | 69                         | 879                       |
| 2     | pine flour       | CSO-DVB-BMA35                  | <310               | 4.3 ± 1.1      | 12.4 ± 1.1             | 3                          | 93                         | 742                       |
| 3     | pine flour       | CSO-DVB-BMA35                  | <224               | 2.7 ± 0.7      | 9.9 ± 0.7              | -1                         | 72                         | 686                       |
| 4     | pine/maple flour | CSO-DVB-BMA35                  | -                  | 1.6 ± 0.1      | 7.5 ± 1.0              | -8                         | 70                         | 388                       |
| 5     | pine flour       | CLO-DVB-BMA35                  | <310               | 3.8 ± 1.9      | 15.7 ± 1.9             | -                          | 54                         | 1559                      |
| 6     | pine flour       | CLO-DVB-BMA20-MA15             | <310               | 4.0 ± 0.9      | 17.6 ± 1.9             | 17                         | 109                        | 2244                      |
| 7     | maple/oak flour  | CLO-DVB-BMA20-MA15             | <470               | 2.1 ± 0.4      | 8.5 ± 2.5              | 11                         | 91                         | 600                       |
| 8     | maple/oak flour  | CLO-DVB-BMA20-MA15             | <310               | 1.8 ± 0.3      | 8.1 ± 2.2              | -12                        | 62                         | 2223                      |
| 9     | maple/oak flour  | CLO-DVB-BMA20-MA15             | <224               | 2.5 ± 0.5      | 11.3 ± 2.3             | -9                         | 59                         | 1064                      |

<sup>a</sup> All resins have 50 wt % of conjugated vegetable oil, and 15 wt % of DVB. The wt percentage of BMA and MA is indicated by the numbers following the corresponding acronyms.

Another interesting aspect from Table III is that the use of mixed wood flours gives worse properties than when a pure wood flour is used in the preparation of the composite.

This is true for the pine/maple mixed flour (entry 4, Table III), when compared with the pure

pine flour (entries 1-3, Table III). One reason for the observed pattern is that the maple flour originally used to prepare the mixture appears to have very low mechanical properties. Unfortunately, we could not get samples of pure maple flour to prepare a control composite and test that hypothesis. A similar situation is observed for composites made with maple/oak mixed flours (entries 7-9, Table III). Although the mechanical properties measured for the maple/oak composite (entry 8, Table III) are overall lower than the ones measured for the pine wood flour composite with the same resin composition and particle size (entry 6, Table III), no controls have been prepared with pure oak, and/or pure maple wood flours.

When CSO is replaced by CLO in pine flour composites (entries 2 and 5, Table III), a significant improvement in tensile strength and storage modulus at 130 °C is observed. These results support the idea that a higher number of carbon-carbon double bonds in the oil (linseed oil has on average 6.0 carbon-carbon double bonds per triglyceride, while soybean oil only possesses 4.5 carbon-carbon double bonds per triglyceride) gives a more crosslinked and stronger material. A similar trend has been observed and recently published by us for soybean and linseed oil-based rice hull composites.<sup>34</sup> As for the Young's modulus of the CSO- and CLO-based composites compared here (entries 2 and 5, Table III), the values measured fall within the standard deviation of the method used and therefore can't be considered statistically different. The appearance of one single  $T_g$  for the CLO-containing composite (entry 5, Table III) is again a result of the higher reactivity of CLO in comparison to CSO, due to its higher number of carbon-carbon double bonds. By reacting faster, CLO is incorporated into the polymer matrix at approximately the same rate as the other comonomers, resulting in a single phase.

When maleic anhydride (MA) is added to the resin formulation, it acts as a compatibilizer between the hydrophobic matrix and the hydrophilic filler. MA can also be polymerized through a standard free radical reaction of its reactive carbon-carbon double bond, which allows it to be easily incorporated into the polymer matrix. It is also known that the anhydride unit can be easily opened in the presence of nucleophiles at elevated temperatures, which should allow the appended anhydride to interact with the ligno-cellulosic fillers rich in carbohydrates.

A comparison of entries 5 and 6 in Table III shows that the addition of MA to the resin formulation in partial replacement of BMA results in a slight improvement in the mechanical properties. Young's modulus and tensile strength are slightly higher for the MA-containing sample, but the values still fall within the standard deviation of the measurements. The storage modulus measured at 130 °C, on the other hand, shows a significant improvement, increasing from 1559 MPa to 2244 MPa after the addition of MA, which supports better stress transfer from the resin to the reinforcement, and indicates that a better filler-resin interaction has been obtained with MA.

Interestingly, the presence of MA in the resin system seems to have an influence on the  $T_g$ 's observed and the corresponding phase separation. Two distinct  $T_g$ 's have been found for a pine flour composite containing MA (entry 6, Table III), even when CLO is used as the major resin component. The same phase separation is observed in all maple/oak composites (entries 7-9, Table III). A plausible explanation for this phenomenon is that when the polymer chains containing MA units start to form, the favorable interactions between MA and the filler restrict the movement and the dispersion of the growing chains, which

ultimately results in the observed phase separation, regardless of the reactivity of the oil used to prepare the resin. A comparison of the tan delta curves of pine flour composites prepared with and without MA is presented in Figure 4.

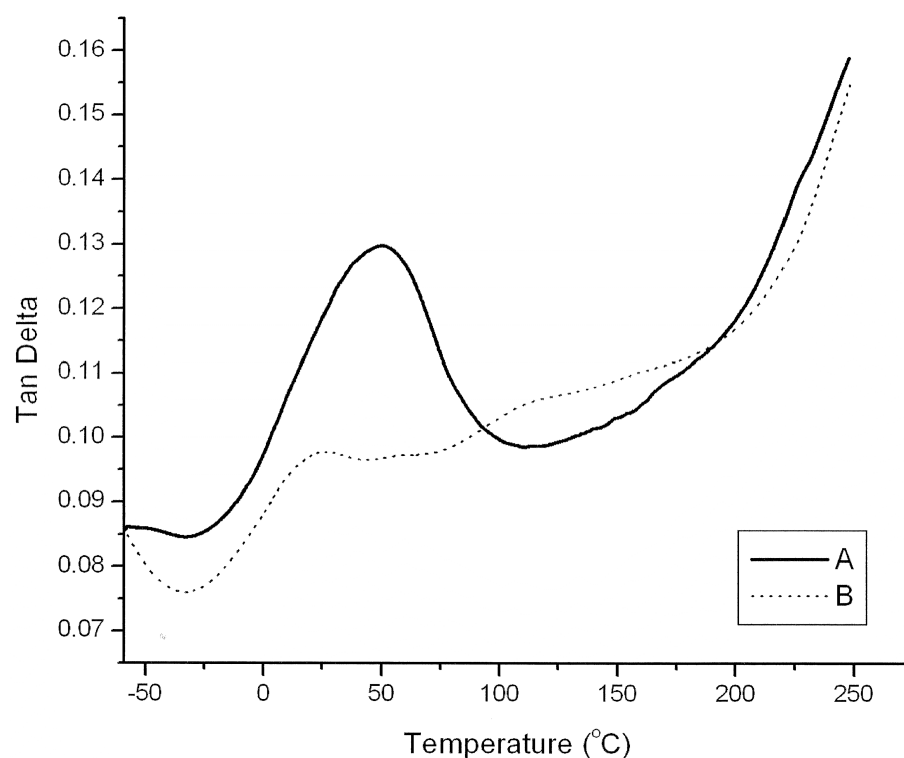


**Figure 4.** Tan delta curves of pine flour composites with resin composition: 50 wt % CLO, 35 wt % BMA, and 15 wt % DVB (A); and 50 wt % CLO, 20 wt % BMA, 15 wt % DVB, and 15 wt % MA (B). Both composites had a filler/resin ratio of 80/20 and have been cured for 4 hours at 180 °C and 600 psi, and post-cured at 200 °C for 2 hours at ambient pressure.

**Wood fiber composites.** For comparison purposes, samples containing mixed hardwood fibers and pine wood flour have been prepared with the same filler/resin ratio and resin composition. The resin was composed of 50 wt % of CLO, 35 wt % of BMA, and 15 wt % of DVB and the filler/resin ratio used was 50/50. As mentioned earlier, a cure sequence of 5 hours at 130 °C and 400 psi, followed by a post-cure step of 2 hours at 150 °C and ambient

pressure, was used for both composites. The properties of both samples are summarized in Table IV.

**Table IV** – Properties of pine flour and hardwood fiber composites.

| Entry          | Filler           | $E$ (GPa)     | Tensile Strength (MPa) | $T_g$ (°C) | $E'$ at 130 °C (MPa) |
|----------------|------------------|---------------|------------------------|------------|----------------------|
| 1 <sup>a</sup> | pine flour mixed | $1.3 \pm 0.4$ | $2.6 \pm 0.6$          | 62         | 152                  |
| 2 <sup>a</sup> | hardwood fiber   | $2.3 \pm 0.2$ | $18.4 \pm 1.5$         | 70         | 1051                 |

<sup>a</sup> Both composites have a 50/50 filler/resin ratio and a resin composition of 50 wt % of CLO, 35 wt % of BMA, and 15 wt % of DVB. The cure employed corresponds to 130 °C for 5 hours at 400 psi, followed by a post-cure of 2 hours at 150 °C and atmospheric pressure.

From the results presented in Table IV, the use of hardwood fiber as a reinforcement resulted in a composite with much higher mechanical properties than the composite reinforced with pine wood flour. The Young's modulus increased from 1.3 GPa to 2.3 GPa, while the tensile strength and storage modulus at 130 °C showed a 7 fold improvement. This increase in mechanical properties is most likely related to the higher aspect ratio and fibrous nature of the wood fibers in comparison to wood flours, where the particles exhibit a more spherical geometry. Also noteworthy is the presence of only one  $T_g$  for both composites due to the use of CLO as the major resin component.

### Conclusions

In this work, we have studied composite systems where the matrix is a free radical copolymer of BMA, DVB, and either conjugated soybean oil or linseed oil. These thermosets have been reinforced with pine, maple, and oak flours, and a mixture of hardwood fibers.



First, we evaluated different filler amounts for pine wood flour composites and determined that a filler load of 80 wt % was the most practical for the preparation of such composites. Then, we examined the effect of cure time on the final properties of the pine flour composites. The results indicate that little variation in the mechanical properties was obtained when the cure time varied from 30 minutes to 5 hours. TGA and DSC experiments indicated that this is a result of factors that compensate for each other. While longer cure times help to completely cure the resin and tend to increase crosslink density and monomer incorporation into the matrix, it is also responsible for partial thermal degradation of the filler components, which impacts the properties negatively. Optimum particle size has been shown to depend on the filler composition, and composites made with mixtures of flours containing oak have exhibited worse mechanical properties than pure pine flour composites. It has been verified that MA is a good filler-resin compatibilizer for the composites studied, because its presence imparts a significant increase in the storage modulus of the composites. Finally, a comparison between wood fiber and wood flour composites indicates that the composites reinforced with fibers show significantly higher mechanical properties.

### **Acknowledgements**

The authors thank the Recycling and Reuse Technology Transfer Center of the University of Northern Iowa for financial support, American Wood Fibers for providing the wood flour and wood fibers, Professor Michael Kessler from the Department of Material Sciences and Engineering at Iowa State University for the use of his facilities, and Dr. Douglas Stokke from the Department of Natural Resource Ecology and Management at Iowa State University for important information concerning the wood flours and the wood fibers.

### References

1. Ashraf, S. M.; Ahmad, S.; Riaz, U. *Polym. Int.* 2007, 56, 1173.
2. Wang, C.; Yang, L.; Ni, B.; Shi, G. *J. Appl. Polym. Sci.* 2009, 114, 125.
3. Sharma, H. O.; Alam, M.; Riaz, U.; Ahmad, S.; Ashraf, S. M. *Int. J. Polym. Mater.* 2007, 56, 437.
4. Gultekin, M.; Beker, U.; Guner, F. S.; Erciyes, A. T.; Yagci, Y. *Macromol. Mater. Eng.* 2000, 283, 15.
5. Bhuyan, S.; Holden, L. S.; Sundararajan, S.; Andjelkovic, D.; Larock, R. C. *Wear* 2007, 263, 965.
6. Sharma, V.; Banait, J. S.; Kundu, P. P. *J. Appl. Polym. Sci.* 2009, 111, 1816.
7. Zhan, M.; Wool, R. P. *J. Appl. Polym. Sci.* 2010, 118, 3274.
8. Zhang, G.; Zhao, L.; Hu, S.; Gan, W.; Yu, Y.; Tang, X. *Polym. Eng. Sci.* 2008, 48, 1322.
9. Sharma, V.; Banait, J. S.; Kundu, P. P. *J. Appl. Polym. Sci.* 2009, 114, 446.
10. Das, G.; Karak, N.; *Prog. Org. Coatings* 2010, 69, 495.
11. Thulasiraman, V.; Rakesh, S.; Sarojadevi, M. *Polym. Comp.* 2009, 30, 49.
12. Espinoza-Perez, J. D.; Ulven, C. A.; Wiesenborn, D. P. *Transactions of the Am. Soc. Agric. Biol. Eng.* 2010, 53, 1167.
13. Lundin, T.; Cramer, S. M.; Falk, R. H.; Felton, C. J. *Mat. Civil Eng.* 2004, 16, 547.
14. Liu, H.; Wu, Q.; Zhang, Q. *Bioresour. Technol.* 2009, 100, 6088.
15. Xu, Y.; Wu, Q.; Lei, Y.; Yao, F. *Bioresour. Technol.* 2010, 101, 3280.
16. Schirp, A.; Loge, F.; Aust, S.; Swaner, P.; Turner, G.; Wolcott, M. *J. Appl. Polym. Sci.* 102, 5191, 2006.
17. Jarukumjorn, K.; Suppakarn, N. *Composites: Part B* 2009, 40, 623.
18. Srebrekoska, V.; Gaceva, G. B.; Dimeski, D. *Maced. J. Chem. Chem. Eng.* 2009, 28, 99.
19. Haque, M. M.; Hasan, M.; Islam, M. S.; Ali, M. E. *Bioresour. Technol.* 2009, 100, 4903.
20. Haq, M.; Burgueno, R.; Mohanty, A. K.; Misra, M. *Composit. Sci. Tech.* 2008, 68, 3344.
21. Li, F.; Hasjim, J.; Larock, R. C. *J. Appl. Polym. Sci.* 2003, 90, 1830.
22. Li, F.; Larock, R. C. *Biomacromolecules* 2003, 4, 1018.
23. Henna, P. H.; Andjelkovic, D. D.; Kundu, P. P.; Larock, R. C. *J. Appl. Polym. Sci.* 2007, 104, 979.

24. Valverde, M.; Andjelkovic, D.; Kundu, P. P.; Larock, R. C. *J. Appl. Polym. Sci.* 2008, 107, 423.
25. Xia, Y.; Henna, P. H.; Larock, R. C. *Macromol. Mater. Eng.* 2009, 294, 590.
26. Henna, P. H.; Andjelkovic, D. D.; Kundu, P. P.; Larock, R. C. *J. Appl. Polym. Sci.* 2007, 104, 979.
27. Kundu, P. P.; Larock, R. C. *Biomacromolecules* 2005, 6, 797.
28. Lu, Y.; Larock, R. C. *Macromol. Mater. Eng.* 2007, 292, 863.
29. Lu, Y.; Larock, R. C. *Macromol. Mater. Eng.* 2007, 292, 1085.
30. Pfister, D. P.; Larock, R. C. *Bioresour. Technol.* 2010, 101, 6200.
31. Quirino, R. L.; Larock, R. C. *J. Appl. Polym. Sci.* 2009, 112, 2033.
32. Bhuyan, S.; Sundararajan, S.; Pfister, D.; Larock, R. C. *Tribol. Int.* 2010, 43, 171.
33. Quirino, R. L.; Larock, R. C. *J. Appl. Polym. Sci.*, 2011, 121, 2039.
34. Quirino, R. L.; Larock, R. C. *J. Appl. Polym. Sci.*, 2011, 121, 2050.
35. [http://www.soystats.com/2008/page\\_21.htm](http://www.soystats.com/2008/page_21.htm)
36. Li, F.; Larock, R. C. *Polym. Int.* 2003, 52, 126.
37. Li, F.; Larock, R. C. *J. Polym. Environ.* 2002, 10, 59.
38. Andjelkovic, D. D.; Min, B.; Ahn, D.; Larock, R. C. *J. Agric. Food Chem.* 2006, 54, 9535.

**CHAPTER 6. SUGAR-CANE BAGASSE COMPOSITES FROM VEGETABLE OILS**

A Paper Submitted to Journal of Applied Polymer Science.

Rafael L. Quirino, Richard C. Larock\*

*Department of Chemistry, Iowa State University, Ames, Iowa 50011*

**Abstract**

Sugar-cane bagasse composites have been prepared by the free radical polymerization of regular or modified vegetable oils with divinylbenzene and *n*-butyl methacrylate, in the presence of dried, ground sugar-cane bagasse. Various cure times and temperatures have been investigated to determine the optimum cure sequence for the new materials. The post-cure time has also been varied and an ideal post-cure treatment of 1 hour at 180 °C at ambient pressure has given the best overall properties. The effect of varying the filler load and resin composition has been assessed by means of tensile tests, DMA, TGA, and Soxhlet extraction, followed by <sup>1</sup>H NMR spectroscopic analysis of the extracts. It has been observed that the initial washing and drying of the filler influences the filler-resin interaction and impacts the final properties of the composites.

**Introduction**

The partial replacement of petroleum-derived plastics and composites by novel bio-based materials from inexpensive, renewable, natural resources, like vegetable oils and agricultural residues, has the potential to greatly impact the plastics and coatings industries. Such natural starting materials tend to be readily available in large quantities, at a low price,

and can possibly afford more bio-degradable materials than the virtually indestructible petroleum-based polymers. Furthermore, new bio-based materials may present properties not currently available in commercial petroleum products, with an overall intrinsic low toxicity. These characteristics make bio-based materials very appealing from an industrial point of view, and research in this area may lead to significant progress towards oil independence and sustainable industrial development.

Currently, a variety of chemicals and materials are prepared from vegetable oils, polysaccharides, wood, or proteins.<sup>1</sup> As an example, bio-oil and syngas are obtained from the pyrolysis of wood and agricultural wastes.<sup>2</sup> Soybean and corn proteins can be denatured and aligned to prepare protein-based bio-polymers,<sup>3,4</sup> and vegetable oils find wide use in paints,<sup>5</sup> biocoatings,<sup>6,7</sup> biofuels,<sup>8</sup> and as building blocks for bio-based resins,<sup>9-17</sup> such as polyurethanes,<sup>9-11</sup> polyester amides,<sup>12</sup> multicomponent thermosets,<sup>13-17</sup> and cyanate esters.<sup>18</sup> Some of these systems have been reinforced with nanoclays,<sup>19</sup> and glass fibers.<sup>20-22</sup>

Alternatively, “green” composites can be prepared by the reinforcement of standard petroleum-derived thermoplastics, like high density polyethylene (HDPE), with natural fillers, such as sugar-cane bagasse<sup>23</sup> or wheat straw.<sup>24</sup> Similarly, polypropylene (PP) has been reinforced with palm and coir fibers.<sup>25</sup> There exist several other possible combinations of thermoplastics and natural fillers that are not explicitly cited here. More recently, some progress on the reinforcement of blends of petroleum-derived unsaturated epoxy resins and epoxidized soybean oil with hemp fibers has been reported.<sup>26</sup>

In an effort to incorporate high biorenewable content into polymer blends, the Larock group at Iowa State University has developed a variety of vegetable oil-based thermosets

with good thermal and mechanical properties.<sup>27-29</sup> Cationic,<sup>27</sup> free radical,<sup>28</sup> and thermal<sup>29</sup> copolymerization of regular and conjugated natural oils in the presence of various petroleum-based co-monomers have yielded materials ranging from elastomers to rigid thermosets. The reactive sites in these vegetable oil-based systems are the carbon-carbon double bonds. Overall, the reactivity of the triglycerides towards the aforementioned polymerization processes can be significantly enhanced if the carbon-carbon double bonds in the fatty acid chains are isomerized and brought into conjugation.<sup>30</sup> More recently, the synthesis of bio-based polymers, making use of alternative polymerization methods, including ring-opening metathesis polymerization (ROMP),<sup>31</sup> and acyclic diene metathesis (ADMET)<sup>32</sup> has also been investigated.

The cationic polymerization of vegetable oils<sup>17,27</sup> in the presence of petroleum-derived co-monomers avoids the entrapment of bubbles in the resin, which are usually seen when AIBN is used as a free radical initiator. It also limits crack formation related to shrinkage of the resin upon cure. Significant improvements in the properties of bio-based polymers can be obtained by simply reinforcing these cationic vegetable oil-based matrices with inorganic<sup>21,22</sup> or natural fillers.<sup>33</sup>

In the preparation of bio-based composites reinforced with spent germ,<sup>34</sup> soybean hulls,<sup>35</sup> corn stover,<sup>36</sup> wheat straw,<sup>37</sup> and rice hulls,<sup>38</sup> it has been demonstrated that peroxide free radical initiators are effective in reacting the carbon-carbon double bonds in the oils and the other co-monomers used in the presence of lignocellulosic materials. The presence of bio-based filler particles minimizes shrinkage of the resin and only minimal micro-cracks have been detected by scanning electron microscopy (SEM) of the soybean hull composites.<sup>35</sup>

Recent studies of natural filler-reinforced composites have suggested that maleic anhydride (MA) can serve as a good filler-resin compatibilizer and helps to improve the stress transfer from the matrix to the reinforcement, resulting in an overall increase in the mechanical properties.<sup>38</sup>

These new bio-based composites contain up to 85 wt % of biorenewable content, including the resin and the filler.<sup>34-38</sup> The technology involved in their preparation is remarkably simple and they have great potential in the automobile and construction industries.

Herein, we report the preparation of bio-based thermosets from vegetable oils with different numbers of carbon-carbon double bonds per triglyceride reinforced with sugar-cane bagasse. Parameters, such as cure sequence, filler load, and resin composition, have been varied and the resulting properties of the composites have been assessed by differential scanning calorimetry (DSC), thermogravimetric analysis (TGA), tensile tests, dynamic mechanical analysis (DMA), and Soxhlet extraction, followed by proton nuclear magnetic resonance (<sup>1</sup>H NMR) spectroscopic analysis of the extracts. The results provide insight into the filler-resin interactions and the thermal stability of the filler present in the composite.

## Experimental

**Materials.** *n*-Butyl methacrylate (BMA) was purchased from Alfa Aesar (Ward Hill, MA). Divinylbenzene (DVB), maleic anhydride (MA), di-*t*-butyl peroxide (TBPO), and tung oil (TUN) were purchased from Sigma-Aldrich (St. Louis, MO). All were used as received. Soybean oil (Great Value brand – Bentonville, AR) was purchased in a local grocery store, and Superb linseed oil was provided by Archer Daniels Midland (Red Wing, MN). Both oils

have been conjugated using a rhodium catalyst, following a method developed and frequently used by our group.<sup>30</sup> The sugar-cane bagasse was generously provided by the U.S. Sugar Corporation (Clewiston, FL).

The sugar-cane bagasse fibers were washed with water and dried at 50 °C overnight. To ensure complete removal of moisture, after being ground to particle sizes <2.0 mm, the filler has been placed in a vacuum oven at 70 °C overnight and been impregnated with the resin right after the drying process.

**General procedure for preparation of the bio-based composites.** The crude resin was obtained by mixing the conjugated or regular vegetable oil, BMA and DVB in a beaker. MA was melted in a hot water bath and quickly added to the crude resin mixture at room temperature under agitation, along with the free radical initiator TBPO. The natural fillers were impregnated with the crude resin and compression molded at 600 psi. The composites were then removed from the mold and post-cured in a convection oven at ambient pressure. In all composites produced, the resin has a vegetable oil content of 50 wt % and the optimum amount of TBPO has been determined to be in preliminary tests an extra 5 wt % of the total resin weight. The vegetable oil used and the amounts of BMA and MA have been varied, as indicated in the text, to produce composites of various compositions.

**Characterization of the composites.** Tensile tests were conducted at room temperature according to ASTM D-638, using an Instron universal testing machine (model 5569) equipped with a video extensometer and operating at a crosshead speed of 2.0 mm/min. Dogbone-shaped test specimens were machined from the original samples to give the following gauge dimensions: 57.0 mm x 12.7 mm x 4.5 mm (length x width x thickness,



respectively). For each composite, seven dogbones were cut and tested. The results presented in the text are the average of these measurements along with the calculated standard deviation.

DMA experiments were conducted on a Q800 DMA (TA Instruments, New Castle, DE) using a three point bending mode with a 10.0 mm clamp. Rectangular specimens of 22.0 mm x 8.5 mm x 1.5 mm (length x width x thickness, respectively) were cut from the original samples. Each specimen was cooled to  $-60\text{ }^{\circ}\text{C}$  and then heated to  $250\text{ }^{\circ}\text{C}$  at  $3\text{ }^{\circ}\text{C}/\text{min}$ . The experiment was conducted using a frequency of 1 Hz and an amplitude of  $14\text{ }\mu\text{m}$  under air. Two runs for each sample were carried out and the results presented in the text reflect the average of the two measurements.

Soxhlet extraction was conducted to determine the amount of soluble materials in the composites. A 2.0 g sample of each composite was extracted for 24 h with dichloromethane ( $\text{CH}_2\text{Cl}_2$ ). After extraction, the solubles were recovered by evaporating the  $\text{CH}_2\text{Cl}_2$  under a vacuum. Both soluble and insoluble materials were dried overnight at  $70\text{ }^{\circ}\text{C}$ . The dried soluble fraction was then dissolved in deuterated chloroform ( $\text{CDCl}_3$ ) and the corresponding  $^1\text{H}$  NMR spectrum was obtained using a Varian Unity spectrometer (Varian Associates, Palo Alto, CA), operating at 300 MHz. The  $^1\text{H}$  NMR spectra helped to determine the identity of the soluble materials in each sample.

DSC experiments were performed on a Q20 DSC (TA Instruments, New Castle, DE) under a  $\text{N}_2$  atmosphere over a temperature range of  $-20\text{ }^{\circ}\text{C}$  to  $400\text{ }^{\circ}\text{C}$ , while heating at a rate of  $20\text{ }^{\circ}\text{C}/\text{min}$ . The samples weighed  $\sim 10\text{ mg}$ .

A Q50 TGA instrument (TA Instruments, New Castle, DE) was used to measure the weight loss of the samples under an air atmosphere. The samples (~10 mg) were heated from room temperature to 650 °C at a rate of 20 °C/min.

### Results and Discussion

**Cure analysis.** *Cure time and temperature.* In order to determine an appropriate cure sequence for the sugar-cane bagasse composites, six different heating treatments have been applied to composites bearing 70 wt % of filler, and a resin composed of 50 wt % of CSO, 20 wt % of BMA, 15 wt % of DVB, and 15 wt % of MA. The mechanical properties of the corresponding materials have been compared, and the results are presented in Table I, along with the percentage of soluble material recovered after Soxhlet extraction of the samples.

**Table I.** Tensile and flexural properties, along with the Soxhlet extraction results, for sugar-cane bagasse composites cured under various cure sequences.<sup>a</sup>

| Entry | Cure Temp./Time                         | Post-cure Temp./Time | $E$ (GPa) | Tensile Strength (MPa) | $E'$ (MPa) at 25 °C | Soluble Content (wt %) <sup>c</sup> |
|-------|---|----------------------|-----------|------------------------|---------------------|-------------------------------------|
| 1     | 180 °C / 5h                             | 200 °C / 2h          | -         | -                      | 1032                | 5                                   |
| 2     | 160 °C / 5h                             | 180 °C / 2h          | 3.2 ± 0.5 | 10.0 ± 1.7             | 1272                | 6                                   |
| 3     | 140 °C / 3h<br>160 °C / 3h <sup>b</sup> | 180 °C / 2h          | 2.9 ± 0.5 | 11.6 ± 1.5             | 597                 | 5                                   |
| 4     | 140 °C / 3h<br>160 °C / 3h <sup>b</sup> | 180 °C / 0.5h        | 2.5 ± 0.4 | 6.8 ± 1.3              | 2437                | 8                                   |
| 5     | 140 °C / 3h<br>160 °C / 3h <sup>b</sup> | 180 °C / 1h          | 3.4 ± 0.4 | 12.6 ± 2.9             | 1137                | 6                                   |
| 6     | 140 °C / 3h<br>160 °C / 3h <sup>b</sup> | 180 °C / 3h          | -         | -                      | 1603                | 7                                   |

<sup>a</sup> The filler/resin ratio is 70/30 and the resin composition is 50 wt % of CSO, 20 wt % of BMA, 15 wt % of DVB, and 15 wt % of MA.

<sup>b</sup> The cure sequence is composed of two stages.

<sup>c</sup> Determined after Soxhlet extraction with CH<sub>2</sub>Cl<sub>2</sub> for 24 hours.

Initially, two cure temperatures have been compared (entries 1 and 2, Table I), maintaining a post-cure time of 2 hours. When the composite is cured at 180 °C for 5 hours (entry 1, Table I), the resulting material is significantly degraded, and dogbone specimens cannot be obtained to conduct the tensile tests. The use of lower cure and post-cure temperatures (entry 2, Table I) results in a completely cured material, with less degradation of the filler, as indicated by the higher storage modulus at 25 °C. Although the material cured at 160 °C for 5 hours (entry 2, Table I) shows good mechanical properties, the dark color and the burnt smell observed, when demolding the sample, suggest that the fillers are still considerably degraded.

Finally, a two step cure process has been tested, in which the sample is heated at 140 °C for 3 hours, and at 160 °C for another 3 hours, before being submitted to the 2 hour post-cure step (entry 3, Table I). In this case, despite the overall longer time in the hot press, the sample was exposed to the maximum temperature for a shorter time, and didn't darken significantly or exhibit any burnt odor after the process. The results for the Young's modulus and tensile strength are comparable to those obtained for the sample cured at 160 °C for 5 hours (entry 2, Table I), as the difference between the numbers fall within the standard deviation of the measurements. While a significantly lower storage modulus at 25 °C is observed (entry 3 *versus* entries 1 and 2, Table I), there is essentially no difference in the soluble content of the samples. This indicates that the changes observed in the mechanical properties of the sugar-cane bagasse composites, when varying the cure times and temperatures, are not related to the crosslink density and/or to the extent of monomer incorporation in the matrix.

While higher temperatures seem to degrade the core structure of the filler, longer cure times slowly degrade the least thermally stable components of the filler, affecting the interface between filler and resin, which results in poor stress transfer from the matrix to the reinforcement, and a lower storage modulus. In conclusion, the two step cure sequence has been chosen as ideal due to concerns about the thermal stability of the filler. A more thorough analysis of the filler's thermal stability will be presented later in the text, when discussing the TGA results.

*Post-cure time.* After establishing the ideal cure process, as discussed above, a study of the post-cure time has been carried out. Samples with the same composition and submitted to the same cure sequence have been post-cured for times varying from 0.5 hour to 3 hours, and their mechanical properties and soluble content have been compared (entries 3-6, Table I). It has been shown previously that the post-cure of vegetable oil-based composites reinforced with rice hulls is crucial in order to get a fully crosslinked material with maximum monomer incorporation into the matrix, and the best mechanical properties possible.<sup>39</sup>

When comparing samples post-cured for 0.5 hour and 1 hour (entries 4 and 5, Table I), it is apparent that the 0.5 hour post-cure step isn't sufficient to fully cure the resin. Besides the significantly lower tensile properties, the sample post-cured for 0.5 hour still exhibits a strong odor of unreacted monomers, indicating that the resin components aren't fully incorporated into the matrix. Further evidence of that is the relatively high percentage of soluble materials recovered after Soxhlet extraction of the material, when compared to entry 5 (Table I). Interestingly, the sample post-cured for 0.5 hour exhibits a significantly higher storage modulus. The DMA experiments have been repeated twice, and similar results have

been found each time. This supports the hypothesis that longer heating times have a negative impact on the filler structure, especially at the filler-matrix interface.

When the post-cure time is increased to 2 hours (entry 3, Table I), the differences in the tensile properties, with respect to the sample post-cured for 1 hour, fall within the standard deviation of the measurements, and similar soluble contents are found. Nevertheless, a significant decrease in storage modulus is again observed.

The tensile properties of the sample post-cured for 3 hours could not be obtained due to severe degradation of the filler during the heat treatment (entry 6, Table I). The increase in storage modulus at 25 °C with respect to entry 3 (Table I) does not follow the trend observed for the other samples and can possibly be related to non-homogeneity of the material after degradation of the filler. Unfortunately, no more than two DMA specimens could be obtained for that particular sample, in order to either confirm or discard the results presented. There is a slight increase in the soluble content that might be a consequence of fragmentation of the resin components, yielding CSO fragments and oligomers that can then be extracted during the Soxhlet extraction process.

Figure 1 depicts the DSC curves of samples post-cured at the same temperature, but for different times. For clarity purposes, the sample post-cured for 0.5 hour has been omitted.

When analyzing the DSC curve of the sample post-cured for 1 hour, some characteristic features are observed. There is a small exothermic peak at 156 °C attributed to residual crosslinking of the matrix components. The sharp endothermic peak at 234 °C is associated with initial thermal degradation of the filler, and all of the other peaks above 250

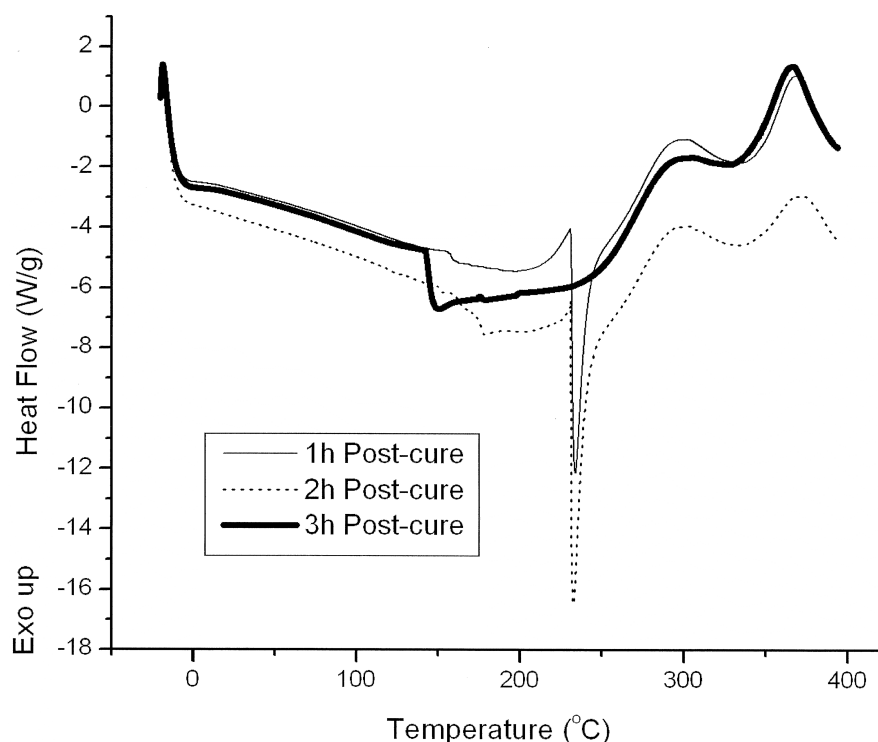


**Figure 1.** DSC curves for 70 wt % filled sugar-cane bagasse composites post-cured at 180 °C for varying times. The resin composition is 50 wt % of CSO, 20 wt % of BMA, 15 wt % of DVB, and 15 wt % of MA, and the cure sequence consists of 3 hours at 140 °C, followed by 3 hours at 160 °C.

°C are related to degradation of the different components of the materials being analyzed.<sup>39</sup> When the composite is post-cured for 2 hours, a very similar DSC curve is obtained, with the same features described for the sample cured for 1 hour. There is only an increase in the temperature of the residual cure peak from 156 °C to 178 °C. On the other hand, the sample post-cured for 3 hours gave a very distinct DSC curve. No exothermic peaks are detected. The endothermic peak occurs at a significantly lower temperature (149 °C), and it is significantly less intense and broader than the ones observed in the other DSC curves. These results confirm that the 3 hour post-cure is responsible for extensive degradation of the material in comparison with the 1 hour and 2 hour processes. Otherwise, except for the

storage modulus, no significant differences have been found between composites post-cured for 1 hour and 2 hours. In view of these facts, a 1 hour post-cure has been chosen as the ideal, and has been used in the preparation of all of the composites in the remainder of this project.

**Filler load evaluation.** The properties of sugar-cane bagasse composites prepared with filler loads varying from 60 wt % to 80 wt % are summarized in Table II. For comparison purposes, the properties of the unreinforced resin and the pure filler have also been included (entries 1 and 5 respectively in Table II). The resin, unless otherwise noted, is composed of 50 wt % of CSO, 20 wt % of BMA, 15 wt % of DVB, and 15 wt % of MA. The composites were cured for 3 hours at 140 °C, followed by another 3 hours at 160 °C, and post-cured for 1 hour at 180 °C.

**Table II.** Characterization of sugar-cane bagasse composites containing various filler loads.<sup>a</sup>

| Entry | Filler Load (wt %) | $E$ (GPa) | Tensile Strength (MPa) | $E'$ (MPa) |                  | $T_7$ (°C) |
|-------|--------------------|-----------|------------------------|------------|------------------|------------|
|       |                    |           |                        | at 25 °C   | at $T_g + 50$ °C |            |
| 1     | 0 <sup>b</sup>     | -         | -                      | 152        | 56               | 327        |
| 2     | 60                 | 3.9 ± 1.2 | 15.7 ± 2.2             | 760        | 447              | 273        |
| 3     | 70                 | 3.4 ± 0.4 | 12.6 ± 2.9             | 1137       | 680              | 265        |
| 4     | 80                 | 2.6 ± 0.1 | 9.8 ± 1.3              | 694        | 302              | 258        |
| 5     | 100 <sup>c</sup>   | -         | -                      | -          | -                | 245        |

<sup>a</sup> The composites were cured for 3 hours at 140 °C, followed by another 3 hours at 160 °C, and post-cured for 1 hour at 180 °C. The resin composition is 50 wt % of CSO, 20 wt % of BMA, 15 wt % of DVB, and 15 wt % of MA.

<sup>b</sup> Unreinforced resin containing 50 wt % of CSO, 35 wt % of BMA, and 15 wt % of DVB.

<sup>c</sup> Non-dried sugar-cane bagasse without resin.

The reinforcing effect of sugar-cane bagasse can be clearly observed when comparing the storage modulus results of the unreinforced resin and a composite containing 60 wt % of

sugar-cane bagasse (entries 1 and 2, Table II). Indeed, a five fold improvement in  $E'$  at 25 °C and an eight fold improvement in  $E'$  at  $T_g + 50$  °C are observed when sugar-cane bagasse is added to the resin. When the filler content is increased from 60 wt % to 80 wt % (entries 2-4, Table II), a decrease in the tensile properties is observed. As indicated by SEM images of soybean<sup>35</sup> and rice hull<sup>38,39</sup> composites with similar resin compositions the higher filler content leads to agglomeration of the ligno-cellulosic particles and formation of weak points within the composite structure.

In the three-point bending mode of deformation, an increase in the filler content from 60 wt % to 70 wt % is beneficial to the flexural properties of the composite, as noted by an increase in the storage modulus (entries 2 and 3, Table II). This behavior is in contrast to what has been observed for the tensile properties, leading to the conclusion that with a filler load of 70 wt %, the particle agglomeration isn't sufficient to have a negative impact on the flexural properties. Instead, the reinforcing nature of the sugar-cane bagasse particles prevails, and an increase in storage modulus results. When the filler content is increased to 80 wt %, there is an excess of filler, as discussed earlier for the tensile properties, and a decrease in the storage modulus is observed (entry 4, Table II).

Homogeneous composites containing less than 60 wt % of sugar-cane bagasse could not be obtained. The filler deposited on the bottom of the mold, and significant resin leakage from the mold during the cure has been observed. The resulting material exhibited a rough surface and the properties could not be measured. Likewise, a mixture of filler and resin beyond the 80/20 ratio doesn't result in viable composites, as the materials crumble too easily



when handled, which is a consequence of the lack of enough resin to hold the filler particles together.

The thermal stability of the sugar-cane bagasse composites is strongly dependent on the filler content, as evident when comparing the  $T_7$  values of the composites containing 60 wt % to 80 wt % of sugar-cane bagasse (entries 2-4, Table II, and Figure 2).  $T_7$  represents the temperature at which 7 wt % of the material has degraded in the TGA experiment. By comparing the  $T_7$  values of the unreinforced resin and the sugar-cane bagasse alone (entries 1 and 5, Table II), it becomes evident that the sugar-cane bagasse is significantly less thermally stable than the vegetable oil-based resin. Therefore, it is expected that a mixture of the two components would result in a material with a thermal stability between those observed for the filler and the resin individually. As the amount of filler increases in the composite (entries 2-4, Table II), a gradual decrease in the  $T_7$  value is observed, and the degradation temperature approaches that of the filler alone (entry 5, Table II). That trend can be better visualized in Figure 2.

Figure 2 illustrates the TGA curves of the unreinforced resin, the sugar-cane bagasse, and composites containing 60 wt % to 80 wt % of sugar-cane bagasse. It is interesting to note that the thermal degradation of the unreinforced resin occurs in one major step, while that of the sugar-cane bagasse can be divided into four well defined steps. The first step corresponds to desorption of water from the filler structure and occurs between 80 °C and 110 °C. The second step, from 251 °C until 320 °C, corresponds to degradation of the hemicellulose. The third step, occurring in the 320 °C to 368 °C temperature range, corresponds to degradation of the cellulose. The lignin component of biomass typically degrades over a wide range of

temperatures.<sup>39</sup> In this case, the values determined from the derivative of the TGA curve (not shown in Figure 2) are 245 °C to 534 °C.

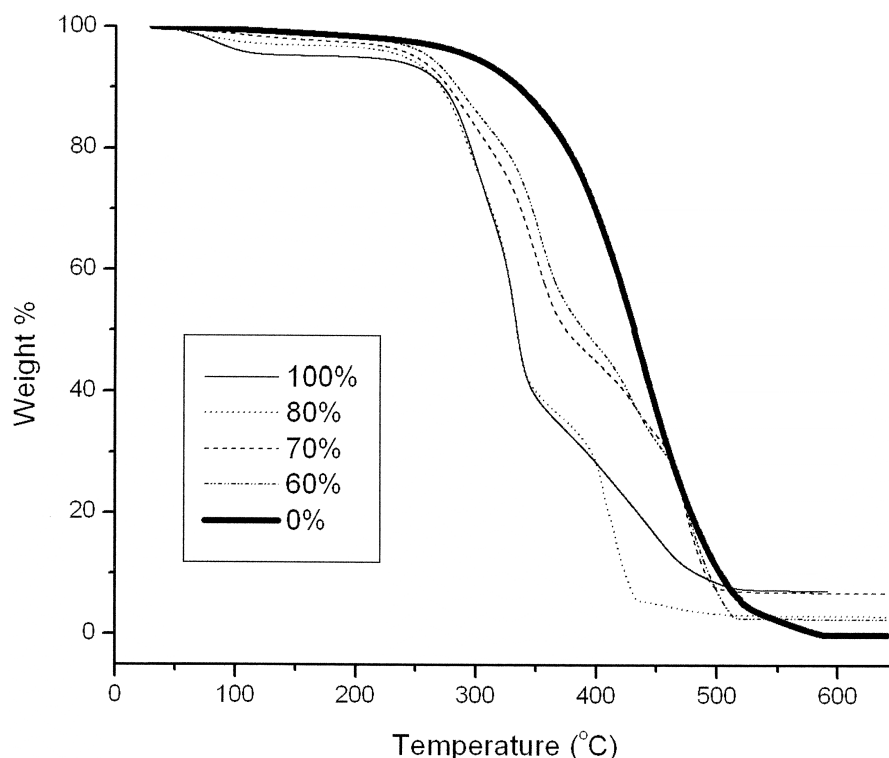


**Figure 2.** TGA curves for CSO-based composites reinforced with varying amounts of sugar-cane bagasse. The resin composition is 50 wt % of CSO, 20 wt % of BMA, 15 wt % of DVB, and 15 wt % of MA, and the cure sequence consists of 3 hours at 140 °C, followed by 3 hours at 160 °C. The composites are post-cured at 180 °C for 1 hour.

The thermal degradation pattern observed for composites containing 60 wt % to 80 wt % of the filler is similar to that obtained for the sugar-cane bagasse alone, with four well defined degradation stages. Significant differences are only observable in the degradation pattern after approximately 400 °C, namely during degradation of the main resin components. In view of the results presented in this section, 60 wt % is considered to be the optimum amount of filler in these sugar-cane bagasse composites, and that filler load has been used for the preparation of all composites in the remainder of this project.

**Resin composition.** It has been previously shown that changes in the resin composition can significantly affect the mechanical properties of bio-based composites.<sup>35,38</sup> The use of vegetable oils with different numbers of carbon-carbon double bonds directly affects the crosslink density of the matrix and, as a consequence, differences in the tensile strength, and Young's and storage moduli have been observed when comparing CSO and CLO-based rice hull composites.<sup>38</sup> Furthermore, the addition of MA as a filler-resin compatibilizer in vegetable oil-based rice hull composites has resulted in a significant improvement in the storage modulus by promoting better stress transfer from the matrix to the reinforcement.<sup>38</sup> The properties of sugar-cane bagasse composites prepared with resins of various compositions are given in Table III.

**Table III.** Characterization of sugar-cane bagasse composites with various resin compositions.<sup>a</sup>

| Entry | Oil (50 wt %) | BMA (wt %) | MA (wt %) | <i>E</i> (GPa) | Tensile Strength (MPa) | <i>T<sub>g1</sub></i> (°C) <sup>b</sup> | <i>T<sub>g2</sub></i> (°C) <sup>b</sup> | <i>E'</i> at <i>T<sub>g2</sub></i> + 50 °C (MPa) | Soluble Content (wt %) <sup>c</sup> |
|-------|---------------|------------|-----------|----------------|------------------------|---|---|--|-------------------------------------|
| 1     | CSO           | 35         | -         | 3.0 ± 0.6      | 9.3 ± 0.4              | 15                                      | 115                                     | 676  | 4                                   |
| 2     | CSO           | 20         | 15        | 3.9 ± 1.2      | 15.7 ± 2.2             | -20                                     | 83                                      | 450  | 3                                   |
| 3     | CLO           | 20         | 15        | 3.2 ± 0.4      | 13.8 ± 0.9             | -24                                     | 76                                      | 1180   | 5                                   |
| 4     | TUN           | 35         | -         | 3.7 ± 0.7      | 16.2 ± 1.2             | 20                                      | 113                                     | 1169   | 2                                   |
| 5     | TUN           | 20         | 15        | 3.5 ± 0.7      | 14.0 ± 0.7             | 10                                      | 74                                      | 895  | 7                                   |

<sup>a</sup> The composites contained 60 wt % of filler, and have been cured for 3 hours at 140 °C, followed by another 3 hours at 160 °C, and post-cured for 1 hour at 180 °C.

<sup>b</sup> Determined by DMA.

<sup>c</sup> Determined after Soxhlet extraction with CH<sub>2</sub>Cl<sub>2</sub> for 24 hours.

From the results in Table III, it is evident that, for composites prepared in the absence of MA, the choice of the oil used to prepare the resin has a strong influence on the tensile and flexural properties of the final composite material. Indeed, significant increases in the tensile strength and in the storage modulus at  $T_g + 50$  °C are observed when tung oil is used as the major resin component in comparison with CSO (entries 1 and 4, Table III). With an average of 7.9 carbon-carbon double bonds per triglyceride, tung oil can form a matrix with a higher crosslink density than CSO (~4.5 carbon-carbon double bonds per triglyceride), which results in overall better mechanical properties. This hypothesis is supported by the soluble content recovered from the corresponding samples after Soxhlet extraction (entries 1 and 4, Table III). Only 2 wt % of soluble material has been recovered from the sample prepared with tung oil, as opposed to 4 wt % recovered from the sample prepared with CSO. An exception to the trend of improved mechanical properties with the use of a more unsaturated oil is the Young's modulus. The difference in the stiffness of samples prepared with TUN and CSO isn't significant and cannot be attributed to the structure of the oils used (entries 1 and 4, Table III).

For MA-containing composites (entries 2, 3, and 5, Table III), the relationship between the oil structure and the mechanical properties isn't as clear as for the composites that do not contain MA. No significant changes in the tensile properties are observed for samples prepared with different oils, as the results obtained for the Young's modulus and the tensile strength fall within the standard deviation of the corresponding measurements. When CLO (~6.0 carbon-carbon double bonds per triglyceride) is used as the major resin component, an increase in the storage modulus at  $T_g + 50$  °C is observed when compared to the sample made from CSO (entries 2 and 3, Table III). However, a decrease in that number

is observed when tung oil is used (entry 5, Table III). The soluble content results are also opposite the expected trend, as more material is recovered from samples prepared with the more unsaturated oils.

These results can't be fully explained, but the deviation from the expected trends are possibly related to the initial treatment applied to the sugar-cane bagasse. The wash and the extended drying to which the fillers have been submitted may have affected the surface of the ligno-cellulosic materials, and therefore altered their polarity, making them less hydrophilic. In that sense, MA no longer works as a compatibilizer between a hydrophobic matrix and a highly hydrophilic filler. On the one hand, this leads to a better interaction between filler and resin even in the absence of MA. On the other hand, the addition of MA to the resin composition represents a decrease in the BMA content. As demonstrated previously with soybean and rice hull composites, the mechanical properties are also closely related to the BMA content of the resin.<sup>35,38</sup>

The trend observed when comparing the mechanical properties of composites made with and without MA is further evidence of the poor compatibilizing effect that MA exhibits in this system. For CSO-containing composites (entries 1 and 2, Table III), the replacement of 15 wt % of BMA with 15 wt % of MA resulted in an expected increase in the tensile properties. Nevertheless, a significant decrease in the storage modulus at  $T_g + 50$  °C is also observed. When tung oil is the major resin component (entries 4 and 5, Table III), the addition of MA results in a decrease in all of the mechanical properties measured. The effect of substituting BMA by MA on the storage modulus can be better visualized in Figure 3,

where the curves of  $E'$  versus temperature for composites prepared with and without MA are plotted.

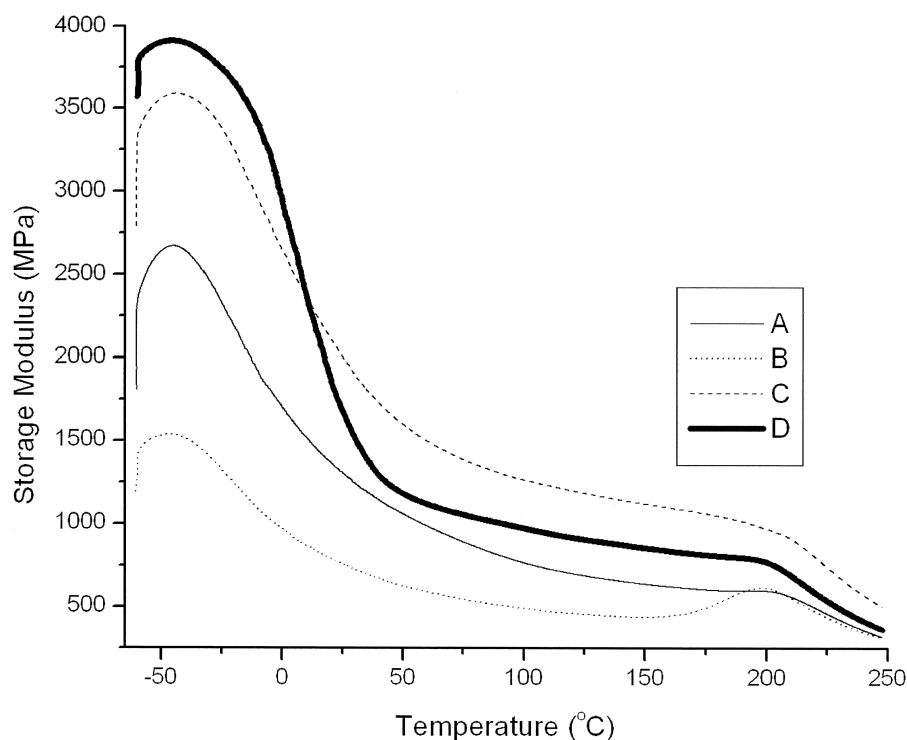


**Figure 3.** Storage modulus versus temperature for composites with the following resin compositions: (A) 50 wt % of CSO, 35 wt % of BMA, and 15 wt % of DVB; (B) 50 wt % of CSO, 20 wt % of BMA, 15 wt % of DVB, and 15 wt % of MA; (C) 50 wt % of TUN, 35 wt % of BMA, and 15 wt % of DVB; (D) 50 wt % of TUN, 20 wt % of BMA, 15 wt % of DVB, and 15 wt % of MA. The composites possess a filler/resin ratio of 60/40, and have been cured for 3 hours at 140 °C and 3 hours at 160 °C, and post-cured for 1 hour at 180 °C.

From a comparison of Figures 3A and 3B, it is clear that the addition of MA to CSO-containing composites results in a lower storage modulus throughout the temperature range investigated. For the tung oil-containing samples (Figures 3C and 3D), the results are a little more complex. Indeed, the expected trend of MA-containing materials exhibiting a higher storage modulus is observed for temperatures below 10 °C. After that, an inversion occurs,

and the MA-containing composite exhibits a lower  $E'$ . Beyond approximately 210 °C, a decrease in  $E'$  indicates initial degradation of the system.

The  $^1\text{H}$  NMR spectra of the extract of sugar-cane bagasse, CSO, and the extract of a composite containing 60 wt % of filler with a resin that's composed of 50 wt % of CSO, 20 wt % of BMA, 15 wt % of DVB, and 15 wt % of MA are presented in Figure 4. In the spectrum of the sugar-cane bagasse extract (Figure 4A), only protons in the aliphatic region have been detected. Although the substance extracted hasn't been thoroughly characterized and identified, the absence of characteristic peaks indicating functional groups and/or multiple bonds in the spectrum implies that this substance is, most likely, a hydrocarbon, that could work as a plasticizer in the composite system. Nevertheless, only 5 wt % of that material has been recovered after Soxhlet extraction (data not included in Table II).

Figure 4C is representative of the extracts of all of the composites prepared in this work. By comparing Figures 4B and 4C, it becomes clear that the vegetable oil is the major component extracted from the composite. Indeed, this has been observed in previous works with soybean and rice hulls,<sup>35,39</sup> and has been attributed to the low reactivity of the oil relative to the other co-monomers present in the matrix.

From the results in Table III, it is evident that all of the composites prepared exhibit two distinct  $T_g$ 's. The appearance of two  $T_g$ 's has been previously attributed to a phase separation of the resin due to a significant difference in the reactivity and rate of polymerization of the different co-monomers that comprise the matrix.<sup>35,38</sup> It has also been previously noted that when more unsaturated oils are used as the major resin component, the

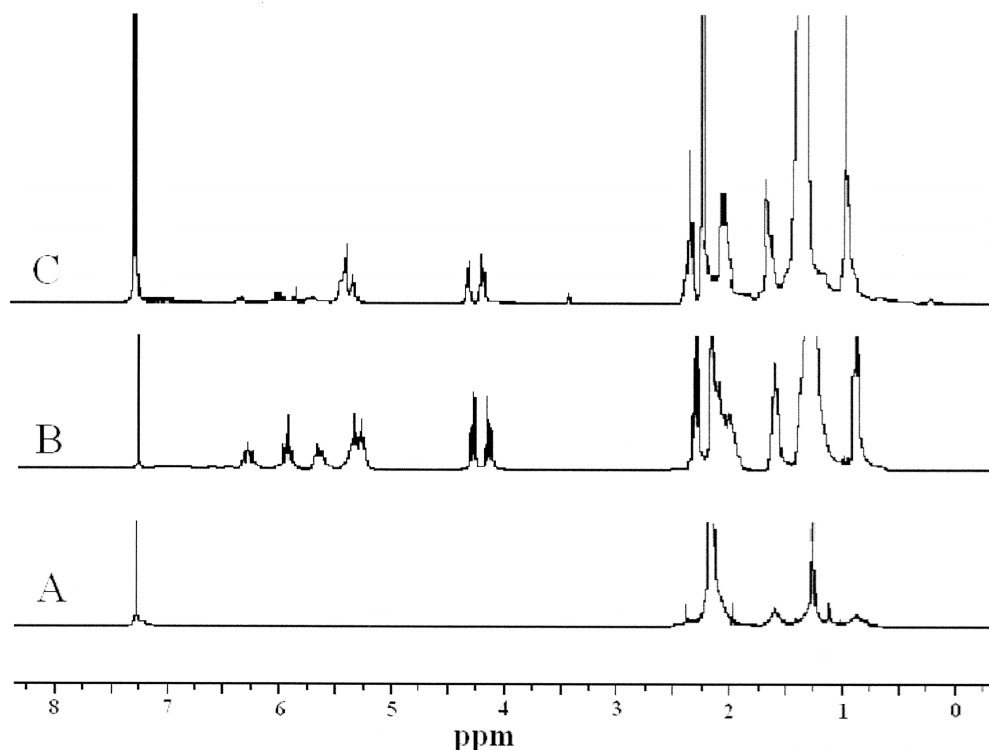


**Figure 4.**  $^1\text{H}$  NMR spectra of (A) the extract of sugar-cane bagasse, (B) CSO, and (C) the extract of a composite containing 60 wt % of filler and a resin that's composed of 50 wt % of CSO, 20 wt % of BMA, 15 wt % of DVB, and 15 wt % of MA cured for 3 hours at 140 °C and for 3 hours at 160 °C, followed by a post-cure at 180 °C for 1 hour.

phase separation is avoided due to their increased reactivity, and only one  $T_g$  is observed as a consequence.<sup>38</sup> Here, two distinct  $T_g$ 's are observed for all of the composites prepared, regardless of the oil used. It is believed that the better filler-resin interaction imparted by the initial wash and drying of the filler makes the diffusion of larger molecules, such as triglycerides, more difficult. Molecules that can diffuse better, react faster, and get incorporated into the growing polymer chains preferentially, which results in the phase separation. It is interesting to note that the  $T_g$ 's of samples prepared with MA are significantly lower than the ones observed for samples that do not contain MA, when the same oil is used (entries 1 and 2, and 4 and 5, Table III).



Figure 5 compares the tan delta curves of samples made with different vegetable oils. It is noticeable that all samples exhibit two tan delta peaks, independent of the oil used, indicative of two distinct  $T_g$ 's. The first  $T_g$  is attributed to the vegetable oil-rich phase, whereas the second  $T_g$  relates to a DVB-rich phase.

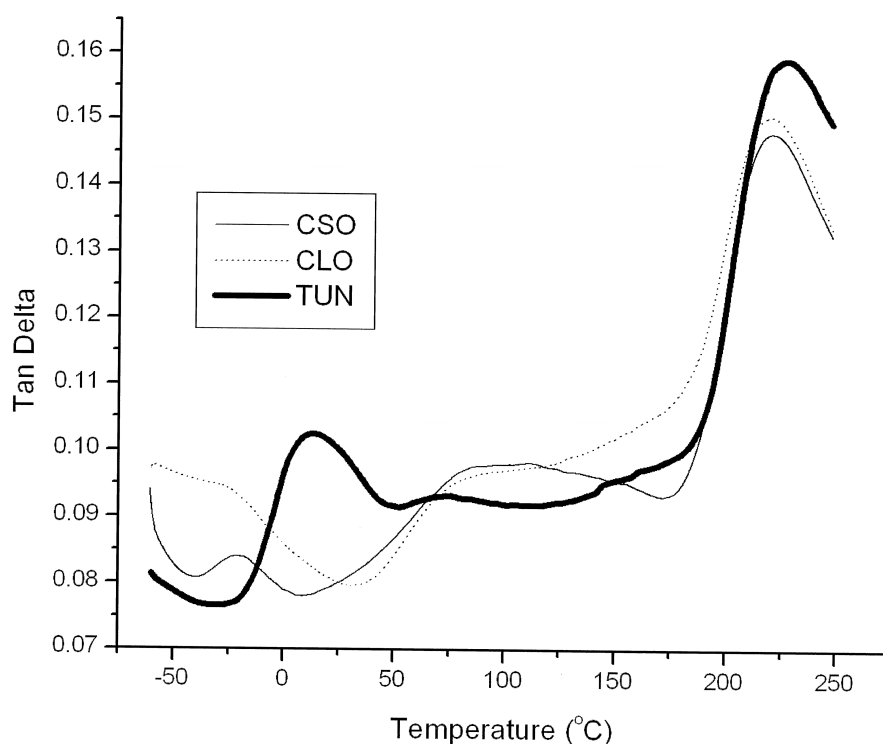


**Figure 5.** Tan delta curves for samples made with (A) CSO, (B) CLO, and (C) tung oil. The composites possess a filler/resin ratio of 60/40, and have been cured for 3 hours at 140 °C and 3 hours at 160 °C, and post-cured for 1 hour at 180 °C. The resin composition is 50 wt % of vegetable oil, 20 wt % of BMA, 15 wt % of DVB, and 15 wt % of MA.

## Conclusions

In this work, we have prepared vegetable oil-based thermoset composites reinforced with sugar-cane bagasse. An initial cure sequence study showed that the changes in mechanical properties, observed when the sample is cured under different temperatures and

times, are related to the thermal stability of the filler. However, the post-cure step, carried out at ambient pressure, right after the cure of the material, has a great impact on the crosslink density of the resin, as shown by the Soxhlet extraction results. An optimum filler load of 60 wt % resulted in the most thermally stable and viable composites. Furthermore, better overall properties are obtained when more unsaturated oils are used as the major resin component. It has been shown that the initial washing and drying of the sugar-cane bagasse affect the filler-resin interaction and result in a phase separation of the matrix, independent of the oil used in the preparation of the composites. Also, with a better interaction between resin and filler, MA no longer acts as a compatibilizer in the system, and an overall decrease in storage modulus is observed when MA is added to the resin composition.

### **Acknowledgements**

The authors thank the Recycling and Reuse Technology Transfer Center of the University of Northern Iowa for financial support, the U. S. Sugar Corporation for the sugar-cane bagasse provided, Professor Michael Kessler from the Department of Material Sciences and Engineering and Dr. Richard Hall from the Department of Natural Resource Ecology and Management at Iowa State University (ISU) for the use of their facilities, and Darren Jarboe from the Center for Crops Utilization Research at ISU for important information on sugar-cane bagasse.

### **References**

1. Huber, G. W.; Iborra, S.; Corma, A. *Chem. Rev.* 2006, 106, 4044.
2. Demirbas, A. *Energy Convers. Manage.* 2009, 50, 2782.
3. Baboi, M.; Srinivasan, G.; Jane, J. L.; Grewell, D. *Int. Polym. Processing* 2007, 22, 489.

4. Srinivasan, G.; Grewell, D. 67th ANTEC, 2009, 2610.
5. Van De Mark, M. R.; Sandefur, K. *in* Industrial Uses of Vegetable Oil, Editor, Erhan, S. Z.; AOCS Press: Peoria, IL 2005, 143.
6. Lu, Y.; Larock, R. C. ChemSusChem 2010, 3, 329.
7. Xia, Y.; Lu, Y.; Larock, R. C. Polymer 2010, 51, 53.
8. Brandao, R. F.; Quirino, R. L.; Mello, V. M.; Tavares, A. P.; Peres, A. C.; Guinhos, F.; Rubim, J. C.; Suarez, P. A. Z. J. Braz. Chem. Soc. 2009, 20, 954.
9. Ashraf, S. M.; Ahmad, S.; Riaz, U. Polym. Int. 2007, 56, 1173.
10. Wang, C.; Yang, L.; Ni, B.; Shi, G. J. Appl. Polym. Sci. 2009, 114, 125.
11. Ionescu, M.; Ji, Y.; Shirley, W. M.; Petrovic, Z. S. *in* Renewable and Sustainable Polymers, Editors, Payne, G. F.; Smith, P. B. ACS Books, Symposium Series 2011, 1063, 73.
12. Sharma, H. O.; Alam, M.; Riaz, U.; Ahmad, S.; Ashraf, S. M. Int. J. Polymer Mater. 2007, 56, 437.
13. Gultekin, M.; Beker, U.; Guner, F. S.; Erciyes, A. T.; Yagci, Y. Macromol. Mater. Eng. 2000, 283, 15.
14. Bhuyan, S.; Holden, L. S.; Sundararajan, S.; Andjelkovic, D.; Larock, R. C. Wear 2007, 263, 965.
15. Sharma, V.; Banait, J. S.; Kundu, P. P. J. Appl. Polym. Sci. 2009, 111, 1816.
16. Zhan, M.; Wool, R. P. J. Appl. Polym. Sci., 2010, 118, 3274.
17. Lu, Y.; Larock, R. C. ChemSusChem, 2009, 2, 136.
18. Zhang, G.; Zhao, L.; Hu, S.; Gan, W.; Yu, Y.; Tang, X. Polym. Eng. Sci. 2008, 48, 1322.
19. Sharma, V.; Banait, J. S.; Kundu, P. P. J. Appl. Polym. Sci. 2009, 114, 446.
20. Thulasiraman, V.; Rakesh, S.; Sarojadevi, M. Polymer Composites 2009, 30, 49.
21. Lu, Y.; Larock, R. C. Macromol. Mater. Eng. 2007, 292, 1085.
22. Henna, P. H.; Kessler, M. R.; Larock, R. C. Macromol. Mater. Eng. 2008, 293, 979.
23. Xu, Y.; Wu, Q.; Lei, Y.; Yao, F. Bioresour. Technol. 2010, 101, 3280.
24. Schirp, A.; Loge, F.; Aust, S.; Swaner, P.; Turner, G.; Wolcott, M. J. Appl. Polym. Sci. 2006, 102, 5191.
25. Haque, M. M.; Hasan, M.; Islam, M. S.; Ali, M. E. Bioresour. Technol. 2009, 100, 4903.
26. Haq, M.; Burgueno, R.; Mohanty, A. K.; Misra, M. Comp. Sci. Tech. 2008, 68, 3344.
27. Andjelkovic, D. D.; Valverde, M.; Henna, P.; Li, F.; Larock, R. C. Polymer 2005, 46, 9674.

28. Valverde, M.; Andjelkovic, D.; Kundu, P. P.; Larock, R. C. *J. Appl. Polym. Sci.* 2008, **107**, 423.
29. Kundu, P. P.; Larock, R. C. *Biomacromolecules* 2005, **6**, 797.
30. Andjelkovic, D. D.; Min, B.; Ahn, D.; Larock, R. C. *J. Agric. Food Chem.* 2006, **54**, 9535.
31. Xia, Y.; Lu, Y.; Larock, R. C. *Polymer* 2010, **51**, 53.
32. Rybak, P. A. Fokou and M. A. R. Meier, *Eur. J. Lipid Sci. Tech.*, 2008, **110**, 797.
33. D. P. Pfister and R. C. Larock, *J. Appl. Polym. Sci.*, 2011, *accepted for publication*.
34. D. P. Pfister, J. R. Baker, P. H. Henna, Y. Lu and R. C. Larock, *J. Appl. Polym. Sci.*, 2008, **108**, 3618.
35. R. L. Quirino and R. C. Larock, *J. Appl. Polym. Sci.*, 2009, **112**, 2033.
36. D. P. Pfister and R. C. Larock, *Bioresour. Technol.*, 2010, **101**, 6200.
37. D. P. Pfister and R. C. Larock, *Composites Part A: Appl. Sci. Manufacturing*, 2010, **41**, 1279.
38. R. L. Quirino and R. C. Larock, *J. Appl. Polym. Sci.*, 2011, **121**, 2050.
39. R. L. Quirino and R. C. Larock, *J. Appl. Polym. Sci.*, 2011, **121**, 2039.

## CHAPTER 7. OAT HULL COMPOSITES FROM CONJUGATED NATURAL OILS

A Paper Submitted to Green Chemistry.

Rafael L. Quirino, Yixin Ma, Richard C. Larock\*

*Department of Chemistry, Iowa State University, Ames, Iowa 50011*

### Abstract

Oat hull composites have been prepared by the free radical polymerization of regular or modified natural oils with divinylbenzene, *n*-butyl methacrylate, and maleic anhydride in the presence of dried, ground oat hulls. Parameters, such as cure time, filler load, cure temperature, and the fatty acid composition of the conjugated natural oil, have been investigated and related to the structure and properties of the composites. Structure-property relationships have been determined with the use of tensile tests, DMA, TGA, and Soxhlet extraction, followed by <sup>1</sup>H NMR spectroscopic analysis of composite extracts. The best overall properties have been obtained for tung oil-based composites bearing 80 wt % of oat hulls cured at 160 °C for 4 hours.

### Introduction

The partial replacement of petroleum-derived plastics and composites by novel bio-based materials from inexpensive, renewable, natural resources has the potential to greatly impact the plastics, coatings, and composites industries. Currently, the polymer industry is responsible for approximately 7% of all oil and gas used worldwide.<sup>1</sup> Natural starting materials, such as natural oils and agricultural residues, tend to be readily available in large

quantities, and may afford more biodegradable materials than the virtually indestructible petroleum-based polymers. Furthermore, new bio-based materials may present properties not currently available in commercial petroleum-based products, with an overall intrinsic low toxicity. These characteristics make bio-based materials very appealing, and the increasing attention bio-renewable chemicals are receiving in both industrial and academic settings may lead to significant progress towards environmental sustainability in the near future.<sup>1,2</sup>

A variety of chemicals and materials are currently prepared from natural oils, polysaccharides, wood, and proteins.<sup>3</sup> As an example, natural oils find wide use in paints,<sup>4</sup> biocoatings,<sup>5,6</sup> biofuels,<sup>7</sup> and as building blocks for bio-based polymeric resins, including polyurethanes,<sup>8-10</sup> polyester amides,<sup>11</sup> multicomponent thermosets,<sup>12-14</sup> and cyanate esters.<sup>15</sup> As a matter of fact, 15% of all soybean oil produced from 2001 to 2005, was employed for industrial uses.<sup>16</sup>

Natural oils are triglycerides that differ from one another with respect to the length of the fatty acid chains, and the number and position of the carbon-carbon double bonds along those fatty acid chains. The final fatty acid composition of a specific natural oil is directly related to its physical and nutritional properties, and varies according to the plant from which the oil is extracted and the corresponding growing conditions.<sup>17</sup> Table I summarizes the fatty acid composition of the most commonly used natural oils.

In recent years, a variety of bio-based polymers, with good thermal and mechanical properties, have been developed through the free radical<sup>18-21</sup> or cationic<sup>22-24</sup> copolymerization of regular or modified natural oils with several petroleum-based comonomers. In such

**Table I.** Approximate fatty acid composition of commonly used natural oils in the preparation of new bio-based materials.

| Oil                   | Linolenic acid (C <sub>18:3</sub> ) <sup>a</sup> content (%) | Linoleic acid (C <sub>18:2</sub> ) <sup>a</sup> content (%) | Oleic acid (C <sub>18:1</sub> ) <sup>a</sup> content (%) | Stearic acid (C <sub>18:0</sub> ) <sup>a</sup> content (%) | Palmitic acid (C <sub>16:0</sub> ) <sup>a</sup> content (%) | Double bonds per triglyceride <sup>b</sup> |
|-----------------------|--|---|--|--|---|--|
| Tung oil <sup>c</sup> | -  | 6   | 4  | -  | 6   | 7.9  |
| Linseed oil           | 56   | 15  | 19   | 4  | 6   | 6.5  |
| Soybean oil           | 8  | 54  | 23   | 4  | 11  | 4.7  |
| Corn oil              | 1  | 60  | 26   | 2  | 11  | 4.5  |
| Fish oil <sup>d</sup> | -  | -   | 11-25  | -  | 10-22   | 9.9  |

<sup>a</sup> The notation in parentheses (C<sub>x,y</sub>), after the fatty acid name, denotes the number of carbon atoms (x), followed by the number of carbon-carbon double bonds (y) in the corresponding fatty acid. The carbon-carbon double bonds in these natural oils possess predominantly a *cis* configuration.

<sup>b</sup> Average number of carbon-carbon double bonds per triglyceride.

<sup>c</sup> Approximately 84 % of the fatty acid chains in tung oil are alpha-eleostearic acid, a naturally conjugated triene.<sup>18</sup>

<sup>d</sup> Fish oil possesses a high percentage of polyunsaturated fatty acids, containing as many as 5 to 6 non-conjugated carbon-carbon double bonds.<sup>22</sup>

systems, the reactive sites are the carbon-carbon double bonds in the triglycerides and the comonomers used. Overall, the reactivity of natural oils towards these polymerization processes can be significantly increased if the carbon-carbon double bonds in the fatty acid chains are conjugated.<sup>25</sup> Furthermore, the crosslink density of the final resin can be varied by using oils with varying numbers of carbon-carbon double bonds per triglyceride, or by varying the comonomers' concentration.

Bio-based materials with improved properties can be obtained by simply reinforcing these free radical or cationic polymeric matrices with various agricultural residues and natural fibers, such as spent germ,<sup>26</sup> soybean hulls,<sup>27</sup> corn stover,<sup>28</sup> wheat straw,<sup>29</sup> rice hulls,<sup>30</sup>

switch grass,<sup>31</sup> and wood flour.<sup>32</sup> These bio-based residues have been added to the aforementioned natural oil-based resins to prepare composites with up to 85 wt % of bio-based content, including the resin and the filler.<sup>26-32</sup>

One of the most promising resin compositions for composite applications investigated by us consists of 50 wt % of conjugated soybean oil (CSO) or conjugated linseed oil (CLO), 20 wt % of *n*-butyl methacrylate (BMA), 15 wt % of divinylbenzene (DVB), and 15 wt % of maleic anhydride (MA).<sup>30</sup> This system has been cured in the presence of an extra 5 wt % of the free radical initiator di-*t*-butyl peroxide (TBPO) with respect to the total resin weight.<sup>30</sup> In such a system, DVB acts as a crosslinker, while MA acts as a filler-resin compatibilizer.<sup>27,30</sup>

Oat hulls, another example of an abundant under-used agricultural by-product, are essentially the outer skin of the oat grain. The large quantity of oat hulls produced and their limited industrial application to date account for their low price. Due to their high pentose biopolymer content, oat hulls have been proposed as an alternative starting material for the production of furfural, which can be converted in the presence of aldehydes into hydrocarbons for biofuel applications through a three step process.<sup>33</sup> Because of their relatively high fiber content (lignin, cellulose, and hemicellulose), low cost, and ready availability, oat hulls are also particularly attractive as an economical and environmentally-friendly reinforcement for biocomposites.

In this work, we have prepared oat hull composites from a series of regular and conjugated natural oils. Parameters, such as cure temperature, filler load, cure time, and the degree of unsaturation of the oils have been varied, and structure-property relationships have been assessed by means of tensile tests, dynamic mechanical analysis (DMA),



thermogravimetric analysis (TGA), Soxhlet extraction followed by proton nuclear magnetic resonance ( $^1\text{H}$  NMR) spectroscopic analysis of the extracts, and differential scanning calorimetry (DSC).

### Experimental

**Materials.** *n*-Butyl methacrylate (BMA) was purchased from Alfa Aesar (Ward Hill, MA). Divinylbenzene (DVB), maleic anhydride (MA), di-*t*-butyl peroxide (TBPO), and tung oil (TUN) were purchased from Sigma-Aldrich (St. Louis, MO). All chemicals were used as received. Soybean oil and corn oil were purchased in a local grocery store. Superb linseed oil was generously provided by Archer Daniels Midland (Red Wing, MN), and Menhaden Norwegian fish oil was generously supplied by Omega Protein (Houston, TX). With the exception of tung oil, the natural oils have been conjugated using a rhodium catalyst, following a method developed and frequently used by our group.<sup>25</sup> The oat hulls, gratefully provided by Quaker Oats (Chicago, IL), have been ground to afford particles <2.0 mm in diameter, and dried in a vacuum oven at 70 °C overnight prior to being impregnated with the crude resin.

**General procedure for preparation of the oat hull composites.** The crude resin was prepared by mixing 50 wt % of regular or conjugated natural oil, 20 wt % of BMA, 15 wt % of DVB, and 15 wt % of MA in a beaker. The mixture was heated to 60 °C under agitation to melt the MA and form a homogeneous liquid. An extra 5 wt % of the total resin weight of the free radical initiator TBPO was added to the homogeneous mixture under agitation. That amount of TBPO had been previously determined to be the optimal amount in preliminary tests. The ground and dried oat hulls were manually mixed with the crude resin in a 6" x 6"

mold using a spatula. The filler/resin ratios varied from 70/30 to 80/20. The actual amount of filler and resin used in the preparation of each composite was tailored to yield a piece with a thickness of approximately 0.5 cm. The impregnated resin was compression molded at 600 psi at different times and temperatures. Cure times varied from 0.5 hours to 6 hours. The resulting composites were then demolded and post-cured in a convection oven for two hours at ambient pressure.

**Characterization of the composites.** Tensile tests were conducted at 25 °C according to ASTM D-638 using an Instron universal testing machine (model 5569) equipped with a video extensometer and operating at a crosshead speed of 2.0 mm/min. The dogbone test specimens had the following gauge dimensions: 57.0 mm x 12.7 mm x 4.5 mm (length, width, and thickness, respectively). For each composite, seven dogbones were cut and tested. The results presented in the text are the average of these measurements along with the calculated standard deviation.

Dynamic mechanical analysis (DMA) was conducted on a Q800 DMA (TA Instruments, New Castle, DE) using a three-point bending mode with a 10.0 mm clamp. Rectangular specimens of 22.0 mm x 8.5 mm x 1.5 mm (length, width, and thickness, respectively) were cut from the samples. Each specimen was cooled to -60 °C and then heated at 3 °C/min to 250 °C. The tests were performed using a frequency of 1 Hz and an amplitude of 14 µm under air. Two runs for each sample were carried out and the results presented in the text reflect the average of the two measurements.

A Q50 TGA instrument (TA Instruments) was used to measure the weight loss of the samples under an air atmosphere. The samples were heated from room temperature to 650 °C at a heating rate of 20 °C/min. The samples weighed approximately 10 mg.

Soxhlet extraction was conducted to determine the amount of soluble materials in the composites. A 2 g sample was extracted for 24 h with dichloromethane (CH<sub>2</sub>Cl<sub>2</sub>). After extraction, the resulting solution was concentrated on a rotary evaporator, and then both the soluble and insoluble materials were dried in a vacuum oven at 70 °C overnight before weighing. The soluble fraction of each extracted sample was dissolved in CDCl<sub>3</sub> and proton nuclear magnetic resonance (<sup>1</sup>H NMR) spectroscopic analysis was carried out. The <sup>1</sup>H NMR spectra were obtained with a Varian Unity spectrometer (Varian Associates, Palo Alto, CA) operating at 300 MHz.

Differential scanning calorimetry (DSC) experiments were carried out in a Q20 DSC (TA Instruments, New Castle, DE) under a N<sub>2</sub> atmosphere over a temperature range of -20 °C to 400 °C at a rate of 20 °C/min. The samples weighed approximately 10 mg.

## Results and Discussion

**Cure temperature analysis.** As observed in our previous studies with various natural fillers,<sup>26-32</sup> the cure temperature has a great impact on the properties of bio-based composites. It has been shown that the thermal stability of the filler is the limiting parameter for the establishment of an optimum cure temperature for a particular filler and resin combination.<sup>27,30,32</sup> After analyzing the TGA curve of the oat hulls (Figure 1D), it has been observed that only 3 wt % of the filler degrades between 140 °C and 240 °C, defining a range of temperatures where the oat hulls can be considered thermally stable. Two temperatures

within that range (160 °C and 180 °C) have been investigated as potential cure temperatures for oat hull composites. The composites have been cured at the chosen temperatures for 5 hours and then post-cured for 2 hours at 180 °C or 200 °C to ensure maximum crosslinking and incorporation of the comonomers into the matrix.

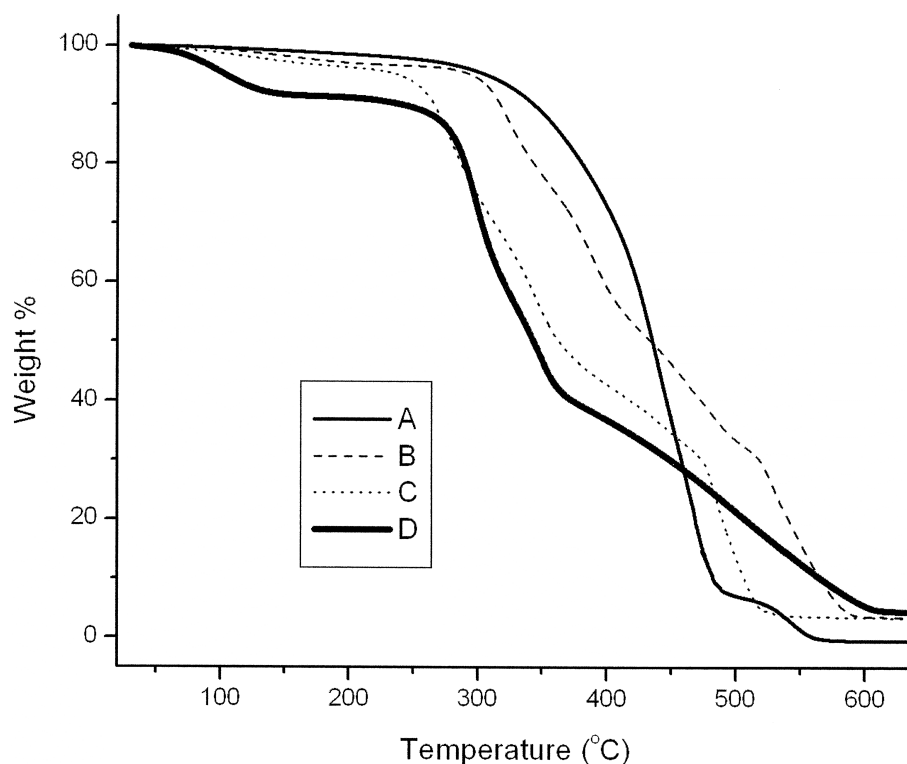


**Figure 1.** TGA curves for: (A) a resin consisting of 50 wt % of CSO, 35 wt % of BMA and 15 wt % of DVB, (B) an oat hull composite cured at 180 °C for 5 hours and post-cured at 200 °C for 2 hours, (C) an oat hull composite cured at 160 °C for 5 hours and post-cured at 180 °C for 2 hours, and (D) oat hulls. The matrix of the composites consists of 50 wt % of CSO, 20 wt % of BMA, 15 wt % of DVB, and 15 wt % of MA.

When comparing the TGA curves of the filler and the pure resin, it is obvious that the resin is more thermally stable than the filler up to 455 °C. Indeed, it has been shown that the scission of carbon-carbon single bonds in triglycerides starts at temperatures ranging from 410 °C to 450 °C, depending on the oil or fat.<sup>7</sup> So it is expected that the major matrix

component degrades at a significant rate at temperatures higher than 450 °C, resulting in a lower thermal stability for the resin in comparison to the filler after that temperature. When comparing the TGA curves of composites cured at 160 °C or 180 °C, a similar degradation pattern can be observed. The most significant difference between the two samples resides in the fact that the sample cured at a lower temperature starts to significantly degrade at 230 °C, whereas the composite cured at 180 °C starts to degrade at 288 °C. These observations suggest that during the cure at 180 °C the material undergoes more degradation than when the cure is carried out at 160 °C. In fact, the higher cure temperature is responsible for a partial degradation of the least thermally stable components of the system, resulting in a material that is richer in more thermally stable components, but with a compromised structure. Similar results have been observed when studying the cure process of rice hull<sup>30</sup> and wood flour<sup>32</sup> composites. The mechanical properties of samples cured at 160 °C and 180 °C are shown in Table II.

**Table II.** Mechanical properties of oat hull composites cured at different temperatures.<sup>a</sup>

| Entry | Cure temperature (°C) | Post-cure temperature (°C) | Young's modulus (GPa) | Tensile strength (MPa) | $T_{g1}$ (°C) | $T_{g2}$ (°C) | Storage modulus (MPa) |                     |
|-------|-----------------------|----------------------------|-----------------------|------------------------|---------------|---------------|-----------------------|---------------------|
|       |                       |                            |                       |                        |               |               | at 25 °C              | at $T_{g2} + 50$ °C |
| 1     | 180                   | 200                        | - <sup>b</sup>        | - <sup>b</sup>         | -5            | 98            | 633                   | 331                 |
| 2     | 160                   | 180                        | 2.5 ± 0.8             | 9.7 ± 2.2              | -1            | 95            | 561                   | 287                 |

<sup>a</sup> Conjugated soybean oil (CSO) was employed as the major resin component (50 wt %), and a filler/resin ratio of 70/30 (weight) was used.

<sup>b</sup> The sample readily crumbled when handled and dogbone specimens could not be obtained to perform the tensile tests.

Due to severe degradation of the composite structure during the cure at 180 °C (entry 1, Table II), dog-bone specimens could not be obtained in order to run tensile tests on that sample. When the cure is carried out at 160 °C (entry 2, Table II), no obvious degradation of the composite is observed and the results for Young's modulus and tensile strength are comparable to commercial (<20%) glass fiber/epoxy composites.

The observation of two distinct  $T_g$ 's in natural oil-based resins and composites has been thoroughly studied and discussed in previous publications and is attributed to a phase separation of the matrix into an oil-rich domain and an oil-poor domain.<sup>30,32</sup> This separation occurs due to the distinctly different reactivity of the natural oil and the other resin components towards free radical polymerization. The gap between the two  $T_g$ 's observed ( $T_{g2} - T_{g1}$ ) is directly related to the extent of the phase separation. When the composite is cured at 180 °C, that gap equals 103 °C, whereas a gap of 96 °C is observed when the sample is cured at 160 °C. The cure at a higher temperature, promotes a higher polymerization rate, affecting primarily the more reactive resin components, and resulting in a more pronounced phase separation.

Also, the higher cure temperature affords a composite with a higher storage modulus, which is possibly related to a slightly higher crosslink density of the matrix. Nevertheless, a difference of only 2 wt % has been detected in the soluble content after Soxhlet extraction of samples cured at the two different temperatures (results not shown in Table II). The Soxhlet extraction results will be discussed in more detail later in the text. Finally, despite the lower storage modulus observed for the composite cured at 160 °C, that temperature does not cause the same degradation of the composite structure as the cure at 180 °C. Therefore, 160 °C will

be used as the cure temperature for preparation of all oat hull composites in the remainder of this project.

**Filler load evaluation.** In order to determine the optimal amount of filler, oat hull composites with 70/30 and 80/20 filler/resin ratios have been prepared. The mechanical properties and extraction results of those samples are presented in Table III. Composites with filler/resin ratios lower than 70/30 cannot be obtained due to excessive resin leakage during the cure. Samples with filler/resin ratios higher than 80/20 result in composites where the excess of filler causes agglomeration of oat hulls and formation of exceedingly large weak regions within the composite's structure.

**Table III.** Mechanical properties and extraction results of oat hull composites with different filler loads.<sup>a</sup>

| Entry | Filler load (wt %) | Young's modulus (GPa) | Tensile strength (MPa) | $T_{g1}$ (°C) | $T_{g2}$ (°C) | Storage modulus (MPa) |                     | Soluble content (wt %) <sup>b</sup> |
|-------|--------------------|-----------------------|------------------------|---------------|---------------|-----------------------|---------------------|-------------------------------------|
|       |                    |                       |                        |               |               | at 25 °C              | at $T_{g2} + 50$ °C |                                     |
| 1     | 70                 | 2.5 ± 0.8             | 9.7 ± 2.2              | -1            | 95            | 561                   | 287                 | 4                                   |
| 2     | 80                 | 2.5 ± 0.7             | 8.2 ± 1.3              | 6             | 90            | 384                   | 170                 | 3                                   |

<sup>a</sup> The composites have been cured at 160 °C for 5 hours and post-cured at 180 °C for 2 hours. CSO has been used as the major resin component (50 wt %).

<sup>b</sup> Determined by Soxhlet extraction with CH<sub>2</sub>Cl<sub>2</sub> for 24 hours.

From the results in Table III, one can clearly see that there is no statistical difference between the Young's modulus and the tensile strength of composites with 70 wt % and 80 wt % of oat hulls (entries 1 and 2, Table III). The phase separation in the matrix of both samples is also very similar, since the value of  $T_{g2} - T_{g1}$  is exactly the same (96 °C) for both composites. The only property that shows a significant difference between the two samples is

the storage modulus ( $E'$ ). At room temperature, the sample containing 80 wt % of filler exhibits a modulus 30% lower than the sample containing 70 wt % of oat hulls. The decrease in  $E'$  between the two samples is 40% when the modulus is measured at  $T_{g2} + 50$  °C. This is the only indication that an increase in the filler load from 70 wt % to 80 wt % might have a negative effect on the composite's properties. Taking into consideration the similarity of the properties measured for oat hull composites with different filler loads and the relative volumes of resin and filler required to prepare such composites, a filler/resin ratio of 80/20 has been chosen as optimal.

As expected, due to the lower filler load, the soluble content recovered after Soxhlet extraction with  $\text{CH}_2\text{Cl}_2$  of the sample listed in entry 1 is slightly higher than that of the sample in entry 2 (Table III). It has been shown with a variety of other fillers that the majority of the soluble material recovered after Soxhlet extraction of similar bio-based composites consists of partially reacted or unreacted comonomers from the resin, most noticeably vegetable oils.<sup>27,30,32</sup> A similar situation is found here. Figure 2 shows a comparison of the  $^1\text{H}$  NMR spectra of conjugated soybean oil (CSO), and the soluble material recovered after Soxhlet extraction of oat hulls and an oat hull composite with a filler/resin ratio of 80/20.

From the spectra presented in Figure 2, it looks like the soluble material recovered from the composite (Figure 2C) is a mixture of CSO and the material recovered from the oat hulls. Although its exact identity is unknown, the latter exhibits features that are characteristic of non-conjugated, unsaturated triglycerides, such as the peak at 2.8 ppm



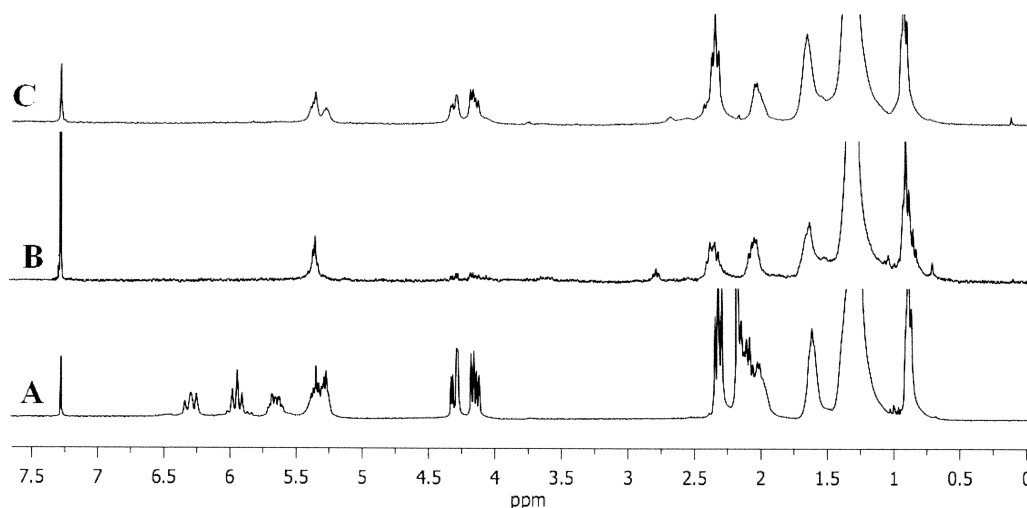


**Figure 2.**  $^1\text{H}$  NMR spectra of (A) conjugated soybean oil (CSO), and the soluble material recovered after Soxhlet extraction with  $\text{CH}_2\text{Cl}_2$  of (B) oat hulls, and (C) a composite prepared from CSO, with a filler/resin ratio of 80/20, cured for 5 hours at  $160\text{ }^\circ\text{C}$ .

related to bisallylic hydrogens and the set of peaks between 4.0 ppm and 4.5 ppm, which are characteristic of the methylene hydrogens on the glycerol unit of the triglycerides. Both features are present in Figure 2C.

The great overlap and complexity of peaks related to aliphatic hydrogens (0.5-2.5 ppm) make it extremely hard to attribute those signals to specific groups in the extracts studied, and therefore won't be discussed in detail here. The two peaks covering the range 5.2-5.4 ppm in Figure 2C correspond well with the vinylic hydrogen peak in Figure 2B (5.35 ppm, also present in Figure 2A) and the first peak (5.25 ppm) of the vinylic hydrogens of conjugated carbon-carbon double bonds in Figure 2A. Those hydrogens correspond to a set of signals that range from 5.2 ppm to 6.35 ppm. The lack of those signals in Figure 2C is an indication that the CSO possibly recovered during the Soxhlet extraction of the composite is most likely present in the form of oligomers, where some of the carbon-carbon double bonds reacted, reducing the conjugation of the system.

**Cure time analysis.** It has been previously shown with wood flour composites that varying the cure time results in opposite effects on the resin and on the filler.<sup>32</sup> Indeed, it has been found that on one hand longer cure times tend to increase the thermal degradation of the filler, which has a negative effect on the mechanical properties of the composite. On the other hand, a positive impact on the resin is seen when the cure lasts longer, because higher crosslink densities and monomer incorporation into the matrix are attained. Overall, one effect compensates for the other and little variation is found between the properties of bio-based composites cured at the same temperature for different times.<sup>32</sup>

Not surprisingly, similar results have been obtained with oat hull composites. The data presented in Table IV show that no statistical difference exists between the Young's modulus ( $E$ ) and the tensile strength of oat hull composites cured between 0.5 hours and 6 hours (entries 1-5, Table IV). From the dynamic mechanical analysis (DMA) of the samples, no particular trend has been observed for the  $T_g$  values of samples cured for different times. Nevertheless, a consistent appearance of two distinct  $T_g$ 's is detected. As discussed earlier, the appearance of two  $T_g$ 's is related to a phase separation of the matrix. Despite the seemingly random variation of the  $T_g$  values with cure time, the overall low temperatures observed for  $T_{g1}$  ( $-7$  °C to  $14$  °C) are consistent with the formation of an oil-rich phase, while the overall high temperatures observed for  $T_{g2}$  ( $89$  °C to  $122$  °C) are consistent with the formation of an oil-poor phase. This phenomenon has already been discussed earlier in the text and is attributed to the distinctly different reactivity of the resin comonomers towards free radical polymerization.

**Table IV.** Mechanical properties of oat hull composites cured for different times.<sup>a</sup>

| Entry | Cure time (h) | Young's modulus (GPa) | Tensile strength (MPa) | $T_{g1}$ (°C) | $T_{g2}$ (°C) | Storage modulus (MPa) |                     |
|-------|---------------|-----------------------|------------------------|---------------|---------------|-----------------------|---------------------|
|       |               |                       |                        |               |               | at 25 °C              | at $T_{g2} + 50$ °C |
| 1     | 0.5           | 2.8 ± 1.0             | 8.8 ± 1.9              | -6            | 100           | 947                   | 409                 |
| 2     | 1             | 2.7 ± 0.9             | 7.7 ± 1.2              | 14            | 122           | 678                   | 285                 |
| 3     | 2             | 2.0 ± 0.3             | 7.2 ± 0.9              | 1             | 94            | 1518                  | 824                 |
| 4     | 4             | 2.4 ± 0.6             | 8.7 ± 1.8              | 7             | 109           | 969                   | 409                 |
| 5     | 5             | 2.5 ± 0.7             | 8.2 ± 1.3              | 6             | 90            | 384                   | 170                 |
| 6     | 6             | 2.6 ± 1.2             | 8.9 ± 1.3              | -7            | 89            | 689                   | 372                 |

<sup>a</sup> The composites have been cured at 160 °C and post-cured at 180 °C for 2 hours. CSO has been used as the major resin component (50 wt %) and a filler/resin ratio of 80/20 has been employed.

The lack of a distinct trend for the storage modulus measured at room temperature and at  $T_{g2} + 50$  °C for samples cured for varying times makes it hard to relate these results to specific changes in the composites' structure. However, it is quite clear that a maximum storage modulus is obtained when the composite is cured for two hours. To help determine the optimal cure time, the samples cured for different times have been submitted to differential scanning calorimetry (DSC) experiments. The corresponding DSC curves are shown in Figure 3. The DSC curve of the sample cured for 0.5 hours is not included in Figure 3 due to its extended overlap with the curve of the sample cured for one hour.

From the DSC curves presented in Figure 3, any transitions occurring after 280 °C are related to degradation of the matrix, as confirmed by the TGA of the pure resin (Figure 1A). This includes the two exothermic peaks at approximately 285 °C and 360 °C. The two glass transition temperatures ( $T_g$ 's) related to the resin occur over a fairly broad temperature range, and are therefore difficult to determine exactly by DSC. Nevertheless, both transitions can be

distinguished in Figure 3 in the temperature ranges  $-20\text{ }^{\circ}\text{C}$  to  $0\text{ }^{\circ}\text{C}$  and  $50\text{ }^{\circ}\text{C}$  to  $100\text{ }^{\circ}\text{C}$ , respectively.

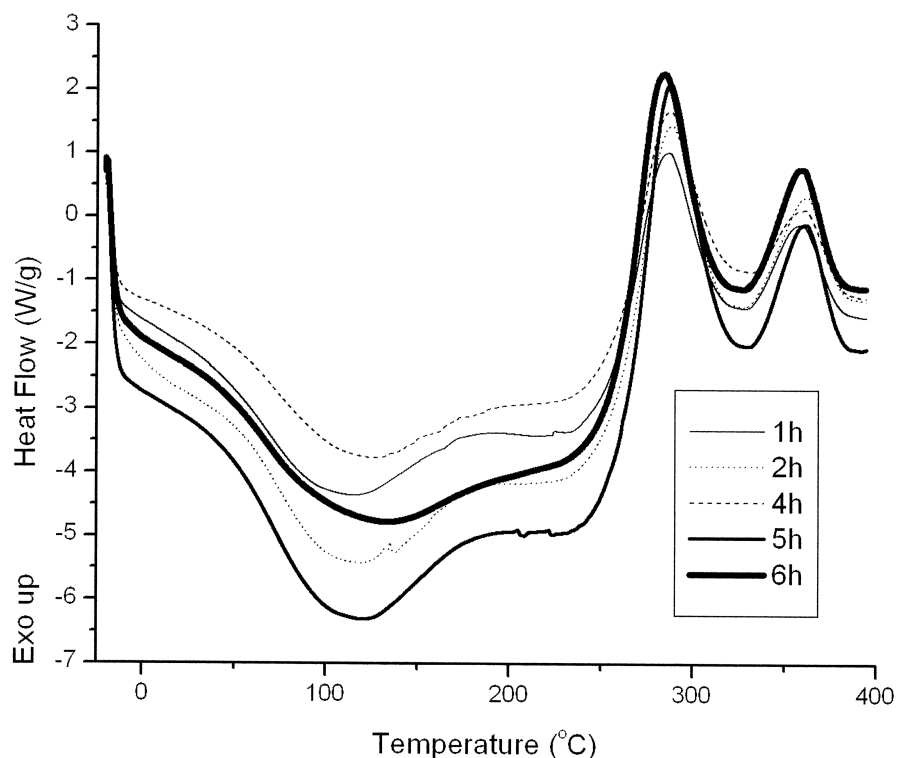


**Figure 3.** Differential Scanning Calorimetry (DSC) curves for oat hull composite samples cured at  $160\text{ }^{\circ}\text{C}$  for varying times. The composites have a filler/resin ratio of 80/20.

The temperature window where transitions related to the cure of the matrix are observed ranges from approximately  $120\text{ }^{\circ}\text{C}$  to  $200\text{ }^{\circ}\text{C}$ . In that temperature range, a small change in the baseline can be observed at approximately  $165\text{ }^{\circ}\text{C}$  for the sample cured for 1 hour, and at approximately  $132\text{ }^{\circ}\text{C}$  for the sample cured for 2 hours (Figure 3). These transitions are most likely associated with further cure of the matrix components, and indicate that these cure times are not sufficient to produce a completely cured matrix. For the sample cured for 4 hours, a series of very small transitions is observed in that temperature

range, but no precise temperature can be attributed to further cure of the resin. When the composite is cured for 5 hours or 6 hours, such transitions are non-existent.

As shown with soybean hulls, the minimum of the DSC curves of bio-based composites reinforced with biomass corresponds to an endothermic peak related to heat absorption during initial volatilization of the least thermally stable components of lignocellulosic materials, such as hemicellulose.<sup>27</sup> The temperature where that peak occurs gives information about the integrity of the filler after the cure. Indeed, that temperature is expected to increase with increasing cure times. As more of the least thermally stable components are degraded, the composite becomes richer in more thermally stable compounds, which results in a higher volatilization temperature. That temperature is 114 °C for the composite cured for 1 hour. It corresponds to 117 °C for the composite cured for 2 hours. When the composite is cured for 4 hours or 5 hours, the same volatilization temperature is observed (123 °C), and after a 6 hour cure, that temperature is 134 °C, correlating really well with the expected trend.

The transitions occurring between 200 °C and 235 °C for composites cured for 1 hour and 5 hours are not yet fully understood and won't be discussed in detail here. Despite the clearly higher storage modulus observed for the sample cured for 2 hours, the lack of clear transitions related to further cure of the resin and the overall results indicate that a 4 hour cure is optimal for preparing oat hull composites with a fully cured resin and without severely degrading the filler. Therefore, this cure time will be used from now on in the preparation of composites from different natural oils.

**Effect of different oils on the properties of oat hull composites.** As explained earlier in the text, different natural oils possess distinctly different triglyceride structures, with particular fatty acid compositions (Table I). It is expected that different composite properties will be obtained when conjugated natural oils with differing numbers of carbon-carbon double bonds per triglyceride are used as the major resin components. When more unsaturated oils are used in the preparation of composites, the formation of materials with higher crosslink densities, and therefore better mechanical properties is expected. The mechanical properties, along with the Soxhlet extraction results from oat hull composites prepared from various conjugated natural oils are presented in Table V.

**Table V.** Mechanical properties and extraction results for oat hull composites made from different natural oils.<sup>a</sup>

| Entry | Oil              | Young's modulus (GPa) | Tensile strength (MPa) | $T_{g1}$ (°C) | $T_{g2}$ (°C) | Storage modulus (MPa) |                     | Soluble content (wt %) <sup>b</sup> |
|-------|------------------|-----------------------|------------------------|---------------|---------------|-----------------------|---------------------|-------------------------------------|
|       |                  |                       |                        |               |               | at 25 °C              | at $T_{g2} + 50$ °C |                                     |
| 1     | CSO <sup>c</sup> | 2.4 ± 0.6             | 8.7 ± 1.8              | 7             | 109           | 969                   | 409                 | 3                                   |
| 2     | CCO <sup>d</sup> | 2.1 ± 0.3             | 10.0 ± 1.1             | -14           | 80            | 1156                  | 581                 | 3                                   |
| 3     | CLO <sup>e</sup> | 2.7 ± 0.5             | 12.8 ± 1.8             | 38            | 83            | 1694                  | 842                 | 2                                   |
| 4     | CFO <sup>f</sup> | 2.2 ± 0.5             | 10.9 ± 0.9             | -             | 97            | 1609                  | 749                 | 3                                   |
| 5     | TUN <sup>g</sup> | 2.9 ± 0.5             | 13.4 ± 2.6             | -             | 65            | 3764                  | 1073                | 2                                   |

<sup>a</sup> The composites have been cured at 160 °C for 4 hours and post-cured at 180 °C for 2 hours. The filler/resin ratio used was 80/20.

<sup>b</sup> Determined by Soxhlet extraction with CH<sub>2</sub>Cl<sub>2</sub> for 24 hours.

<sup>c</sup> CSO = conjugated soybean oil

<sup>d</sup> CCO = conjugated corn oil

<sup>e</sup> CLO = conjugated linseed oil

<sup>f</sup> CFO = conjugated fish oil

<sup>g</sup> TUN = tung oil

For the Young's modulus, very little variation is detected when different oils are used as the major resin component. The values vary from 2.1 GPa for conjugated corn oil (CCO -

entry 2, Table V) to 2.9 GPa for tung oil (TUN - entry 5, Table V) and all values fall within the standard deviation of the measurements. Some trends start to become evident when the tensile strength is analyzed. Despite the low value observed for conjugated soybean oil (CSO - entry 1, Table V), the tensile strength of that sample overlaps with those of samples prepared from CCO and conjugated fish oil (CFO) when the standard deviations are taken into account (entries 2 and 4, Table V). However, there is a definite increase in the tensile strength of the composite when conjugated linseed oil (CLO) or TUN are used as the major resin component (entries 3 and 5, Table V). When the tensile properties of composites prepared from these two oils are compared, no statistical differences are observed (entries 3 and 5, Table V).

A comparison of the tensile results of oat hull composites prepared from different oils with the information provided in Table I helps explain the observed trends. Indeed, the fatty acid composition of corn and soybean oils is very similar, which results in a similar number of carbon-carbon double bonds per triglyceride. As a consequence, there is virtually no difference in the tensile properties of composites prepared from CSO and CCO. For fish oil, approximately 32% of the fatty acid chains are eicosa-5,8,11,14,17-pentaenoic acid (EPA) and approximately 25% of the fatty acid chains are docosa-4,7,10,13,16,19-hexaenoic acid (DHA).<sup>22</sup> Despite the significant amount of polyunsaturated fatty acids and the high number of carbon-carbon double bonds per triglyceride (9.9), there is also approximately 47% of mono-unsaturated and completely saturated fatty acids. This mix of highly saturated and unsaturated fatty acids results in composites with tensile properties similar to those prepared from CSO and CCO. For CLO and TUN, the similarity in the tensile properties can be explained by the high amount of conjugated carbon-carbon double bonds in both oils. After

conjugation, CLO has approximately 71% of its fatty acids with conjugated carbon-carbon double bonds, while TUN naturally possesses 84% of conjugated fatty acids.

The number of carbon-carbon double bonds in the oils used for the preparation of oat hull composites also explains the  $T_g$  results obtained. While CSO, CCO, and CLO exhibit two distinct  $T_g$ 's, the use of CFO and TUN results in composites with only one  $T_g$ , as determined by DMA. The tan delta curves used to determine the  $T_g$  values of the oat hull composites prepared from different natural oils are presented in Figure 4 and clearly show two peaks for CSO and CCO, while only one peak is observed for CFO and TUN. In the case of CLO, the first tan delta peak is in fact composed of two very discrete peaks in the temperature ranges  $-30\text{ }^{\circ}\text{C}$  to  $0\text{ }^{\circ}\text{C}$  and the  $0\text{ }^{\circ}\text{C}$  to  $50\text{ }^{\circ}\text{C}$ . It is possible that a third phase also rich in CLO is formed, but the non-reproducibility of such phase separation with other fillers makes it hard to evaluate the origin of this phenomenon. A higher carbon-carbon double bond content results in a more reactive oil after conjugation. Oils with more than 6.5 carbon-carbon double bonds per triglyceride exhibit reactivity similar to the other comonomers in the resin, and therefore their use as the major matrix component results in a single phase.

The storage moduli of oat hull composites prepared from different oils tend to increase with the number of carbon-carbon double bonds per triglyceride. In that regard, the storage moduli obtained at room temperature and at  $T_{g2} + 50\text{ }^{\circ}\text{C}$  for CSO and CCO are very close, which correlates well with their similar number of carbon-carbon double bonds per triglyceride (4.7 and 4.5, respectively – Table I). When the number of carbon-carbon double bonds per triglyceride is increased to 6.5 (CLO – entry 3, Table V), increases of 45-47% in



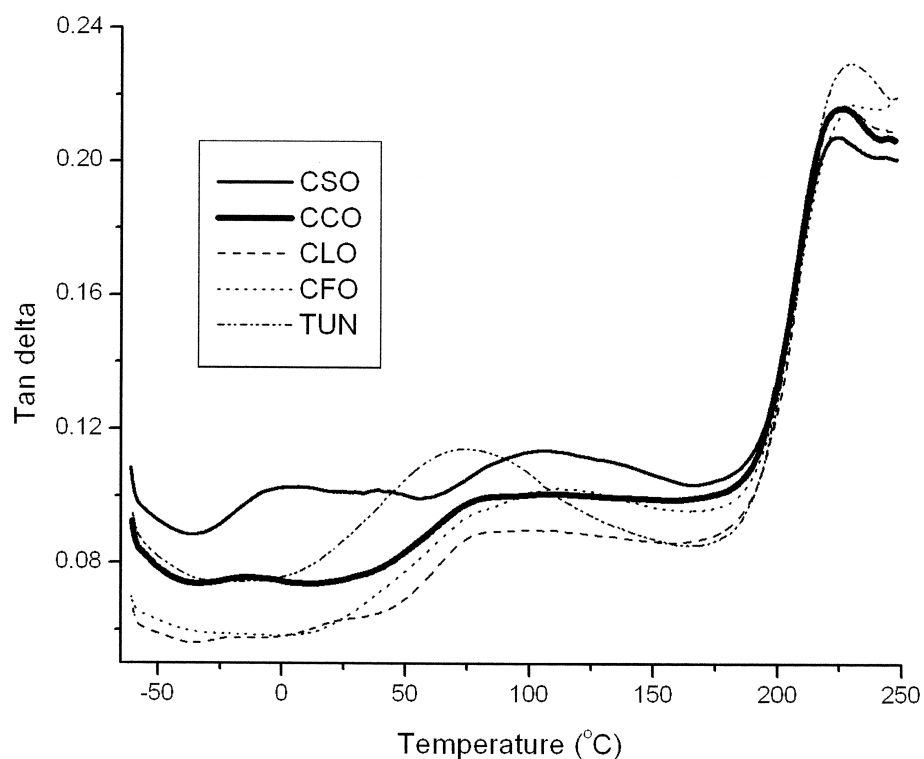


**Figure 4.** Tan delta curves for oat hull composites prepared from different conjugated natural oils. The composites have been cured at 160 °C for 4 hours and have a filler/resin ratio of 80/20.

the storage modulus at room temperature and at  $T_{g2} + 50$  °C are observed. The use of CFO as the major resin component results in composites with a storage modulus very similar to the CLO sample, despite its higher number of carbon-carbon double bonds per triglyceride (9.9). As explained earlier, CFO also possesses a high mono-unsaturated and saturated fatty acid content, which negatively impact mechanical properties, such as the storage modulus. Not surprisingly, the use of TUN results in the highest storage modulus of the series of samples analyzed, with an impressive increase of 122% at room temperature and an increase of 27% at  $T_{g2} + 50$  °C with respect to the sample prepared from CLO.

The storage modulus *versus* temperature curves for oat hull composites prepared from various conjugated natural oils are shown in Figure 5. The already discussed trends of increase in storage modulus with the number of carbon-carbon double bonds per triglyceride can be clearly seen from -60 °C to approximately 25 °C. With the exception of TUN, most of the samples exhibit a rubbery plateau that ranges from approximately 50 °C to 200 °C. Due to its higher crosslink density and lower mobility of its polymer chains, TUN exhibits a much narrower rubbery plateau (~100 °C to 200 °C). When the storage modulus of the different samples is compared at  $T_{g2} + 50$  °C (in the rubbery plateau), the aforementioned trend is still observed, but smaller differences between the values are detected. Above 200 °C, the samples lose their ability to restore the energy input during the test and a sudden decrease in storage modulus is observed for all of the samples.

Finally, the Soxhlet extraction results for samples prepared from various oils don't show any significant variation. It was expected that more unsaturated oils would be more easily incorporated into the matrix. In fact, since all of the oils used possess a significant content of conjugated carbon-carbon double bonds, they are all incorporated to the same extent under the cure conditions employed here.

### Conclusions

In this work, we have prepared conjugated natural oil-based thermoset composites reinforced with oat hulls. An initial cure temperature study showed that the changes in mechanical properties observed when the sample is cured under different temperatures are related to the thermal stability of the filler, and that a temperature of 160 °C is sufficient to

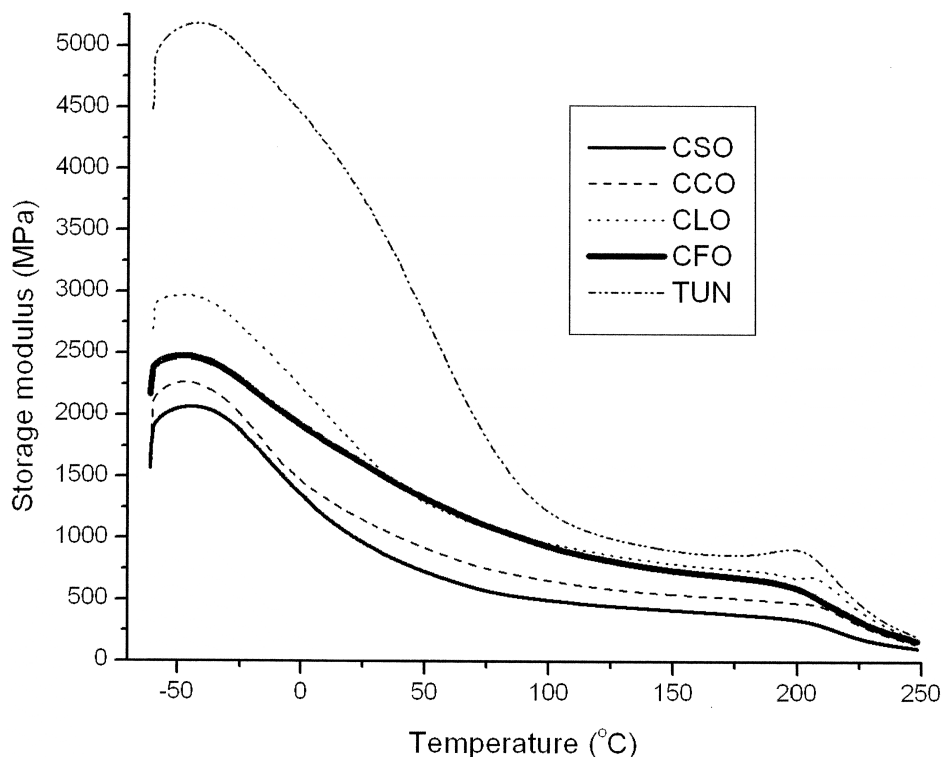


**Figure 5.** Storage modulus *versus* temperature for oat hull composites prepared from different conjugated natural oils. The composites have been cured at 160 °C for 4 hours and have a filler/resin ratio of 80/20.

completely cure the resin without severely damaging the filler. After taking into consideration practical aspects involved in the preparation of the composites and the mechanical data obtained, a filler load of 80 wt % has been chosen as optimal for the system under investigation. The cure time has also been investigated and it has been shown that a 4 hour cure is optimal for oat hull composites. Finally, it has been observed that composites with better overall properties are formed when more unsaturated oils are used as the major resin component, with the best material being obtained from tung oil.

### Acknowledgements

The authors thank the Recycling and Reuse Technology Transfer Center of the University of Northern Iowa for financial support, Quaker Oats for the oat hulls provided, and Professor Michael Kessler from the Department of Material Sciences and Engineering and Dr. Richard Hall from the Department of Natural Resource Ecology and Management at Iowa State University (ISU) for the use of their facilities.

### References

1. C. K. Williams and M. A. Hillmyer, *Polym. Rev.*, 2008, **48**, 1.
2. J. J. Bozell, *Clean-Soil Air Water*, 2008, **36**, 641.
3. G. W. Huber, S. Iborra and A. Corma, *Chem. Rev.*, 2006, **106**, 4044.
4. M. R. Van De Mark and K. Sandefur, in *Industrial Uses of Vegetable Oil*, Editor, S. Z. Erhan, AOCS Press: Peoria, IL 2005, 143.
5. Y. Lu and R. C. Larock, *ChemSusChem*, 2010, **3**, 329.
6. Y. Xia, Y. Lu and R. C. Larock, *Polymer*, 2010, **51**, 53.
7. R. F. Brandao, R. L. Quirino, V. M. Mello, A. P. Tavares, A. C. Peres, F. Guinhos, J. C. Rubim and P. A. Z. Suarez, *J. Braz. Chem. Soc.*, 2009, **20**, 954.
8. S. M. Ashraf, S. Ahmad and U. Riaz, *Polym. Int.*, 2007, **56**, 1173.
9. C. Wang, L. Yang, B. Ni and G. Shi, *J. Appl. Polym. Sci.*, 2009, **114**, 125.
10. M. Ionescu, Y. Ji, W. M. Shirley and Z. S. Petrovic, in *Renewable and Sustainable Polymers*, Editors, G. F. Payne and P. B. Smith, *ACS Books*, Symposium Series 2011, 73.
11. H. O. Sharma, M. Alam, U. Riaz, S. Ahmad and S. M. Ashraf, *Int. J. Polymer Mater.*, 2007, **56**, 437.
12. M. Gultekin, U. Beker, F. S. Guner, A. T. Erciyes and Y. Yagci, *Macromol. Mater. Eng.*, 2000, **283**, 15.
13. M. Zhan and R. P. Wool, *J. Appl. Polym. Sci.*, 2010, **118**, 3274.
14. Y. Lu and R. C. Larock, *ChemSusChem*, 2009, **2**, 136.
15. G. Zhang, L. Zhao, S. Hu, W. Gan, Y. Yu and X. Tang, *Polym. Eng. Sci.*, 2008, **48**, 1322.
16. M. N. Belgacem and A. Gandini, in *Monomers, Polymers and Composites from*

- Renewable Resources, Editors, M. N. Belgacem and A. Gandini, *Elsevier*, Amsterdam, 2008, 39.
17. M. A. R. Meier, J. O. Metzger and U. S. Schubert, *Chem. Soc. Rev.*, 2007, **36**, 1788.
  18. F. Li and R. C. Larock, *Biomacromolecules*, 2003, **4**, 1018.
  19. P. P. Kundu and R. C. Larock, *Biomacromolecules*, 2005, **6**, 797.
  20. P. H. Henna, D. D. Andjelkovic, P. P. Kundu and R. C. Larock, *J. Appl. Polym. Sci.*, 2007, **104**, 979.
  21. M. Valverde, D. Andjelkovic, P. P. Kundu and R. C. Larock, *J. Appl. Polym. Sci.*, 2008, **107**, 423.
  22. D. W. Marks, F. Li, C. M. Pacha and R. C. Larock, *J. Appl. Polym. Sci.*, 2001, **81**, 2001.
  23. F. Li and R. C. Larock, *J. Appl. Polym. Sci.*, 2000, **78**, 1044.
  24. D. D. Andjelkovic, M. Valverde, P. Henna, F. Li and R. C. Larock, *Polymer*, 2005, **46**, 9674.
  25. D. D. Andjelkovic, B. Min, D. Ahn and R. C. Larock, *J. Agric. Food Chem.*, 2006, **54**, 9535.
  26. D. P. Pfister, J. R. Baker, P. H. Henna, Y. Lu and R. C. Larock, *J. Appl. Polym. Sci.*, 2008, **108**, 3618.
  27. R. L. Quirino and R. C. Larock, *J. Appl. Polym. Sci.*, 2009, **112**, 2033.
  28. D. P. Pfister and R. C. Larock, *Bioresour. Technol.*, 2010, **101**, 6200.
  29. D. P. Pfister and R. C. Larock, *Composites Part A: Appl. Sci. Manufacturing*, 2010, **41**, 1279.
  30. R. L. Quirino and R. C. Larock, *J. Appl. Polym. Sci.*, 2011, **121**, 2050.
  31. D. P. Pfister and R. C. Larock, *J. Appl. Polym. Sci.*, 2011, *in press*.
  32. R. L. Quirino, J. Woodford and R. C. Larock, *J. Appl. Polym. Sci.*, 2011, *accepted for publication*.
  33. A. Corma, O. Torre, M. Renz and N. Vollandier, *Angew. Chem. Int. Ed.*, 2011, **50**, 2375.

## CHAPTER 8. Rh-BASED BIPHASIC ISOMERIZATION OF CARBON-CARBON DOUBLE BONDS

A Paper Submitted to Green Chemistry.

Rafael L. Quirino, Richard C. Larock\*

*Department of Chemistry, Iowa State University, Ames, Iowa 50011*

### Abstract

The biphasic conjugation of soybean and other natural oils, as well as the isomerization of various alkenes, has been examined using a rhodium catalyst. A maximum yield, of conjugated soybean oil, of 96% has been obtained when the reaction is run at 80 °C under argon with ethanol as the polar solvent, using triphenylphosphine monosulfonate sodium salt (tppms) as the ligand, and the surfactant sodium dodecyl sulfate (SDS). The optimized conditions have been tested with other substrates, and the products have been analyzed by <sup>1</sup>H NMR, GC/MS, and ICP-MS.

### Introduction

The positional isomerization of carbon-carbon double bonds in organic molecules is a reaction long known and studied.<sup>1-4</sup> More recently, carbon-carbon double bond migrations in allylic sulphides have been carried out in the presence of Ru homogeneous catalysts to produce cycloaddition precursors widely used in organic synthesis.<sup>5</sup> The carbon-carbon double bond migration in terminal olefins, to produce internal alkenes, has been promoted by Ru-carbene complexes,<sup>6</sup> and used in the total synthesis of complex natural products.<sup>7</sup>

Heterogeneous catalysts have also been used in the isomerization of 1-hexene and 1-pentene.<sup>8,9</sup> In vegetable oils, the isomerization of carbon-carbon double bonds to produce conjugated species has been first reported as a side reaction during the bleaching of vegetable oils.<sup>10</sup> Later on, isomers of conjugated linoleic acid were detected as by-products in the heterogeneous catalytic hydrogenation of soybean oil.<sup>11,12</sup> Since then, the production of conjugated fatty acids and triglycerides using heterogeneous catalysts has been studied and optimized.<sup>13-16</sup>

The presence of carbon-carbon double bonds in natural oils is extremely important for their industrial application as biorenewable starting materials. The unsaturation in natural oils can give rise to networks of triglyceride repeating units, known as biopolymers.<sup>17-23</sup> Besides the degree of unsaturation of the oil, the reactivity of the carbon-carbon double bonds is of major importance in such processes. Indeed, systems where the transition state is stabilized by conjugation have an overall higher reactivity. Conjugated vegetable oils are also useful as drying oils for paints and coatings.<sup>24</sup> While some natural oils can be used without further structural modification to produce coatings,<sup>25</sup> cheaper and more readily available vegetable oils can be conjugated in order to increase their drying properties and reduce production costs.<sup>24</sup>

Conjugated vegetable oils can also be used as a source of conjugated linoleic acid (CLA).<sup>24</sup> CLA has been shown to possess anticancer and antiatherosclerosis activity, and serves as a fat reducing agent.<sup>24</sup> Vegetable oils with a high content of linoleic acid have great potential for the production of CLA upon conjugation.

As already mentioned, several conjugation processes for vegetable oils have been developed to date.<sup>10-16</sup> In most of these processes, transition metal hydrides interact with the unsaturation in the triglyceride through an addition-elimination mechanism and the carbon-carbon double bonds “move” along the fatty acid chain to yield conjugated species. In 2001, the Larock group at Iowa State University developed a very efficient homogeneous conjugation system that used a Rh-based pre-catalyst ( $[\text{RhCl}(\text{C}_8\text{H}_{14})_2]_2$ ) and gave more than 95% conversion for several natural oils, including linoleic acid and ethyl linoleate.<sup>24</sup> In situ ligand exchange, which converts the pre-catalyst into the presumed active species  $[\text{RhH}(\text{ttp})_3]$  (where ttp = tris-*p*-tolylphosphine) occurs easily under the reaction conditions.<sup>24</sup> The conjugation of vegetable oils in the presence of this catalyst system has been carried out under mild reaction conditions (60 °C and argon) for 24 hours and affords no hydrogenation products, a typical side product in such processes.<sup>26</sup>

Due to the high yields obtained using the earlier procedure, the mild reaction conditions, and the absence of hydrogenated products,<sup>24,26</sup> related catalysts looked very promising for the preparation of drying oils, CLA, and natural oil-based reactive monomers for biopolymers, as well as the isomerization of carbon-carbon double bonds in simple dienes and olefins. Although very efficient, this prior Rh catalyst is completely discarded after conjugation. Being a homogeneous catalyst, filtration of the products to recover the metal complex is very difficult and time consuming. Therefore, the catalyst's reuse is currently not an attractive process, despite its high price.

Finding procedures that can lead to recyclable and reusable catalysts for the conjugation/isomerization of mono and polyenes represents a key step towards the



development of greener technologies for preparing olefins and conjugated polyenes of all types. Many alternatives to homogeneous catalysts have been proposed, including solid catalysts.<sup>8,9,11-16</sup> More recently, polymer-bound complexes, and active species tethered to inorganic supports have shown reactivities similar to their homogeneous counterparts, with the advantage of being more easily recoverable.<sup>27-30</sup>

The alternative we investigate here consists of the conversion of Larock's homogeneous Rh catalyst into an ethanol-soluble complex that works under biphasic conditions. This catalyst has the potential advantage of using an environmentally friendly solvent and being easily recovered using simple liquid/liquid separation techniques for subsequent use, without the need for further purification of the active species or the products.

Figure 1 illustrates the system studied.

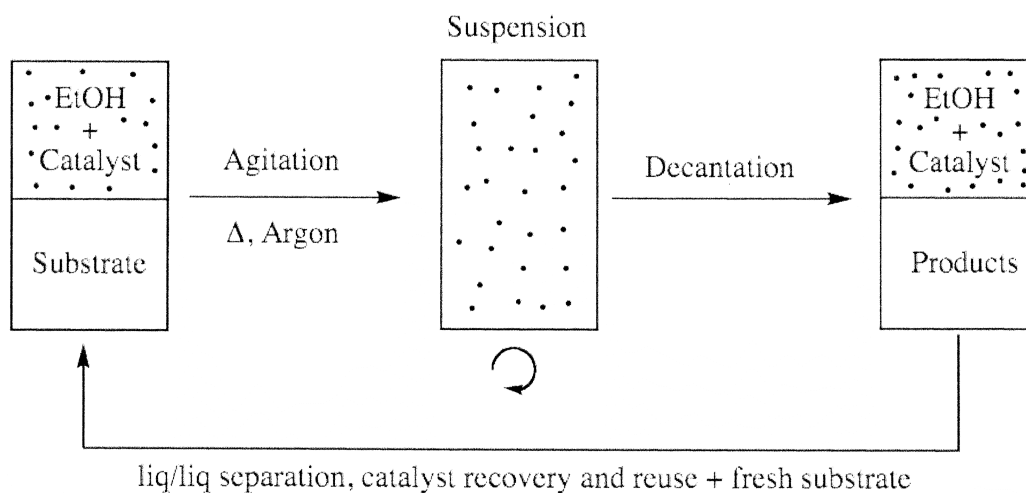


**Figure 1.** Biphasic catalytic system for the conjugation of carbon-carbon double bonds.

Other reactions have been successfully carried out under biphasic conditions. For instance, cross-coupling reactions using water and surfactants at room temperature have been

reported by Lipshutz and co-workers.<sup>31</sup> Also, fluorous-soluble catalysts for hydroformylation reactions have been studied by I. T. Horvath.<sup>32</sup> F. Joo has studied aqueous biphasic hydrogenation reactions,<sup>33</sup> and Li and co-workers have demonstrated the importance of surfactants in biphasic reactions.<sup>34</sup>

The successful biphasic reactions cited above do not include the isomerization of carbon-carbon double bonds. Indeed, to the best of our knowledge, the conjugation of vegetable oils under biphasic conditions has not been reported in the literature. Therefore, the approach proposed here significantly broadens the range of catalysts useful for the conjugation of vegetable oils.

### Experimental

**Materials.** Rhodium trichloride hydrate ( $\text{RhCl}_3 \cdot x\text{H}_2\text{O}$ ) was generously supplied by Kawaken Fine Chemicals Co., Ltd. (Tokyo, Japan). Ruthenium trichloride hydrate ( $\text{RuCl}_3 \cdot x\text{H}_2\text{O}$ ) was purchased from Alfa Aesar (Ward Hill, MA). Cyclooctene, 4-(diphenylphosphino)benzoic acid (dppba), 1,4-cyclohexadiene, 1,5-cyclooctadiene, 1,5-hexadiene, 1-nonene, methyl linoleate, and the surfactants cetyltrimethylammonium bromide (CTAB), Brij 76, Brij 700, and polyoxyethanyl- $\alpha$ -tocopheryl sebacate (PTS) were purchased from Aldrich (St. Louis, MO). Absolute ethanol (EtOH) was purchased from Pharmco-Aaper (Shelbyville, KY). 3-(Diphenylphosphino)benzenesulfonic acid sodium salt (tppms) was purchased from TCI (Tokyo, Japan). Sodium dodecyl sulfate (SDS), tin dichloride dihydrate ( $\text{SnCl}_2 \cdot 2\text{H}_2\text{O}$ ), methanol (MeOH), 1-propanol (PrOH), 2-propanol (*i*PrOH), and *tert*-butanol (*t*BuOH) were purchased from Fisher Chemical (Fair Lawn, NJ). 1-Heptene, 1-decene, and 1,7-octadiene were purchased from J. T. Baker (Phillipsburg, NJ). Soybean oil (*Carlini*

brand, Batavia, IL), grape seed oil (*GrapeOla* brand, Irvine, CA), sunflower oil (*Wesson* brand, Irvine, CA), sesame oil (*Loriva* brand, San Leandro, CA), peanut oil (*Planters* brand, Winston-Salem, NC), and olive oil (*HyVee* brand, West Des Moines, IA) were purchased in a local grocery store. Linseed oil was generously supplied by Archer Daniels Midland (Red Wing, MN). Menhaden Norwegian fish oil was supplied by Virginia Prime (Houston, TX).

**Synthesis of the pre-catalyst  $[\text{RhCl}(\text{C}_8\text{H}_{14})_2]_2$ .** In a three-necked round-bottomed flask,  $\text{RhCl}_3 \cdot x\text{H}_2\text{O}$  was dissolved in a previously degassed mixture of *i*PrOH and deionized water (4:1). One equivalent of cyclooctene was added to the flask and the mixture was stirred for fifteen minutes under argon and then allowed to stand at room temperature for five days. The resulting crystals were filtered, washed with absolute EtOH, and dried under vacuum. An overall yield of 72% was obtained for this process. This procedure is adapted from a previously published literature process.<sup>35</sup>

**Isomerization of carbon-carbon double bonds under biphasic conditions.** In a capped vial, the surfactant was dissolved in 5 g of the substrate, and the mixture was degassed and flushed three times with argon, while stirring at room temperature to remove the  $\text{O}_2$  dissolved in the substrate that could potentially oxidize the phosphine-based ligands. In a separate vial, the pre-catalyst, the ligands, and  $\text{SnCl}_2 \cdot 2\text{H}_2\text{O}$  were dissolved in 5 mL of the alcohol/deionized water mixture. This vial was also degassed and flushed with argon for the same aforementioned reason. The amount of  $\text{SnCl}_2 \cdot 2\text{H}_2\text{O}$  was fixed at eight times that of the pre-catalyst based on an optimization study previously conducted.<sup>24</sup> Using a canula, the mixture containing the substrate and the surfactant was transferred to the vial containing the catalyst solution. The system was stirred in an oil bath under argon. After 24 hours, the vial

was removed from the oil bath and allowed to cool to room temperature. The products and the catalyst solution separated into two distinct phases. Aliquots of the products were taken using a glass syringe, and were analyzed by  $^1\text{H}$  NMR spectroscopy, GC/MS, and ICP-MS for determination of the yield and concentration of Rh in the products.

**Recycle of the catalyst.** After the first cycle (24 hours), the reaction vial was removed from the oil bath and allowed to cool to room temperature. The products and the catalyst solution separated into two distinct phases. Using a glass syringe, the product phase was carefully removed from the vial, and a mixture containing 5 g of fresh substrate and surfactant was degassed and charged to the reaction vial using a canula. The same reaction conditions described for the first cycle were employed during subsequent cycles.

**Analysis of the products.** The product aliquots were dissolved in deuterated chloroform ( $\text{CDCl}_3$ ) and the corresponding  $^1\text{H}$  NMR spectra were obtained using a Varian Unity spectrometer (Varian Associates, Palo Alto, CA) operating at 300 MHz. The yield of conjugated products from the isomerization of carbon-carbon double bonds in triglycerides can be easily determined by  $^1\text{H}$  NMR spectroscopy.<sup>26</sup> Indeed, after normalization of the spectra with respect to the methylene protons of the glycerol unit (4.0-4.3 ppm), the final yield of conjugated product ( $C$ ) can be calculated using the following equation:

$$C = (B - H) \times 100;$$

where  $B$  corresponds to the disappearance of the bisallylic protons at 2.7-2.8 ppm relative to the starting material, and  $H$  is a measurement of the carbon-carbon double bonds hydrogenated during the reaction.  $B$  can be defined by:

$$B = 1 - (b'/b);$$

where  $b'$  and  $b$  are the areas of the peaks related to the bisallylic protons in the products and in the starting material, respectively.  $H$ , on the other hand, is calculated through:

$$H = 1 - [(d'-1)/(d-1)];$$

where  $d'$  and  $d$  are the areas of the peaks related to the vinylic protons (5.1-6.4 ppm) in the products and in the starting material, respectively. It is noteworthy that the formula used to calculate  $H$  takes into account the methyne hydrogen from the glycerol unit, which generates a peak in the 5.0-5.5 ppm range in the  $^1\text{H}$  NMR spectrum. Figure 2 shows an example of the  $^1\text{H}$  NMR spectra of non-conjugated and conjugated soybean oils with the corresponding assigned peaks.

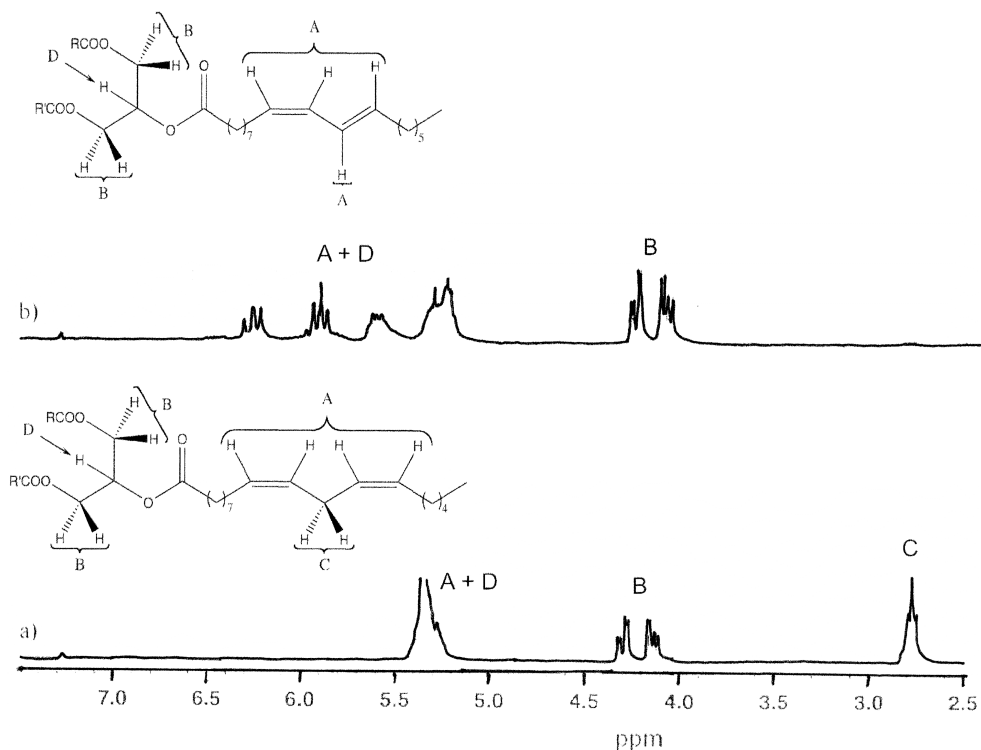


**Figure 2.**  $^1\text{H}$  NMR spectra of: a) regular soybean oil along with the corresponding chemical structure and peak assignments, and b) conjugated soybean oil along with the corresponding chemical structure and peak assignments.

For the ICP-MS analysis, the aliquots from selected samples were first dissolved in 2-propanol to give a final concentration of 1 mg/mL of the products. These solutions underwent then an 11 fold dilution in 1% HCl before the analysis. The analyses were performed on a Thermo Finnigan Element ICP-MS spectrometer, and the experimental parameters were set as 1150 W forward power, 1.02 L/min. carrier gas flow, 100  $\mu$ L/min. sample flow rate, using an ESI self-aspirating nebulizer.

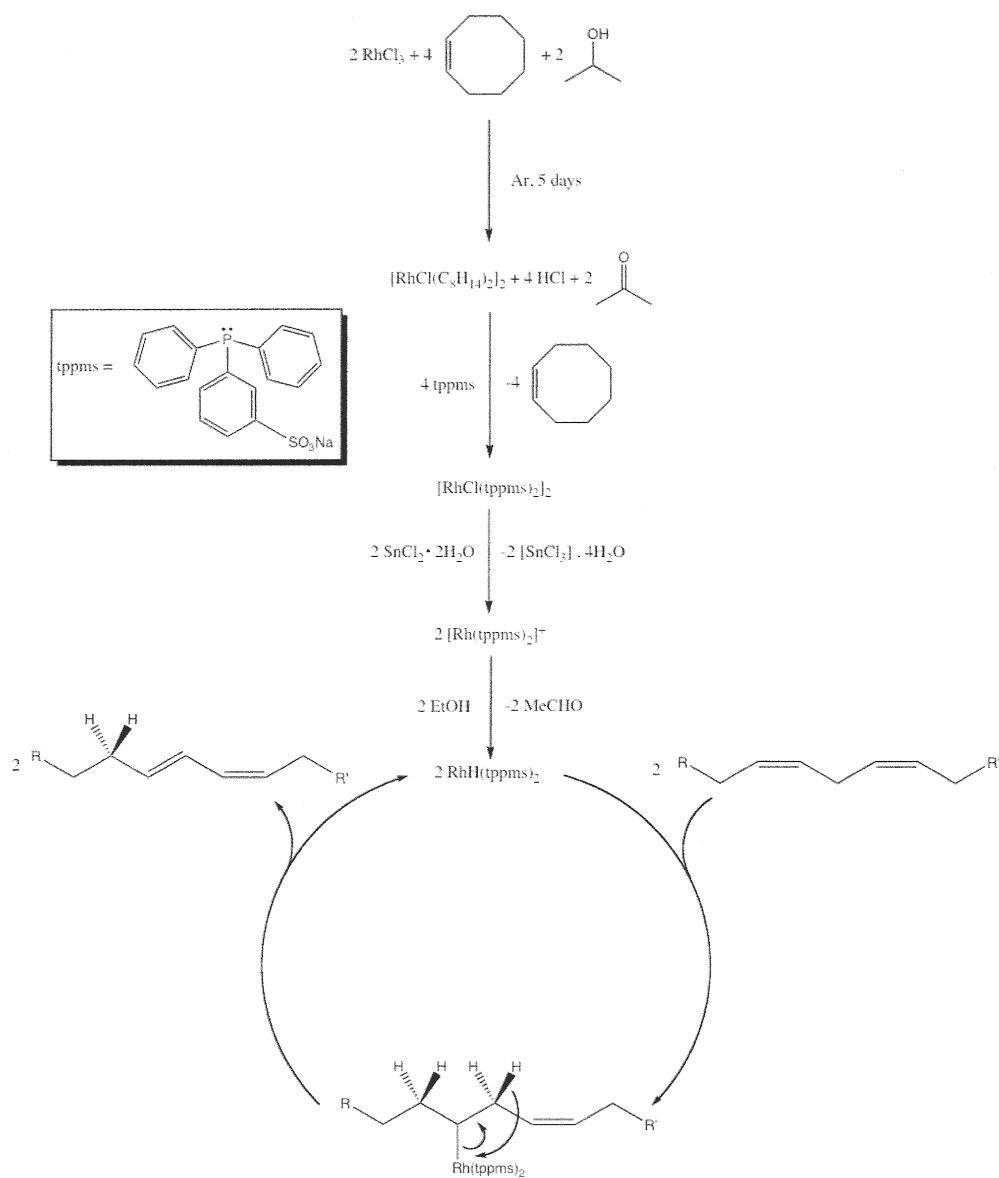
For the GC/MS analyses, the aliquots were dissolved in chloroform to give an approximate concentration of 0.2 mg/mL. For the triglycerides analyzed, a 200 mg aliquot of the products was initially mixed with 2 mg of NaOH and 0.3 mL of MeOH at 50 °C. After 2 hours the mixture was cooled to room temperature and 1 mL of chloroform was added. After phase separation, the organic product was checked by  $^1\text{H}$  NMR spectroscopy to verify that the triglyceride was successfully converted into the corresponding methyl esters. The sample was then appropriately diluted for the GC/MS analysis as mentioned above. The prepared solutions were manually injected in a Varian 3400 gas chromatograph (Palo Alto, CA) coupled to a Magnum GCMS ion-trap mass spectrometer. A 30.0 m J&W DB-5 column from Agilent (Santa Clara, CA) with 0.25 mm internal diameter and 0.25  $\mu$ m film thickness capillary column was used as the stationary phase and the following temperature program was used for all samples: 160-200 °C (at 10 °C/min.), 200 °C for 6 min., 200-220 °C (at 10 °C/min.), 220-230 °C (at 5 °C/min.), 230 °C for 1 min., 230-280 °C (at 30 °C/min.), and 280 °C for 3 min. *MassLynx* software and data-base were used to identify each peak in the chromatograms obtained, and the areas under the peaks were used to determine the concentration of each compound.

## Results and Discussion

**Screening of reaction conditions.** As mentioned earlier, the procedure developed by the Larock group for the isomerization of carbon-carbon double bonds using a homogeneous catalyst is very efficient, but not practical on a large scale or industrially.<sup>24</sup> In order to convert that catalyst into a complex able to operate under biphasic conditions, water-soluble ligands, such as tppms and dppba, have been introduced into the reaction system to replace ttp. Although the goal of this work is not to investigate the mechanistic aspects of the catalyst formation and the conjugation/isomerization reactions, a proposed, plausible mechanism for the in situ formation of the active catalyst and the conjugation of carbon-carbon double bonds in dienes is given in Figure 3.

The first step depicted in Figure 3 is the reduction of  $\text{Rh}^{3+}$  and formation of the pre-catalyst  $[\text{RhCl}(\text{C}_8\text{H}_{14})_2]_2$ . Secondly, a ligand exchange results in the dimer  $[\text{RhCl}(\text{tppms})_2]_2$ , which breaks down into  $[\text{Rh}(\text{tppms})_2]^+$  after abstraction of  $\text{Cl}^-$  by the strong Lewis acid  $\text{SnCl}_2 \cdot 2\text{H}_2\text{O}$ . The active metal hydride, readily formed in the presence of ethanol, is assumed to add across one carbon-carbon double bond and, subsequently, to eliminate a hydride from an adjacent carbon. The overall process results in a conjugated product.

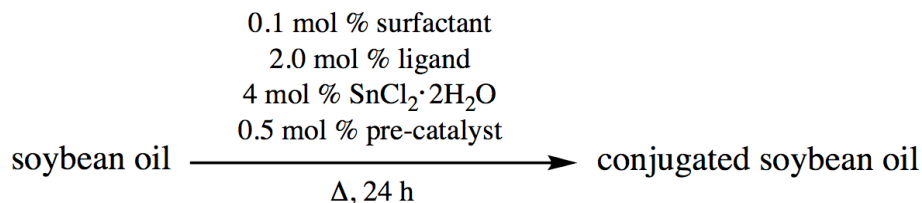
The results of the isomerization reactions of soybean oil, carried out under various conditions, are presented in Table I. Soybean oil has been chosen as the model system to screen several reaction conditions due to the easy identification of its isomerization products using  $^1\text{H}$  NMR spectroscopy, as explained earlier.<sup>26</sup>



**Figure 3.** Proposed reaction mechanism for *in situ* formation of the presumed active catalyst  $[\text{RhH}(\text{tppms})_2]$  and conjugation of the carbon-carbon double bonds in dienes.

Initially, water was chosen as the polar phase to carry out the isomerization of the carbon-carbon double bonds in soybean oil (entries 1 and 2, Table I). Due to a significant difference in polarity between water and soybean oil, no isomerization products were



**Table I.** Screening of reaction conditions for the isomerization of soybean oil.

| Entry <sup>a</sup> | Temp. (°C) | Gas | Pre-catalyst (0.5 mol %)   | Ligand (2 mol %) | EtOH (mL) | Water (mL) | Surfactant (0.1 mol%) | Yield (%) <sup>b</sup> |
|--------------------|------------|-----|--|------------------|-----------|------------|-----------------------|------------------------|
| 1                  | 60         | Ar  | [RhCl(C <sub>8</sub> H <sub>14</sub> ) <sub>2</sub> ] <sub>2</sub> | tppms            | -         | 5.0        | -                     | 0                      |
| 2                  | 60         | Ar  | [RhCl(C <sub>8</sub> H <sub>14</sub> ) <sub>2</sub> ] <sub>2</sub> | dppba            | -         | 5.0        | -                     | 0                      |
| 3                  | 60         | Ar  | [RhCl(C <sub>8</sub> H <sub>14</sub> ) <sub>2</sub> ] <sub>2</sub> | tppms            | 2.5       | 2.5        | -                     | 0                      |
| 4                  | 60         | Ar  | [RhCl(C <sub>8</sub> H <sub>14</sub> ) <sub>2</sub> ] <sub>2</sub> | dppba            | 2.5       | 2.5        | -                     | 0                      |
| 5                  | 60         | Ar  | [RhCl(C <sub>8</sub> H <sub>14</sub> ) <sub>2</sub> ] <sub>2</sub> | tppms            | 5.0       | -          | -                     | 48                     |
| 6                  | 60         | Ar  | [RhCl(C <sub>8</sub> H <sub>14</sub> ) <sub>2</sub> ] <sub>2</sub> | dppba            | 5.0       | -          | -                     | 6                      |
| 7                  | 60         | Ar  | [RhCl(C <sub>8</sub> H <sub>14</sub> ) <sub>2</sub> ] <sub>2</sub> | tppms            | 5.0       | -          | SDS                   | 76                     |
| 8                  | 60         | Ar  | [RhCl(C <sub>8</sub> H <sub>14</sub> ) <sub>2</sub> ] <sub>2</sub> | tppms            | 5.0       | -          | CTAB                  | 25                     |
| 9                  | 60         | Ar  | [RhCl(C <sub>8</sub> H <sub>14</sub> ) <sub>2</sub> ] <sub>2</sub> | tppms            | 5.0       | -          | Brij 700              | 20                     |
| 10                 | 60         | Ar  | [RhCl(C <sub>8</sub> H <sub>14</sub> ) <sub>2</sub> ] <sub>2</sub> | tppms            | 5.0       | -          | Brij 76               | 24                     |
| 11                 | 60         | Ar  | [RhCl(C <sub>8</sub> H <sub>14</sub> ) <sub>2</sub> ] <sub>2</sub> | tppms            | 5.0       | -          | PTS                   | 0                      |
| 12                 | 60         | Ar  | RhCl <sub>3</sub> ·xH <sub>2</sub> O                               | tppms            | 5.0       | -          | SDS                   | 0                      |
| 13                 | 60         | Ar  | RuCl <sub>3</sub> ·nH <sub>2</sub> O                               | tppms            | 5.0       | -          | SDS                   | 0                      |
| 14                 | 40         | Ar  | [RhCl(C <sub>8</sub> H <sub>14</sub> ) <sub>2</sub> ] <sub>2</sub> | tppms            | 5.0       | -          | SDS                   | 28                     |
| 15                 | 80         | Ar  | [RhCl(C <sub>8</sub> H <sub>14</sub> ) <sub>2</sub> ] <sub>2</sub> | tppms            | 5.0       | -          | SDS                   | 89                     |
| 16                 | 80         | air | [RhCl(C <sub>8</sub> H <sub>14</sub> ) <sub>2</sub> ] <sub>2</sub> | tppms            | 5.0       | -          | SDS                   | 0                      |

<sup>a</sup> Reaction carried out at 60 °C in 5.0 mL of EtOH, using 0.5 mol % of [RhCl(C<sub>8</sub>H<sub>14</sub>)<sub>2</sub>]<sub>2</sub>, 2.0 mol % of tppms, and 0.1 mol % of SDS, under argon.

<sup>b</sup> No significant yield of hydrogenated products has been detected.

detected, no matter what the ligand used. Indeed, it is believed that the surface tension between the two phases prevented the catalyst from mixing with the substrate even upon agitation at 60 °C. In an attempt to reduce the difference in polarity between the two phases, a 1:1 mixture of water and EtOH has been used as the polar solvent (entries 3 and 4, Table I)

with no significant formation of conjugated products. When EtOH is used as the sole polar solvent, a 48% yield of conjugated product is obtained in the presence of the ligand tppms (entry 5, Table I). When dppba is used as the ligand, a very low 6% yield of conjugated product results (entry 6, Table I), possibly due to its higher solubility in polar solvents. The ligand triphenylphosphine-3,3',3''-trisulfonic acid trisodium salt (tppts) hasn't been tried because of its higher solubility in polar solvents.

Problems in aqueous/organic biphasic catalysis are mainly related to poor miscibility of the phases. This is especially true for reactions involving higher olefins or non-polar molecules having twelve or more carbon atoms, for which the immiscibility of the catalyst solution yields very low reaction rates.<sup>34</sup> Indeed, in those cases, the contact between catalyst and substrate is very limited, and to solve this issue, surfactants are normally added to lower the surface tension and increase the contact/miscibility. Among the surfactants investigated, anionic SDS gives the highest yield (entry 7, Table I). The cationic surfactant CTAB, and the neutral, non-ionic, Brij-based surfactants yield 20-25% of conjugated soybean oil (entries 8-10, Table I). The use of the surfactant solution known as PTS results in no conjugated products (entry 11, Table I), possibly due to the presence of water in the commercial version of the surfactant.

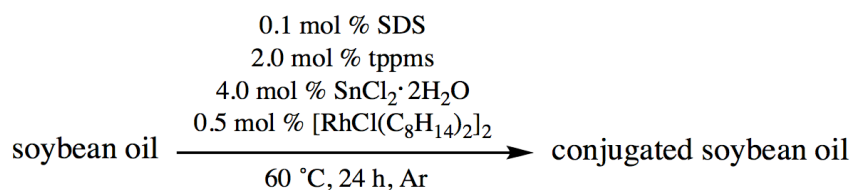
As mentioned before, the whole concept of the biphasic catalyst developed in this work is based on substitution of the ligand in a homogeneous catalyst previously studied.<sup>26</sup> In an attempt to skip the synthesis of the pre-catalyst  $[\text{RhCl}(\text{C}_8\text{H}_{14})_2]_2$  and still have a one-pot procedure, the direct use of  $\text{RhCl}_3 \cdot x\text{H}_2\text{O}$  as the rhodium source has been investigated, but no conjugated products have been detected after 24 hours (entry 12, Table I). Similarly,

$\text{RuCl}_3 \cdot n\text{H}_2\text{O}$  has been used to replace the pre-catalyst and once again no conjugated products have been detected (entry 13, Table I).

As expected, the efficiency of the reaction depends greatly on the temperature. There is a significant decrease in the yield of conjugated product when the reaction temperature is lowered to 40 °C (entry 14, Table I). On the other hand, an increase in the reaction temperature from 60 °C to 80 °C results in an increase in the yield of conjugated product from 76% to 89% (entries 7 and 15, respectively). If the reaction is run under air (entry 16, Table I), instead of argon, no conjugation occurs, most likely due to oxidation of the phosphine ligands in the presence of the  $\text{O}_2$  from the air. Although this is a very plausible explanation, the final catalyst solution hasn't been tested for the presence of phosphine oxide to confirm that hypothesis.

Since the polarity of the solvent is of major relevance to the efficiency of the process being investigated, several alcohols, with varying carbon chain lengths, have been tested and the results are presented in Table II. Because of the low boiling point of the shorter chain alcohols, a temperature of 60 °C has been used for all alcohols.

As expected, the yield of conjugated soybean oil in the presence of MeOH was lower than that obtained with EtOH (entries 1 and 2, Table II). Indeed, the higher polarity of shorter chain alcohols compromises their miscibility with the substrate, resulting in a lower yield for the reaction. When alcohols containing three or more carbons are used (entries 3-5, Table II), the catalyst solution becomes completely miscible with the soybean oil, and no conjugated products are obtained. In view of these results, EtOH is the ideal solvent to run the biphasic isomerization of soybean oil.

**Table II.** Conjugation of soybean oil under biphasic conditions in the presence of various alcohols.

| Entry <sup>a</sup> | Alcohol (5 mL) | Yield (%) |
|--------------------|----------------|-----------|
| 1                  | MeOH           | 21        |
| 2                  | EtOH           | 76        |
| 3                  | PrOH           | 0         |
| 4                  | <i>i</i> PrOH  | 0         |
| 5                  | <i>t</i> BuOH  | 0         |

<sup>a</sup> Reaction carried out at 60 °C in 5.0 mL of EtOH, using 0.5 mol % of [RhCl(C<sub>8</sub>H<sub>14</sub>)<sub>2</sub>]<sub>2</sub>, 2.0 mol % of tppms, and 0.1 mol % of SDS, under argon.

In order to illustrate the quick deactivation of the catalyst during the reaction, aliquots of the reaction mixture were taken, using a glass syringe, at pre-determined time intervals. The yield of conjugated product from each aliquot was determined immediately after its collection by means of <sup>1</sup>H NMR spectroscopy, as discussed earlier. A curve of the reaction yield *versus* reaction time is presented in Figure 4. It is noticeable that the catalyst is significantly deactivated after eight hours of reaction with a yield of conjugated product of approximately 70%. During the following 16 hours, only a slight increase of 6% in the yield is detected.

**Optimization of reaction conditions.** The use of surfactants makes the loss of the metal to the products more likely, which may account for a decrease in the catalyst's activity upon reuse. To solve this new issue, an excess of the water-soluble ligand (tppms) is most likely

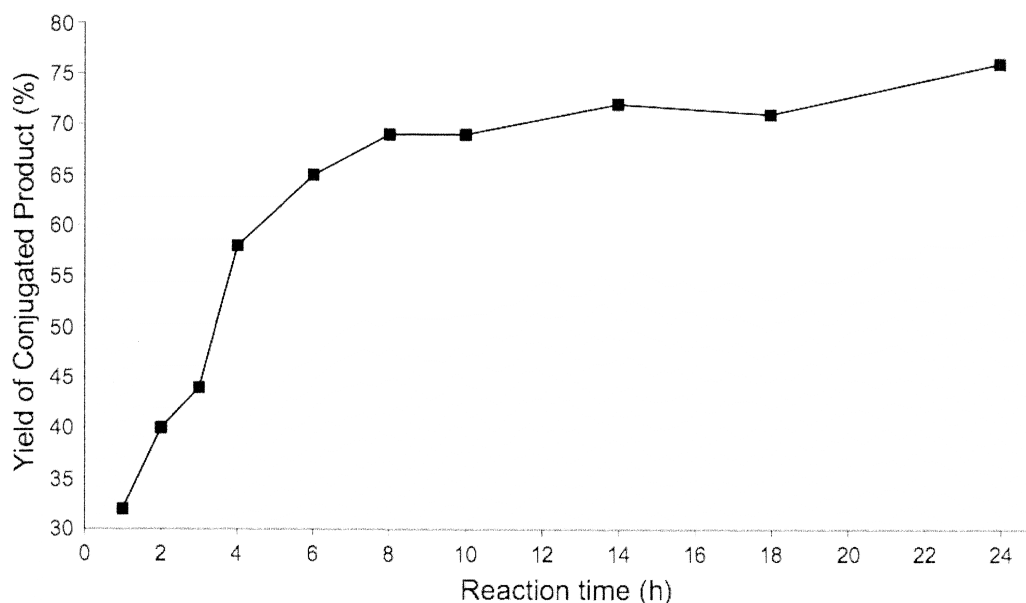


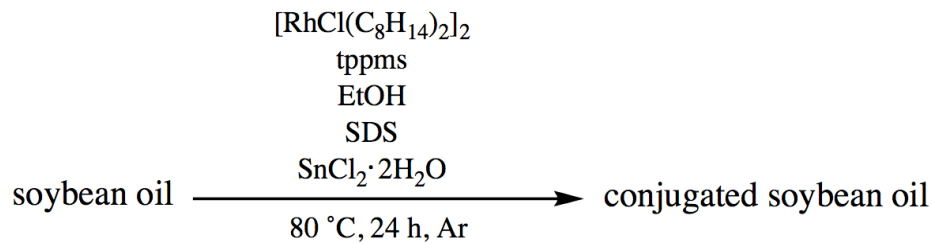
**Figure 4.** Yield of conjugated product *versus* reaction time for the biphasic conjugation of soybean oil.

necessary to prevent metal leach and improve the recyclability of the catalyst. An optimization study of the reaction conditions is presented in Table III. Factors, such as the amount of EtOH, the catalyst concentration, the amount of surfactant, the ligand/pre-catalyst ratio, and the surfactant/ligand ratio have been varied in order to determine the optimum conditions for the conjugation of soybean oil.

Maintaining the amount of pre-catalyst at 0.5 mol %, the amount of the ligand tppms at 2.0 mol %, and the amount of SDS at 0.1 mol %, the concentration of the catalyst solution has been changed by varying the volume of EtOH used in the reaction (entries 1-3, Table III). A decrease in the yield of the reaction from 89% to 18% is noticed with increasing volumes of EtOH, which corresponds to a decrease in the catalyst concentration. Obviously, when higher volumes of EtOH are used, there is reduced contact between the catalyst and the substrate during the reaction, so lower reaction rates are expected, which explains the lower

yields obtained after 24 hours. If a volume of EtOH lower than 5 mL is used, the solubility of the catalyst in the polar phase is compromised and erratic data is obtained (not shown in Table III).

**Table III.** Optimization of reaction conditions for the conjugation of soybean oil.



| Entry | $[\text{RhCl}(\text{C}_8\text{H}_{14})_2]_2$<br>(mol%) | tppms (mol%) | EtOH (mL) | SDS (mol%) | Yield (%) |
|-------|--|--------------|-----------|------------|-----------|
| 1     | 0.5  | 2.0          | 5.0       | 0.1        | 89        |
| 2     | 0.5  | 2.0          | 10.0      | 0.1        | 49        |
| 3     | 0.5  | 2.0          | 15.0      | 0.1        | 18        |
| 4     | 0.5  | 2.0          | 5.0       | 0.2        | 95        |
| 5     | 0.5  | 2.0          | 5.0       | 0.3        | 88        |
| 6     | 0.5  | 1.5          | 5.0       | 0.2        | 56        |
| 7     | 0.5  | 2.5          | 5.0       | 0.2        | 96        |
| 8     | 0.5  | 3.0          | 5.0       | 0.2        | 90        |
| 9     | 0.2  | 0.8          | 2.0       | 0.2        | 0         |
| 10    | 0.3  | 1.2          | 5.0       | 0.2        | 14        |
| 11    | 0.4  | 1.6          | 5.0       | 0.2        | 35        |

Establishing the optimum volume of EtOH at 5 mL, and keeping the amount of the pre-catalyst constant at 0.5 mol %, and the amount of the ligand tppms constant at 2.0 mol %, the effect of varying the amount of SDS has been evaluated. An increase in the amount of SDS from 0.1 mol % to 0.2 mol % results in an increase in the yield of conjugated product from 89% to 95% (entries 1 and 4, Table III). This improvement in the reaction efficiency

shows that a higher concentration of surfactant helps to minimize the surface tension between the two phases and therefore results in better exposure of the catalyst to the substrate molecules. When the amount of surfactant is increased to 0.3 mol %, the yield of the reaction drops to 88% (entry 5, Table III), indicating that the excess of SDS favors the formation of micelles, and it no longer improves the catalyst/substrate contact.

Fixing the amount of SDS at its optimum value of 0.2 mol %, and keeping the amount of the pre-catalyst constant at 0.5 mol %, the ligand/pre-catalyst ratio has been changed by varying the amount of ligand introduced into the reaction system. Up to this point, a ligand/pre-catalyst ratio of 4 has been used, and the optimum conditions are represented by entry 4 in Table III. Reducing the ligand/pre-catalyst ratio to 3 results in a decrease in the yield of the reaction to 56% (entry 6, Table III). In this case, it appears that there is an insufficient amount of ligand to keep the metal in the polar phase. According to the reaction mechanism presented in Figure 3, each equivalent of the pre-catalyst  $[\text{RhCl}(\text{C}_8\text{H}_{14})_2]_2$  results in two equivalents of the active catalyst  $[\text{RhH}(\text{tppms})_2]$  needed for conjugation. Ideally, a ligand/pre-catalyst ratio of 4 would be required to maintain all of the rhodium in the polar phase. However, as discussed earlier, an excess of the ligand may be necessary to compensate for the use of a surfactant that helps to improve the miscibility between the catalyst solution and the substrate. When a ligand/pre-catalyst ratio of 5 is used (entry 7, Table III), the yield increases slightly to 96%, and if the ligand/pre-catalyst ratio is 6 (entry 8, Table III), the yield drops to 90%. These results match very well with the expected trends. Considering the cost-effectiveness of the process, a ligand/pre-catalyst ratio of 4 is considered the ideal value.

Once the optimum ligand/pre-catalyst ratio has been established, an attempt has been made to reduce the amount of pre-catalyst used by decreasing the volume of the catalyst solution, but still maintaining the same ligand/pre-catalyst ratio and the same catalyst concentration (entry 9, Table III). In that case, the low volume of catalyst solution compromised the phase separation of the system and no conjugated product was detected. When a higher concentration of the catalyst is used (entries 10 and 11, Table III) with a ligand/pre-catalyst ratio of 4 and a volume of EtOH equal to 5 mL, very low yields are obtained. After these reactions, a precipitate was found at the bottom of the reaction flask. The low yields are attributed to coagulation and precipitation of the catalyst during the reaction at those high concentrations, which indicates poor solubility of the catalyst in EtOH beyond a rhodium concentration of about 0.012 M.

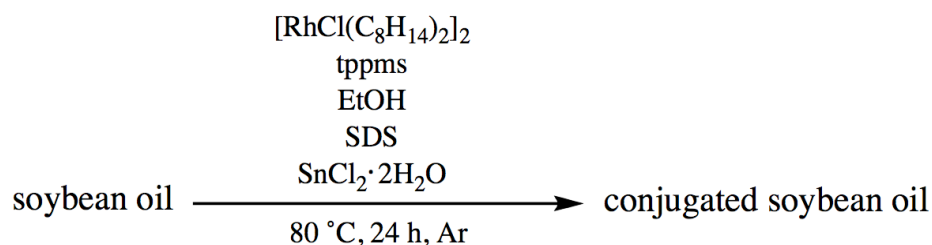
In view of the results presented, the optimal conditions for the conjugation of carbon-carbon double bonds in soybean oil with the proposed system is represented by entry 4, in Table III. An assessment of the catalyst's recyclability is addressed next.

**Catalyst recycle and reuse.** In order to evaluate the potential for catalyst recycle and reuse, and to further understand the trends observed in Table III, ICP-MS analysis of the products of five selected samples has been carried out to determine the amount of rhodium that leached from the catalyst solution into the products. The results, summarized in Table IV, reveal that the yield of conjugated products depends greatly on the miscibility of the two phases in the system, as well as the stability of the catalyst in the polar phase. For instance, the decrease observed in the yield, when the volume of EtOH was increased from 5 mL to 10 mL (entries 1 and 2, Table IV), has been attributed to poorer miscibility between the catalyst



solution and the substrate for higher volumes of polar solvent. From the ICP-MS results, it is indeed clear that a significantly lower concentration of Rh is found in the products when a higher volume of EtOH is used. This confirms that there is less contact between substrate molecules and the catalyst species when using higher solvent volumes.

**Table IV.** ICP-MS results for selected samples.



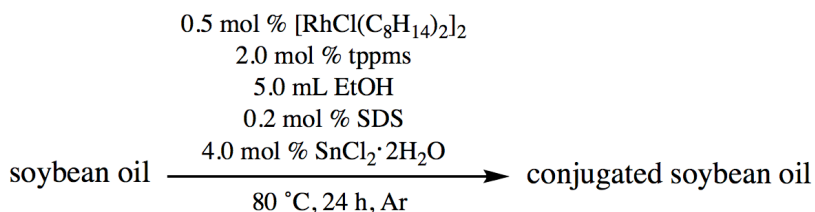
| Entry | $[\text{RhCl}(\text{C}_8\text{H}_{14})_2]_2$<br>(mol%) | tppms<br>(mol%) | EtOH (mL) | SDS<br>(mol%) | Rh Conc.<br>(ppm) | Yield<br>(%) |
|-------|--|-----------------|-----------|---------------|-------------------|--------------|
| 1     | 0.5  | 2.0             | 5.0       | 0.1           | 69.45             | 89           |
| 2     | 0.5  | 2.0             | 10.0      | 0.1           | 4.50              | 49           |
| 3     | 0.5  | 2.0             | 5.0       | 0.2           | 21.95             | 95           |
| 4     | 0.5  | 1.5             | 5.0       | 0.2           | 53.34             | 56           |
| 5     | 0.5  | 3.0             | 5.0       | 0.2           | 22.00             | 90           |

Surprisingly, when an increased amount of the surfactant SDS is used at constant EtOH volume (entries 1 and 3-5, Table IV), less Rh is found among the products. Although this could explain the improved yield observed for entry 3 (Table IV), it is still not obvious how a surfactant can decrease metal leaching during a biphasic reaction. It is possible that by decreasing the surface tension between the two phases, the surfactant promotes an easier transfer of the catalyst from one phase to the other, so the Rh complex can more easily interact with the substrate in the non-polar phase, and return to the polar solution, where it exhibits higher solubility and stability.

Changes in the amount of the EtOH-soluble ligand tppms directly affect the stability of the catalyst in the polar phase, and, as a consequence, the yield of the reaction (entries 3-5, Table IV). When the amount of tppms is reduced from its optimum value (entries 3 and 4, Table IV), more Rh leaches into the products, which ultimately affects the yield of the reaction. On the other hand, when an excess of tppms is employed (entry 5, Table IV) in the reaction, there is a tendency for the Rh particles to stay in the polar phase, and once again the contact between catalyst and substrate may be slightly compromised. This has a slight impact on the yield of the reaction, but does not change the amount of Rh found in the products.

After optimization of the reaction conditions, attempts at recycling and reusing the catalyst have been made. The experimental conditions employed for the second cycle of the catalyst and the corresponding results are described in Table V.

**Table V.** Recycling results.



| Entry          | Additions for 2 <sup>nd</sup> cycle | Yield (%) |
|----------------|-------------------------------------|-----------|
| 1 <sup>a</sup> | -                                   | 95        |
| 2              | -                                   | 18        |
| 3              | 2.0 mol % tppms                     | 11        |
| 4              | 0.2 mol % SDS                       | 21        |
| 5              | 0.2 mol % SDS + 2.0 mol % tppms     | 18        |

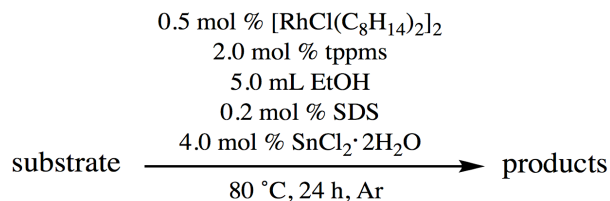
<sup>a</sup> First cycle of catalyst under optimized conditions.

A significant decrease in the catalyst's activity has been detected after the first cycle (entries 1 and 2, Table V). Although the specific reasons for such a drop in activity are currently unknown, coagulation and precipitation of the catalyst have been observed within the first three hours of reaction during the second cycle. It is believed that coagulation of the catalyst is a result of reduction of Rh(I) under the reaction conditions, which would be responsible for deactivation of the catalyst. In an attempt to avoid such a rapid deactivation, fresh tppms has been added to the system for the second cycle (entry 3, Table V), but the yield obtained was even lower than the recycle carried out without addition of extra ligand. Indeed, the extra tppms added had an effect similar to that observed in entry 5, Table IV, where the catalyst had a tendency to stay in the polar phase, making the interaction between substrate and catalyst more difficult. The addition of fresh SDS (entry 4, Table V) slightly improved the yield upon catalyst recycle. In this case, it is possible that the extra surfactant added compensates for any SDS removed from the system with the products of the first cycle. Finally, addition of both SDS and tppms in the second cycle does not result in any improvement in the yield of conjugated product, indicating that the effects of both additions cancel each other out.

Another possibility for the dramatic loss in activity is Rh leaching into the products during the reaction. However, for the first cycle of the catalyst under optimized conditions, only 4% of the Rh initially added as catalyst has been found in the products (entry 3, Table IV). Deactivation of the catalyst by complexation with the surfactant is also possible. In fact, the exact deactivation mechanism for the catalyst remains unknown for the time being. This problem is part of our future research efforts on the development of more efficient catalysts for the conjugation of carbon-carbon double bonds.

**Other substrates tested.** In order to evaluate the scope of the biphasic procedure, unsaturated molecules other than soybean oil have been submitted to the reaction conditions optimized for the model system. The results shown in Table VI for a range of natural oils, as well as for methyl linoleate, and shorter chain dienes and alpha-olefins, have been obtained through  $^1\text{H}$  NMR spectroscopic and GC-MS analysis of the corresponding product mixtures.

All of the vegetable oils used in this study have approximately the same molecular weight, with structures differing only in the number and distribution of the carbon-carbon double bonds in the fatty acid chains. On average, sunflower oil has 4.8 carbon-carbon double bonds per molecule, while peanut oil has 2.3 double bonds. The corresponding number for sesame oil is 3.6, and, for soybean, linseed, grape seed, and olive oils, the numbers are 4.5, 6.2, 3.4, and 2.4, respectively. Among the natural oils tested as substrates for the biphasic conjugation of carbon-carbon double bonds, fish oil is the only one with a significantly different structure. It possesses longer fatty acid chains overall and an average of 3.6 carbon-carbon double bonds per triglyceride. Although the number and distribution of carbon-carbon double bonds in the different natural oils has a great impact on their flavor, color, viscosity, and nutritional value, there is no direct correlation between the number of carbon-carbon double bonds per molecule and the yield of conjugated products. Indeed, complete conjugation of the carbon-carbon double bonds has been observed for sunflower, peanut, and sesame oils (entries 1-3, Table VI). Soybean and linseed oils exhibit high, but incomplete conversion. In fact, a 95% yield of conjugated products has been obtained for those oils (entries 4 and 5, Table VI). Grape seed, fish, and olive oils are conjugated less efficiently (entries 6-8, Table VI). Although relatively high yields of conjugated oils have

**Table VI.** Conjugation/isomerization results for various substrates under our “optimized” reaction conditions.

| Entry | Substrate                 | Conversion (%) | Conjugated Products (%) <sup>a</sup> | Non-conjugated Isomers (%) <sup>b</sup> |
|-------|---------------------------|----------------|--------------------------------------|---|
| 1     | sunflower oil             | 100            | 100                                  | 0                                       |
| 2     | peanut oil                | 100            | 100                                  | 0                                       |
| 3     | sesame oil                | 100            | 100                                  | 0                                       |
| 4     | soybean oil               | 95             | 95                                   | 0                                       |
| 5     | linseed oil               | 95             | 95                                   | 0                                       |
| 6     | grapeseed oil             | 88             | 88                                   | 0                                       |
| 7     | fish oil                  | 82             | 82                                   | 0                                       |
| 8     | olive oil                 | 71             | 71                                   | 0                                       |
| 9     | methyl linoleate          | 52             | 52                                   | 0                                       |
| 10    | 1,5-cyclooctadiene        | 100            | 73 <sup>c</sup>                      | 25 <sup>d</sup>                         |
| 11    | 1,4-cyclohexadiene        | 100            | 0                                    | 100 <sup>e</sup>                        |
| 12    | <i>trans</i> -isolimonene | 6              | 6                                    | 0                                       |
| 13    | 1,7-octadiene             | 57             | 2                                    | 55                                      |
| 14    | 1,5-hexadiene             | 76             | 19                                   | 23 <sup>f</sup>                         |
| 15    | 1-decene                  | 40             | -                                    | 40                                      |
| 16    | 1-nonene                  | 79             | -                                    | 79                                      |
| 17    | 1-heptene                 | 51             | -                                    | 51                                      |

<sup>a</sup> Mixture of all isomers where the carbon-carbon double bonds are conjugated.

<sup>b</sup> Mixture of all isomers (excluding any unreacted starting material) where the carbon-carbon double bonds are not conjugated.

<sup>c</sup> Bi-1-cycloocten-1-yl has been detected as the major product for the reaction.

<sup>d</sup> A 2% yield of cyclooctene has been detected by GC-MS.

<sup>e</sup> Bi-1-cyclohexen-3-yl has been detected as the major product for the reaction.

<sup>f</sup> A 34% yield of unidentifiable products have been detected by GC-MS.

been obtained with the process reported here, it is unclear to us, at the moment, the reasons for the differences obtained for the different oils examined. Similar trends for the percent conjugation of various vegetable oils have also been observed when our earlier homogeneous catalyst was employed.<sup>24</sup>

A significant decrease in the yield of conjugated products is observed when methyl linoleate is employed as the substrate (entry 9, Table VI). The lower molecular weight of methyl linoleate, when compared to the natural oils tested (entries 1-8, Table VI), may, in fact, compromise the phase separation of the system, which is crucial for the catalyst to work properly, as noted in Table II, when longer chain alcohols have been used as the polar phase. Although a clear phase separation is still observed in the EtOH/methyl linoleate mixture, it is believed that a significant portion of methyl linoleate is miscible with the polar phase, resulting in a lower yield of conjugated product.

When cyclic dienes are exposed to the optimized reaction conditions, complete reaction of the substrates is observed (entries 10 and 11, Table VI). In these cases, however, a coupling product is formed preferentially. For the reaction of 1,5-cyclooctadiene, 73% of the products consist of bi-1-cycloocten-1-yl, a conjugated diene, that is most likely formed through initial conjugation of the carbon-carbon double bonds in the starting material, followed by the coupling of two units. An hydrogenation step is also required during the process to yield the observed major product. Besides the observed coupling product, 25% of the reaction mixture contains non-conjugated positional isomers of 1,5-cyclooctadiene. In addition, a small percentage (2%) of cyclooctene is detected among the products. The reaction of 1,4-cyclohexadiene affords bi-1-cyclohexen-3-yl as the only observed product. In

this case, however, the final product is not conjugated, and no hydrogenated products have been detected. The mechanism of these coupling reactions hasn't been thoroughly investigated in this work. Therefore, any assumptions about the steps involved in formation of the observed products is pure speculation. When *trans*-isolimonene was submitted to the optimized reaction conditions (entry 12, Table VI), only 6% of the starting material is converted into the conjugated species 1-methyl-4-isopropyl-1,3-cyclohexadiene. In this case, the vast majority of the starting material (94%) remained unreacted.

When linear dienes, such as 1,7-octadiene and 1,5-hexadiene, are employed as substrates (entries 13 and 14, Table VI), a mixture of several possible positional isomers is observed. In the case of 1,7-octadiene, the final mixture contained 23% of 1,6-octadiene, 21% of 1,4-octadiene, 8% of 2,6-octadiene, 2% of 2,4-octadiene, 2% of 1,5-cyclooctadiene, and 1% of cyclooctene, besides 43% of unreacted starting material. This product distribution, along with the long reaction time required, suggests a very low activity for our Rh catalyst with such dienes. In fact, the major product is one where only one carbon-carbon double bond has moved from its original position to the adjacent carbon. In that regard, it is not surprising that the natural oils investigated (entries 1-8, Table VI) gave, overall, much higher conversion and yields of conjugated products, since the carbon-carbon double bonds in those triglycerides are naturally separated by only one methylene group. Along the same lines, the reaction of 1,5-hexadiene affords 14% of 1,4-hexadiene, 11% of 1,3-hexadiene, 9% of cyclohexene, 8% of 2,4-hexadiene, and 34% of other unidentified compounds, besides 24% of unreacted starting material. Similarly, alpha-olefins react under the optimized conditions to give a number of possible positional isomers (entries 15-17, Table VI), with the majority closely resembling the starting material. 1-Decene, for instance, afforded 19% of 2-decene,

16% of 3-decene, 3% of 4-decene, and 2% of 5-decene, besides 60% of unreacted starting material. In the case of 1-nonene, the final mixture was composed of 39% of 2-nonene, 35% of 3-nonene, and 5% of 4-nonene, besides 21% of the starting material. For 1-heptene, the product mixture contained 29% of 2-heptene, 23% of 3-heptene, and 49% of the starting material.

With the exception of 1,5-cyclooctadiene, little or no hydrogenation has been detected for any of the substrates tested. It is also noteworthy that the reaction conditions have been initially optimized using soybean oil as the model system. Since biphasic reactions are extremely sensitive to the miscibility of the catalyst solution and the substrates, it is expected that significant changes in the activity of the catalyst would result when substrates with different structures are used. The difference is not so significant for the various natural oils tested due to their similar chemical structures, but factors, such as the amount of EtOH, the catalyst concentration, the ligand/metal ratio, the reaction time, and the temperature may need to be adjusted for each individual substrate in order to give the highest yield of conjugated products possible. An alternative is immobilization of the rhodium catalyst on an inorganic support to form a heterogeneous tethered catalyst. This approach is under active investigation.

### Conclusions

In this work, we have successfully converted a known and active homogeneous rhodium catalyst into a biphasic system for the conjugation of carbon-carbon double bonds. The biphasic reaction developed involves a polar catalyst solution and a non-polar phase composed of the substrate. The new catalytic system has the advantage of easy product



isolation and catalyst recycle, using simple liquid/liquid separation techniques, although catalyst recycle has not yet proven to be an efficient process. The research effort reported in this work constitutes the first steps leading to a technology that can significantly reduce the costs and the environmental impact of catalytic carbon-carbon double bond conjugation processes requiring expensive rare metal species. The process has been optimized using soybean oil as the model system and screening various reaction conditions. A maximum yield of 96% has been obtained when the reaction is run at 80 °C under argon with ethanol as the polar solvent, using tppms as the ligand, and SDS as the surfactant. The optimized reaction conditions have been tested with other substrates, including various natural oils, cyclic and linear dienes, and alpha olefins. The products have been analyzed by <sup>1</sup>H NMR spectroscopy, and GC/MS and ICP-MS analysis. The results obtained give some insight about the reactivity of the catalyst. They indeed suggest a very low activity for our Rh catalyst with dienes in general. In fact, significant conjugated products are only observed for starting materials where the carbon-carbon double bonds are separated by a single methylene group.

### Acknowledgements

The authors thank the National Science Foundation (NSF) Engineering Research Center for Biorenewable Chemicals (CBiRC) at Iowa State University for funding this project, and graduate student C. Ebert and Professor R. S. Houk of the Chemistry Department at Iowa State University for help with the ICP-MS analyses.

### References

1. J. E. Arnet and R. Pettit, *J. Am. Chem. Soc.* 1961, **83**, 2954.

2. J. Kiji and M. Iwamoto, *J. Am. Chem. Soc.* 1968, **41**, 1483.
3. T. Mizuta, H. Samejima and T. Kwan, *J. Am. Chem. Soc.* 1968, **41**, 727.
4. R. A. Johnson and S. Seltzer, *J. Am. Chem. Soc.* 1973, **95**, 5700.
5. N. Kuznik, S. Krompiec, T. Bieg, S. Baj, K. Skutil and A. Chrobok, *J. Organomet. Chem.* 2003, **665**, 167.
6. U. L. Dharmasena, H. M. Foucault, E. N. Santos, D. E. Fogg and S. P. Nolan, *Organometallics* 2005, **24**, 1056.
7. T. J. Donohoe, T. J. C. O'Riordan and C. P. Rosa, *Angew. Chem. Int. Ed.* 2009, **48**, 1014.
8. S. Pariente, P. Trens, F. Fajula, F. D. Renzo and N. Tanchoux, *Appl. Cat. A: Gen.* 2006, **307**, 51.
9. I. Coletto, R. Roldan, C. Jimenez-Sanchidrian, J. P. Gomez and F. J. Romero-Salguero, *Catalysis Today* 2010, **149**, 275.
10. J. H. Mitchell Jr. and H. R. Kraybill, *J. Am. Chem. Soc.* 1942, **64**, 988.
11. M. Y. Jung and Y. L. Ha, *J. Agric. Food Chem.* 1999, **47**, 704.
12. M. O. Jung, S. H. Yoon and M. Y. Jung, *J. Agric. Food Chem.* 2001, **49**, 3010.
13. A. Bernas, N. Kumar, P. Maki-Arvela, N. V. Kul'kova, B. Holmbom, T. Salmi and D. Y. Murzin, *Appl. Cat. A: Gen.* 2003, **245**, 257.
14. A. Bernas, N. Kumar, P. Laukkanen, J. Vayrynen, T. Salmi and D. Y. Murzin, *Appl. Cat. A: Gen.* 2004, **267**, 121.
15. P. Pakdeechanuan, K. Intarapichet, L. N. Fernando and I. U. Grun, *J. Agric. Food Chem.* 2005, **53**, 923.
16. O. A. Simakova, A. Leino, B. Campo, P. Maki-Arvela, K. Kordas, J. Mikkola and D. Y. Murzin, *Catalysis Today* 2010, **150**, 32.
17. M. A. R. Meier, J. O. Metzger and U. S. Schubert, *Chem. Soc. Rev.* 2007, **36**, 1788.
18. S. M. Ashraf, S. Ahmad and U. Riaz, *Polym. Int.* 2007, **56**, 1173.
19. C. Wang, L. Yang, B. Ni and G. Shi, *J. Appl. Polym. Sci.* 2009, **114**, 125.
20. V. Thulasiraman, S. Rakesh and M. Sarojadevi, *Polymer Composites* 2009, **30**, 49.
21. P. H. Henna, D. D. Andjelkovic, P. P. Kundu and R. C. Larock, *J. Appl. Polym. Sci.* 2007, **104**, 979.
22. D. D. Andjelkovic, M. Valverde, P. Henna, F. Li and R. C. Larock, *Polymer* 2005, **46**, 9674.
23. P. P. Kundu and R. C. Larock, *Biomacromolecules* 2005, **6**, 797.
24. R. C. Larock, X. Dong, S. Chung, C. K. Reddy and L. E. Ehlers, *J. Am. Oil Chem. Soc.* 2001, **78**, 447.

25. H. Wexler, *Chem. Rev.* 1964, **64**, 591.
26. D. D. Andjelkovic, B. Min, D. Ahn and R. C. Larock, *J. Agric. Food Chem.* 2006, **54**, 9535.
27. D. E. Bergbreiter, *Chem. Rev.* 2002, **102**, 3345.
28. I. Steiner, R. Aufdenblatten, A. Togni, H. Blaser and B. Pugin, *Tetrahedron: Asymmetry* 2004, **15**, 2307.
29. J. M. Fraile, J. I. Garcia and J. A. Mayoral, *Coord. Chem. Rev.* 2008, **252**, 624.
30. J. Lu and P. H. Toy, *Chem. Rev.* 2009, **109**, 815.
31. B. H. Lipshutz and S. Ghorai, *Aldrichimica Acta* 2008, **14**, 59.
32. I. T. Horvath, *Acc. Chem. Res.* 1998, **31**, 641.
33. F. Joo, *Acc. Chem. Res.* 2002, **35**, 738.
34. M. Li, H. Fu, M. Yang, H. Zheng, Y. He, H. Chen and X. Li, *J. Mol. Cat. A: Chem.* 2005, **235**, 130.
35. A. V. Ent and A. L. Onderdelinden, *Inorg. Synth.* 1990, **28**, 90.

## CHAPTER 9. GENERAL CONCLUSIONS

This dissertation discusses several aspects of the preparation of bio-based composites made from various natural oil-based resins reinforced with ligno-cellulosic residues. Each one of the projects covered here focuses on a specific filler and has the goal of studying the influence of parameters, such as filler load, cure conditions, and resin composition, in the final mechanical properties of the bio-based composites. The information gathered in the study of one particular system is used on following projects to tailor the focus of the parameters investigated. The structure-property relationships determined for different systems provides us a broader base of knowledge on bio-based composites. The fillers investigated include soybean hulls, rice hulls, wood flours, wood fibers, sugar-cane bagasse, and oat hulls.

The development of a recyclable rhodium-based catalyst for the isomerization/conjugation of carbon-carbon double bonds in triglycerides is also addressed in this dissertation. The outcomes of this project may be quite valuable for future research in biphasic catalysis, as well as in the preparation of more affordable bio-based polymers.

The biocomposites investigated in Chapter 2 consist of a conjugated soybean oil-based resin reinforced with soybean hulls. An initial cure study revealed that heating the composite for 5 hours at 130 °C, followed by a post-cure at 150 °C for 2 hours resulted in the best mechanical properties. It is also observed that the properties of the composites tend to decrease whenever good dispersion of the filler in the matrix is compromised by factors such as filler/resin ratio or filler particle size. As the pressure applied during cure is increased up to 276 psi, an overall increase in the mechanical properties is observed. Beyond that point,

the properties decrease with increasing pressures. A phase separation of the matrix occurs upon cure due to a difference in the reactivity of CSO and the other resin components towards free radicals, suggesting that better results might be achieved by using more reactive oils, such as conjugated linseed oil. In terms of resin composition, a significant dependence of the properties on the DVB content is observed. Replacement of DVB by DCPD affects considerably the mechanical properties due to differences in the reactivity of these two compounds.

As part of the same project, Chapters 3 and 4 involve a study of rice hull composites prepared from a more reactive oil, CLO. While Chapter 3 is concerned with physical aspects of the system, such as cure analysis, pressure, filler load, pre-treatment of the filler (drying and grinding), Chapter 4 focuses on chemical aspects related to the resin composition, with special attention given to the incorporation of maleic anhydride as a filler-resin compatibilizer.

The results presented in Chapter 3 indicate an optimal cure temperature of 180 °C, and it has been shown that the post-cure step is crucial in order to get a fully cured resin and the best CLO incorporation into the matrix. A pressure of 600 psi during the cure has resulted in the stiffest material. The use of 70 wt % of dried and ground rice hulls affords the best overall properties. SEM analysis provides evidence of a weak filler-resin interaction due to differences in the hydrophilicity of the matrix and the reinforcement. A Si X-ray map of the composites indicated the presence of significant amounts of silica in the rice hulls, which may account for the high thermal stability and mechanical properties obtained.

The variations introduced in the resin composition of rice hull composites in Chapter 4 include a comparison of CLO and CSO as the major resin components. The results show that composites made from CLO exhibit better overall properties than those made from CSO. The relative amounts of BMA, DVB, and MA have also been varied. The data obtained show an overall improvement in the composites' properties whenever MA is added as a co-monomer in the resin. MA acts as a compatibilizer between the filler particles and the matrix. These results have been corroborated by SEM images showing a better filler-resin interaction when the matrix contains MA.

Bio-based composites made from either conjugated soybean oil- or conjugated linseed oil-based thermosets reinforced with pine, maple, and oak flours, and a mixture of hardwood fibers is the subject of Chapter 5. Initial experiments with pine wood flour composites indicated that a filler load of 80 wt % is the most practical for the preparation of wood flour composites. Little variation in the mechanical properties was observed when the cure time varied from 30 minutes to 5 hours. TGA and DSC analyses indicate that this is a result of factors that compensate for each other. While longer cure times help to completely cure the resin and tend to increase crosslink density and monomer incorporation into the matrix, they are also responsible for partial degradation of the filler, negatively impacting the mechanical properties. Composites reinforced with mixtures of flours containing oak exhibit worse mechanical properties than those containing exclusively pine flour. Finally, a comparison between wood fiber and wood flour composites indicates that the composites reinforced with fibers show significantly better mechanical properties.

In Chapter 6, CSO-, CLO-, and tung oil-based thermosets reinforced with sugar-cane bagasse have been prepared and studied. An initial cure sequence evaluation showed that the changes in mechanical properties, observed when the sample is cured under different temperatures and times, are related to the thermal stability of the filler. Furthermore, the post-cure step has a great impact on the crosslink density of the resin. An optimum filler load of 60 wt % results in the most thermally stable and viable composites. Better properties are usually obtained when more unsaturated oils are used as the major resin component. It has been shown that the initial washing and drying of the sugar-cane bagasse affect the filler-resin interaction and result in a phase separation of the matrix, independent of the oil used. Also, with a better interaction between resin and filler, MA no longer acts as a compatibilizer in the system, and an overall decrease in storage modulus is observed whenever MA is added to the resin composition.

The focus of Chapter 7 is the preparation and investigation of oat hull composites from various conjugated natural oils. An initial cure temperature study showed that a temperature of 160 °C is sufficient to completely cure the resin without severely damaging the filler. After taking into consideration practical aspects involved in the preparation of the composites and the mechanical data obtained, a filler load of 80 wt % was chosen as optimal for this particular system. The cure time has also been investigated and it has been shown that a 4 hour cure is ideal for oat hull composites. Finally, it has been observed that composites with better properties are formed when tung oil is used as the major resin component.

In Chapter 8, the successful conversion of a known and active homogeneous rhodium catalyst into a biphasic system for the conjugation of carbon-carbon double bonds in triglycerides is presented. The biphasic reaction developed involves a polar catalyst solution and a non-polar phase composed of the substrate. The new catalytic system has the advantage of easy product isolation and catalyst recycle, using simple liquid/liquid separation techniques. This technology can significantly reduce the costs of catalytic carbon-carbon double bond conjugation processes that require expensive rare metal species. The process has been optimized using soybean oil as the model system and a maximum yield of 96% has been obtained when the reaction is run at 80 °C under argon with ethanol as the polar solvent, using tppms as the ligand, and SDS as the surfactant. The optimized reaction conditions have been tested with other substrates, including various natural oils, cyclic and linear dienes, and alpha olefins. The results obtained suggest a very low activity of the catalyst with dienes in general. In fact, significant conjugated products are only observed for starting materials where the carbon-carbon double bonds are separated by a single methylene group.

The technology developed for the use of vegetable oils in the preparation of diverse bio-based materials, such as thermosetting resins and composites, is tremendously useful and the research effort in that area is expanding rapidly. Bio-based thermosets with a wide range of properties have been prepared from regular and modified oils by their free radical, cationic, thermal, and ring opening metathesis polymerization in the presence of various vinylic comonomers. In general, a similarity in the reactivities of the comonomers is of great importance in maximizing the oil incorporation and the homogeneity of the products obtained.



The aforementioned bio-based resins have been reinforced with inorganic and natural fillers to afford high bio-based content thermosetting composites. In comparison to the pure resins, significant improvements have been obtained in the mechanical properties by the addition of the fillers.

Despite the great accomplishments observed to date in the development of bio-based materials, achieving composites with properties similar and sometimes even better than commercially available materials, future research efforts in the area should include the design of hybrid composites, where inorganic fillers and natural fibers can be used simultaneously as reinforcements. In such systems, the beneficial aspects of either kind of reinforcement can be combined to yield materials with new and interesting properties. Another area where improvements can yield more promising materials is the surface treatment of natural fibers. A variety of processes can be tested in an effort to modify the ligno-cellulosic surface of natural fillers and afford better filler-resin interactions.

Other resin systems can also be sought by the incorporation of other comonomers and by applying other modifications in the structure of the triglycerides. Improvements on recycling the catalysts involved in the conjugation of carbon-carbon double bonds in triglycerides will also help the systems discussed here to become more economically viable.

## ACKNOWLEDGEMENTS

I would like to thank Dr. Larock for his support, kindness, and wise guidance during my time at Iowa State University. I feel truly grateful and honored to have had the chance to work in his research group and learned so much from him. I am also sincerely thankful to Dr. Kessler. The interaction with his students, the courses taught, and his advices were very important and appreciated components of my education at Iowa State University. I also want to thank Dr. Zhao, Dr. Jeffries, and Dr. Verkade for their time and interest.

I thank my fellow group members, in special Dr. Pfister, Dr. Valverde, Dr. Henna, Dr. Lu, Ying Xia, and Tom Garrison for their friendship and all the productive discussions we have had during the past five years. Likewise, I appreciate all the help provided by Patti Boone and those in the Chemistry Department Office. Their incredibly efficient work makes bureaucracy seem an outdated term.

None of this would have been possible without my faith in God and the constant incentive of my loving family. Larissa, Gabriela, Nathan, mom, dad, Alba, Hécio, Leticia, and Igor, you are my inspiration and the ultimate reason behind all my effort. Thank you so much!

**CURRICULUM VITAE****RAFAEL L. QUIRINO**

Ph.D. candidate, Chemistry Department

Major professor: Dr. Richard C. Larock

3701 Gilman Hall, Iowa State University, Ames, IA 50011

(515) 451-2460 / rquirino@iastate.edu

**(a) Education**

|                                   |                             |                         |
|-----------------------------------|-----------------------------|-------------------------|
| Iowa State University             | Major: Chemistry (3.88 GPA) | Ph.D. in 2011 (planned) |
| Universidade de Brasília (Brazil) | Major: Physical Chemistry   | M.S. in 2006            |
| Universidade de Brasília (Brazil) | Major: Chemistry            | B.S. in 2004            |
| Lycée Jeane D'Arc (France)        | High School                 | Bac. in 1999            |

**(b) Features**

- Fields of expertise: synthesis and characterization of biopolymers and biocomposites, biofuels, catalysis, and oleochemistry
- Relevant course work: Physical Organic Chemistry I and II, Organic Synthesis I, Polymer Processing and Characterization, Polymer Properties, Spectroscopic Identification of Organic Compounds, Molecular Catalysis and Processes, Heterogeneous Catalysis
- Fluent in English, French, and Portuguese
- Residence in France from 1997 to 2001
- Contacts in academia in France, Brazil and the U.S.

**(c) Appointments**

|             |  |
|-------------|--|
| 2006 – 2011 | Teaching and Research Assistant in alternating years (Iowa State University) |
| 2005 – 2006 | Chemistry teacher (high school level) at IPEB (Brazil)                       |
| 2004 – 2006 | Research Assistant at Universidade de Brasília (Brazil)                      |

2001 – 2004 Teaching Assistant at Universidade de Brasília (Brazil) and Fellowship through EMBRAPA (Brazil)

#### (d) Teaching Experience

- Mentored the research of a graduate student at Iowa State University
- Mentored the research of six undergraduate students in both Brazil and the U.S.
- Taught General Chemistry, Physical Chemistry, and Organic Chemistry classes at the undergraduate level as a teaching assistant in both Brazil and the U.S.
- Worked as a Chemistry teacher at the High School level for one year and six months in Brazil

#### (e) Awards

1. 2<sup>nd</sup> edition of the Petrobras Prize of Technology (Brazil, 2007)
2. Alpha Chi Sigma Award for Excellence in Research, Chemistry Department, Iowa State University (2011)

#### (f) Publications

1. Oliveira, E.; Quirino, R. L.; Suarez, P. A.Z.; Prado, A. G. S.; Heats of combustion of biofuels obtained by pyrolysis and by transesterification and of biofuel/diesel blends; *Thermochimica Acta*, v. 450, p. 87-90, 2006.
2. Quirino, R. L.; Larock, R. C.; Synthesis and properties of soy hull-reinforced biocomposites from conjugated soybean oil; *J. Appl. Polym. Sci.*, v. 112, p. 2033-2043, 2009.
3. Quirino, R. L.; Tavares, A. P.; Peres, A. C.; Rubim, J. C.; Suarez, P. A. Z.; Studying the influence of alumina catalysts doped with tin and zinc oxides in the soybean oil pyrolysis reaction; *J. Am. Oil Chem. Soc.*, v. 86, p. 167-172, 2009.
4. Brandao, R. F.; Quirino, R. L.; Mello, V. M.; Tavares, A.; Peres, A. C.; Guinhos, F.; Rubim, J.; Suarez, P. A. Z.; Synthesis, characterization and use of Nb<sub>2</sub>O<sub>5</sub>-based catalysts in producing biofuels by transesterification, esterification and pyrolysis; *J. Braz. Chem. Soc.*, v. 20, p. 954-966, 2009.
5. Santos, A. L. F.; Mello, V. M.; Iha, O. K.; Ribeiro, R. A. M.; Quirino, R. L.; Suarez, P. A. Z; Agro-industrial residues as low-price feedstock for diesel-like fuel production by thermal cracking. *Bioresource Technology*, v. 101, p. 6157-6162, 2010.
6. Quirino, R. L.; Larock, R. C.; Rice hull biocomposites. I. Preparation of a linseed-oil-based resin reinforced with rice hulls. *Journal of Applied Polymer Science*, v.121, 2039-2049, 2011.

7. Quirino, R. L.; Larock, R. C.; Rice hull biocomposites, Part 2: Effect of the resin composition on the properties of the composite. *Journal of Applied Polymer Science*, v. 121, 2050-2059, 2011.
8. Quirino, R. L.; Woodford, J.; Larock, R. C.; Cure sequence study of wood flour and wood fiber biocomposites. *Journal of Applied Polymer Science*, *accepted for publication*, 2011.
9. Quirino, R. L.; Daher, L. O.; Rubim, J. C.; Suarez, P. A. Z.; Synthesis, characterization and application of alumina doped with TiO<sub>2</sub> and ZrO<sub>2</sub> in soybean oil cracking. *Submitted for publication*.
10. Quirino, R. L.; Larock, R. C.; Rh-based biphasic isomerization of carbon-carbon double bonds. *Submitted for publication*.
11. Quirino, R. L.; Larock, R. C.; Sugar-cane bagasse composites from vegetable oils. *Submitted for publication*.
12. Quirino, R. L.; Ma, Y.; Larock, R. C.; Oat hull composites from conjugated natural oils. *Submitted for publication*.

#### (g) Book Chapters

1. Quirino, R. L.; Larock, R. C.; Bioplastics, Biocomposites, and Biocoatings from Natural Oils. *ACS books, Symposium Series*, v. 1063, Renewable and Sustainable Polymers, Ch. 3, 37-59, 2011.
2. Quirino, R. L.; Kessler, M.; Vegetable Oil-based Resins and Composites. In *Sustainable Composites and Advanced Materials*. *Manuscript under preparation*.

#### (h) Oral Presentations

1. Quirino, R. L.; Suarez, P. A. Z.; Guinhos, F.; Cardoso, E. V.; Rubim, J. C.; Borges, E.; Tavares, A.; The influence of metal oxide catalysts in the selectivity of the soybean oil pyrolysis reaction's products. 96<sup>th</sup> American Oil Chemist's Society Annual Meeting, Salt Lake City, UT, 2005.
2. Quirino, R. L.; Pfister, D.; Larock, R. C.; Biorenewable composites reinforced with under-used agricultural co-products. Recycle and Reuse Technology Transfer Center, University of Northern Iowa, Cedar Falls, IA, 2007.
3. Quirino, R. L.; Larock, R. C.; Synthesis and tensile properties of soy hull-reinforced biocomposites from conjugated soybean oil. 236<sup>th</sup> American Chemical Society National Meeting and Exposition, Philadelphia, PA, 2008.
4. Quirino, R. L.; Larock, R. C.; Development of a Rh-biphasic catalyst for the conjugation of soybean oil. 44<sup>th</sup> ACS Midwest Regional Meeting, Iowa City, IA, 2009.

5. Quirino, R. L.; Larock, R. C.; Linseed and soybean oil-based biopolymers reinforced with rice hulls. 45<sup>th</sup> ACS Midwest Regional Meeting, Wichita, KS, 2010.
6. Quirino, R. L.; Woodford, J.; Larock, R. C.; Biobased wood flour composites from soybean and linseed oils. 241<sup>st</sup> ACS National Meeting and Exposition, Anaheim, CA, 2011.
7. Quirino, R. L.; Larock, R. C.; Vegetable oil-derived composites reinforced with sugar-cane bagasse. Larock Retirement Symposium, Ames, IA, 2011.

#### **(i) Poster presentations**

1. Quirino, R. L.; Tavares, A.; Peres, A. C.; Rubim, J. C.; Suarez, P. A. Z.; Study of the influence of catalysts based on alumina doped with Tin and Zinc oxides in the soybean oil cracking reaction. I Midwest Chemistry Graduate Workshop; I BCS Regional Meeting of Distrito Federal, Brasilia, DF, 2006.
2. Quirino, R. L.; Ribeiro, R. A. M.; Santos, A. L. F.; Rubim, J. C.; Suarez, P. A. Z.; Pyrolysis of animal and vegetable feedstock for the production of biofuels. I Midwest Chemistry Graduate Workshop; I BCS Regional Meeting of Distrito Federal, Brasilia, DF, 2006.
3. Quirino, R. L.; Larock, R. C.; Synthesis and mechanical properties of soy hull-reinforced biocomposites from conjugated soybean oil. Biobased Industry Outlook Conference, Ames, IA, 2008.
4. Quirino, R. L.; Larock, R. C.; Preparation of biocomposites using conjugated vegetable oils and soy hulls. Chemistry Department Open House, Ames, IA, 2008.
5. Quirino, R. L.; Larock, R. C.; Conjugation of polyenes. CBiRC, NSF Site Visit, Ames, IA, 2009.
6. Quirino, R. L.; Larock, R. C.; Progress on the biphasic conjugation of soybean oil. CBiRC Working Meeting, Ames, IA, 2009.
7. Quirino, R. L.; Larock, R. C.; Latest results on the isomerization of C=C. CBiRC, NSF Site Visit, Ames, IA, 2010.
8. Quirino, R. L.; Larock, R. C.; Polyene conjugation and tethered catalyst for selective hydrogenation. CBiRC Working Meeting, Ames, IA, 2010.
9. Quirino, R. L.; Larock, R. C.; Polyene conjugation and tethered catalyst for selective hydrogenation. CBiRC, NSF Site Visit, Ames, IA, 2011.

#### **(j) Masters Thesis**

1. Quirino, R. L.; Study of the influence of catalysts based on alumina doped with TiO<sub>2</sub> and ZrO<sub>2</sub> in the soybean oil cracking reaction. Masters Thesis,

University of Brasilia, Brasilia-DF, Brazil, 2006. Major Prof.: Dr. Paulo Suarez.

**(k) Doctorate Dissertation**

1. Quirino, R. L.; Natural oil-based composites reinforced with natural fillers, and conjugation/isomerization of carbon-carbon double bonds. Doctorate Dissertation, Iowa State University, Ames, IA, 2011. Major Prof.: Dr. Richard C. Larock.